

C. BROWN

Spacecraft Mission Design, Second Edition

AIAA
Education Series

J. S. PRZEMIENIECKI EDITOR-IN-CHIEF

Spacecraft Mission Design

Second Edition

This page intentionally left blank

Spacecraft Mission Design

Second Edition

Charles D. Brown
Wren Software, Inc.
Castle Rock, Colorado



EDUCATION SERIES

J. S. Przemieniecki
Series Editor-in-Chief
Air Force Institute of Technology
Wright-Patterson Air Force Base, Ohio

Published by
American Institute of Aeronautics and Astronautics, Inc.
1801 Alexander Bell Drive, Reston, VA 20191

American Institute of Aeronautics and Astronautics, Inc., Reston, Virginia

1 2 3 4 5

Library of Congress Cataloging-in-Publication Data

Brown, Charles D., 1930—

Spacecraft mission design / Charles D. Brown. — 2nd ed.
p. cm.

Includes bibliographical references and index.

ISBN 1-56347-262-7 (alk. paper)

1. Space flight—Planning. 2. Astrodynamics. 3. ORBWIN.

I. Title.

TL790.B735 1998 629.4'1—dc21 98-12675

Copyright © 1998 by the American Institute of Aeronautics and Astronautics, Inc. All rights reserved.
Printed in the United States of America. No part of this publication may be reproduced, distributed, or
transmitted, in any form or by any means, or stored in a database or retrieval system, without the prior
written permission of the publisher.

Data and information appearing in this book are for informational purposes only. AIAA is not responsible
for any injury or damage resulting from use or reliance, nor does AIAA warrant that use or reliance
will be free from privately owned rights.

Foreword

The original publication of *Spacecraft Mission Design* by Charles D. Brown brought another text/software combination into the AIAA Education Series. This approach, which is used in many modern textbooks, allows students to perform “hands on” computations as if they were engaged in the real-life design activity. The second edition of this text includes updated software and a separate chapter on lunar trajectories as well as many improvements based on five years of classroom use. The text emphasizes the fundamentals of spacecraft mission design without going into the details of the mathematical treatment of orbital mechanics and astrodynamics. It provides an excellent overview of the subject, starting with two-body motion, moving on to orbital maneuvers and special Earth orbits and leading finally to interplanetary missions and the applications software package ORBWIN: AIAA Mission Design Software. The text was originally written for use in a spacecraft course, which has been taught by the author at Colorado University since 1981. It is a natural companion to the more advanced text *Introduction to Mathematics and Methods of Astrodynamics* by Richard H. Battin, also published in the AIAA Education Series. With the national commitment to space exploration, as evidenced by the building of the International Space Station, *Spacecraft Mission Design* fills a need for an introductory textbook in aerospace engineering curricula.

Mr. Brown is eminently qualified to write on the subject, having been one of the leaders at Martin Marietta in various design teams such as the Mariner 9, the first spacecraft to orbit another planet in 1971; the Viking spacecraft; and the Magellan spacecraft, which produced successful imaging of the planet Venus and was the first planetary spacecraft to fly on the Space Shuttle. In 1992, Mr. Brown received the Goddard Memorial Trophy for his Magellan project leadership and the NASA Public Service Medal, just to mention a few of his achievements and awards.

The Education Series of textbooks and monographs published by the American Institute of Aeronautics and Astronautics embraces a broad spectrum of theory and application of different disciplines in aeronautics and astronautics, including aerospace design practice. The series also includes texts on defense science, engineering, and management. The complete list of textbooks published in the series (over 50 titles) can be found on the end pages of this volume. The series provides teaching texts as well as reference materials for practicing engineers, scientists, and managers.

J. S. Przemieniecki
Editor-in-Chief
AIAA Education Series

This page intentionally left blank

About the Author

Charles Brown has had a distinguished career as the manager of planetary spacecraft projects and as a college-level lecturer in spacecraft design. During his 30 years with Martin Marietta, he led the design team that produced propulsion systems for Mariner 9 and Viking Orbiter. Among other projects, he directed the team that produced the successful Venus-imaging spacecraft, Magellan. Magellan was launched on Space Shuttle *Atlantis* in 1989 and completed the first global map of the surface of Venus. Magellan was the first planetary spacecraft to fly on the Shuttle and the first planetary launch by the United States in 10 years.

Mr. Brown has instructed a popular spacecraft design course at Colorado University since 1981. This book was originally written for use in that course. Mr. Brown also is the author of *Spacecraft Propulsion*, published by AIAA, and he writes software for Wren Software, Inc., a small software company he founded in 1984. He was corecipient of the Dr. Robert H. Goddard Memorial Trophy in 1992 for Magellan leadership. He has also received the Astronauts' Silver Snoopy Award in 1989; the NASA Public Service Medal in 1992 for Magellan and in 1976 for Viking Orbiter; and the Outstanding Engineering Achievement Award, 1989 (a team award), from the National Society of Professional Engineers for Magellan.

This page intentionally left blank

Table of Contents

Preface	xi
Chapter 1. Introduction	1
1.1 Arrangement of the Book	1
1.2 ORBWIN: AIAA Mission Design Software	1
1.3 Study of Two-Body Motion	1
Chapter 2. Two-Body Motion	5
2.1 Circular Orbits	5
2.2 General Solution	7
2.3 Elliptical Orbits	11
2.4 Parabolic Orbits	18
2.5 Hyperbolic Orbits	22
2.6 Time Systems	26
2.7 Coordinate Systems	32
2.8 Classical Orbital Elements	35
Problems	36
Chapter 3. Orbital Maneuvers	39
3.1 In-Plane Orbit Changes	39
3.2 Hohmann Transfer	43
3.3 Bielliptical Transfer	45
3.4 Plane Changes	45
3.5 Combined Maneuvers	48
3.6 Propulsion for Maneuvers	49
Problems	51
Chapter 4. Observing the Central Body	53
4.1 Effect of the Launch Site	53
4.2 Orbit Perturbations	57
4.3 Ground Track	63
4.4 Spacecraft Horizon	68
4.5 Constellations	74
Problems	78

Chapter 5. Special Earth Orbits	81
5.1 Geosynchronous Orbit	81
5.2 Sun-Synchronous Orbit	87
5.3 Molniya Orbit	89
5.4 Low Earth Orbit	91
Problems	93
Chapter 6. Interplanetary Trajectories	95
6.1 Patched Conic Approximation	96
6.2 Highly Simplified Example	98
6.3 Patched Conic Procedure	100
6.4 Locating the Planets	101
6.5 Design of the Transfer Ellipse	106
6.6 Design of the Departure Trajectory	108
6.7 Design of the Arrival Trajectory	115
6.8 Gravity-Assist Maneuver	120
6.9 Cycler Orbits	126
6.10 Establishing Planetary Orbit	129
Problems	130
Chapter 7. Lunar Trajectories	133
7.1 Motion of the Earth–Moon System	133
7.2 Time of Flight and Injection Velocity	134
7.3 Sphere of Influence	135
7.4 Lunar Patched Conic	136
Problems	141
Appendix A. ORBWIN: AIAA Mission Design Software	143
A.1 Introduction to ORBWIN	143
A.2 Quick Tour of ORBWIN	143
A.3 Orbit Definition Example	149
A.4 Utilities	152
A.5 Interesting Orbits—Examples	156
Appendix B. Mission Design Glossary	161
Appendix C. Mission Design Data	167
References	179
Index	181

Preface

This book, now in its second edition, is called *Spacecraft Mission Design*, as opposed to *Orbital Mechanics* or *Astroynamics*, to convey its emphasis on purpose. Mission design distinctly includes the idea of achieving a result as opposed to simply studying principles. This book is an outgrowth of my spacecraft design course at Colorado University, and it is first of all a teaching tool. It is my objective to make the concepts clear enough, with enough examples worked out, that you can be self-taught if need be. This second edition includes the changes and improvements from five years of classroom use and adds material in places where students had problems. The accompanying software has been totally rewritten to make it easier to use and compatible with WindowsTM. Sections on lunar trajectories, constellation design, and cycler orbits have been added along with additional astronomical reference material. A specific energy method for definition of conics of unknown type has been added in Chapter 2, Sec. 2.2.

College upperclassmen, graduates, practicing engineers, and managers who want to know more about mission design all can benefit from this book. The subject is treated using elementary mathematics (which is adequate and easier to understand). Derivations are generally avoided in favor of emphasis on the assumptions involved and hence on the conditions under which the resulting expressions can be used. Other works, notably Battin's *An Introduction to the Mathematics and Methods of Astrodynamics* (AIAA Education Series, AIAA, Washington, DC, 1987), do an excellent job of describing the mathematical elegance underlying this field. My objective is to take the shortest route to practical understanding.

This book is different than other books in the field in three primary ways: First, the book includes ORBWIN: AIAA Mission Design Software. ORBWIN allows you to proceed directly from understanding concepts into professional work. It also provides you with the accuracy, speed, and convenience of personal computing. Second, an entire chapter is devoted to interplanetary trajectories, which I believe are the most interesting type of mission design. Third, I like a book that will fit in your briefcase. This book has been kept thin by focusing on the most general and most practical tools needed for early spacecraft design studies. Although material has been added in this new edition, the original focus has been maintained. Everyone who works in aerospace should know at least this much about mission design.

I wish to thank Lockheed Martin Corporation, the Jet Propulsion Laboratory, and Colorado University for giving me the opportunity to work and to teach in this fascinating field. I also want to thank the many brilliant professionals at these institutions from whom I learned so much.

Charles D. Brown

February 1998

1

Introduction

You need nothing more than this book and the ORBWIN software that comes with it to design a mission to anywhere in the solar system. Are you interested in how the Mars Sample Return mission will be flown? Or would you like to study a mission to Titan, one of Saturn's moons and a candidate for life? Or are you interested in the feasibility of a mission to Pluto, the last unexplored planet? Have at it.

1.1 Arrangement of the Book

The first three chapters of the book describe the basic equations of two-body motion including the design of maneuvers and the special relations involved in observing the central body. Chapters 5 and 6 give examples of mission designs of several of the most important orbit types. Chapter 6 also covers the interesting complexities of interplanetary orbits and includes a detailed example.

The appendices were designed to provide the working professional with ready reference material. Appendix A is the manual for ORBWIN: AIAA Mission Design Software. Appendix B is a glossary of mission design terms, which are unusually obtuse. Equations, design data, and conversion factors are in Appendix C.

1.2 ORBWIN: AIAA Mission Design Software

This book includes ORBWIN: AIAA Mission Design Software. With ORBWIN you can do complete mission designs with the accuracy, speed, and downright convenience of personal computing. You no longer need to have a mainframe to do quality work in this field.

1.3 Study of Two-Body Motion

Much of the history of mathematical and physical thought was inspired by curiosity about the motion of the planets—the very same laws that govern the motion of spacecraft. The first observations of the celestial bodies predate recorded history. The inertial position of the vernal equinox vector was observed and recorded in stone constructions—Stonehenge, for example—as early as 1800 B.C. Written evidence of stellar observations was left by the Egyptians and the Babylonians from about 3500 years ago. (The Babylonians of this era divided time into 60 even units, a tradition that survives to this day.¹)

In about 350 B.C. Aristotle explained the wandering motion of the planets by proposing that the universe was composed of 55 concentric rotating spheres centered in the Earth. The outermost sphere contained the fixed stars; its rotation is a very adequate explanation of the observed motion of stars in the night sky and

SPACECRAFT MISSION DESIGN

the irresistible image of a celestial sphere. The rotation of the inner sphere containing the moon was also a simple, descriptive idea. The motion of the planets, however, was much more difficult. Not only were the observing instruments crude and the mathematical tools nonexistent, the Earth is a singularly poor observation post for heliocentric motion. Usually the planets move slowly eastward across a background of fixed stars; however, at times they reverse direction and move westward. The retrograde loop of Mars is renowned. To explain this motion, Aristotle invented the remaining 53 concentric spheres. Each planet was located in one of the spheres, and its motion was influenced by the rotation of several other spheres.²

At about the same time a Greek named Aristarchus proposed a much simpler theory in which the sun and stars were fixed and the planets rotated about the sun, but this theory was not accepted. Aristotle's theory dominated scientific thought for 1800 years.

In about 150 A.D. the Greek astronomer Ptolemy presented a more elaborate Earth-centered theory, which held that the planets moved around the Earth in small circles called epicycles, whose centers moved around in large circles called deferents. The tables of planetary motion computed by Ptolemy based on this theory were used for 1400 years.

In 1543 Nicholas Copernicus broke with Aristotle's theory and advocated sun-centered rotation. His theory neatly explained the retrograde motion of the planets as observed from Earth; however, measured positions were so crude at the time that they fit Ptolemy's conception as well as that of Copernicus.

In about 1610 the Italian scientist Galileo Galilei made two observations that reinforced the theory of Copernicus. First, he observed the motion of moons orbiting Jupiter; thus at least some bodies must not orbit Earth. Second, he observed moonlike phases of the sunlight on Venus that could not be explained by Ptolemy's theory. Galileo attracted the wrath of the Catholic Church and was forced to recant his observations.

In the late 1500s Tycho Brahe made the first accurate measurements of the positions of the planets as a function of time. His achievement is all the more remarkable because the telescope had not yet been invented. Brahe himself believed in Ptolemy's theory of the universe, but his careful observations allowed Johannes Kepler to describe mathematically the heliocentric motion of the planets and to lay to rest the ancient theories of Aristotle and Ptolemy.

In early 1600, Kepler presented his three laws of planetary motion, which are the basis of our understanding of planetary (and spacecraft) motion.

First Law: The orbit of each planet is an ellipse, with the sun at one focus.

Second Law: The line joining the planet to the sun sweeps out equal areas in equal times.

Third Law: The square of the period of a planetary orbit is proportional to the cube of its mean radius.

In addition, Kepler contributed Kepler's equation, which relates position and time. Kepler's equation is the most famous transcendental equation ever discovered. Solving it for the time elapsed since periapsis when one is given orbital elements is trivial; solving it for orbital elements when one is given the time elapsed since periapsis was the "Mount Everest" of mathematics for three centuries.

INTRODUCTION

3

With Kepler's laws, the world had a description of planetary motion, but the underlying cause of the motion was yet to come, and that would require the genius of Isaac Newton. Newton was 23 and a student at Cambridge in 1665 when an epidemic of the plague broke out. He moved to the relative safety of the countryside, where he spent the most productive two years of his life. Just one of his achievements during that period was to develop the physics of planetary motion. He postulated that all masses are attracted to one another with a force proportional to the product of their masses and inversely proportional to the square of the distance between them. He further postulated that the mass of symmetrical bodies could be concentrated at their centers. To test these assumptions, he formulated the differential equations of motion for the planets and invented calculus to solve them. The result confirmed Kepler's laws. By 1666 one man understood planetary motion, but it would be another 20 years before the world had the news.

Newton put this incredible piece of work aside and neither published it nor discussed it until 20 years later, when he was questioned by his friend Edmund Halley about planetary motion. Newton casually replied that he had already worked it out and had it somewhere among his papers. At the urging of an astonished Halley, Newton published his work in 1687 in *Principia*.²

With the understanding at the outset that we will consider no principles newer than those of the seventeenth century, let us proceed to see how we might send a spacecraft to Pluto.

This page intentionally left blank

2

Two-Body Motion

All of the celestial bodies, from a fleck of dust to a supernova, are attracted to each other in accordance with Newton's law of universal gravitation:

$$F_g = MmG/r^2 \quad (2.1)$$

where

F_g = universal gravitational force between bodies

M, m = mass of the two bodies

G = universal gravitational constant

r = distance between the center of masses of the two bodies

The motion of a spacecraft in the universe is governed by an infinite network of attractions to all celestial bodies. A rigorous analysis of this network would be impossible; fortunately, the motion of a spacecraft in the solar system is dominated by one central body at a time. This observation leads to the very useful two-body assumptions:

- 1) The motion of a spacecraft is governed by attraction to a single central body.
- 2) The mass of the spacecraft is negligible compared to that of the central body.
- 3) The bodies are spherically symmetric with the masses concentrated at the centers.
- 4) No forces act on the bodies except for gravitational forces and centrifugal forces acting along the line of centers.

If the two-body assumptions hold, it can be shown that conic sections are the only possible paths for orbiting bodies and that the central body must be at a focus of the conic.⁴

The two-body assumptions are very nearly true. Table 2.1 shows the most significant relative accelerations on a low Earth orbiter. The influence of Earth on the spacecraft is more significant than any other influence by more than a factor of 1000. The oblateness of the Earth also leads to errors in two-body solutions; however, these errors are small and can be accurately predicted.

No explicit solution has been found for the N -body problem except for $N = 2$; however, numerical solutions are available for the N -body situation. These solutions require a large computing capacity and are used only when the two-body solution is suspect (e.g., a Mercury orbiter) or when high accuracy is required (e.g., navigation calculations).

2.1 Circular Orbits

Figure 2.1 shows the forces on a spacecraft in a circular orbit under two-body conditions. The gravitational force on the spacecraft is defined by Eq. (2.1); the

SPACECRAFT MISSION DESIGN

Table 2.1 Accelerations on a low Earth orbiter

Body	Acceleration, g
Earth	0.9
Sun	6×10^{-4}
Moon	3×10^{-6}
Jupiter	3×10^{-8}
Venus	2×10^{-8}

Source: From Ref. 3, p. 11; reproduced through the courtesy of Dover Publications, Inc.

centrifugal force on the spacecraft is

$$F_c = mV^2/r \quad (2.2)$$

where

F_c = centrifugal force on the spacecraft

V = velocity of the spacecraft

m = mass of the spacecraft

r = radius from the spacecraft center of mass to the central body center of mass

For circular, steady-state motion to occur, the gravitational and centrifugal forces must be equal; therefore

$$mV^2/r = MmG/r^2 \quad (2.3)$$

$$V = \sqrt{MG/r} \quad (2.4)$$

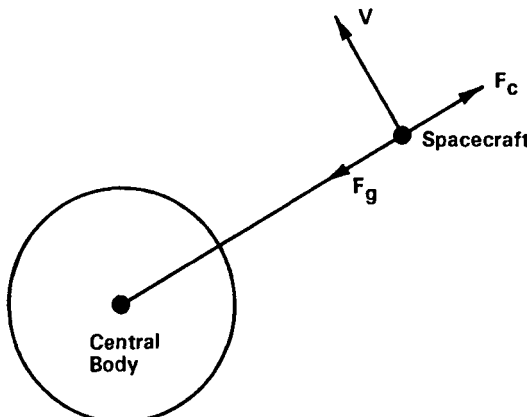


Fig. 2.1 Two-body motion—circular orbit.

TWO-BODY MOTION

7

It is convenient to assign a gravitational parameter μ , which is the product of the central body mass and the universal gravitational constant. In other words,

$$\mu = MG \quad (2.5)$$

allows the simplification

$$V = \sqrt{\mu/r} \quad (2.6)$$

for circular orbits.

The gravitational parameter is a property of the central body; a table that lists values for each of the major bodies in the solar system is given in Appendix C. (Substantial improvement in the accuracy of planetary constants is one of the by-products of planetary exploration.)

The period of a circular orbit, derived with equal simplicity, is given by

$$P = \text{circumference}/\text{velocity} = 2\pi\sqrt{r^3/\mu} \quad (2.7)$$

Example 2.1 Circular Orbit Velocity and Period

What is the velocity of the Space Shuttle in a 150-n mile circular orbit? From Appendix C, for Earth,

$$R_0 = 6378.14 \text{ km}$$

$$\mu = 398,600 \text{ km}^3/\text{s}^2$$

Spacecraft altitude h is specified more frequently than radius r in practical applications. It is understood that altitude, used as an orbital element, is given with respect to the mean equatorial radius R_0 .

Calculate r (the conversion factor for nautical miles to kilometers is given in Table C.10 of Appendix C):

$$r = R_0 + h = 6378.14 + (150)(1.852) = 6655.94 \text{ km}$$

Calculate Shuttle velocity for a circular orbit by using Eq. (2.6):

$$V = \sqrt{398,600/6655.94} = 7.739 \text{ km/s}$$

Calculate orbit period by using Eq. (2.7):

$$P = 2\pi\sqrt{r^3/\mu} = 2\pi\sqrt{(6655.94)^3/398,600} = 5404 \text{ s} \approx 90 \text{ min}$$

2.2 General Solution

Circular motion is a special case of two-body motion. Solving the general case requires integration of the equations of motion; this solution is summarized in the work of Koelle⁴ and elsewhere. The conclusions that can be drawn from the general solution are more interesting than the solution itself:

- 1) Kepler's laws of planetary motion are confirmed and generalized to allow orbits of any conic section, not just elliptical orbits. (Two-body motion is often called Keplerian motion.)

- 2) The sum of the potential energy and kinetic energy of the orbiting body, per unit mass, is a constant at all points in the orbit and is

$$\varepsilon = (V^2/2) - (\mu/r) \quad (2.8)$$

where ε is the total mechanical energy per unit mass, or specific energy, of an object in any orbit about a central body. The kinetic energy term in Eq. (2.8) is $V^2/2$ and the potential energy term is $-\mu/r$. Potential energy is considered to be zero at infinity and negative at radii less than infinity. Equation (2.8) can be reduced to

$$\varepsilon = -(\mu/2a) \quad (2.9)$$

where a is the semimajor axis (see Fig. 2.3). The total energy of any orbit depends on the semimajor axis of the orbit only. For a circular orbit, $a = r$ and specific energy is negative. For an elliptical orbit, a is positive and specific energy is negative. Thus, for all closed orbits specific energy is negative. For parabolic orbits, $a = \infty$ and specific energy is zero; as we will see, a parabolic orbit is a boundary condition between hyperbolas and ellipses. For hyperbolic orbits, a is negative and specific energy is positive. Figure 2.2 shows the relative energy for orbit types.

At a given radius, velocity and specific energy increase in the following order: circular, elliptical, parabolic, hyperbolic; total spacecraft energy increases in the same order. Additional energy must be added to a spacecraft to change an orbit from circular to elliptical. Energy must be removed to change from an elliptical to a circular orbit. Both adding and removing energy requires a force on the vehicle and in general that means consumption of propellant.

A particularly useful form of Eq. (2.9) is

$$a = -(\mu/2\varepsilon) \quad (2.10)$$

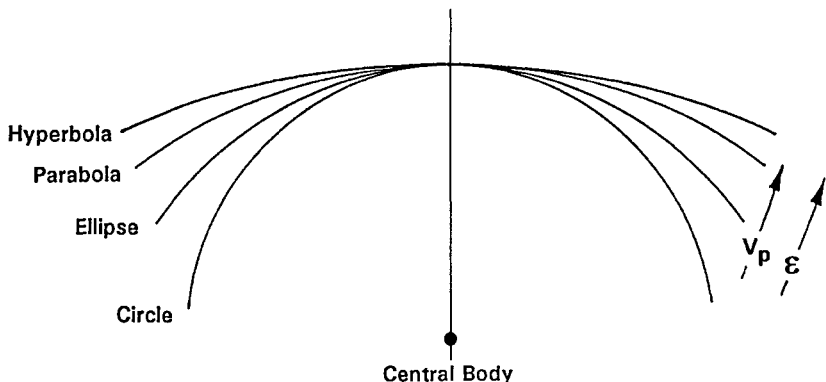


Fig. 2.2 Relative energy of orbit types.

TWO-BODY MOTION

9

- 3) Total angular momentum of the orbiting body is a constant, equal to the cross product of the radius and the velocity vectors:

$$\mathbf{H} = \mathbf{r} \times \mathbf{V} \quad (2.11)$$

where \mathbf{H} is the angular momentum per unit mass (or specific momentum) and is a vector quantity. From vector mechanics, the magnitude of \mathbf{H} can be determined by

$$H = r V \cos \gamma \quad (2.12)$$

where

H = magnitude of the specific momentum, km^3/s

r = magnitude of the radius vector (the distance from the spacecraft to the center of mass of the central body), km/s

V = magnitude of the velocity vector, km/s

γ = flight path angle (the angle between the local horizontal and the velocity vector; see Fig. 2.3), deg

Eccentricity e defines the shape of a conic orbit and is equal to c/a in Fig 2.3. Eccentricity equals zero for a circular orbit, is less than one for an elliptical orbit, equal to one for a parabolic orbit, and is greater than one for a hyperbolic orbit. Specific energy and eccentricity are related as follows:

$$e = \sqrt{1 - (H^2/\mu a)} \quad (2.13)$$

The most useful relation resulting from the general two-body solution is the energy integral (also called the vis-viva integral), which yields the general relation for the velocity of an orbiting body:

$$V = \sqrt{(2\mu/r) - (\mu/a)} \quad (2.14)$$

Equation (2.13) yields spacecraft velocity at any point on any conic orbit. For each conic it can be reduced, if desired, to a specific relation.

For a circle, $a = r$, and

$$V = \sqrt{\mu/r} \quad (2.6)$$

as was derived for circular orbits in the previous section.

For an ellipse, $a > 0$, and

$$V = \sqrt{(2\mu/r) - (\mu/a)} \quad (2.14)$$

For a parabola, $a = \infty$, and

$$V = \sqrt{2\mu/r} \quad (2.15)$$

For a hyperbola, $a < 0$, and

$$V = \sqrt{(2\mu/r) + (\mu/a)} \quad (2.16)$$

Table 2.2 summarizes the distinguishing characteristics of the four conic orbits. It is important to note that Eqs. (2.8–2.14) are general equations. They are valid at any point on any orbit and can be used in cases where the orbit type is not known. These relations also are summarized in Table 2.1.

Table 2.2 Characteristics of conic orbits

Element	Circle	Ellipse	Parabola	Hyperbola
Eccentricity e	Zero	<1	1	>1
Semimajor axis a	$= r$	Positive	∞	Negative
Specific energy ε	Negative	Negative	Zero	Positive

Defining an Orbit Given r , V , and γ

Equations 2.8–2.14 can be used to define an orbit and discover its type given only r , V , and γ at a point. This situation arises when an arrival orbit has been changed by a planetary encounter. The steps required are

- 1) Given r and V , the specific energy can be calculated from Eq. (2.8).
- 2) With specific energy, the semimajor axis can be obtained from Eq. (2.10).
- 3) Given r , V , and γ , the magnitude of specific momentum can be obtained from Eq. (2.12).
- 4) With specific momentum and the semimajor axis, eccentricity can be obtained from Eq. (2.13).
- 5) From the characteristics of the eccentricities, the orbit type can be determined from inspection, Table 2.2.

Eccentricity and the semimajor axis define a conic orbit. Knowing these two elements and the orbit type, any other element can be obtained using the relations derived in subsequent sections.

Example 2.2 Defining an Orbit Given r , V , and γ

An Earth-orbiting spacecraft has been observed to have a velocity of 10.7654 km/s at an altitude of 1500 km and a flight path angle of 23.174 deg; determine the orbit elements e and a and the orbit type.

The orbital radius is $1500 + 6378.14 = 7878.14$ km. Determine the specific energy from Eq. (2.8):

$$\varepsilon = \frac{(10.7654)^2}{2} - \frac{398600.4}{7878.14} = 7.351169 \text{ km}^2/\text{s}^2$$

[One of the problems with using Eq. (2.8) is the subtraction of two large numbers, which reduces accuracy. Intermediate steps must be taken to four or five places.]

With ε set, a can be calculated from Eq. (2.10):

$$a = -\frac{398600.4}{2(7.351169)} = -27111.36 \text{ km}$$

The negative semimajor axis indicates that the orbit is a hyperbolic departure. Calculating specific momentum from Eq. (2.12),

$$H = (7878.14)(10.7654)\cos(23.174) = 77968.2 \text{ km}^3/\text{s}$$

TWO-BODY MOTION

11

With the semimajor axis and specific momentum, eccentricity can be calculated from Eq. (2.13)

$$e = \sqrt{1 - \frac{(77968.2)^2}{(398600.4)(-27111.36)}} = 1.250$$

An eccentricity larger than one confirms that the orbit is a hyperbolic departure.

2.3 Elliptical Orbits

Elliptical orbits are by far the most common orbits. All planets and most space-craft move in elliptical orbits. The geometry of an elliptical orbit is shown in Fig. 2.3.

Defining an Elliptical Orbit

An elliptical orbit is most frequently defined in terms of these orbital elements:

a = semimajor axis

e = eccentricity

r_a = apoapsis radius

r_p = periapsis radius

The periapsis of an orbit is the point of closest approach to the central body or the point of minimum radius. The apoapsis is the point of maximum radius. The apoapsis, periapsis, and center of mass of the central body are joined by the line of apsides.

Periapsis and apoapsis are general terms for orbits about any central body; there are also body-specific terms:

General:	Periapsis	Apoapsis
Sun:	Perihelion	Aphelion
Earth:	Perigee	Apogee
Moon:	Perilune	Apolune

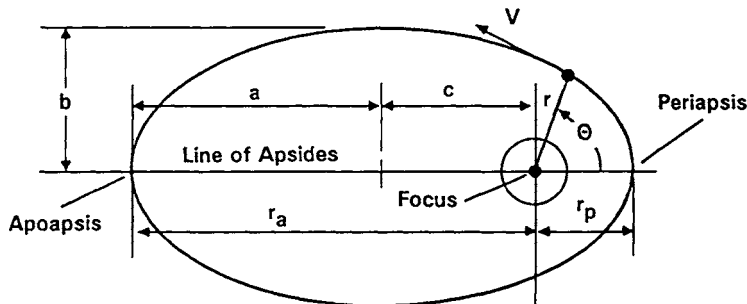


Fig. 2.3 Elliptical orbit.

By inspection, the long axis of an elliptical orbit is the sum of the apoapsis radius and the periapsis radius. It is useful to define the semimajor axis a as one-half of the long axis. Therefore,

$$a = (r_a + r_p)/2 \quad (2.17)$$

The semimajor axis is one of the classical orbital elements. It defines the size of the orbit and indicates the energy of the orbit. In astronomical work the semimajor axis is often called the mean distance; this term is misleading, however, because the semimajor axis is not equal to the time-average radius.

Similarly, the distance between elliptical foci is $2c$, and

$$c = (r_a - r_p)/2 \quad (2.18)$$

Eccentricity e is one of the classical orbital elements. As previously stated, eccentricity defines the shape of an orbit, and it is defined as

$$e = c/a \quad (2.19)$$

Thus,

$$e = (r_a - r_p)/(r_a + r_p) \quad (2.20)$$

The semiminor axis b of an ellipse is related to a and c as follows:

$$a^2 = b^2 + c^2 \quad (2.21)$$

As shown in Fig. 2.4, a spacecraft position in orbit is defined by the radius r and the position angle θ , called the true anomaly, which is measured from the periapsis to the spacecraft in the direction of motion. Given an orbit defined by e and a , the radius to a position can be calculated using the true anomaly as follows:

$$r = \frac{a(1 - e^2)}{(1 + e \cos \theta)} \quad (2.22)$$

$$r = \frac{r_p(1 + e)}{(1 + e \cos \theta)} \quad (2.23)$$

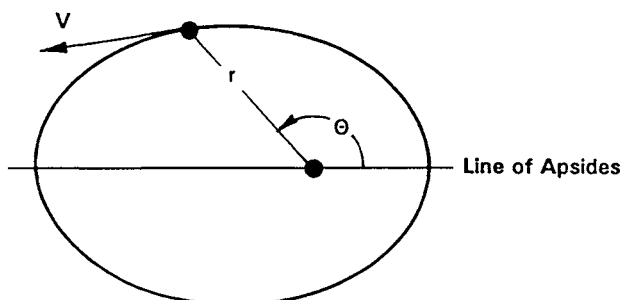


Fig. 2.4 Spacecraft position in orbit.

TWO-BODY MOTION

13

Given a defined orbit, the true anomaly can be calculated from the radius as follows:

$$\cos \theta = [r_p(1 + e)/re] - 1/e \quad (2.24)$$

$$\cos \theta = [a(1 - e^2)/re] - 1/e \quad (2.25)$$

Example 2.3 True Anomaly at a Point

Given an elliptical Earth orbit with a perigee radius of 6500 km and apogee radius of 60,000 km, find the true anomaly of the spacecraft position as it enters the Van Allen belt at an altitude of about 500 km.

Find the eccentricity by using Eq. (2.20):

$$e = \frac{60,000 - 6500}{60,000 + 6500} = 0.8045$$

Find true anomaly at an altitude of 500 km (Earth radius is from Appendix C):

$$r = 6378.14 + 500 = 6878.14 \text{ km}$$

From Eq. (2.24)

$$\cos \theta = \frac{(6500)(1 + 0.8045)}{(6878.14)(0.8045)} - \frac{1}{0.8045}$$

$$\theta = 28.755 \text{ deg}$$

Note that the altitude (or radius) defines two positions on an orbit; therefore, the radius in this example will be 6878.14 km when the true anomaly is either 28.755 deg or 331.245 deg.

It is sometimes necessary to design an elliptical orbit to pass through two given points, as shown in Fig. 2.5; two points are sufficient to design a unique elliptical orbit. Intercept trajectories and interplanetary orbits are designed in this way.

From Eq. (2.23), the relations for r_1 and r_2 can be given as

$$r_1 = \frac{r_p(1 + e)}{1 + e \cos \theta_1} \quad (2.26)$$

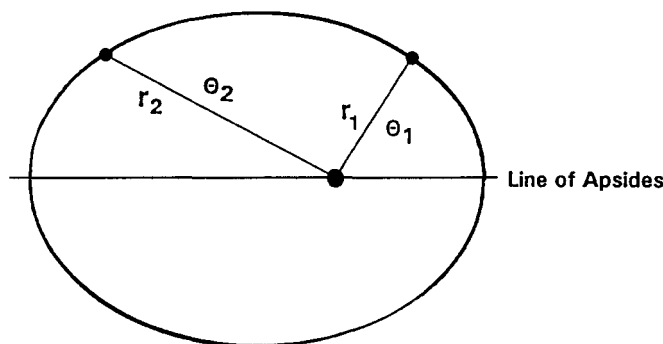


Fig. 2.5 Elliptical orbit defined by two points.

$$r_2 = \frac{r_p(1+e)}{1+e \cos \theta_2} \quad (2.27)$$

Equations (2.26) and (2.27) are two equations with two unknowns; they can be solved to produce the equations defining an orbit from two points:

$$e = \frac{r_2 - r_1}{r_1 \cos \theta_1 - r_2 \cos \theta_2} \quad (2.28)$$

$$r_p = r_1 \frac{(1 + e \cos \theta_1)}{1 + e} \quad (2.29)$$

Example 2.4 Defining an Ellipse from Two Points

Design a transfer ellipse from Earth at a heliocentric position of $r = 1.00$ AU and a longitude of 41.26° to Pluto at $r = 39.5574$ AU and a longitude of 194.66° . Place the line of apsides at a longitude of 25° .

The true anomaly of a spacecraft at Earth's position is $41.26 \text{ deg} - 25 = 16.26 \text{ deg}$. Similarly, at Pluto's position, the true anomaly is $194.66 \text{ deg} - 25 = 169.66 \text{ deg}$.

The radii of date of the planets are

$$r_1(\text{Earth}) = 1.49598 \times 10^8 \text{ km}$$

$$r_2(\text{Pluto}) = 5.9177 \times 10^9 \text{ km}$$

Find the eccentricity by using Eq. (2.28):

$$e = \frac{5.9177 \times 10^9 - 1.49598 \times 10^8}{(1.49598 \times 10^8) \cos 16.25 - (5.9177 \times 10^9) \cos 169.66} \\ = 0.9670$$

Find r_p by using Eq. (2.29):

$$r_p = (1.49598 \times 10^8) \frac{(1 + 0.9670 \cos 16.25)}{(1 + 0.9670)} = 1.4666 \times 10^8 \text{ km}$$

Any of the remaining elements of this colossal transfer ellipse can be found from e and r_p .

Defining Parameters at a Point

Having defined the orbit, it is now possible to define the parameters at any point on the orbit. The radius and true anomaly define the orbit point. The parameters of interest at a point are flight path angle γ , velocity V , and time since periaxis t .

Flight path angle. Flight path angle is defined as the angle between the local horizontal and the velocity vector, as shown in Fig. 2.6. It might seem strange to consider local horizontal and vertical in a 0-g situation; however, the horizontal at any point can be defined as perpendicular to the radius vector.

TWO-BODY MOTION

15

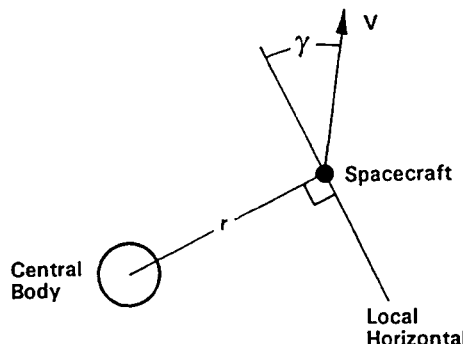


Fig. 2.6 Flight path angle.

The relation between radius and flight path angle can be readily derived by noting that

$$\tan \gamma = dr/r d\theta \quad (2.30)$$

Differentiating Eq. (2.30) and rearranging yields

$$\tan \gamma = \frac{e \sin \theta}{1 + e \cos \theta} \quad (2.31)$$

Flight path angle varies with orbital position as shown in Fig. 2.7. As a spacecraft flies around an orbit, its flight path angle is zero at periapsis; it is positive as the spacecraft rises to apoapsis. It is zero again at apoapsis and negative as the spacecraft descends to periapsis.

Velocity. Velocity at any point is calculated from the general velocity equation as previously discussed:

$$V = \sqrt{(2\mu/r) - (\mu/a)} \quad (2.14)$$

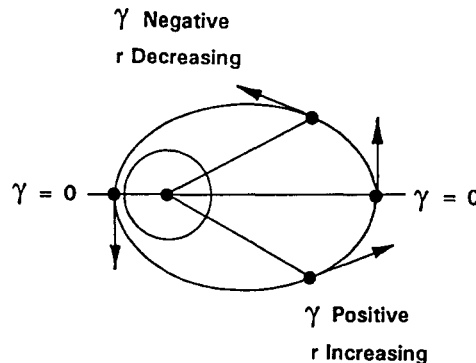


Fig. 2.7 Flight path angle as a function of position.

Another useful velocity relationship can be obtained from the equation for angular momentum. From Eq. (2.11), the angular momentum vector is

$$\mathbf{H} = \mathbf{r} \times \mathbf{V} \quad (2.11)$$

Angular momentum is constant for any point on an orbit; therefore,

$$r_1 V_{t1} = r_2 V_{t2} \quad (2.32)$$

Where V_t is tangential velocity component.

Since flight path angle is zero at periapsis and apoapsis,

$$r_p V_p = r_a V_a \quad (2.33)$$

Time since periapsis. The time taken by a spacecraft to move from periapsis to a given true anomaly (time since periapsis) is computed using the famous Kepler equation:

$$t = (E - e \sin E)/n \quad (2.34)$$

where

t = time since periapsis

E = eccentric anomaly, rad

e = eccentricity of orbit

n = mean motion

Figure 2.8 shows the geometric relationship between the eccentric anomaly and the true anomaly.

The eccentric anomaly traces a point on a circle, with radius equal to a , that circumscribes the elliptical orbit. As eccentricity goes to zero, the eccentric anomaly and true anomaly merge. The relation between eccentric and true anomaly is

$$\cos E = (e + \cos \theta)/(1 + e \cos \theta) \quad (2.35)$$

If the spacecraft were traveling on the circumscribing circle shown in Fig. 2.8, rather than the elliptical orbit, it would have an angular velocity equal to the mean

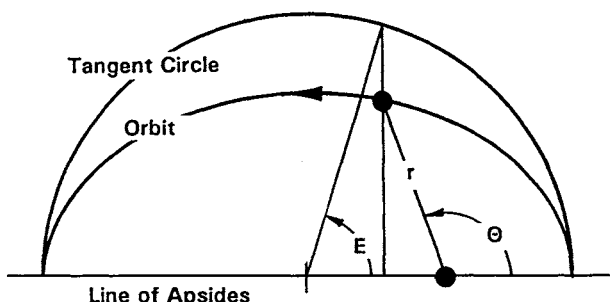


Fig. 2.8 Eccentric anomaly and true anomaly.

motion,

$$n = \sqrt{\mu/a^3} \quad (2.36)$$

Equation (2.34) does not yield time values greater than one half of the orbit period. For true anomalies greater than π , the result obtained from Eq. (2.34) must be subtracted from the orbit period to obtain the correct time since periaxis. Note also that in using Eqs. (2.34) and (2.35), all angles must be expressed in radians.

Kepler's equation has attracted the attention of mathematicians for centuries. It is tractable when being used to calculate the time since periaxis given the orbit parameters. The historic interest, however, stems from attempts to deduce orbit parameters knowing the time since periaxis. Obtaining a solution in this direction is very difficult indeed. Many of the great mathematical minds of all time attempted to solve Kepler's equation—Newton, Euler, Gauss, Laplace, and Lagrange, to name a few. It is interesting to speculate as to how mathematics would have developed if Kepler's equation were trivial.

Orbital period. When $E = 2\pi$, Kepler's equation reduces to Kepler's third law, the relation for elliptical orbit period:

$$P = 2\pi/n \quad (2.37)$$

$$P = 2\pi\sqrt{a^3/\mu} \quad (2.38)$$

where P equals the orbital period in seconds. The orbital period for a circular orbit, given by Eq. (2.7), is a special case of Eq. (2.38), with $a = r$.

Example 2.5 Parameters at a Point

The elements of the Magellan mapping orbit about Venus are as follows:

$$a = 10,424.1 \text{ km}$$

$$e = 0.39433$$

The mapping pass is started at a true anomaly of 280 deg. What are the altitude, flight path angle, velocity, and time since periaxis at this point?

Calculate the radius by using Eq. (2.22)

$$r = \frac{10424.1[1 - (0.39433)^2]}{(1 + 0.39433 \cos 280 \text{ deg})} = 8239 \text{ km}$$

$$h = 8239 - 6052 = 2187 \text{ km}$$

Calculate the flight path angle by using Eq. (2.31):

$$\tan \gamma = \frac{0.39433 \sin 280 \text{ deg}}{1 + 0.39433 \cos 280 \text{ deg}}$$

$$\gamma = -19.97 \text{ deg}$$

Calculate the velocity by using Eq. (2.14):

$$V = \sqrt{\frac{2(324858.81)}{8239} - \frac{(324858.81)}{10424.1}} = 6.906 \text{ km/s}$$

Calculate the eccentric anomaly by using Eq. (2.35) (in preparation for calculation of time since periapsis):

$$\theta = 280 \text{ deg} = 4.8869 \text{ rad}$$

$$\cos E = \frac{0.39433 + \cos 4.8869}{1 + 0.39433 \cos 4.8869}$$

$$E = 1.01035 \text{ rad}$$

Calculate the mean motion by using Eq. (2.36):

$$n = \sqrt{\frac{324858.81}{(10424.1)^3}} = 0.0005355 \text{ s}^{-1}$$

Calculate the time since periapsis by using Eq. (2.34):

$$t = \frac{1.01035 - 0.39433 \sin 1.01035}{0.0005355} = 1263 \text{ s}$$

Recall that Eq. (2.34) gives the time since periapsis in the shortest direction. Since the true anomaly is greater than 180 deg, the result of Eq. (2.34) must be subtracted from orbit period. Calculate the orbit period by using Eq. (2.37),

$$P = 2\pi / 0.0005355 = 11,733 \text{ s}$$

The time at which the mapping starts, measured in the direction of flight, is

$$t = 11,733 - 1263 = 10,470 \text{ s or } 174.5 \text{ min}$$

Summary of Relations for Elliptical Orbits

There are myriad relations between the principle elements of elliptical orbits that can be derived algebraically from the foregoing definitions; many of these are tabulated in the work of Wood⁵ and elsewhere. The relations in Table 2.3 are an adequate working set.

2.4 Parabolic Orbits

A parabolic orbit would be achieved by an object falling from an infinite distance toward a central body. Such a fall essentially describes the motion of comets, and as a result, comets approach parabolic orbits. The process is reversible. If an object were propelled to the velocity for a parabolic orbit, it would just reach infinity.

A parabolic orbit, shown in Fig. 2.9, represents the boundary condition between an elliptic orbit and a hyperbolic orbit. A parabola can be considered an ellipse

TWO-BODY MOTION

19

Table 2.3 Relations defining an elliptical orbit

 Eccentricity e

$$e = \frac{c}{a} \quad (2.19) \quad e = \frac{r_a}{a} - 1 \quad (2.39)$$

$$e = \frac{(r_a - r_p)}{(r_a + r_p)} \quad (2.20) \quad e = 1 - \frac{r_p}{a} \quad (2.40)$$

$$e = \frac{r_2 - r_1}{r_1 \cos \theta_1 - r_2 \cos \theta_2} \quad (2.28)$$

 Flight path angle γ

$$\tan \gamma = \frac{e \sin \theta}{1 + e \cos \theta} \quad (2.31)$$

 Mean motion n

$$n = \sqrt{\mu/a^3} \quad (2.36)$$

 Period P

$$P = 2\pi/n \quad (2.37)$$

$$P = 2\pi \sqrt{a^3/\mu} \quad (2.38)$$

 Radius (general) r

$$r = \frac{a(1 - e^2)}{1 + e \cos \theta} \quad (2.22)$$

$$r = \frac{r_p(1 + e)}{1 + e \cos \theta} \quad (2.23)$$

 Radius of apoapsis r_a

$$r_a = a(1 + e) \quad (2.41)$$

$$r_a = 2a - r_p \quad (2.42)$$

$$r_a = r_p \frac{(1 + e)}{(1 - e)} \quad (2.43)$$

(continued)

SPACECRAFT MISSION DESIGN

Table 2.3 Relations defining an elliptical orbit (continued)

 Radius of periapsis r_p

$$r_p = a(1 - e) \quad (2.44)$$

$$r_p = r_a \frac{(1 - e)}{(1 + e)} \quad (2.45)$$

$$r_p = 2a - r_a \quad (2.46)$$

$$r_p = \frac{r_1(1 + e \cos \theta_1)}{1 + e} \quad (2.29)$$

 Semimajor axis a

$$a = \frac{(r_a + r_p)}{2} \quad (2.17)$$

$$a = \frac{\mu r}{2\mu - V^2 r} \quad (2.47)$$

$$a = \frac{r_p}{(1 - e)} \quad (2.48)$$

$$a = \frac{r_a}{(1 + e)} \quad (2.49)$$

 Time since periapsis t

$$t = (E - e \sin E)/n \quad (2.34)$$

$$\cos E = \frac{e + \cos \theta}{1 + e \cos \theta} \quad (2.35)$$

 True anomaly θ

$$\cos \theta = \frac{r_p(1 + e)}{re} - \frac{1}{e} \quad (2.24)$$

$$\cos \theta = \frac{a(1 - e^2)}{re} - \frac{1}{e} \quad (2.25)$$

 Velocity V

$$V = \sqrt{\frac{2\mu}{r} - \frac{\mu}{a}} \quad (2.14)$$

$$r_p V_p = r_a V_a \quad (2.33)$$

TWO-BODY MOTION

21

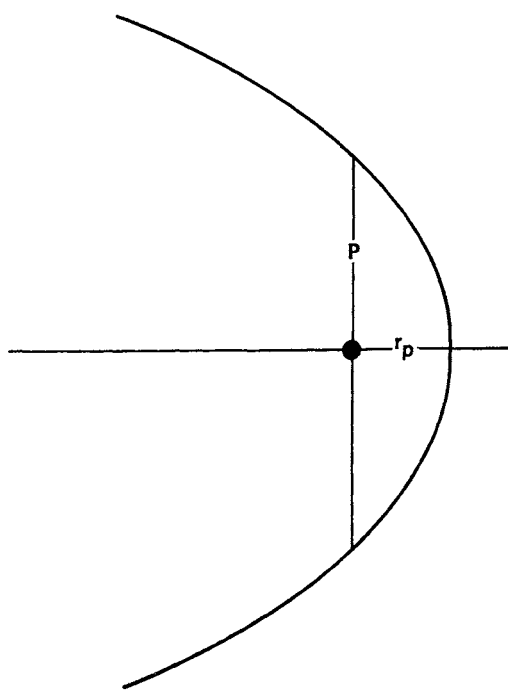


Fig. 2.9 Parabolic orbit.

with an infinite semimajor axis. The arms become parallel as r approaches infinity and when $e = 1$ and $a = \infty$. The velocity along a parabolic orbit is

$$V = \sqrt{2\mu/r} \quad (2.15)$$

Parabolic orbits are the least energetic open orbits. The velocity on a parabolic orbit is the minimum velocity needed for a spacecraft to escape the central body; i.e., parabolic velocity is the escape velocity. Note that the escape velocity is an inverse function of the square root of the radius; the greater the spacecraft altitude, the lower the escape velocity.

Example 2.6 Escape Velocity

What is the escape velocity from the surface of the moon?
For the moon, Appendix C gives

$$\mu = 4902.8 \text{ km}^3/\text{s}^2$$

$$R_0 = 1738 \text{ km}$$

From Eq. (2.15) the lunar escape velocity is

$$V = \sqrt{(2)(4902.8)/1738} = 2.375 \text{ km/s}$$

Parabolic orbits are an interesting boundary condition but not a useful spacecraft trajectory.

2.5 Hyperbolic Orbits

Hyperbolic orbits are used for Earth departure on planetary flights and for planetary arrival and targeting. Hyperbolic planetary flyby orbits are used for energetic gravity-assist maneuvers that change the direction and magnitude of spacecraft velocity without expending spacecraft resources. At any radius, a spacecraft on a hyperbolic orbit has a greater velocity than it would on a parabolic orbit; thus all hyperbolas are escape trajectories. Figure 2.10 shows the geometry of a hyperbolic trajectory. The orbital parameters are similar to those of an ellipse:

r_p = periapsis radius

a = semimajor axis, the distance from the center to the periapsis

b = semiminor axis, the distance from the asymptote to a parallel passing through the central body

e = eccentricity, c/a (greater than 1)

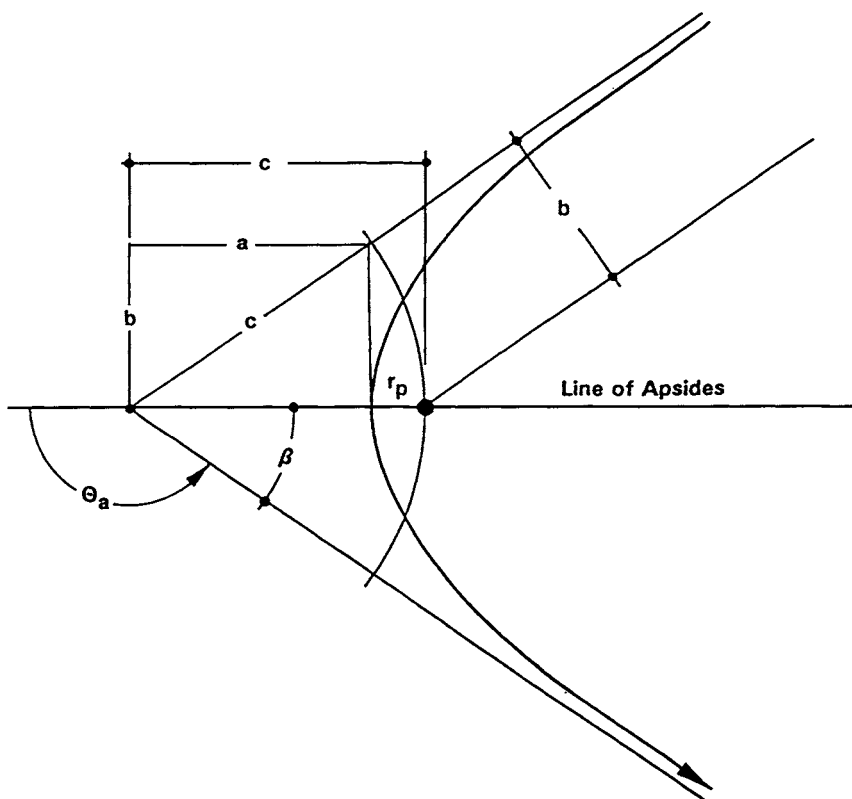


Fig. 2.10 Elements of hyperbola.

TWO-BODY MOTION

23

β = angle of the asymptote

θ_a = true anomaly of the asymptote

It is important to note that the semimajor axis of a hyperbola is considered negative; however, the equations in this book are adjusted to accept a positive semimajor axis.

As with an ellipse,

$$c^2 = a^2 + b^2 \quad (2.21)$$

$$e = c/a \quad (2.19)$$

The angle of the asymptote is

$$\cos \beta = 1/e \quad (2.50)$$

The position of a spacecraft on a hyperbolic orbit is defined by radius and true anomaly; in a manner similar to that for ellipses,

$$r = \frac{a(e^2 - 1)}{1 + e \cos \theta} \quad (2.51)$$

$$\cos \theta = a(e^2 - 1)/re - 1/e \quad (2.52)$$

The true anomaly of the asymptote θ_a is

$$\theta_a = 180 \text{ deg} \pm \beta \quad (2.53)$$

In the region between the minimum θ_a and the maximum θ_a , the hyperbolic radius is infinite. From Eq. (2.52), the true anomaly of the asymptote can also be expressed as

$$\cos \theta_a = -1/e \quad (2.54)$$

The flight path angle relation is the same as for an ellipse and is derived in the same way:

$$\tan \gamma = e \sin \theta / (1 + e \cos \theta) \quad (2.31)$$

The velocity at any point on a hyperbola is

$$V = \sqrt{(2\mu/r) + (\mu/a)} \quad (2.16)$$

The velocity on a hyperbolic trajectory is greater than the velocity on a parabola at any radius. The parabolic velocity goes to zero for an infinite radius; on a hyperbolic trajectory, the velocity at infinity is finite and equal to

$$V_\infty = \sqrt{\mu/a} \quad (2.55)$$

V_∞ is the velocity in excess of the escape velocity and is called the hyperbolic excess velocity (V_{HE}) when Earth escape is intended. For all situations other than

Earth escape, V_∞ is the preferable term. For the equations in this text, V_{HE} and V_∞ may be used interchangeably.

$$V_\infty = V_{\text{HE}} = \sqrt{\mu/a} \quad (2.56)$$

$$V = \sqrt{(2\mu/r) + V_{\text{HE}}^2} \quad (2.57)$$

V_{HE} is the velocity that must be added to the Earth's velocity to achieve departure on a planetary mission. It is traditional to express the energy required of a launch vehicle for a planetary mission as C3, which is the square of V_{HE} :

$$C3 = V_{\text{HE}}^2 \quad (2.58)$$

C3 is used to describe hyperbolic departure from Earth; it is not used to describe an arrival at a planet.

Example 2.7 Hyperbolic Earth Departure

The elements of the departure hyperbola of the Viking I Mars Lander were⁶

$$a = 18,849.7 \text{ km}$$

$$e = 1.3482$$

What C3 value was provided by the lander's Titan IIIE launch vehicle? From Eqs. (2.56) and (2.58),

$$C3 = V_{\text{HE}}^2 = \frac{398,600.4}{18,849.7} = 21.146 \text{ km}^2/\text{s}^2$$

The angle of the asymptote is given by Eq. (2.50) as

$$\cos \beta = 1/1.3482 = 0.7417$$

$$\beta = 42.12 \text{ deg}$$

Gravity-Assist Maneuvers

The angle through which a spacecraft velocity vector is turned by an encounter with a planet is $180 \text{ deg} - 2\beta$. This type of encounter is called a gravity-assist maneuver; it is a very energetic maneuver that can be accomplished without expending spacecraft resources.

The 1989 Galileo mission would not have been possible without multiple gravity-assist turns at Venus and Earth. Gravity-assist trajectories were also used by Voyager to target from one outer planet to the next at a substantial reduction in time of flight. The Ulysses mission, to take scientific data over the polar region of the sun, would not be possible in any year without a gravity turn out of the ecliptic. As shown in Fig. 2.11, Ulysses uses the gravitational attraction of Jupiter to bend its trajectory out of the ecliptic plane and send it on its way over the polar region of the sun. The design of this important maneuver will be discussed in Chapter 6.

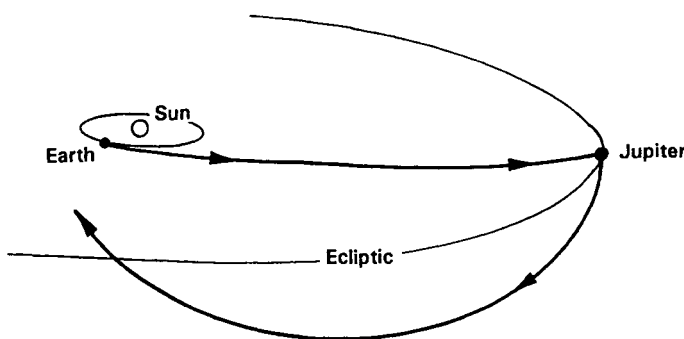


Fig. 2.11 Ulysses mission gravity-assist maneuver.

Time of Flight

The time since periaxis can be determined in a manner analogous to that for elliptical orbits with the aid of the hyperbolic eccentric anomaly F :

$$t = (e \sinh F - F)/n \quad (2.59)$$

$$\cosh F = (e + \cos \theta)/(1 + e \cos \theta) \quad (2.60)$$

where

t = time since periaxis passage, s

F = hyperbolic eccentric anomaly, rad

e = eccentricity

a = semimajor axis, km

θ = true anomaly

n = mean motion

This expression for F yields inaccurate results for e values near 1. See Ref. 3, page 191, for a universal variable solution for near-parabolic orbits.

The following hyperbolic relations are useful in solving for time:

$$F = \ln(\cosh F + \sqrt{\cosh^2 F - 1}) \quad (2.61)$$

$$\sinh F = \frac{1}{2}[\exp(F) - \exp(-F)] \quad (2.62)$$

Example 2.8 Time Since Periapsis—Hyperbola

On August 24, 1989, Voyager 2 flew past the north pole of Neptune.⁷ The elements of the Voyager 2 encounter hyperbola were:

$$a = 19,985 \text{ km}$$

$$e = 2.45859$$

During departure, Voyager 2 passed Triton, one of the moons of Neptune, at a radius of 354,600 km. What was the time since periaxis for the encounter with Triton?

Calculate the mean motion by using Eq. (2.25):

$$n = \sqrt{\frac{6,871,307.8}{(19,985)^3}} = 0.0009278 \text{ s}^{-1}$$

Calculate the cosine of the true anomaly by using Eq. (2.52):

$$\cos \theta = \frac{19,985[(2.45859)^2 - 1]}{(354,600)(2.45859)} - \frac{1}{2.45859} = -0.2911$$

From Eq. (2.60)

$$\cosh F = \frac{2.45859 - 0.2911}{1 + (2.45859)(-0.291096)} = 7.6236$$

From Eq. (2.61)

$$F = \ln [7.326 + \sqrt{(7.6236)^2 - 1}] = 2.720$$

From Eq. (2.62),

$$\sinh F = \frac{1}{2}[\exp(2.720) - \exp(-2.720)] = 7.5577$$

Finally, calculate time since periapsis by using Eq. (2.59):

$$t = \frac{(2.45859)(7.5577) - 2.720}{0.0009278} = 17095 \text{ s or } 4.75 \text{ h}$$

Summary of Relations Defining a Hyperbolic Orbit

Additional relations for hyperbolic orbits can be found by algebraic manipulation or on page 201 of Ref. 5 and elsewhere. Table 2.4 summarizes the most frequently used equations. The equations in Table 2.4 have been arranged to accept semimajor axis as a positive number. V_{HE} denotes an Earth-centered hyperbola; V_{∞} is the general case. V_{∞} and V_{HE} are used interchangeably in Table 2.4.

2.6 Time Systems

Mission design calculations, especially ephemeris calculations, require a more precise definition of how time is measured and of the relationship between time and planetary position. Five different time measurement systems must be understood.

Apparent Solar Time

The most ancient measure of time is the apparent solar day. It is the time interval between two successive solar transits across a local meridian, i.e., two successive high noons. Two motions are involved in this definition; the rotation of the Earth about its axis and the revolution of the Earth about the sun, as shown in Fig. 2.12. The apparent solar day can be measured by a sundial and was an adequate standard for thousands of years.

TWO-BODY MOTION

27

Table 2.4 Relations defining a hyperbolic orbit

Angle of asymptote β			
$\tan \beta = b/a$	(2.63)	$\tan \beta = b V_{\text{HE}}^2 / \mu$	(2.64)
$\tan \beta = \frac{2br_p}{b^2 - r_p^2}$	(2.65)	$\cos \beta = 1/e$	(2.50)
Eccentricity e			
$e = 1/\cos \beta$	(2.66)	$e = 1 + (r_p/a)$	(2.67)
$e = \sqrt{1 + (b^2/a^2)}$			
Flight path angle γ			
$\tan \gamma = \frac{e \sin \theta}{1 + e \cos \theta}$			
Mean motion n			
$n = \sqrt{\mu/a^3}$			
Radius (general) r			
$r = a(e^2 - 1)/(1 + e \cos \theta)$			
Radius of periapsis r_p			
$r_p = b\sqrt{(e-1)/(e+1)}$	(2.69)	$r_p = a(e-1)$	(2.70)
$r_p = c - a$	(2.71)	$r_p = b \tan(\beta/2)$	(2.72)
$r_p = \frac{2\mu + \mu(e-1)}{V_p^2}$	(2.73)	$r_p = -\frac{\mu}{V_{\text{HE}}^2} + \sqrt{\left(\frac{\mu}{V_{\text{HE}}^2}\right)^2 + b^2}$	(2.74)
$r_p = -a + \sqrt{a^2 + b^2}$			

(continued)

Table 2.4 Relations defining a hyperbolic orbit (continued)Semimajor axis a

$$a = b/\sqrt{e^2 - 1} \quad (2.76)$$

$$a = r_p/(e - 1) \quad (2.77)$$

$$a = \mu/V_{\text{HE}}^2 \quad (2.78)$$

$$a = (b^2 - r_p^2)/2r_p \quad (2.79)$$

$$a = \frac{\mu r_p}{r_p V_p^2 - 2\mu} \quad (2.80)$$

Semiminor axis b

$$b = r_p \sqrt{(e + 1)/(e - 1)} \quad (2.81)$$

$$b = a\sqrt{e^2 - 1} \quad (2.82)$$

$$b = r_p \sqrt{(2\mu/r_p V_{\text{HE}}^2) + 1} \quad (2.83)$$

Time since periapsis t

$$t = (e \sinh F - F)/n \quad (2.59)$$

$$\cosh F = \frac{(e + \cos \theta)}{(1 + e \cos \theta)} \quad (2.60)$$

$$F = \ell_n (\cosh F + \sqrt{\cosh^2 F - 1}) \quad (2.61)$$

$$\sinh F = \frac{1}{2} [\exp(F) - \exp(-F)] \quad (2.62)$$

True anomaly θ

$$\cos \theta = \frac{a(e^2 - 1)}{re} - \frac{1}{e} \quad (2.52)$$

True anomaly of asymptote θ_a

$$\theta_a = 180 \text{ deg} \pm \beta \quad (2.53)$$

$$\cos \theta_a = -\frac{1}{e} \quad (2.54)$$

Velocity V

$$V_\infty = V_{\text{HE}} = \sqrt{\mu/a} \quad (2.56) \quad V = \sqrt{(2\mu/r) + V_{\text{HE}}^2} \quad (2.57)$$

$$V = \sqrt{(2\mu/r) + (\mu/a)} \quad (2.16) \quad C3 = V_{\text{HE}}^2 \quad (2.58)$$

TWO-BODY MOTION

29

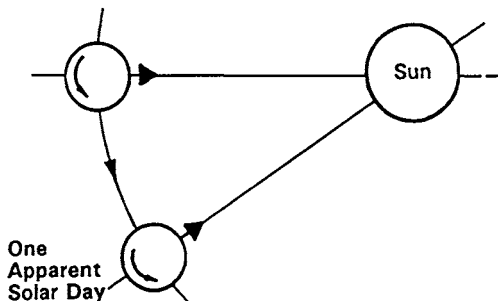


Fig. 2.12 Apparent solar day.

Mean Solar Time

One of the problems with apparent solar time is that the days are all of different lengths. This variation occurs because the Earth's axis is not perpendicular to the ecliptic plane, the Earth's orbit is not circular, and the Earth's axis wobbles slightly with respect to the ecliptic plane. These effects are all small, regular, and predictable; therefore, it is possible to establish a mean solar day that has an invariant length. A mean solar day is defined based on the assumptions that the Earth is in a circular orbit with period exactly equal to the actual period of the Earth's orbit and that the Earth's axis is perpendicular to the ecliptic plane. The mean solar day is the common time standard; it is the time you read from your watch. Seconds, minutes, and hours are defined in duration by dividing a mean solar day into equal parts. A mean solar day is equal to exactly 24 h, or 1440 min, or 86,400 s.

Sidereal Time

For some purposes, notably astronomy, it is necessary to measure time with respect to the fixed stars rather than the solar zenith. A mean sidereal day is the mean time required for the Earth to rotate once on its axis with respect to fixed stars, or with respect to inertial space. A mean sidereal day is slightly shorter than a mean solar day, as shown in Fig. 2.13. A sidereal day is subdivided into sidereal hours, minutes, and seconds just as a solar day is; however, the lengths are slightly different:

$$\begin{aligned} 1 \text{ mean solar day} &= 1.0027379093 \text{ mean sidereal days}^8 \\ &= 24 \text{ h}, 3 \text{ min}, 56.5536 \text{ s of sidereal time} \\ &= 86,636.55536 \text{ sidereal seconds} \\ &= 86,400.00000 \text{ mean solar seconds} \end{aligned}$$

$$1 \text{ mean sidereal day} = 86,164.091 \text{ mean solar seconds}$$

Time Zones and Universal Time

Another problem with solar time is that the time of day is different at every longitude on Earth. Up until the mid-1800s every town in the United States set its

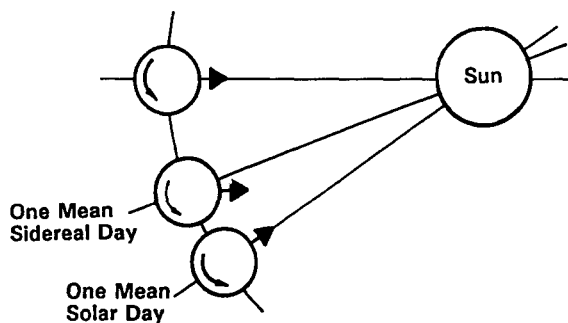


Fig. 2.13 Mean sidereal day. (From Ref. 3, p. 102; reproduced courtesy of Dover Publications, Inc.)

clock by local high noon. The advent of railroads changed all that. To operate a train schedule it was necessary to standardize time. The Earth is now subdivided into 24 standard time zones, each encompassing approximately 15° of longitude. Greenwich, England, is the index mark for time zones. The mean solar time at Greenwich is called Universal time (UT). (Greenwich mean time, an early standard used prior to 1925, was similar to universal time except that a new day was started at noon rather than at midnight.) Table 2.5 shows the conversion of universal time to local mean solar times for the United States. Interestingly enough, universal time is computed from solar motion in mean sidereal time and then converted to mean solar time. Universal time is expressed by the 24-h clock method; i.e., 4 p.m. is stated as 16:00.

Julian Days

The Julian day system is a means of providing a unique number to all days that have elapsed since a standard reference day in the distant past. The day selected for the starting point of the system is January 1, 4713 B.C. The days are in mean solar measure. The Julian day (JD) numbers are never repeated and are not partitioned

Table 2.5 Conversion of UT to local time

Eastern Standard Time	(EST)	+	5 h	=	UT
Eastern Daylight Time	(EDT)	+	4 h	=	UT
Central Standard Time	(CST)	+	6 h	=	UT
Central Daylight Time	(CDT)	+	5 h	=	UT
Mountain Standard Time (MST)		+	7 h	=	UT
Mountain Daylight Time (MDT)		+	6 h	=	UT
Pacific Standard Time	(PST)	+	8 h	=	UT
Pacific Daylight Time	(PDT)	+	7 h	=	UT

TWO-BODY MOTION

31

into weeks or months. As a result, the number of days between two dates may be obtained by subtracting Julian day numbers.

There are 36,525 mean solar days in a Julian century and 86,400 s in a day. The Julian century does not refer to some time system; it is merely a count of a fixed number of days. Ephemeris calculations are done in Julian days and Julian centuries.

This curious system was devised by Joseph Scaliger in 1582 to provide a calendar suitable for recording astronomical observations.⁹ The starting date was selected because it is the starting point of three cycles: the 28-year solar cycle, the 19-year lunar cycle, and the 15-year tax cycle in use at the time. In spite of the general inconvenience of the system, it is still, four centuries later, the only generally recognized system of unique day numbers.

A Julian day starts at noon UT rather than at midnight, an astronomical custom; astronomers find it disconcerting for the day number to change in the middle of a night's observations. This custom has a curious effect on the conversion of Julian days to equivalent Gregorian calendar (the common calendar) days, as shown in Fig. 2.14. Julian dates may be calculated from calendar dates using Eq. (2.84), adapted from a remarkably compact relation devised by Thomas C. Van Flandern (see Ref. 10). The result is accurate for dates between 1901 A.D. and 2099 A.D.

$$J = 367Y - 7 \left[\frac{Y + (M + 9)/12}{4} \right] + \frac{275M}{9} + D + 1,721,013.5 \quad (2.84)$$

where

J = Julian day number

Y = calendar year

M = calendar month number (e.g., July = 7)

D = calendar day and fraction

All divisions must be integer divisions. Only the integer is kept; the fraction is discarded.

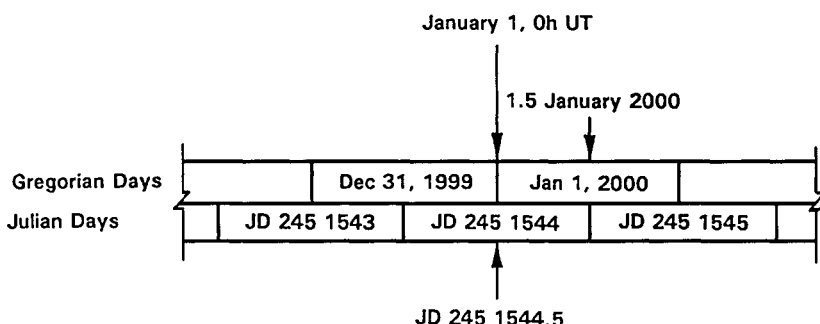


Fig. 2.14 Conversion of Gregorian days to Julian days.

Example 2.9 Conversion to Julian Days

What is the number of the Julian day that starts at noon UT on January 1, 2000? That is, find the Julian day for

$$M = 1$$

$$Y = 2000$$

$$D = 1.5$$

From Eq. (2.84),

$$J = 367(2000) - 7\{[2000 + (1 + 9)/12]/4\} + 275(1)/9 + 1.5 + 1,721,013.5$$

$$J = 734,000 - 3500 + 30 + 1.5 + 1,721,013.5 = 2,451,545$$

2.7 Coordinate Systems

Four types of coordinate systems are common in mission design work: 1) the geocentric-inertial system, 2) the heliocentric-inertial system, 3) the geographic-body-fixed system, and 4) the International Astronomical Union (IAU) cartographic system (for the planets). The systems are designed to make various types of motion easy to visualize; selection of the proper coordinate system has a profound effect on the difficulty of a given type of problem. Each system is defined by the selection of the origin, selection of axes, and the determination of what is fixed.

A body-fixed coordinate system measures all motion relative to that body with the assumption that the body is stationary. Our daily experience is in body-fixed coordinates where the sun appears to rise in the east and set in the west. An inertially fixed coordinate system is one which is referenced to stellar positions. The vernal equinox vector is the primary reference in such systems.

Vernal Equinox

There are two equinoxes in a year, one in the spring and one in the fall. On these days the Earth is located at the intersection line of the equatorial and ecliptic planes. The axis of rotation of the Earth is in a plane perpendicular to the sun's rays; as a result the length of the day and night is the same everywhere on Earth. As shown in Fig. 2.15, the vernal equinox vector is the vector from the center of mass of the Earth to the center of mass of the sun on the spring (northern hemisphere) equinox day, which occurs around March 21.

The vernal equinox was first observed more than 5000 years ago; at that time the vector passed through Aries (a constellation in the zodiac also called the Ram). The sign of the Ram, Γ , is used to this day to indicate the vernal equinox; however, over the years the vector has moved through Aries and into Pisces (the Fishes).¹¹ This small precession of the equinoxes, about 0.014 deg per year, does not prevent consideration of the vector as fixed for most purposes; however, this precession and the motion of the ecliptic plane are important for ephemeris calculations. Ephemeris tabulations are noted to indicate the instant of time that defines the exact position of the reference axes.

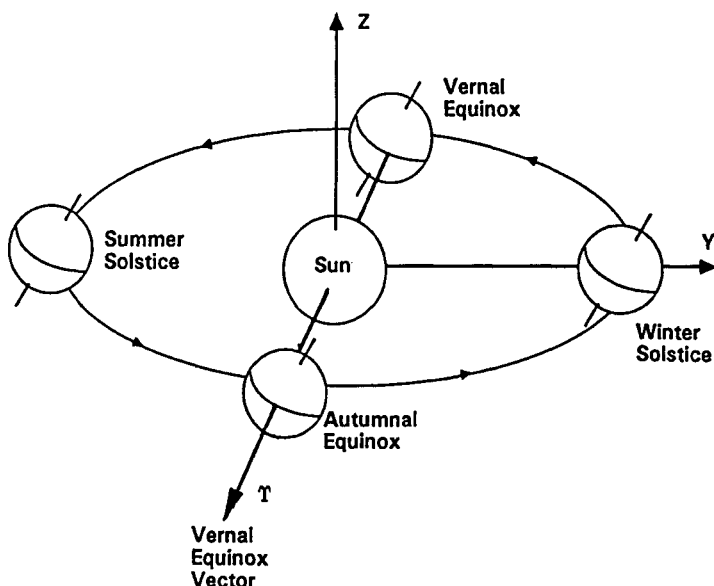


Fig. 2.15 Vernal equinox. (From Ref. 3, p. 54; reproduced courtesy of Dover Publications, Inc.)

Geocentric-Inertial Coordinate System

For most orbital calculations the coordinate system of choice is the geocentric-inertial system, shown in Fig. 2.16. The origin for the geocentric system is the center of mass of the central body, which is usually, but not necessarily, the Earth. The equatorial plane (the plane of the Earth's equator) is the reference plane. The X axis is the vernal equinox vector, and the Z axis is the spin axis of the Earth; north is positive. The axes are fixed in inertial space or fixed with respect to the stars.

Positions are measured by latitude and longitude; longitudes are measured eastward (i.e., counterclockwise as viewed from celestial north) from the vernal equinox vector and centered in the Earth. North latitudes are measured in the positive Z direction from the equatorial plane, and south latitudes are measured in a negative Z direction.

Heliocentric-Inertial System

The heliocentric-inertial system is used for interplanetary mission design. The ecliptic plane, the plane that contains the center of mass of the sun and the orbit of the Earth, is the reference plane for the heliocentric system. The system is identical to the geocentric-inertial system shown in Fig. 2.16 except for the reference plane and the central body. The origin for the system is centered in the sun, and the system is fixed with respect to the stars. The equatorial plane is inclined at an angle of approximately 23.5 deg with respect to the ecliptic. The X axis for the heliocentric system is the vernal equinox vector, which is common to the ecliptic

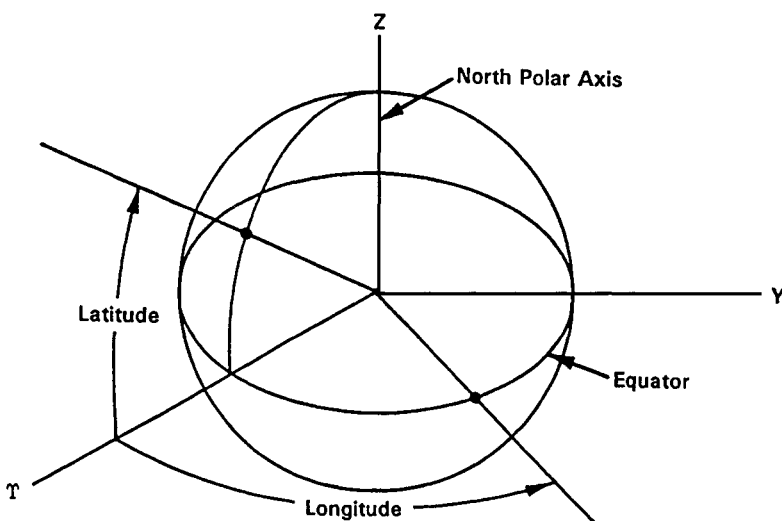


Fig. 2.16 Geocentric-inertial coordinate system.

plane and the equatorial plane. The Z axis is perpendicular to the ecliptic; positive is north. Latitude and longitude are measured as in the geocentric system.

Geographic-Body-Fixed Coordinate System

The geographic-body-fixed coordinate system, shown in Fig. 2.17, has been used for centuries to locate and map positions on the Earth. The system is Earth-centered and body-fixed; the surface of the Earth is divided into a grid of latitude and longitude measured in degrees. Spacecraft ground track is commonly plotted in this coordinate system.

Longitude is a spherical angle measured around the polar axis, starting at the prime meridian. The prime meridian is the great circle passing through Greenwich, England, and the Earth's poles. Longitude is measured in degrees east or west from the prime meridian (the highest longitude being 180°). The longitude of New York is approximately 75° W. Both east and west longitudes are positive.

Latitude is a spherical angle measured around the center of the Earth starting from 0° at the equator. Latitude is measured north or south of the equator with the highest latitude being 90° . Both north and south latitudes are positive. Philadelphia and Denver are at approximately 40° N.

The geographic system is most frequently mapped as a Mercator projection, which projects an Earth map on a cylinder wrapped around the equator.

International Astronomical Union Cartographic Coordinates

The International Astronomical Union (IAU) cartographic system is a body-centered, body-fixed system for mapping solar system bodies. International agreement has been established by the IAU on the placement of the north polar axis, the

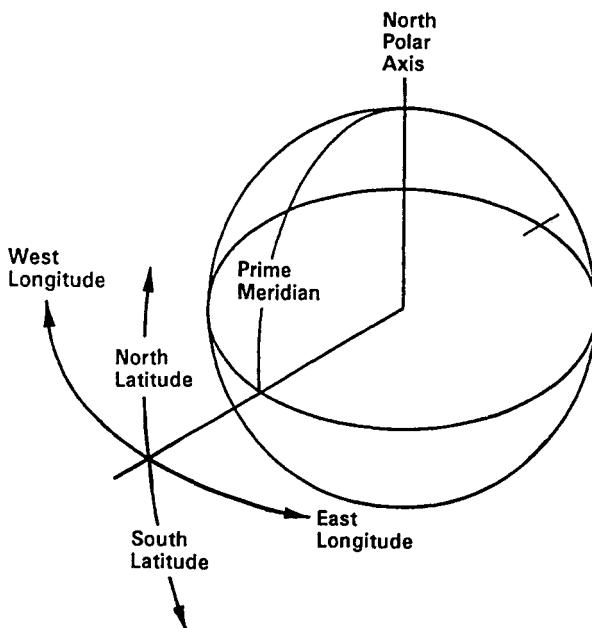


Fig. 2.17 Geographic-body-fixed coordinate system.

equatorial plane, and the prime meridian for the planets and their satellites.¹² The north pole is placed in the northern celestial hemisphere regardless of the direction of rotation of the body. Parameters specifying the orientation of the north pole and the location of the prime meridian vary slowly with time and can be obtained from Ref. 12.

Longitudes are reckoned in an eastward direction from the prime meridian, i.e., in a counterclockwise direction as viewed from the north pole. Unlike the geographic system, longitudes increase from 0° to 360° ; latitudes north of the equator are positive, and southern latitudes are negative.

2.8 Classical Orbital Elements

There are a number of independent parameters describing the size, shape, and spatial position of an orbit. Six of these have become the parameters of choice to define and describe an orbit. These six parameters (see Fig. 2.18) are called the classical orbital elements:

e = Eccentricity: the ratio of minor to major dimensions of an orbit defines the shape.

a = Semimajor axis: The orbit size is defined by one half of the major axis dimension. (Circular orbits are defined by radius.)

i = Inclination: the angle between the orbit plane and the reference plane or the angle between the normals to the two planes.

ω = Argument of periapsis: the angle from the ascending node to the periapsis, measured in the orbital plane in the direction of spacecraft motion. The *ascending*

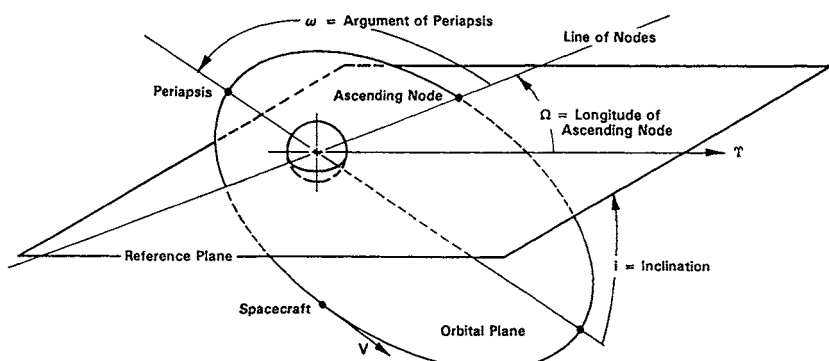


Fig. 2.18 Classical orbital elements.

node is the point where the spacecraft crosses the reference plane headed from south to north. The *line of nodes* is the line formed by the intersection of the orbit plane and the reference plane. The ascending node and the descending node are on this line.

Ω = Longitude of the ascending node: the angle between the vernal equinox vector and the ascending node measured in the reference plane in a counterclockwise direction as viewed from the northern hemisphere.

Θ = True anomaly: the sixth element locates the spacecraft position on the orbit. (Time since periapsis is also used as this orbital element.³⁾

For orbits about the Earth or planets, the elements are located with respect to the geocentric system. For interplanetary orbits the elements are given with respect to the heliocentric system. The coordinate system, the orbital elements, and the orbit itself are fixed in inertial space and do not rotate with the central body.

Problems

2.1 An Earth satellite is in an orbit with a perigee altitude of 400 km and an eccentricity of 0.6. Find

- the perigee velocity
- the apogee radius
- the apogee velocity
- the orbit period
- the satellite velocity when its altitude is 3622 km
- the true anomaly at altitude 3622 km
- the flight path angle at altitude 3622 km

2.2 The LANDSAT C Earth resources satellite is in a near-polar, near-circular orbit with a perigee altitude of 917 km, an eccentricity of 0.00132, and an inclination of 89.1 deg. What are the apogee altitude, the orbit period, and the perigee velocity?

TWO-BODY MOTION

37

2.3 Two radar fixes on an unidentified Earth orbiter yield the following positions:

Altitude = 1545 km at a true anomaly of 126 deg

Altitude = 852 km at a true anomaly of 58 deg

What are the eccentricity, altitude of perigee, and semimajor axis of the spacecraft orbit?

2.4 What is the escape velocity from a geosynchronous orbit, $r = 42163$ km? What velocity increase would be required for a geosynchronous satellite to escape?

2.5 The Magellan spacecraft was placed in an elliptical orbit around Venus with a periapsis altitude of 250 km and a period of 3.1 h. What is the apoapsis altitude?

2.6 Consider an elliptical Earth orbit with a semimajor axis of 12,500 km and an eccentricity of 0.472. What is the time from periapsis passage to a position with a true anomaly of 198 deg?

2.7 A spacecraft is approaching Venus with $V_\infty = 10$ km/s and $b = 10,000$ km. What will be the periapsis radius at Venus?

2.8 A hyperbolic Earth departure trajectory has a periapsis velocity of 15 km/s at an altitude of 300 km. Find

- (a) the hyperbolic excess velocity
- (b) the radius when the true anomaly is 100 deg
- (c) the velocity when the true anomaly is 100 deg
- (d) the time from periapsis to a true anomaly of 100 deg

2.9 Voyager I's closest approach to Saturn was at a periapsis radius of 124,000 km; the hyperbolic excess velocity was 7.51 km/s. What was the angle through which the spacecraft velocity vector was turned by Saturn?

This page intentionally left blank

3

Orbital Maneuvers

Orbital maneuvering is based on the fundamental principle that an orbit is uniquely determined by the position and velocity at any point. Conversely, changing the velocity vector at any point instantly transforms the trajectory to correspond to the new velocity vector. For example, to change from a circular orbit to an elliptical orbit, the spacecraft velocity must be increased to that of an elliptic orbit, as shown in Fig. 3.1.

In Fig. 3.1,

$$V(\text{circle}) + \Delta V = V(\text{ellipse}) \quad (3.1)$$

3.1 In-Plane Orbit Changes

Any conic orbit can be converted to any other conic orbit by adjusting velocity; a spacecraft travels on the trajectory defined by its velocity at a point. Circular trajectories can be converted to ellipses, ellipses can be changed in eccentricity, and circles or ellipses can be changed to hyperbolas—all by adjusting velocity.

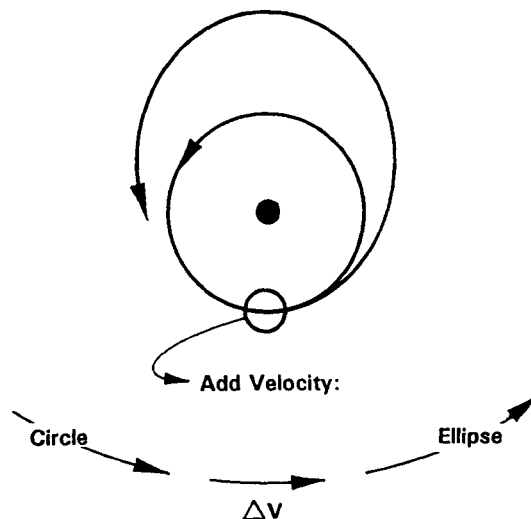


Fig. 3.1 Changing a circular orbit to an elliptical orbit.

Example 3.1 Simple Coplanar Orbit Change

Consider an initial circular, low Earth orbit at a 300-km altitude. What velocity increase would be required to produce an elliptical orbit with a 300-km altitude at periapsis and a 3000-km altitude at apoapsis?

The velocity on the initial circular orbit is, from Eq. (2.6),

$$V = \sqrt{\frac{398,600.4}{(300 + 6378.14)}} = 7.726 \text{ km/s}$$

The semimajor axis on the final orbit is, from Eq. (2.17),

$$a = \frac{(300 + 6378.14) + (3000 + 6378.14)}{2} = 8028.14 \text{ km}$$

The velocity at periapsis is, from Eq. (2.14),

$$V = \sqrt{\frac{2(398,600.4)}{6678.14}} - \frac{398,600.4}{8028.14} = 8.350 \text{ km/s}$$

The velocity increase required to convert the initial circular orbit to the final elliptical orbit is $8.350 - 7.726 = 0.624 \text{ km/s}$. The velocity should be increased at the point of desired periapsis placement. Table 3.1 shows the results of various velocity changes from an initial 300-km Earth orbit. In Table 3.1 it is assumed that the magnitude of velocity is changed without changing the direction. The radius at the point at which the velocity is changed remains unchanged. Velocity changes made at the periapsis change the apoapsis radius but not the periapsis radius, and vice versa. As would be expected, the plane of orbit in inertial space does not change as velocity along the orbit is changed. Orbital changes are a reversible process.

Finite Burn Losses

Up to this point it has been assumed that velocity is changed at a point on the trajectory, i.e., that a velocity change is instantaneous. If this assumption is not valid, serious energy losses can occur; these losses are called finite burn losses. Figure 3.2 shows a situation where finite burn losses are significant. The case illustrated in this figure is for a Venus orbit insertion burn using relatively small rocket engines. As shown in Fig. 3.2 the finite burn losses could exceed 20%, or 700 m/s, in this case. This example is not general; each suspect situation requires

Table 3.1 Effect of velocity change

ΔV , km/s	Impulse location	Resulting trajectory
0.624	Periapsis	Ellipse: $h_p = 300 \text{ km}$, $h_a = 3000 \text{ km}$
-0.029	Apoapsis	Ellipse: $h_p = 200 \text{ km}$, $h_a = 300 \text{ km}$
3.200	Periapsis	Parabola: $h_p = 300 \text{ km}$, $e = 1.0$
4.490	Periapsis	Hyperbola: $h_p = 300 \text{ km}$, $e = 1.5$

ORBITAL MANEUVERS

41

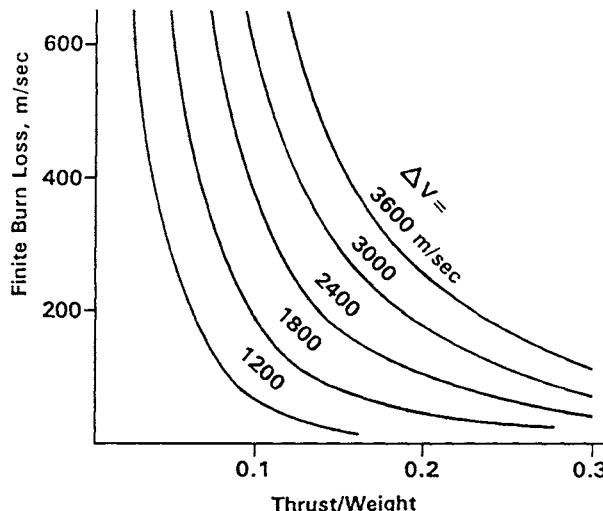


Fig. 3.2 Finite burn losses.

a numerical integration to evaluate. Low thrust-to-weight ratios cause finite burn loss and should thus be avoided; situations where thrust-to-weight ratio is less than about 0.5 should be analyzed by numerical integration.

General Coplanar Maneuver

Figure 3.3 shows the general coplanar maneuver, which changes the initial orbit velocity V_i to an intersecting coplanar orbit with velocity V_f . The velocity on the final orbit is equal to the vector sum of the initial velocity and the velocity change vector. Applying the cosine law,

$$\Delta V^2 = V_i^2 + V_f^2 - 2V_i V_f \cos \alpha \quad (3.2)$$

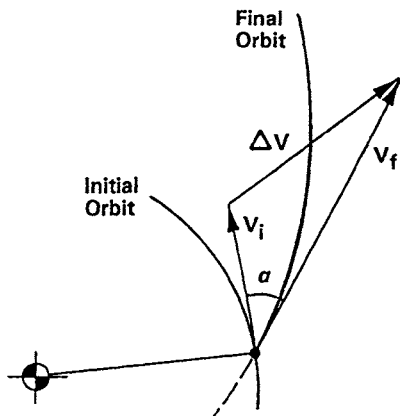


Fig 3.3 Generalized coplanar maneuver.

where

- ΔV = the velocity added to a spacecraft initial velocity to change from the initial orbit to the final orbit; ΔV can be either positive or negative
- V_i = the velocity on the initial orbit at the point of intersection of the two orbits
- V_f = the velocity on the final orbit at the point of intersection of the two orbits
- α = the angle between vectors V_i and V_f

The transfer can be made at any intersection of two orbits. Note that the necessary velocity change is lowest when the orbits are tangent and $\alpha = 0$.

Example 3.2 General Coplanar

Referring to Fig. 3.3, consider an initial direct, circular Earth orbit of radius 9100 km and a final direct, coplanar, elliptical orbit with $e = 0.1$ and $r_p = 9000$ km. What velocity change is required to make the transfer?

The velocity on the initial orbit is, from Eq. (2.6),

$$V = \sqrt{\frac{398,600.4}{9100}} = 6.618 \text{ km/s}$$

For the final orbit, the semimajor axis is, from Eq. (2.50),

$$a = 9000/(1 - 0.1) = 10,000 \text{ km}$$

The velocity at the point of intersection is, from Eq. (2.14),

$$V = \sqrt{\frac{2(398,600.4)}{9100} - \frac{398,600.4}{10,000}} = 6.910 \text{ km/s}$$

The true anomaly on the final orbit (at the intersection points) is, from Eq. (2.24),

$$\cos \Theta = \frac{9000 (1.1)}{9100 (0.1)} - \frac{1}{0.1}$$

$$\Theta = 28.464 \text{ deg and } 331.536 \text{ deg}$$

The flight path angle on the final orbit (at the intersection points) is, from Eq. (2.31),

$$\tan \gamma = \frac{(0.1) \sin(28.464)}{1 + (0.1) \cos(28.464)}$$

$$\gamma = 2.508 \text{ deg and } -2.508 \text{ deg}$$

At either of the intercept points, the velocity change necessary to convert from the initial to the final orbit is, from Eq. (3.2),

$$\Delta V^2 = (6.618)^2 + (6.910)^2 - 2(6.618)(6.910) \cos(2.508)$$

$$\Delta V = 0.4158 \text{ km/s}$$

3.2 Hohmann Transfer

Suppose you need to transfer between two nonintersecting orbits; how can you do it? The Hohmann transfer, shown in Fig. 3.4, answers this need in a most efficient way. The Hohmann transfer, devised by Walter Hohmann in 1925, employs an elliptical transfer orbit that is tangent to the initial and final orbits at the apsides.¹³

To design a Hohmann transfer between two circular, coplanar orbits, set the periapsis radius of the transfer ellipse equal to the radius of the initial orbit, and set the apoapsis radius equal to the radius of the final orbit:

$$r_{pt} = r_i \quad (3.3)$$

$$r_{at} = r_f \quad (3.4)$$

With these two radii set, the transfer ellipse is defined.

There are two velocity increments required to accomplish the transfer. One increment changes the initial velocity of the spacecraft to the velocity needed on the transfer ellipse, and a second increment changes from the velocity needed on the transfer ellipse to the velocity needed on the final orbit:

$$\Delta V_1 = V_{pt} - V_i \quad (3.5)$$

$$\Delta V_2 = V_{at} - V_f \quad (3.6)$$

where

V_{pt} = the periapsis velocity on the transfer ellipse

V_{at} = the apoapsis velocity on the transfer ellipse

V_i = the spacecraft velocity on the initial orbit

V_f = the spacecraft velocity on the final orbit

A transfer between two circular orbits is shown in Fig. 3.4, but the transfer could

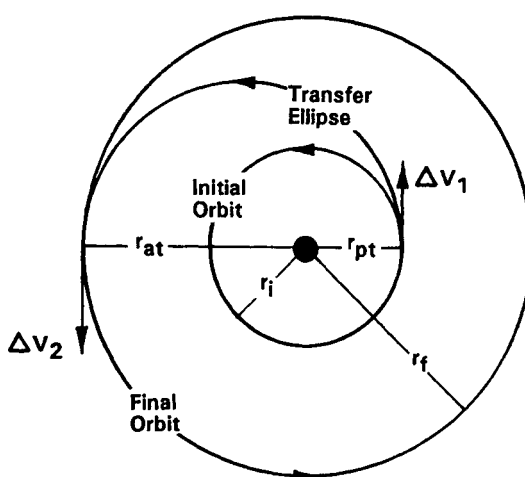


Fig. 3.4 Hohmann transfer.

as well have been between elliptical orbits. Similarly, the transfer could have been from a high orbit to a low orbit.

Example 3.3 Hohmann Transfer

Design a Hohmann transfer from a circular Mars orbit of radius 8000 km to a circular Mars orbit of radius 15,000 km.

From Appendix C for Mars,

$$\mu = 42,828.3 \text{ km}^3/\text{s}^2$$

The velocity on the initial orbit is, from Eq. (2.6),

$$V = \sqrt{\frac{42,828.3}{8000}} = 2.314 \text{ km/s}$$

Similarly, the velocity on the final orbit is found to be 1.690 km/s.

The semimajor axis of the transfer ellipse is, from Eq. (2.17),

$$a = (8000 + 15,000)/2 = 11,500 \text{ km}$$

The velocity at periaxis of the transfer ellipse is, from Eq. (2.14),

$$V_p = \sqrt{\frac{2(42,828.3)}{8000} - \frac{42,828.3}{11,500}} = 2.642 \text{ km/s}$$

Similarly the velocity at apoaxis is

$$V_a = \sqrt{\frac{2(42,828.3)}{15,000} - \frac{42,828.3}{11,500}} = 1.409 \text{ km/s}$$

There is another, possibly easier way to calculate the velocity at apoaxis by using Eq. (2.32):

$$V_a = \frac{(8000)(2.642)}{15,000} = 1.409 \text{ km/s}$$

The velocity change required to enter the transfer orbit is found by using Eq. (3.5):

$$\Delta V_1 = 2.642 - 2.314 = 0.328 \text{ km/s}$$

Similarly from Eq. (3.6), the velocity change to “circularize” is 0.281 km/s, and the total velocity change for the transfer is 0.609 km/s.

The time required to make the transfer is one half the period of the transfer ellipse, or from Eq. (2.38),

$$P = 2\pi \sqrt{\frac{(11,500)^3}{42,828.3}} = 37,442 \text{ s}$$

The time for transfer is 18,271 s, or about 5.2 h.

The efficiency of the Hohmann transfer stems from the fact that the two velocity changes are made at points of tangency between the trajectories; therefore, only the magnitude of the velocity is changed without the energy losses associated with a change in direction.

3.3 Bielliptical Transfer

In cases where a transfer is being made from an initial orbit to a final orbit with much greater radius, it may be more efficient in terms of energy to use a bielliptical transfer.

As shown in Fig. 3.5, the bielliptic is a three-impulse transfer. The first impulse converts the initial orbit to the first transfer ellipse. The second impulse establishes the second transfer orbit. The second transfer ellipse has a periapsis radius equal to that of the final orbit. The apoapsis radius is much larger than the final orbit radius and is a design variable. (It can be shown that an infinite apoapsis is the most efficient but least practical approach.) Chobotov has shown that for transfers where the final orbit radius is more than 15.58 times the initial radius, the bielliptical transfer is more efficient than the Hohmann transfer.¹⁴ However, the energy savings is 8% or less, and the maneuver requires more velocity changes. The bielliptical transfer offers an excellent opportunity for a low-energy plane change at the apoapsis of the transfer ellipses (the ΔV_2 point in Fig. 3.5).

3.4 Plane Changes

So far only in-plane changes to orbits have been considered. What happens when a spacecraft must change orbit planes to accomplish its mission? Such a change is accomplished by applying an out-of-plane impulse at the intersection of the initial and final orbit planes, as shown in Fig. 3.6. By inspection of Fig. 3.6, or from the law of cosines,

$$\Delta V = 2V_i \sin(\alpha/2) \quad (3.7)$$

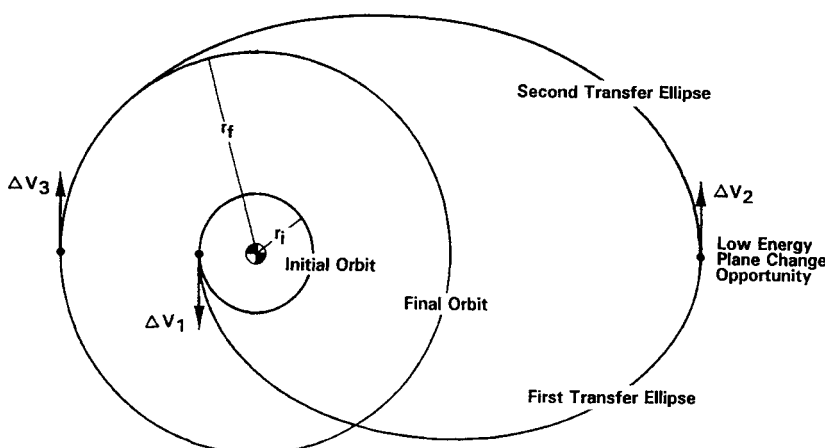


Fig. 3.5 Bielliptical transfer.

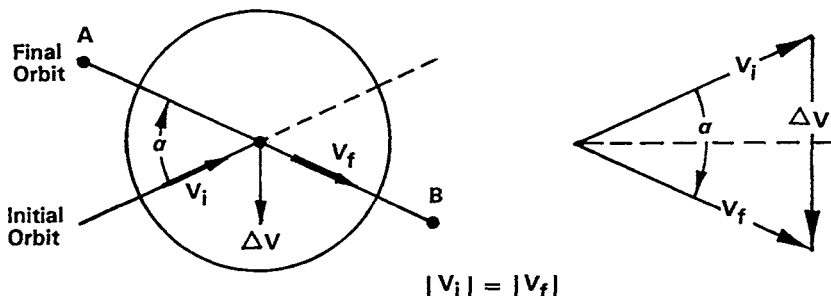


Fig. 3.6 Plane change maneuver.

where

ΔV = the velocity change required to produce a plane change

V_i = the velocity of the spacecraft on the initial orbit at the intersection of the initial and final orbit planes

α = the angle of the plane change

Spacecraft speed is unaltered by the plane change; thus,

$$|V_i| = |V_f| \quad (3.8)$$

Orbit shape is unaffected; therefore, eccentricity, semimajor axis, and radii are unchanged.

Plane changes are expensive as far as energy is concerned. A 10-deg plane change in low Earth orbit requires a velocity change of 1.4 km/s. Equation (3.7) shows that it is important to change planes through the smallest possible angle and at the lowest possible velocity. The lowest possible velocity occurs at the greatest radius, i.e., at the apoapsis.

The maximum displacement between positions on the initial and final orbits occurs at 90 deg from the point of plane change. There are two such points, A and B, in Fig. 3.6.

General Plane Change

A change in orbit plane can result in a change in inclination, the longitude of the ascending node, or both, as shown in Fig. 3.7. A spherical triangle, with one side and two angles known, is formed by i_i , $180 - i_f$, and $\Delta\Omega$. To design a plane change with the desired effect on inclination and longitude of ascending node, the necessary angle of plane change can be found from the cosine law of spherical trigonometry¹⁵:

$$\cos \alpha = \cos i_i \cos i_f + \sin i_i \sin i_f \cos(\Delta\Omega) \quad (3.9)$$

The velocity change ΔV required to provide a plane change α can be obtained from Eq. (3.7). The argument of latitude on the initial orbit, at which the maneuver must be performed, is given by the sine law of spherical trigonometry¹⁵:

$$\sin A_{La} = \frac{\sin i_f \sin(\Delta\Omega)}{\sin \alpha} \quad (3.10)$$

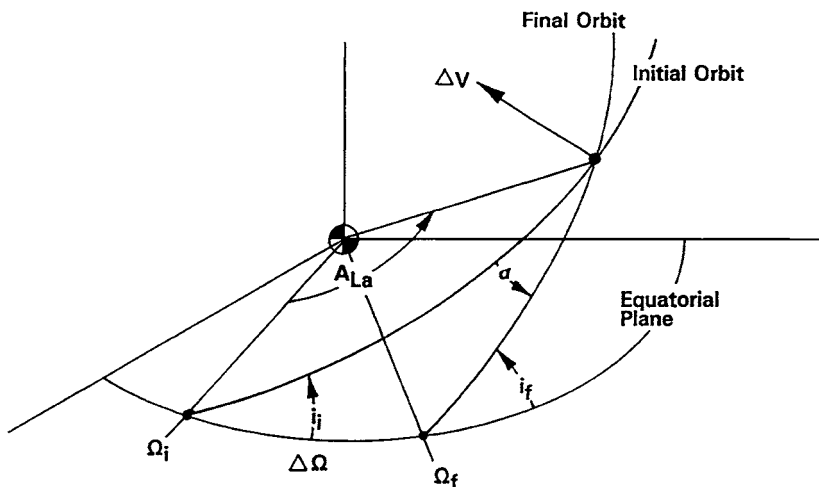


Fig. 3.7 General plane change.

and

$$A_{La} = \omega_i + \Theta_i \quad (3.11)$$

where

A_{La} = the argument of latitude, which is the angle from the reference plane to the spacecraft position, measured in the direction of motion; equal to the true anomaly plus the argument of periaxis

ω_i = the argument of periapsis on the initial orbit

Θ_i = the true anomaly on the initial orbit at which the plane change must occur

$\Delta\Omega$ = the change in longitude of the ascending node caused by the plane change ($\Delta\Omega = \Omega_f - \Omega_i$)

α = the angle between initial and final planes

Example 3.4 General Plane Change

Consider an initial circular Earth orbit with the following characteristics:

$$h = 275 \text{ km}$$

$$i = 28.5 \text{ deg}$$

$$\Omega = 60^\circ \text{ West}$$

It is desired to make a plane change to a circular orbit with the following final characteristics:

$$h = 275 \text{ km}$$

$$i = 10 \text{ deg}$$

$$\Omega = 100^\circ \text{ West}$$

Design the plane change.

The angle of the plane change, from Eq. (3.9), is

$$\cos \alpha = \cos(28.5) \cos(10) + \sin(28.5) \sin(10) \cos(40)$$

$$\alpha = 21.730 \text{ deg}$$

The argument of latitude on the initial orbit at which the impulse must be applied, from Eq. (3.10), is

$$\sin A_{La} = \frac{\sin(10) \sin(40)}{\sin(21.730)}$$

$$A_{La} = 17.547 \text{ deg}$$

The velocity on the initial and final orbit, found by using Eq. (2.6), is 7.740 km/s. The velocity change required for the plane change, from Eq. (3.7), is

$$\Delta V = 2(7.740) \sin(21.730/2) = 2.918 \text{ km/s}$$

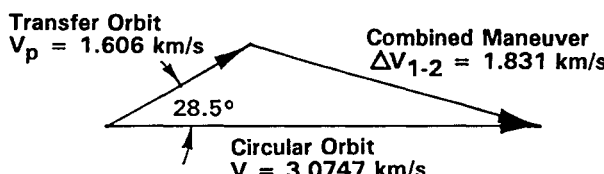
If spacecraft velocity is changed at the reference plane, i.e., at one of the nodes, the inclination of the orbit will be changed, and the longitude of the ascending node will not be changed. The change in inclination will be

$$\Delta i = \alpha \quad (3.12)$$

where α is the angle between initial and final velocity vectors. Inclination is the only orbital parameter changed by adding out-of-plane velocity at one of the nodes.

3.5 Combined Maneuvers

Significant energy savings can be made if in-plane and out-of-plane maneuvers can be combined. The savings result from the fact that any side of a vector triangle is always smaller than the sum of the other two sides. The maneuvers necessary to establish a geosynchronous orbit provide an excellent example of combined maneuver savings. The final two maneuvers, shown in Fig. 3.8, are an in-plane orbit circularization and a 28.5-deg plane change. The plane change maneuver at



Separate Maneuvers:

1) Plane Change Maneuver $\Delta V = 0.791 \text{ km/s}$

2) Circularization Maneuver $\Delta V = 1.469 \text{ km/s}$

Total $\Delta V = 2.260 \text{ km/s}$

Fig. 3.8 Combined maneuver.

ORBITAL MANEUVERS

49

a velocity of 1.606 km/s would require a ΔV of 0.791 km/s. The circularization maneuver would change the velocity at apoapsis on the transfer ellipse to the circular orbit velocity of 3.0747 km/s; this maneuver would require a ΔV of 1.4687 km/s. The total for velocity change for the two maneuvers, conducted separately, would be 2.260 km/s. Combining the two maneuvers, however, requires a velocity change of only 1.831 km/s, a savings of 0.429 km/s. (See Chapter 5 for a complete description of the geosynchronous mission design.) Watch for opportunities to combine maneuvers. Every plane change offers an opportunity of this kind.

If a plane change can be incorporated into a bielliptic transfer at the apoapsis of the intermediate orbit, substantial energy savings can be made. Note, however, that a bielliptical transfer requires a more complicated propulsion system than a Hohmann transfer with a plane change.

3.6 Propulsion for Maneuvers

The ultimate result of maneuver design is reflected in the propellant mass required to accomplish it. Converting a velocity change to an equivalent propellant mass is a process that is both simple and accurate for space conditions. Consider a spacecraft being accelerated by an unbalanced force as shown in Fig. 3.9. Assume that thrust is the only unbalanced force acting on the spacecraft; thus drag is zero, and weight is balanced by centrifugal forces. These assumptions describe a common condition in space flight. Further assume that the mass of the spacecraft is decreasing at the propellant mass flow rate of dm/dt .

The thrust force on the spacecraft is equal to the change in momentum of the exhaust gas, which has been accelerated from rest to the exhaust gas average

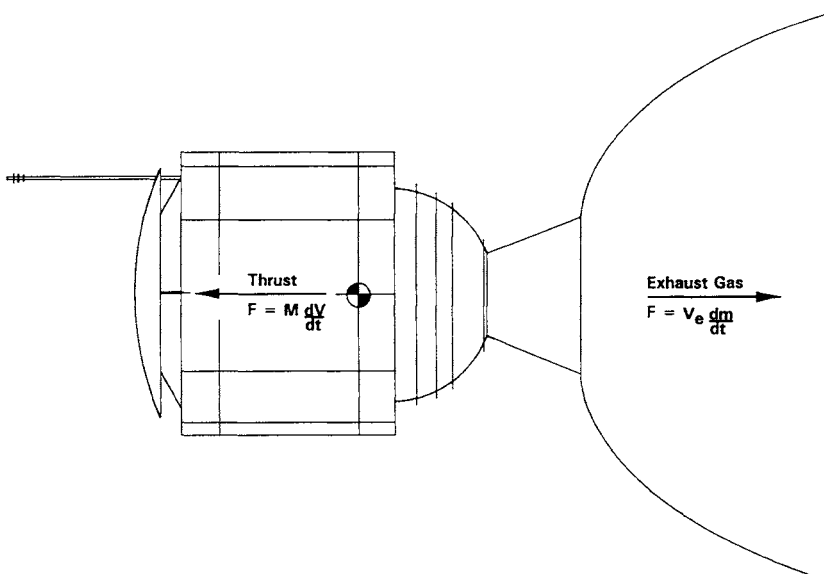


Fig. 3.9 Thrust acting on a spacecraft.

velocity V_e ; thus,

$$F = V_e \left(\frac{dm}{dt} \right) \quad (3.13)$$

The force on the spacecraft may also be expressed as

$$F = M \left(\frac{dV}{dt} \right) \quad (3.14)$$

where

M = the mass of the spacecraft at any instant

dV/dt = the acceleration of the spacecraft

Setting Eq. (3.13) equal to Eq. (3.14), substituting $-dM$ for dm , and integrating yields

$$\Delta V = V_e \ln(M_i/M_f) \quad (3.15)$$

where M_i and M_f are the initial and final masses of the spacecraft before and after the propellant is burned.

The usefulness of Eq. (3.15) can be improved by introducing the concept of specific impulse I_{sp} , which is the thrust produced by a unit propellant flow rate. The units for specific impulse are $s - lb_f/lb_m$ (or simply s , where "s" stands for seconds). By definition, thrust is

$$F = I_{sp} \left(\frac{dw}{dt} \right) \quad (3.16)$$

where dw/dt is the propellant weight flow rate (in lb_m/s). It can be shown that

$$V_e = I_{sp}/g_c \quad (3.17)$$

where g_c is the gravitational constant ($g_c = 32.174 \text{ ft/s}^2$). Now Eq. (3.17) can be simplified; a very useful equation results:

$$\Delta V = g_c I_{sp} \ln(M_i/M_f) \quad (3.18)$$

The importance of Eq. (3.18) is that the difference between M_i and M_f is the propellant mass M_p necessary to produce velocity change ΔV . For a given spacecraft mass, the ΔV required for a maneuver can be converted accurately to propellant mass. There are additional, secondary masses associated with containing the propellants, but these are usually small in comparison with the propellant mass.

Since velocity change is usually known and the propellant weight is unknown, Eq. (3.18) can be rearranged into the following more useful forms:

$$M_i/M_f = \exp(\Delta V/g_c I_{sp}) \quad (3.19)$$

$$M_p = M_i [1 - \exp(-\Delta V/g_c I_{sp})] \quad (3.20)$$

$$M_p = M_f [\exp(\Delta V/g_c I_{sp}) - 1] \quad (3.21)$$

where M_p is the mass of propellant consumed producing velocity change ΔV . A handy feature of Eqs. (3.18–3.21) is that masses appear as a ratio; therefore, initial

ORBITAL MANEUVERS

51

Table 3.2 Typical specific impulses

Propellant	I_{sp} , s
Cold gas	50
Monopropellant hydrazine	230
Solid propellant	290
Nitrogen tetroxide/MMH	310
Liquid oxygen/liquid hydrogen	460

and final spacecraft weights can be used directly without conversion to mass. Note that specific impulse, velocity change, and g_c must be in the same system of units, usually the English system.

Typical steady-state, specific impulse values that can be expected from current propulsion systems operating in a vacuum are summarized in Table 3.2 (in English units). Note that if Eq. (3.18), in any of its forms, is used when drag or gravity losses are important, serious errors will result.

Example 3.5 Combined Maneuver Savings

It has been shown that a combined maneuver for the final impulse in establishing a geosynchronous orbit saves 0.429 km/s over the use of two separate maneuvers. What are the propellant weight savings for a spacecraft that has a burnout weight of 1025 kg and that uses a solid rocket motor for the impulse?

The first order of business is to get compatible units. The velocity and specific impulse must be in English units; the weights can remain in metric units. Conversion factors are given in Appendix C. First convert ΔV to English units:

$$\Delta V = (0.429 \text{ km/s})(3280.84 \text{ ft/km}) = 1407.5 \text{ ft/s}$$

From Eq. (3.21),

$$M_p = 1025 \left[\left(\exp \frac{1407.5}{(32.174)(290)} \right) - 1 \right]$$

$$= 167 \text{ kg}$$

A propellant weight savings of 167 kg (368 lb) is a substantial reward for careful mission design.

Problems

3.1 The Magellan approach hyperbola at Venus had the following elements:

$$a = 17,110 \text{ km}$$

$$e = 1.3690$$

The spacecraft was placed in a nearly polar, elliptical mapping orbit with the following elements:

$$a = 10,424.1 \text{ km}$$

$$e = 0.39433$$

If the two orbits were tangent at periapsis, what velocity change was required to establish the mapping orbit? Was it a velocity increase or decrease?

3.2 The Thor-Delta placed GEOS-A in a 500-km-altitude circular parking orbit. Design a Hohmann transfer to lift it to a 36,200-km-radius circular orbit. Define each velocity change, and find the time required for the transfer.

3.3 Determine how much propellant weight would be required for the Space Shuttle *Columbia* to make a 3-deg plane change in its 275-km-altitude circular parking orbit under the following conditions:

Columbia initial weight = 220,000 lb

Specific impulse of propulsion system = 320 s

3.4 Determine the velocity change required to convert a direct, circular, Earth orbit with a radius of 15,000 km into a coplanar, direct, elliptical orbit with the following elements:

Periapsis altitude = 500 km

Apoapsis radius = 22,000 km

Would the velocity change have been different if the orbits had been about Mars?

3.5 Design a plane change for the following circular Earth orbit:

Altitude = 1000 km

Inclination = 37 deg

Longitude of ascending node = 30°

which results in an inclination of 63 deg and a longitude of the ascending node of 90° West. What are the angle of the plane change and the change in velocity?

4

Observing the Central Body

One of the principle uses of spacecraft is for observation of a central body from the unique position of space. The position of a spacecraft over the central body is determined by the orbital parameters already discussed and by the properties of the launch, launch site, and perturbations to the orbit. This chapter discusses each of these effects and also discusses the view from a spacecraft given its position. Observations of the Earth are charted from space in the geographic coordinate system; observations of other planets are recorded in the similar IAU cartographic system.

4.1 Effect of the Launch Site

Both the latitude of the launch location and the allowable launch azimuth range have a profound effect on orbital parameters. In general, southerly launches allow polar orbits, and easterly launches take advantage of the Earth's rotation and produce low-inclination orbits. The more nearly equatorial the launch site is, the greater the range of orbit inclinations that can be achieved.

Figure 4.1 shows a launch site at latitude La and a launch azimuth Az . Latitude is measured on a great circle through the north pole, perpendicular to the equatorial

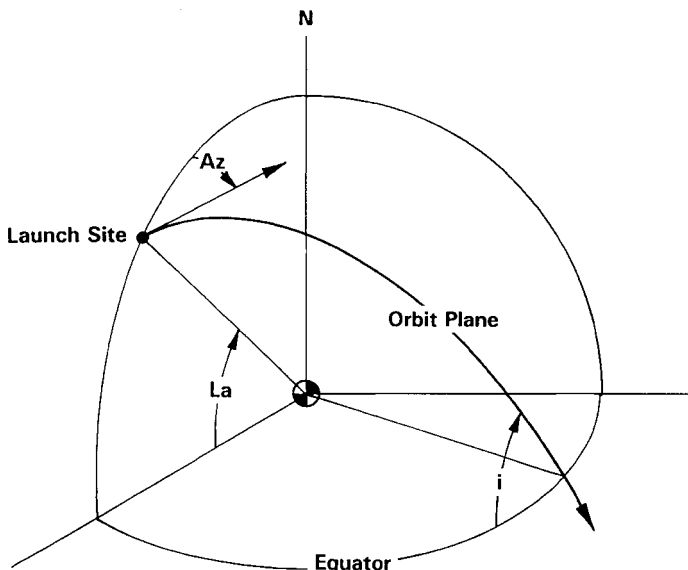


Fig. 4.1 Launch azimuth and altitude.

plane. Azimuth is measured from true north, which is a vector in the latitude circle, to the launch direction vector. The launch direction vector is in the orbit plane. On the first orbit after launch, the spacecraft crosses the equatorial plane at the orbit inclination angle i .

A right spherical triangle is formed by the side La and by the two angles Az and i . From spherical trigonometry,

$$\cos i = \cos La \sin Az \quad (4.1)$$

where

i = the orbit inclination

Az = the launch azimuth, the angle from true north to the departure trajectory

La = the latitude of the launch platform

Equation (4.1) assumes a nonrotating Earth. To adjust for a rotating Earth, adjust the azimuth and orbital velocity by adding the Earth's eastward rotational vector, as shown in Fig. 4.2. In Fig. 4.2,

V_e = the eastward rotational velocity of Earth

V_o = the orbital velocity over a nonrotating Earth

V'_o = the orbital velocity corrected for Earth's rotation

Az' = the launch azimuth corrected for Earth's rotation

The rotating Earth correction of the azimuth is usually small enough to be neglected; however, the velocity addition is important. Missions requiring high launch energy (e.g., geosynchronous or planetary missions) usually launch due east to obtain the maximum benefits of Earth rotation.

Equation (4.1) produces a minimum inclination when the launch azimuth is due east (90°) or west (270°). The latitude of the launch site is numerically equal to the minimum orbital inclination that can be achieved from that site.

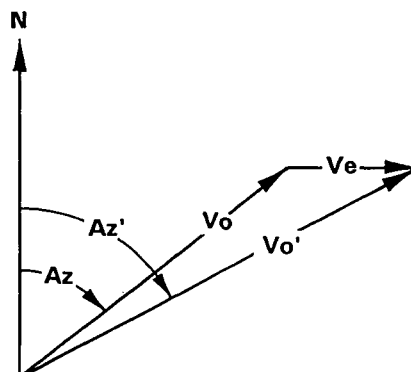


Fig. 4.2 Adjusting for Earth rotation.

OBSERVING THE CENTRAL BODY

55

Launch Latitude

The latitudes of the launch sites of the world are listed in Table 4.1. The United States operates two major launch sites. The eastern test range at Cape Canaveral, Florida, is called the Kennedy Space Flight Center (KSC) by NASA and Cape Canaveral or Eastern Test Range (ETR) by the Air Force; in this book we will use ETR. The western test range, near Lompoc, California, is called either Vandenberg Air Force Base or WTR; we will use WTR. These two sites were chosen for their advantageous latitude and coastal positions.

The minimum orbit inclination that a U.S. spacecraft can have without a plane change is 28.5°, the latitude of ETR. The European Space Agency has a launch site in South America at a latitude of 5.5° N. The former USSR, with launch sites at latitudes of 46°, 48.4°, and 62.8° has difficulty achieving low orbit inclinations.

Launch Azimuth

Given a launch site, the desired orbit inclination is obtained by selection of a launch azimuth in accordance with Eq. (4.1). However, the usable range of launch azimuths is restricted by safety considerations. The area underneath a departing launch vehicle is clearly unsafe if the vehicle malfunctions, and even a normal launch sheds spent stages. The location of downrange populated areas limits the acceptable launch azimuth range for a launch complex. Figure 4.3 shows the acceptable azimuth range for ETR and WTR. The restrictions on launch azimuth

Table 4.1 Worldwide launch sites

Launch site	Country	Latitude	Longitude
ETR	United States	28° 30' N	80° 33' W
WTR	United States	34° 36' N	120° 36' W
Wallop Island	United States	37° 51' N	75° 28' W
Kourou	Europe, ESA	5° 32' N	52° 46' W
San Marco	Italy	2° 56' S	40° 12' E
Plesetsk	Soviet Union	62° 48' N	40° 24' E
Kapustin Yar	Soviet Union	48° 24' N	45° 48' E
Tyuratam (Baikonur)	Soviet Union	45° 54' N	63° 18' E
Thumba	UN/India	8° 35' N	76° 52' E
Sriharikota	India	13° 47' N	80° 15' E
Shuang-Ch'Eng-Tzu	China	40° 25' N	99° 50' E
Xichang	China	28° 06' N	102° 18' E
Tai-yuan	China	37° 46' N	112° 30' E
Wuzhai	China	38° 35' N	111° 27' E
Kagoshima	Japan	31° 14' N	131° 05' E
Osaki	Japan	30° 24' N	130° 59' E
Takesaki	Japan	30° 23' N	130° 58' E
Woomera	Australia/U.S.	31° 07' S	136° 32' E
Yavne	Israel	31° 31' N	34° 27' E

From Ref. 11, page 617, reproduced here through the courtesy of Wertz and Larson.



Fig. 4.3 Acceptable launch azimuth range for the United States.

and the latitudes of ETR and WTR control the inclination capabilities of the United States as shown in Table 4.2. Polar orbits, with $i \approx 90$ deg, can be achieved by launching south out of WTR. Polar orbits cannot be achieved from ETR without a plane change.

Direct orbit. Orbita are classified as direct or retrograde depending on their direction of rotation about the central body. In a direct orbit, a spacecraft rotates counterclockwise around the central body as viewed from the north pole; orbit inclination is between 0 and 90 deg. (All planets are in direct orbits around the sun.) The launch azimuth for direct orbits is 0 to 180 deg. Direct orbits are usually achieved by launches from ETR.

Retrograde orbit. In a retrograde orbit, a spacecraft rotates clockwise around the central body as viewed from the north pole; orbit inclination is between 90 and 180 deg. Launch azimuths for retrograde orbits are between 180 and 360 deg; the United States can achieve retrograde orbits only by launching from WTR.

Example 4.1 Effect of Launch Azimuth

The Solar Mesosphere Explorer spacecraft was launched on a two-stage Delta into a circular orbit with the following characteristics:

$$\begin{aligned} \text{Altitude} &= 500 \text{ km} \\ \text{Inclination} &= 97.4 \text{ deg} \\ \text{Period} &= 94.6 \text{ min} \end{aligned}$$

What was the launch azimuth, and where was the launch site?

Table 4.2 Orbit inclinations from U.S. launch sites

Site	La	Az, deg	i , deg
ETR	28.5°	35	59.7
		90	28.5
		120	40.4
WTR	34.5°	170	81.8
		180	90.0
		300	135.5

OBSERVING THE CENTRAL BODY

57

WTR is the only U.S. launch site that can achieve an inclination of 97.4 deg. (Technically, an inclination of 97.4 deg could be achieved from ETR with a plane change maneuver called a dog leg, but this maneuver is expensive and highly unlikely.)

The latitude of WTR is 34.5° from Table 4.2. The launch azimuth can be obtained by rearranging Eq. (4.1) as follows:

$$\sin Az = \frac{\cos i}{\cos La} = \frac{\cos 97.4}{\cos 34.5} = -0.1563$$

$$Az = 188.99 \text{ deg}$$

Since the inclination is greater than 90 deg the orbit is retrograde. In fact, the orbit is sun-synchronous, a type of orbit that will be discussed in Chapter 5.

4.2 Orbit Perturbations

In our analysis of two-body motion, we have assumed that the mass of the central body is spherically symmetrical and can be considered concentrated at the geometric center. In addition, we have assumed that gravitational attraction is the only force acting on the spacecraft. Both of these assumptions are very nearly true, but for refined calculations it is necessary to consider the orbit perturbations caused by forces due to 1) oblateness of the Earth, 2) drag, 3) attraction of the sun, 4) attraction of the moon, and 5) solar radiation pressure. The relative importance of these forces is shown in Fig. 4.4. For each effect the logarithm of the disturbing acceleration, normalized to 1 g, is plotted as a function of altitude. Earth's gravity is the dominant acceleration at altitudes above 100 km (below 100 km, re-entry

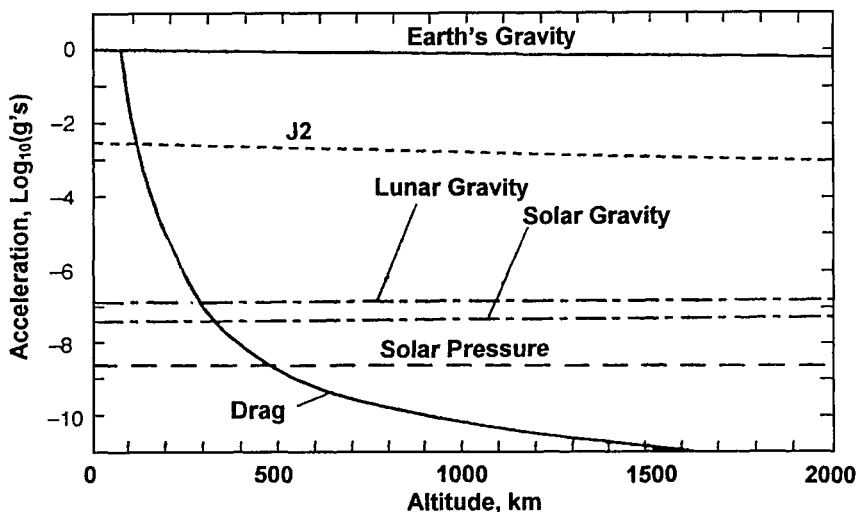


Fig. 4.4 Relative importance of orbit perturbations. (From Ref. 16, p. 99; reproduced courtesy of Wiley.)

conditions prevail and atmospheric drag dominates). At altitudes below about 200 km, atmospheric drag must be considered in projecting the life of a spacecraft. For orbits above 200 km the effects of Earth's oblateness J_2 is the major force, second only to Earth's gravity. In this section the effects of central body oblateness on spacecraft orbits will be considered.

The Earth is not spherically symmetric. The equatorial radius is 6378.14 km and the polar radius 6356.77 km.¹² This oblateness is caused by the axial rotation rate of the Earth. All planets share this oblateness to one degree or another. Oblateness of the planets causes two orbital perturbations: 1) regression of nodes and 2) rotation of apsides.

Regression of Nodes

An equatorial bulge causes a component of the gravitational force to be out of the orbit plane, as shown in Fig. 4.5. The out-of-plane force causes the orbit plane to precess gyroscopically; the resulting orbital rotation is called regression of nodes. Regression of nodes can be approximated by an expression of the following form^{11,15}:

$$\frac{d\Omega}{dt} = \frac{-3nJ_2R_0^2(\cos i)}{2a^2(1-e^2)^2} \quad (4.2)$$

where

- $d\Omega/dt$ = rate of change of the longitude of the ascending node, rad/s
 R_0 = mean equatorial radius of the central body
 a = semimajor axis of the orbit
 i = inclination of the orbit
 e = eccentricity of the orbit
 n = mean motion
 J_2 = zonal coefficient, a constant peculiar to each celestial body

This equation is derived by expressing the gravitational force as a polynomial, by assuming that longitudinal variations in force can be ignored, and by observing that J_2 dominates all terms.

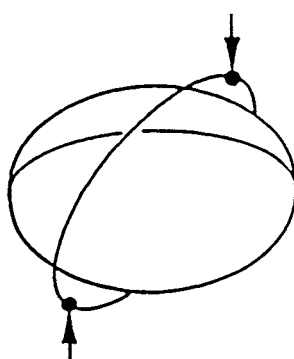


Fig. 4.5 Regression of nodes.

OBSERVING THE CENTRAL BODY

59

Table 4.3 Zonal coefficients

Planet	J_2
Venus	0.000027
Earth	0.00108263
Mars	0.001964
Jupiter	0.01475
Saturn	0.01645
Uranus	0.012
Neptune	0.004
(Moon)	0.0002027

Table 4.3 shows J_2 for the planets.¹² Oblateness is large for the gaseous outer planets, which have high rotation rates; it is small for Venus, which is almost stationary.

For Earth orbits Eq. (4.2) can be reduced to

$$\frac{d\Omega}{dt} = -2.06474 \times 10^{14} \frac{\cos i}{a^{3.5}(1-e^2)^2} \quad (4.3)$$

Equation (4.3) yields nodal regression in degrees per mean solar day.

Figure 4.6 (arrangement of Fig. 4.6 based on the work of Bate³) shows the nodal regression rate for some circular Earth orbits. Elliptical orbits of low eccentricity exhibit nodal regression very nearly equal to that of a circular orbit of the same

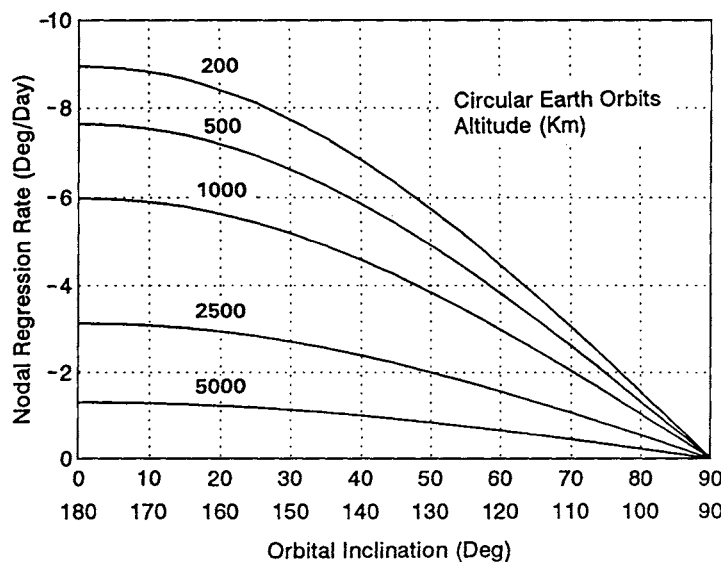


Fig. 4.6 Nodal regression rates for various orbital inclinations.

semimajor axis. As shown in Fig. 4.6, regression of nodes is greater at low inclinations and low altitudes, where it can reach 9 deg per mean solar day. For orbits above 10,000 km in altitude, the regression of nodes is less than 0.5 deg per mean solar day and can be ignored for most purposes. Care must be taken, however, in the analysis of geosynchronous orbits. Even though the regression is small at that altitude, it is cumulative and important in planning for station keeping.

The orbit plane rotates clockwise for direct orbits and counterclockwise for retrograde orbits. For direct orbits, regression of nodes adds to the apparent westward motion caused by the rotation of the Earth.

Taking advantage of the regression of nodes makes a sun-synchronous orbit possible. In such an orbit, regression of nodes is used to hold the orbit plane at a constant angle with respect to the sun vector; see Chapter 5 for details.

Example 4.2 Regression of Nodes

What is the regression of nodes for the STS30, which achieved a near-circular orbit with the following characteristics:

$$\text{Periapsis altitude} = 270 \text{ km}$$

$$\text{Apoapsis altitude} = 279 \text{ km}$$

$$\text{Inclination} = 28.5 \text{ deg}$$

The semimajor axis is, from Eq. (2.17),

$$a = \frac{(270 + 6378.14) + (279 + 6378.14)}{2} = 6652.6 \text{ km}$$

The mean motion is, from Eq. (2.36),

$$n = \sqrt{398,600.4/(6652.6)^3} = 0.001164$$

From Table 4.3, $J_2 = 1.08263 \times 10^{-3}$. Eccentricity, 0.00068, can be considered to be zero. From Eq. (4.2) the regression of nodes is

$$\begin{aligned} \frac{d\Omega}{dt} &= -1.5(0.001164)(1.08263 \times 10^{-3}) \frac{(6378.14)^2}{(6652.64)^2} \cos 28.5 \\ \frac{d\Omega}{dt} &= -1.5265 \times 10^{-6} \text{ rad/s} = -7.556 \text{ deg/day} \end{aligned}$$

(Correction for eccentricity would produce a regression of nodes of -7.5559 deg/day.)

Rotation of Apsides

Rotation of apsides is an orbit perturbation due to the Earth's bulge and is similar to regression of nodes (see Fig. 4.7). Rotation of apsides is caused by a greater than normal acceleration near the equator and subsequent overshoot at periapsis. A rotation of periapsis results. This motion occurs only in elliptical orbits. The

OBSERVING THE CENTRAL BODY

61

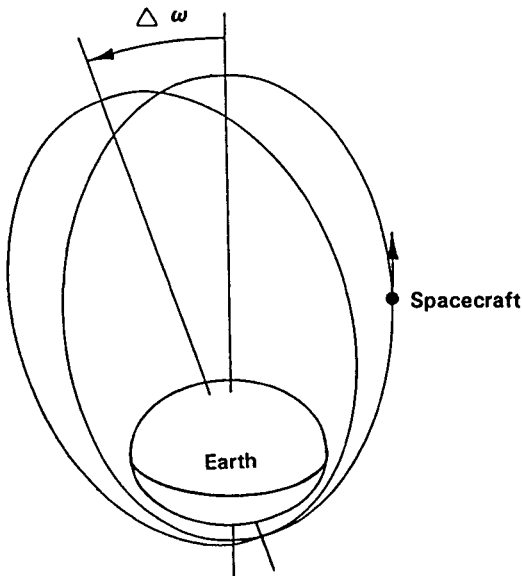


Fig. 4.7 Rotation of apsides.

polynomial expansion described for Eq. (4.2) produces the following description of the motion^{11,15}:

$$\frac{d\omega}{dt} = \frac{3nJ_2R_0^2(4 - 5\sin^2i)}{4a^2(1 - e^2)^2} \quad (4.4)$$

where

- $d\omega/dt$ = apsidal rotation rate, rad/s
- R_0 = mean equatorial radius of central body
- e = orbit eccentricity
- i = orbit inclination
- n = mean motion

For an Earth orbit Eq. (4.4) can be reduced to

$$\frac{d\omega}{dt} = 1.0324 \times 10^{14} \frac{(4 - 5\sin^2i)}{a^{3.5}(1 - e^2)^2} \quad (4.5)$$

Equation (4.5) produces apsidal rotation rate in degrees per mean solar day.

Figure 4.8 (arrangement of Fig. 4.8 based on the work of Bate³) shows the apsidal rotation rate, in degrees per mean solar day, for orbits with perigee altitudes of 200 km and various apogee altitudes and inclinations. Figure 4.8 shows that apsidal rotation can be either positive or negative and is greater for low inclination or low altitude orbits.

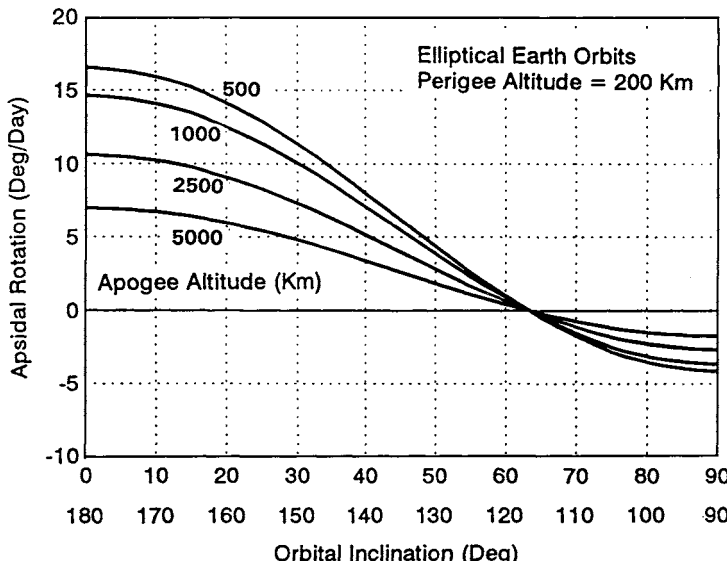


Fig. 4.8 Apsidal rotation for various orbital inclinations.

Example 4.3 Rotation of Apsides

What is the rotation of apsides for an Earth orbit with the following characteristics:

$$\begin{aligned} \text{Periapsis altitude} &= 185 \text{ km} \\ \text{Apoaapsis altitude} &= 555 \text{ km} \\ \text{Inclination} &= 30 \text{ deg} \end{aligned}$$

The semimajor axis is, from Eq. (2.17),

$$a = (6563.14 + 6933.14)/2 = 6748.14 \text{ km}$$

The eccentricity is, from Eq. (2.20),

$$e = \frac{6933.14 - 6563.14}{6933.14 + 6563.14} = 0.027415$$

The mean motion is, from Eq. (2.36),

$$n = \sqrt{\frac{398,600.4}{(6748.14)^3}} = 1.1389 \times 10^{-3}$$

OBSERVING THE CENTRAL BODY

63

From Table 4.3, $J_2 = 1.08263 \times 10^{-3}$. From Eq. (4.4), the rotation of apsides is

$$\frac{d\omega}{dt} = \frac{0.75(1.1389 \times 10^{-3})(1.08263 \times 10^{-3})(6378.14)^2[4 - 5 \sin^2(30)]}{(6748.14)^2[1 - (0.027415)^2]^2}$$

$$\frac{d\omega}{dt} = 2.2753 \times 10^{-6} \text{ rad/s} = 11.26 \text{ deg/day}$$

Since this is an Earth orbit, the same result could be obtained from Eq. (4.5).

It can be seen from Eq. (4.4) that when $\sin^2 i = 4/5$, apsidal rotation is zero regardless of eccentricity. This inclination, 63.435 or 116.565 deg, is called the *critical inclination*. The Molniya orbit is at the critical inclination (see Chapter 5). Note that critical inclination is independent of J_2 and therefore is the same for all celestial bodies.

4.3 Ground Track

The ground track (or ground trace) of a spacecraft is the locus of nadir positions traced on the surface of the central body by a spacecraft as a function of time. Figure 4.9 shows the ground track of a spacecraft in a direct, circular low Earth orbit for the first three orbits after launch from ETR.

Spacecraft ground track is the result of three motions:

- The motion of the spacecraft in orbit
- The rotation of the central body
- The perturbation of the orbit caused by the equatorial bulge of the central body

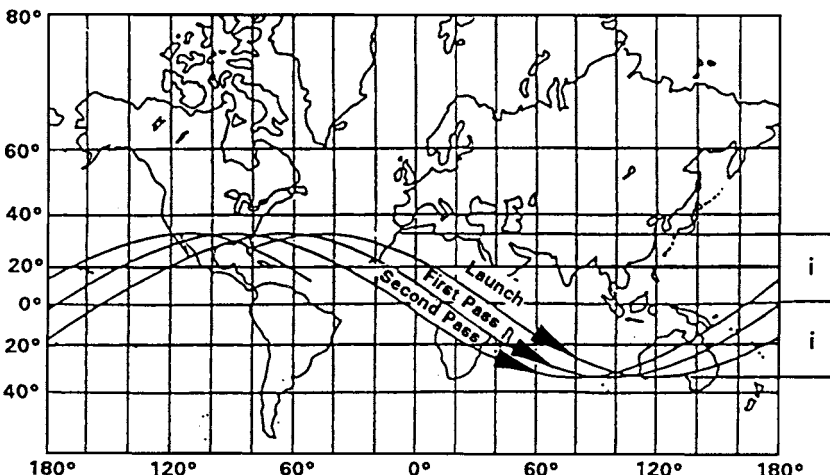


Fig. 4.9 Ground track of a low Earth orbit.

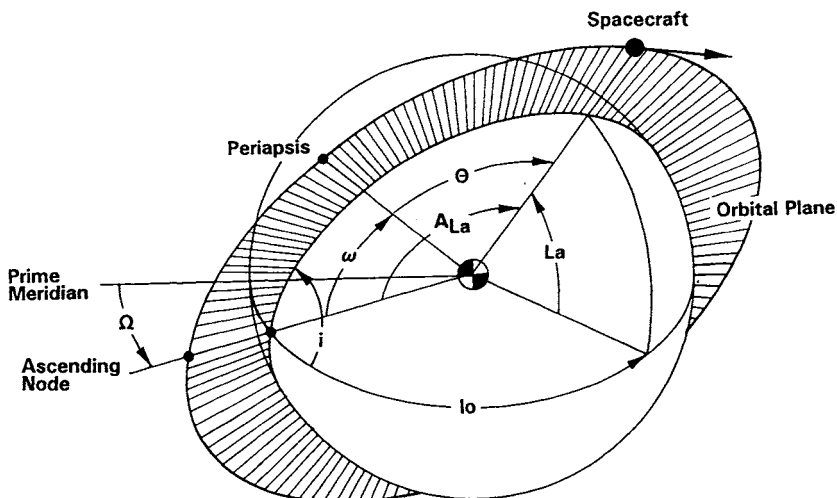


Fig. 4.10 Spacecraft position.

Consider a spacecraft in orbit over the surface of a central body, as shown in Fig. 4.10. In the figure,

La = latitude of spacecraft at time t

Lo = longitude of spacecraft at time t

Ω = longitude of ascending node at the last crossing (measured from the prime meridian)

i = orbit inclination

A_{La} = the argument of latitude (the angle in the orbital plane from the ascending node to the spacecraft position; $A_{La} = \omega + \Theta$)

lo = longitudinal angle to spacecraft position measured in the equatorial plane from the ascending node

t = time to travel from the ascending node to the current position, s

ω = argument of periapsis

Θ = true anomaly of the current position

For a right spherical triangle,

$$\sin La = \sin i \sin A_{La} \quad (4.6)$$

$$\sin lo = \tan La / \tan i \quad (4.7)$$

The argument of latitude is measured in the direction of motion and is equal to the true anomaly plus the argument of periapsis. The maximum latitude occurs when A_{La} is 90 deg and numerically equal to the orbit inclination. When A_{La} is 0 or 180 deg, the spacecraft position is on the equator, and the latitude is 0°. When A_{La} is between 0 and 180 deg, the spacecraft is in the northern hemisphere, and latitude is noted as north for Earth and as positive for the other planets. When A_{La}

OBSERVING THE CENTRAL BODY

65

is between 180 and 360 deg, latitude is noted as south for Earth and as negative for the other planets.

The longitude of the spacecraft for a spherical nonrotating Earth would be

$$Lo = \Omega + lo \quad (4.8)$$

For a rotating Earth, the spacecraft longitude must be adjusted to account for the Earth's rotation rate of 360 deg per mean sidereal day (86,164 s). This adjustment Re is added to western longitudes and subtracted from eastern longitudes and is expressed as

$$Re = 360t/86,164 = 0.0041781t \quad (4.9)$$

Regression of Nodes

The longitude of the spacecraft ground track must be further adjusted to account for regression of nodes $\Delta\Omega$. The orbit plane rotates westward for direct orbits and eastward for retrograde orbits. For direct orbits, regression of nodes adds to the apparent westward motion caused by the rotation of the Earth.

Sign of Adjustments

In calculating the longitude of the ground track, it is important to keep track of the sign of each of the three adjustments made to the longitude of the ascending node due to regression of nodes, Earth's rotation (or apparent westward progression), and orbital motion. The signs vary with orbit direction and hemisphere as shown in Fig. 4.11.

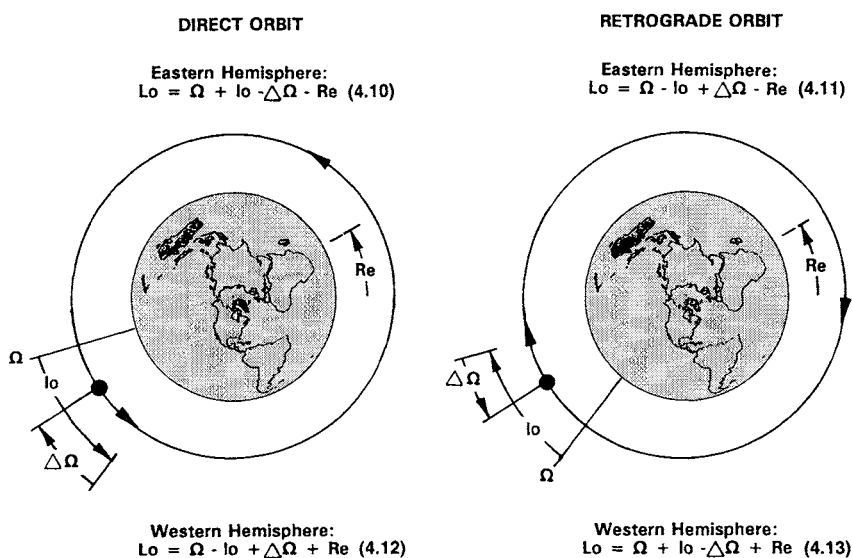


Fig. 4.11 Adjustments to longitude.

In Fig. 4.11,

Lo = longitude of the ground track

Ω = longitude of the ascending node at the last equatorial crossing

$\Delta\Omega$ = adjustment for regression of nodes since passing the ascending node

lo = longitudinal angle to spacecraft position measured in the equatorial plane from the ascending node

Re = longitudinal adjustment for rotation of Earth since passing the ascending node

When using the geocentric coordinate system, the calculation of longitude can be simplified by ignoring the east/west longitude convention and making all calculations in east (or west) longitude measure in accordance with Eq. (4.10) and Eq. (4.11). As a final step, convert the resulting east longitude to the east/west measure. To convert, reduce the east longitude to less than 360° by subtracting all full revolutions. If the residual East longitude Lo' is greater than 180° , the West longitude is

$$Lo = 360^\circ - Lo' \quad (4.14)$$

For example, 1020° East longitude would become 60° West longitude. The IAU cartographic system used for planets other than Earth has been simplified by eliminating the east/west convention.

Example 4.4 Ground Track of Space Shuttle *Atlantis*

The elements of the May 1989 flight of the Space Shuttle *Atlantis* were as follows⁴¹:

Perigee altitude = 270 km

Apogee altitude = 279 km

Eccentricity = 0.000676

Semimajor axis = 6652.64 km

Period = 90.00 min

Argument of periapsis = 25 deg

Inclination = 28.5 deg

Longitude of ascending node = 167° East (third orbit)

Find the latitude and longitude of *Atlantis* for a true anomaly of 20° deg.

The true anomaly at the ascending node was $360^\circ - 25^\circ = 335^\circ$ deg.

Calculate the eccentric anomaly by using Eq. (2.35) in preparation for calculating the time since passing the ascending node. (Note that this orbit is so nearly circular that a circular period could be used.)

$$\cos E = \frac{(0.000676 + \cos 335)}{1 + (0.000676)(\cos 335)} = 0.9064$$

$$E = 0.4360 \text{ rad}$$

Calculate mean motion by using Eq. (2.36):

$$n = \sqrt{\frac{398,600.4}{(6652.64)^3}} = 0.0011635$$

OBSERVING THE CENTRAL BODY

67

Calculate the time since passing the ascending node by using Eq. (2.34):

$$t = \frac{(0.4360) - (0.000676)(\sin 0.4360)}{0.0011635} = 374.5 \text{ s}$$

Recall that Eq. (2.34) has the curious property of calculating the shortest time since periapsis; that is, the calculated time is always shorter than one half of the orbit period. This property is convenient in this case, because Eq. (2.34) produces the time being sought.

Repeating the preceding steps yields a time of 299.6 s from periapsis to a true anomaly of 20 deg; therefore, the time from the ascending node to the current position is 674.1 s.

The argument of latitude A_{La} for the current position is 20 deg + 25 deg = 45 deg. From Eq. (4.6) the current latitude of the *Atlantis* is

$$\sin La = (\sin 28.5)(\sin 45) = 0.3374$$

$$La = 19.72^\circ \text{ North}$$

The latitude is north because A_{La} is between 0 and 180 deg.

In preparation for calculating longitude, we need 1) the longitudinal angle, 2) the rotation of the Earth since passing the ascending node, and 3) the regression of nodes since passing the ascending node.

From Eq. (4.7) the longitudinal angle is

$$\sin lo = \tan(19.72)/\tan(28.5) = 0.660$$

$$lo = 41.31^\circ$$

The longitudinal adjustment for the rotation of the Earth since passing the ascending node is, from Eq. (4.9),

$$Re = 0.0041781(674.1) = 2.82 \text{ deg}$$

The regression of nodes can be calculated most simply from Eq. (4.3) since the central body is Earth:

$$\begin{aligned} \frac{d\Omega}{dt} &= \frac{-2.06474 \times 10^{14}(\cos 28.5)}{(6652.64)^{3.5}[1 - (0.000676)^2]^2} = -7.556 \text{ deg/day} \\ &= 8.745 \times 10^{-5} \text{ deg/s} \end{aligned}$$

The regression since passing the ascending node is

$$\Delta\Omega = (8.745 \times 10^{-5})(674.1) = 0.059 \text{ deg}$$

We now have everything we need to calculate longitude. For the sake of simplicity, we will calculate longitude in east longitude measure and convert later. From Eq. (4.10) for a direct orbit, the longitude of *Atlantis* is

$$Lo = 167 + 41.31 - 0.059 - 2.82 = 205.43^\circ \text{ East}$$

Convert east longitude to the east–west convention used for Earth by using Eq. (4.14):

$$Lo = 360 - 205.43 - 154.6^\circ \text{ West}$$

If we were proceeding to calculate additional positions, we would now calculate the rotation of apsides to reposition the perigee for the next point.

4.4 Spacecraft Horizon

The spacecraft horizon, shown in Fig. 4.12, forms a circle on the spherical surface of the central body. The spacecraft horizon circle encloses the area in which:

- 1) The spacecraft can be seen from the central body.
- 2) Two-way microwave communication can be established with the spacecraft from the central body.
- 3) The spacecraft can observe the central body.

The line from the spacecraft to the local horizon is, at all points, perpendicular to the line from the center of the central body to the horizon, as shown in Fig. 4.13. In Fig. 4.13,

R_s = the radius to the surface of the central body at the spacecraft position; for most calculations it can be assumed that R_s is equal to the mean equatorial radius R_0

h_s = the instantaneous altitude of the spacecraft above the local terrain

s_w = the swath width, which is an arc on the surface of the central body running from spacecraft horizon to horizon

β_h = the horizon angle, which is centered at the spacecraft center of mass and measured from the nadir to the horizon

α_h = the central angle, which is centered at the central body center of mass and measured from the spacecraft horizon to the nadir vector

D_h = the horizon distance, which is measured from the spacecraft to the horizon

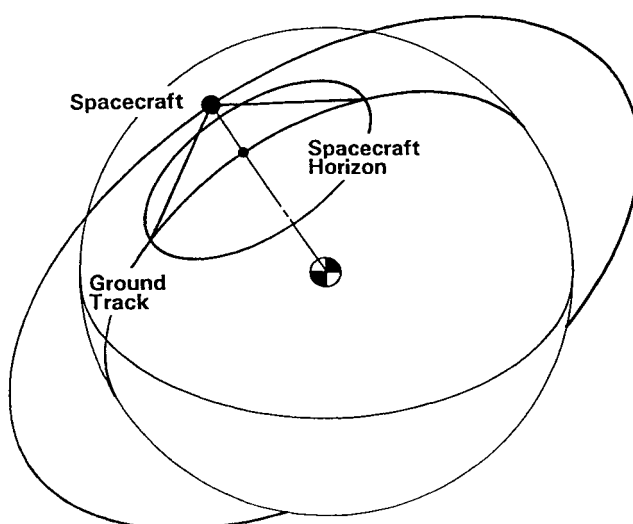


Fig. 4.12 Spacecraft horizon.

OBSERVING THE CENTRAL BODY

69

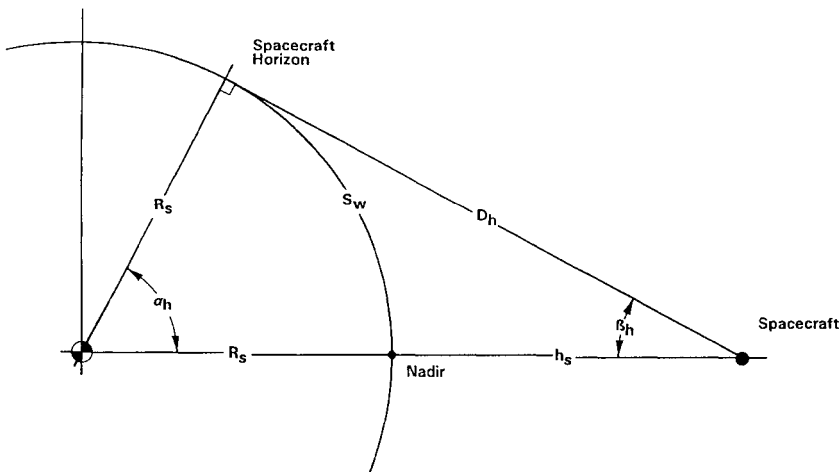


Fig. 4.13 Horizon angle and distance.

Figure 4.13 shows that the spacecraft position, the horizon point, and the central body center of mass form a plane right triangle with one side R_s and hypotenuse $R_s + h_s$. Note that $R_s + h_s$ is equal to the orbital radius r regardless of surface irregularities.

The central angle to the horizon α_h can be found from

$$\cos \alpha_h = R_s / (R_s + h_s) = R_s / r \quad (4.15)$$

Similarly, the angle from the nadir to the spacecraft horizon β_h can be determined from

$$\sin \beta_h = R_s / r \quad (4.16)$$

The distance from the spacecraft to the horizon D_h is, therefore,

$$D_h = r \cos \beta_h \quad (4.17)$$

As the spacecraft moves over the surface, the locus of horizon circles forms a ribbon, or swath, of land centered on the ground track, as shown in Fig. 4.14. The swath width S_w is a linear measurement on the spherical surface of the central body from horizon to horizon:

$$S_w = 2\alpha_h R_s \quad (4.18)$$

Note that Eqs. (4.15), (4.16), and (4.18) use the instantaneous radius to the surface of the central body R_s , which is a function of position. For most purposes it is adequate to substitute the mean equatorial radius R_0 ; however, for very precise work (e.g., cartography) it is necessary to make adjustments for the oblateness of the central body and for terrain roughness. Mapping spacecraft often carry radar altimeters for this reason.

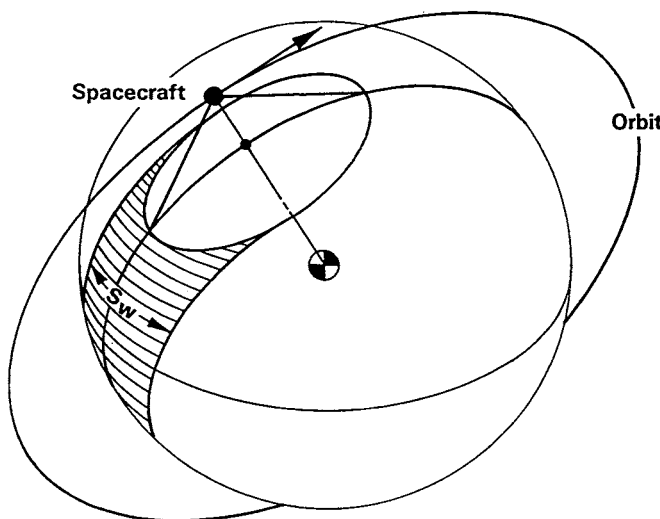


Fig. 4.14 Spacecraft swath.

Example 4.5 Swath Width

The LANDSAT D is in a circular, near-polar Earth orbit at an altitude of 709 km. What is the swath width when it passes over mile-high Denver, Colorado?

Spacecraft altitude, when used as an orbital element, refers to the mean equatorial radius; therefore,

$$r = 6378.14 + 709 = 7087.14 \text{ km}$$

The radius of the surface at Denver is

$$R_s = 1.609 + 6378.14 = 6379.75 \text{ km}$$

From Eq. (4.15) the central angle to the spacecraft horizon is

$$\begin{aligned} \cos \alpha_h &= 6379.75 / 7087.14 = 0.9002 \\ \alpha_h &= 0.4506 \text{ rad} = 25.82 \text{ deg} \end{aligned}$$

From Eq. (4.18), the swath width is

$$S_w = 2(0.4506)(6379.75) = 5749 \text{ km}$$

How much difference would it have made if we had ignored the altitude of Denver and used the mean equatorial radius as R_s ? The central angle would become

$$\begin{aligned} \cos \alpha_h &= 6387.14 / 7087.14 = 0.8999 \\ \alpha_h &= 0.4511 \text{ rad} \end{aligned}$$

OBSERVING THE CENTRAL BODY

71

The swath width would be

$$S_w = 2(0.4511)(6378.14) = 5754 \text{ km}$$

Assuming that $R_s = R_0$ causes an error in swath width of about 0.1% at a surface altitude of 5280 ft. The difference is negligible for most purposes.

Field of View

The field of view of an observing instrument is a spherical angle, centered at the instrument, which defines the portion of the horizon circle that can be viewed by the instrument. Figure 4.15 shows an instrument field of view *Fov* centered at the nadir. The nadir angle β_i is

$$\beta_i = Fov/2 \quad (4.19)$$

The angle that β_i subtends at the center of the central body is α_i . As shown in Fig. 4.15, we now have a plane triangle with sides D_i , r , and R_s . The two sides R_s and r are known from the orbit. The opposite angle β_i is known from the instrument field of view. From plane trigonometry, for triangles of this type,

$$\sin \Gamma' = (r/R_s) \sin \beta_i \quad (4.20)$$

$$\Gamma = 180 \text{ deg} - \Gamma' \quad (4.21)$$

[The supplementary angle Γ' is used in Eq. (4.20) in cases where Γ is obtuse.] The angle α_i can be expressed as

$$\alpha_i = 180 \text{ deg} - (\beta_i + \Gamma) = \Gamma' - \beta_i \quad (4.22)$$

The distance to the surface at the edge of the field of view D_i is

$$D_i = R_s(\sin \alpha_i / \sin \beta_i) \quad (4.23)$$

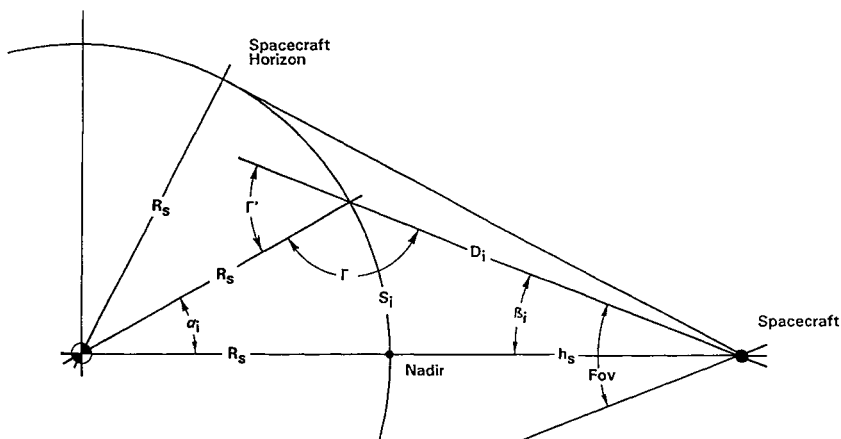


Fig. 4.15 Instrument field of view.

The swath width of the instrument, measured on the surface, is

$$S_i = 2\alpha_i R_s \quad (4.24)$$

In Eq. (4.24), α_i must be in radians; the resulting swath width will be in the same units as R_s .

Equations (4.20–4.24) are perfectly general relationships between the nadir angle and the central angle and can be used for numerous computations associated with the horizon circle (e.g., communication times, pointing to a ground target, and swath widths with a slant angle).

Example 4.6 Field of View

The LANDSAT D (circular orbit, 709 km altitude) multispectral scanner has a field of view of 14.90 deg centered on the nadir.¹⁷ What is the swath width of the instrument?

From Eq. (4.19),

$$\beta_i = 14.90/2 = 7.45 \text{ deg}$$

From Eq. (4.20),

$$\begin{aligned} \sin \Gamma' &= \frac{(7087.14) \sin 7.45}{6378.14} = 0.1441 \\ \Gamma' &= 8.284 \text{ deg} \end{aligned}$$

From Eq. (4.22) the central angle is

$$\alpha_i = 8.284 - 7.45 = 0.834 \text{ deg} = 0.01456 \text{ rad}$$

The instrument swath width is, from Eq. (4.24),

$$S_i = 2(0.01456)(6378.14) = 185.7 \text{ km}$$

Field of View at a Slant Angle

Up to this point we have been considering the field of view as being centered directly beneath the spacecraft. Some instruments require a view at a slant angle j from the nadir to the instrument center. (Synthetic aperture radars are a classic example; they have been called side-looking radars for this reason). Figure 4.16 shows the field of view of an instrument centered at a slant angle. The swath width can be obtained by solving for the central angles, α_1 and α_2 , using Eqs. (4.20–4.22) for the inside triangle given by R_s , r , and β_1 ; and again for the outside triangle given by R_s , r , and β_2 . Then the swath width of the instrument can be obtained by modifying Eq. (4.24) as follows:

$$S_i = R_s(\alpha_2 - \alpha_1) \quad (4.25)$$

Spacecraft Communication

For communications calculations it is desirable to reverse the point of view and anchor the horizon circle at the ground station. The circle is slightly reduced in size

OBSERVING THE CENTRAL BODY

73

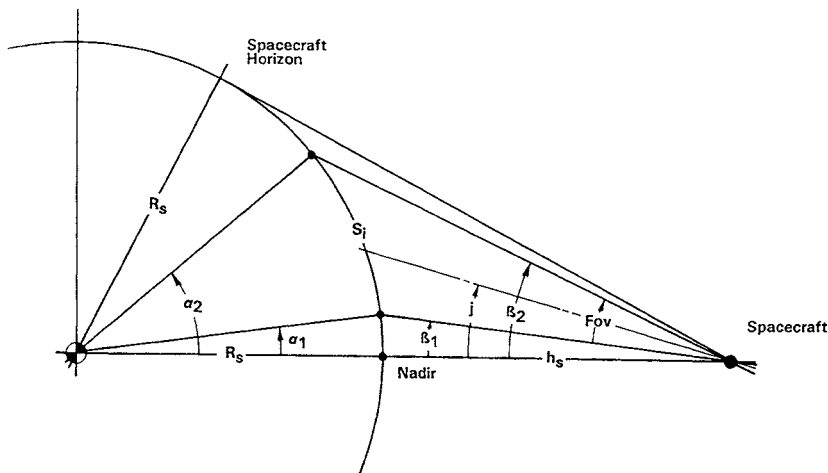


Fig. 4.16 Field of view at a slant angle.

to account for the poor communication when the spacecraft is near the horizon. The circle is also modified to account for local terrain obstructions. Direct microwave communication between the ground station and the spacecraft can occur when the spacecraft flies through the resulting modified circle.

For any orbit, the time available for communication is proportional to the central angle of the ground track inside the communication circle α_c . If the nadir angle β_h is reduced to β_c to eliminate bad communication at the horizon, we can use Eqs. (4.20–4.22) to get the central angle α_c .

For circular orbits, the time available for communication T_c is

$$T_c = 2\alpha_c \sqrt{r^3/\mu} \quad (4.26)$$

where α_c is in radians.

For an elliptical orbit, α_c is the arithmetic difference between the true anomaly entering the communication circle and the true anomaly leaving it. The maximum distance to the station D_c is

$$D_c = R_s (\sin \alpha_c / \sin \beta_c) \quad (4.27)$$

Example 4.7 Communication Time

What is the maximum communication time for a spacecraft in a 300-km orbit if the spacecraft passes directly over the station?

Calculate the nadir angle to the horizon by using Eq. (4.16):

$$\sin \beta_h = 6378.14 / 6678.14 = 0.95507$$

$$\beta_h = 72.76 \text{ deg}$$

Arbitrarily reducing the horizon angle by 3 deg to eliminate communication problems near the horizon yields $\beta_c = 69.76$ deg.

From Eq. (4.20),

$$\sin \Gamma' = \frac{6678.14 (\sin 69.76)}{6378.14} = 0.9824$$

$$\Gamma' = 79.23 \text{ deg}$$

From Eq. (4.22),

$$\alpha_c = 79.23 - 69.76 = 9.47 \text{ deg} = 0.16527 \text{ rad}$$

A pass directly over the station would cover an arc of $2\alpha_c$, and from Eq. (4.27) the communication time is

$$T_c = 2(0.16527) \sqrt{\frac{(6678.14)^3}{398,600.4}} = 285.7 \text{ s} = 4.8 \text{ min}$$

For a low Earth orbit, the time over a ground station is uncomfortably short. The advent of the TDRSS communication satellite constellation has eliminated this operating constraint. Spacecraft now communicate with TDRSS from almost any location, and the signal is relayed to Earth.

For additional information on horizon, swath width, and related problems, consult the work of Wertz and Larson,¹¹ which has excellent coverage of the subject.

4.5 Constellations

The many applications requiring whole Earth coverage or even continuous whole Earth coverage has led to the study of spacecraft constellations. A constellation is a special arrangement of spacecraft in one or more orbits that will achieve a given objective. Some of the early constellations are described in Table 4.4. The simplest constellation, and one of the earliest, is a group of three spacecraft evenly spaced in a geosynchronous orbit. This constellation, fully described in Chapter 5, will

Table 4.4 Early constellations

Name	Description	Capability
Communication	Three spacecraft in geosynchronous orbit	Continuous coverage of Earth's surface below 70°
LANDSAT 7	One spacecraft in circular polar retrograde orbit: $h = 705 \text{ km}$, $i = 98.2^\circ$	Complete Earth coverage every 16 days
TDRSS	Two spacecraft in geosynchronous orbit	Nearly continuous communication with spacecraft in low Earth orbit
GPS	Six circular polar orbits, $h = 20,200 \text{ km}$, four spacecraft in each	At least five spacecraft in view continuously, anywhere on the Earth

OBSERVING THE CENTRAL BODY

75

provide continuous coverage of all of the Earth's surface at latitudes less than 70° (see Figs. 5.1 and 5.4).

A new constellation in the process of construction is Iridium; its purpose is global communication from individual cell phones. When complete there will be at least one spacecraft in view continuously from any point on Earth. The constellation will be composed of six circular polar orbits at an altitude of 780 km, with 11 spacecraft in each. There are several other communication constellations under study.

The variables in constellation design are numerous; they include: orbit type, number of planes, orbit inclination, number of spacecraft per orbit, and orbit altitude. The analysis of constellations is a trial and error process; there are no universal laws. One of several processes that will work follows:

- 1) First set the orbital altitude and calculate the central half-angle α_h from Eq. (4.29).
- 2) Then establish a satisfactory coverage map; see Fig. 4.17.
- 3) From the coverage map, set the number of orbit planes and number of spacecraft per plane.

It requires care in design to prevent orbital perturbations from distorting a constellation. Circular orbits are preferred over elliptical orbits to avoid distortion because of apsidal rotation. (However, Russia uses a constellation of elliptical orbits at an inclination of 63.4 deg. Can you think why this works?)

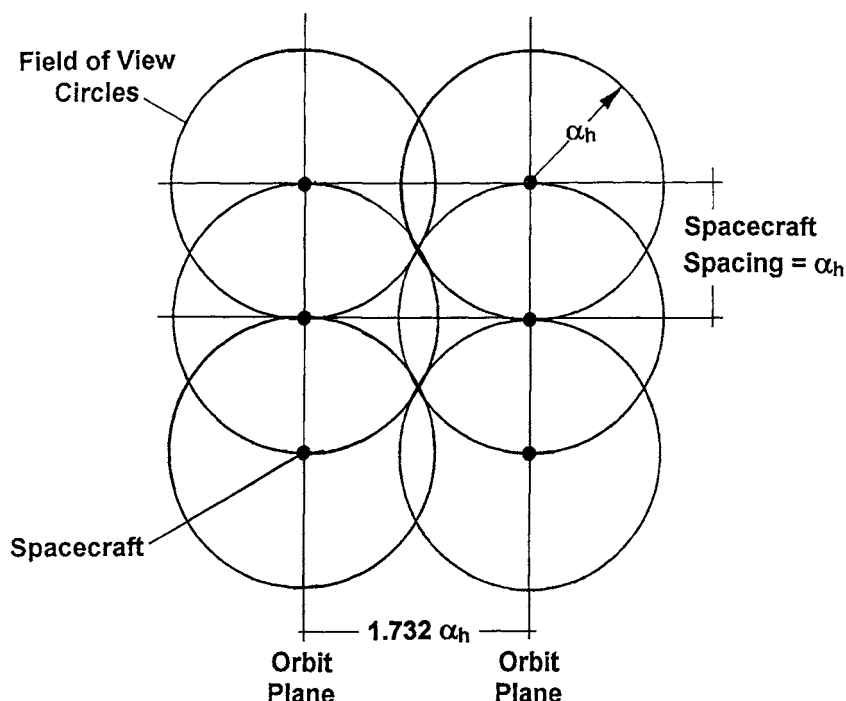


Fig. 4.17 A constellation geometry (equatorial view).

All of the orbital planes must have the same inclination and altitude to equalize regression of nodes for all spacecraft. Otherwise, it would require a great deal of orbit correction and propellant consumption to correct distortion. An exception to this rule is a constellation combining polar orbits with equatorial orbits. The perturbations of all of the orbits is zero. It would also be possible to minimize perturbations by using very high orbits at any desired inclinations.

It is desirable to minimize the number of planes even at the expense of more spacecraft. A spare spacecraft is often placed in each plane. In the event of a failure the spare spacecraft can be maneuvered into the position of the failed machine. Recall that it requires far more energy to change planes than to maneuver in-plane. Fewer planes also facilitate bringing the constellation on line. Initial service can often be started with one spacecraft per plane.¹¹ Fewer planes also mean smaller impact from a single spacecraft failure.

Launch vehicle costs go up nonlinearly with altitude. Hence, low orbits are more desireable than high orbits. It is obvious that fewer spacecraft are cheaper than many.

There has been considerable research into constellations for continuous global coverage. In the 1960s Easton and Brescia researched constellations with two perpendicular orbit planes and concluded that it would take six spacecraft to provide continuous coverage.⁴⁰

In the 1970s Walker researched constellations of circular orbits with equal altitudes and inclinations and concluded that complete coverage could be done with five spacecraft.¹⁹ In the 1980s Draim found and patented a constellation of elliptical orbits that require only four spacecraft for full coverage.^{11,42}

Walker Constellations

Walker's work is extensive, and a constellation of regularly spaced, circular orbits with equal altitudes and inclinations is often called a Walker constellation. Walker constellations are described with a three-number notation:

t = total number of spacecraft

p = number of orbit planes

f = relative spacing between spacecraft in adjacent planes, any integer from zero to $p - 1$

The parameters t , p , and f , plus inclination, fully define a Walker constellation. In a 15,5,1 constellation, the number of spacecraft in a plane is t/p or 3. The spacing of the ascending nodes about the equator is $360/p$ or 72° . The spacing of spacecraft in any plane is $360/3$ or 120° . The phase angle between spacecraft in adjacent planes ϕ is

$$\phi = 360f/t \quad (4.28)$$

For a 15,5,1 constellation, $\phi = 24$ deg. (A 15,5,1 Walker constellation at 65-deg inclination is described fully in Ref. 11, pp. 190, 191.)

Spacing

The key parameter in spacecraft and orbit plane spacing is the central half-angle α_h ; see Fig. 4.13. (Note that the central angle $2\alpha_h$ is given by the ORBWIN

OBSERVING THE CENTRAL BODY

77

software field of view function.) The central half-angle is the radius of the field of view circle on the surface of the Earth, which in turn describes how much of the surface is covered from a given position. When the central angle is 90 deg, one quarter of the planet surface is being covered; therefore, two orbit planes at an altitude that gives a central angle of at least 90 deg can cover the entire surface (given enough spacecraft in each orbit). Any orbit altitude that produces a central angle less than 90 deg requires at least three orbit planes for global coverage. The altitude corresponding to a central angle of 90 deg can be calculated from Eq. (4.15), which can be rearranged as follows:

$$r = R_s / \cos \alpha_h \quad (4.29)$$

For an Earth orbit and $\alpha_h = 45$ deg

$$r = 6378.14 / 0.7071 = 9020 \text{ km}$$

Therefore, constellations with orbital altitudes greater than 2642 km can be designed for global coverage with two planes. Note, however, that a constellation with altitude 2642 km and two planes will not give continuous global coverage because the field of view circles would be tangent at best and could not overlap.

Example 4.8 Constellation Design

Design a constellation to meet the following requirements:

- 1) Provide continuous global coverage (at least one spacecraft in view at all times from any point on Earth)
- 2) Maintain circular polar orbits

The equatorial geometry will control the design. The objective is to make the equatorial spacing just barely provide coverage; there will be overlapping coverage at all other locations on the globe. It is often possible to compromise the coverage requirements in the equatorial region to reduce overlap elsewhere. However, in this example we will take the requirement literally. One efficient equatorial geometry is shown in Fig. 4.17.

The geometry in Fig. 4.17 defines a family of continuous coverage constellations since

$$\alpha_h = \frac{360}{1.732p} = \frac{207.85}{p} \quad (4.30)$$

where p is the number of planes in a constellation (p must be an integer greater than one) and

$$s = 360/\alpha_h \quad (4.31)$$

where s is the number of spacecraft in an orbit. Note that s must be rounded up to the next integer. By setting the number of planes equal to the integers from two to eight, the characteristics of this family of constellations may be calculated; see Table 4.5. (The number of planes can be incremented upward, beyond eight, until the resulting radius is subsurface.) Note that α_h cannot be larger than 90 deg.

**Table 4.5 Some continuous global coverage constellations
(Circular polar orbits)**

Planes	Spacecraft per plane	α_h , deg	Altitude, km
2	7	51.95	3970
3	11	34.63	1373
4	14	25.98	717

One of the compromises in constellation design is evident from Table 4.5. The desirability of fewer planes would indicate two planes; however, high orbits entail substantially higher launch vehicle costs. With cost data on launch vehicles and spacecraft a selection of least expensive constellations could be made.

In this example it was assumed that the spacecraft instruments could use the spacecraft field of view from horizon to horizon. This is not normally the case (see Fig. 4.15). Accounting for realistic instrument field of view increases the number of spacecraft required.

Problems

- 4.1** The orbit of the GOES-B spacecraft has the following elements:

$$\begin{aligned} \text{Inclination} &= 28.8 \text{ deg} \\ \text{Eccentricity} &= 0.732 \\ \text{Period} &= 10.6 \text{ h} \end{aligned}$$

What are the rotation of apsides and regression of nodes?

- 4.2** The Russian communication spacecraft Molniya has the following orbital elements:

$$\begin{aligned} \text{Perigee altitude} &= 300 \text{ km} \\ \text{Inclination} &= 63.4 \text{ deg} \\ \text{Semimajor axis} &= 26,562 \text{ km} \\ \text{Longitude of ascending node} &= 120^\circ \text{ West} \\ \text{Argument of perigee} &= 270 \text{ deg} \end{aligned}$$

If the current spacecraft position is at a true anomaly of 170 deg, what are the current latitude and longitude? What is the spacecraft swath width from this position?

- 4.3** A constellation of global positioning satellites was launched in the 1990s to provide accurate worldwide position data. The constellation contains six orbit planes, each at an inclination of 55 deg. The circular orbits will be at an altitude of 20,182 km. How many spacecraft were placed on each orbit to provide continuous coverage along the ground track?

OBSERVING THE CENTRAL BODY

79

4.4 The Viking Mars orbiter had an orbital period of 24.8 h (one Martian day) and a periapsis altitude of 1500 km. The infrared thermal mapper instrument, carried by the orbiter, had a field of view of 3 deg; what was the swath width of the instrument when the true anomaly was 23 deg?

4.5 What is the maximum communication time and distance between the Viking orbiter and lander if the orbiter passes directly over the lander at periapsis?

4.6 The encounter hyperbol of the Voyager spacecraft at Neptune had an eccentricity of 2.4586. What was the width of the horizon (swath width) as the spacecraft streaked over the north pole at a periapsis altitude of 4850 km?

This page intentionally left blank

5

Special Earth Orbits

In this chapter the mission designs of four important orbit types—geosynchronous, sun-synchronous, Molniya, and low Earth—are analyzed.

5.1 Geosynchronous Orbit

A spacecraft in a circular, equatorial orbit with a period equal to one sidereal day has a rotation rate exactly equal to the rotation rate of the Earth's surface directly below. The spacecraft appears to be stationary as observed from Earth. This is called a geosynchronous orbit. The north polar view of a geosynchronous orbit is shown to scale in Fig. 5.1. Positions on this orbit are so important commercially that they are rationed by international agreement. Most of the world's communications satellites and meteorological satellites are positioned on this ring.

The importance of this orbit was well understood long before it could be reached. Arthur C. Clarke emphasized what could be accomplished from such an orbit in 1945 in an essay in *Wireless World*.²¹ It was 1963, however, before launch vehicle and electronics technology would enable the world's first geosynchronous satellite,

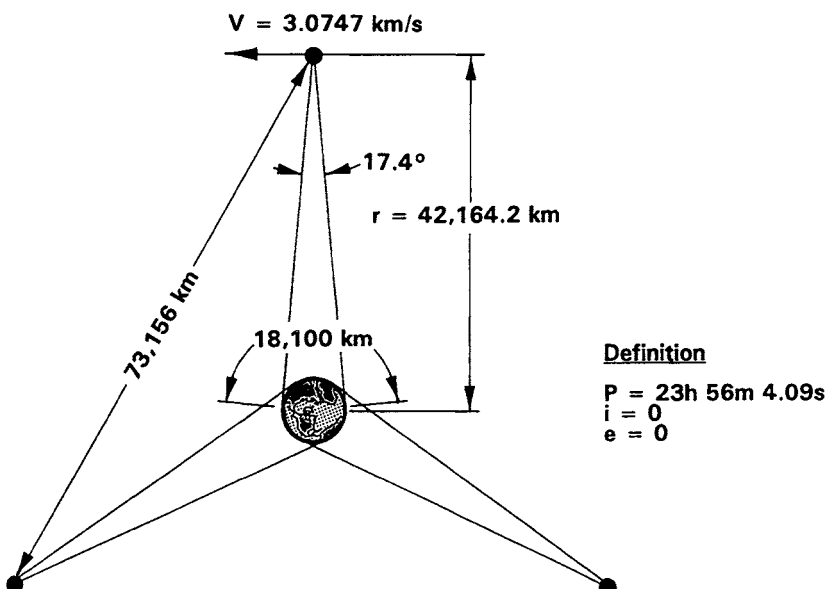


Fig. 5.1 Geosynchronous orbit.

Syncom II. In 1964 Syncom III brought the Olympic games directly from Japan to the United States in real time, a feat that had never before been possible.

Geosynchronous Mission Design

By definition, the period of a geosynchronous orbit must be equal to the time required for the Earth to rotate once with respect to the stars. This period is one sidereal day and is 23 h 56 min 4.09 s, or 86,164.09 s, long.

Equation (2.7) can be rearranged to yield the radius of a circular orbit given the period:

$$r = (P^2 \mu / 4\pi^2)^{1/3} \quad (5.1)$$

From Eq. (5.1) the radius of a geosynchronous orbit can be obtained as follows:

$$r = [(86,164.09)^2 398,600.4 / 4\pi^2]^{1/3} = 42,164.17 \text{ km}$$

$$h = r - R_0$$

$$h = 42,164.17 - 6378.14 = 35,786 \text{ km}$$

Surprisingly, placing a spacecraft in geosynchronous orbit requires as much energy as launching a planetary flight. As shown in Fig. 5.2, four distinct velocity changes are required:

- 1) Launch to low Earth orbit
- 2) Hohmann transfer from the parking orbit to $r = 42,164.2 \text{ km}$
- 3) Plane change from $i = 28.5 \text{ deg}$ to the equatorial plane
- 4) Circularization of the transfer ellipse to form the geosynchronous orbit

Launch to Low Earth Orbit

A launch to geosynchronous orbit would be made due east out of ETR (for a U.S. spacecraft) to: 1) take advantage of the Earth's rotational velocity and 2) provide the minimum orbit inclination. In a typical launch, the Space Shuttle accelerates

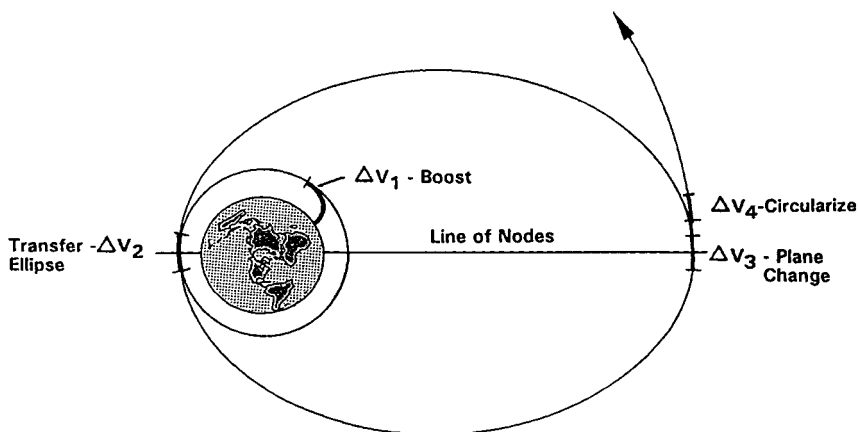


Fig. 5.2 Velocity increments needed to achieve geosynchronous orbit.

SPECIAL EARTH ORBITS

83

the spacecraft to a 280-km circular parking orbit. The velocity of the spacecraft in the parking orbit, from Eq. (2.6), is

$$V = \sqrt{\mu/r} = \sqrt{398,600.4/6658.14} = 7.737 \text{ km/s}$$

The launch vehicle contributes 7.329 km/s, and the rotation of the Earth contributes 408 m/s. In addition, the launch vehicle contributes the potential energy of the spacecraft and the substantial energy that goes to gravity and drag losses.

Parking Orbit to Transfer Ellipse

The perigee radius of the Hohmann transfer ellipse must be tangent to the parking orbit. The apogee radius must be 42,164.2 km to match the geosynchronous orbit; thus, the semimajor axis is 24,411.2 km. The line of apsides must be in the equatorial plane, so that the apogee will be a point in the geosynchronous orbit. Therefore, the velocity increase needed to change the parking orbit to the transfer ellipse must take place on the equator. An upper stage usually performs this burn at the first equatorial crossing. Note that two impulses are required of this stage. A single stage with restart capability or two stages are required.

The velocity at the perigee of the transfer ellipse is, from Eq. (2.14),

$$V_p = \sqrt{\frac{2(398,600.4)}{6658.14} - \frac{398,600.4}{24,411.2}}$$

$$V_p = 10.169 \text{ km/s}$$

The required velocity increase is

$$\Delta V_2 = 10.169 - 7.737 = 2.432 \text{ km/s}$$

Plane Change and Circularization

A plane change is required to rotate the transfer ellipse from an inclination of 28.5 to 0 deg. Equation (3.7) shows that to conserve energy it is important to make the plane change at the lowest velocity that will occur on the entire mission. The lowest velocity occurs at the apogee of the transfer ellipse; that velocity is

$$V_a = \sqrt{\frac{2(398,600.4)}{42,164.2} - \frac{398,600.4}{24,411.2}}$$

$$V_a = 1.606 \text{ km/s}$$

Apogee velocity could also be obtained from Eq. (2.33):

$$r_p V_p = r_a V_a$$

$$V_a = r_p V_p / r_a = 6658.14(10.169)/42,164.2$$

$$V_a = 1.606 \text{ km/s}$$

The velocity change that would be required to make a 28.5-deg plane change at a velocity of 1.606 km/s is 0.791 km/s. Note that if the plane change were made after

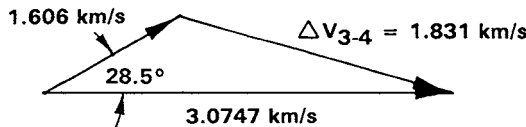


Fig. 5.3 Vector diagram for the final impulse.

circularization, the velocity change required would be 1.514 km/s. In practice, the plane change is combined with the circularization burn because

- 1) Less ΔV is required with a combined burn.
- 2) A solid motor can be used for the burn if restart is not required.

The solid motor that performs this burn is often called a kick stage.

The velocity on a geosynchronous orbit is

$$V = \sqrt{398,600.4/42,164.2} = 3.0747 \text{ km/s}$$

The vector diagram for the combined maneuver is shown in Fig. 5.3. From the law of cosines [see Eq. (3.2)], the velocity change required for the combined maneuver is 1.831 km/s. Note that if two individual maneuvers were used, the velocity change required would have been 2.260 km/s. It is always advantageous to combine individual burns in this fashion; watch for plane changes that can be combined with in-plane maneuvers.

The total velocity change required to place a spacecraft in geosynchronous orbit is 12.0 km/s as shown below:

ΔV_1 boost to parking orbit	= 7.737
ΔV_2 for transfer ellipse	= 2.432
ΔV_3 and V_4 plane change and circularization	= 1.831
Total ΔV	12.000 km/s

The required total ΔV will vary slightly with the selection of parking orbit altitude. If we had chosen a 180-km parking orbit altitude, the total ΔV would have been 12.09 km/s. The parking orbit altitude is usually chosen to accommodate launch vehicle constraints rather than ΔV considerations.

View from Geosynchronous Orbit

As shown in Fig. 5.4, three spacecraft positioned on this orbit can observe the Earth's entire surface except for the extreme polar regions. The horizon angle from a geosynchronous spacecraft can be obtained from Eq. (4.16):

$$\sin \beta = 6378.14/42,164.17 = 0.15127$$

$$\beta = 8.70 \text{ deg} = 0.518 \text{ rad}$$

The broad expanse shown in Fig. 5.4 represents a field of view of only 17.4 deg to the spacecraft. Figure 5.1 shows why this is true.

The central angle is, from Eq. (4.15),

$$\cos \alpha = 0.15127$$

$$\alpha = 81.30 \text{ deg} = 1.4189 \text{ rad}$$

SPECIAL EARTH ORBITS

85

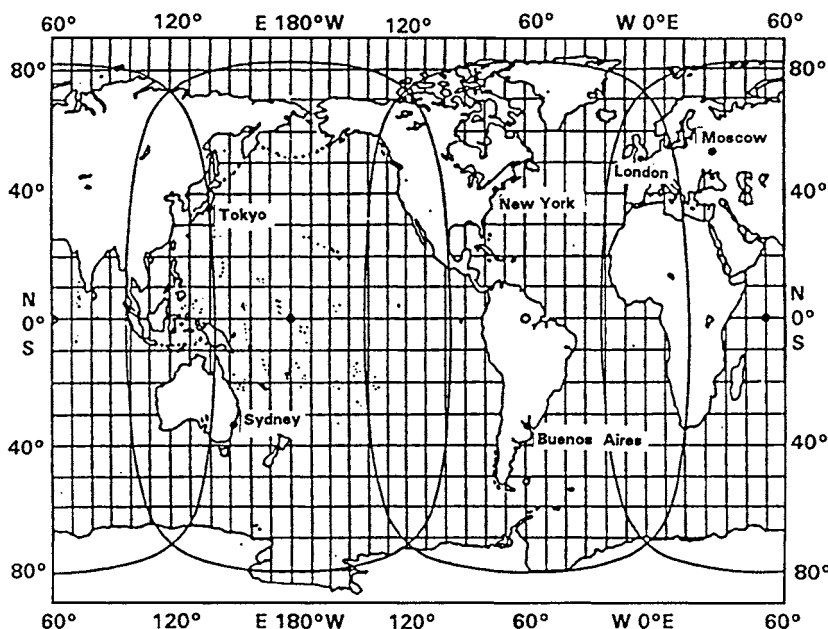


Fig. 5.4 View from geosynchronous orbit.

The swath width is, from Eq. (4.18),

$$S_w = (2)(1.4189)(6378.14) = 18,100 \text{ km}$$

The horizon circles shown in Fig. 5.4 are 18,100 km across, a vast field of view.

Orbital Errors

Once in orbit the spacecraft should occupy a fixed longitude position at zero latitude. Any errors made by the launch vehicle or the kick stage will result in apparent motion of the spacecraft as summarized in Table 5.1. The spacecraft must have propulsion capability to correct these errors.

Table 5.1 Geosynchronous orbital errors

Error	Apparent motion
Radius too long	Westward drift at 0.013 deg/day/km
Radius too short	Eastward drift at 0.013 deg/day/km
$e \neq 0$	East/west reciprocating drift amplitude = $2e$
$i \neq 0$	North/south figure eights amplitude = $2i$

Source: Ref. 22, pp. 68–70.

Radius errors. Since orbit period is critical to this mission, it is not surprising that an accurate radius is critical. A 1-km error in radius would produce a period error of about 3 s. At the end of the first day, the spacecraft would be about 9.2 km out of position. At geosynchronous altitude 1° of longitude is equivalent to 735.9 km; therefore, a drift of 9.2 km/day would be about 0.013° of longitude per day. If the radius is long, the orbit period is long, and the drift is westward. Conversely, if radius is short, the period is short, and the drift is eastward. Note that this type of error increases continuously with time.

As shown in Fig. 5.5, to correct the radius, a Hohmann transfer ellipse is established from the current radius to the desired radius; then the orbit is circularized at the correct radius. Two velocity changes, equal in magnitude and opposite in direction, are required.

Eccentricity errors. An eccentricity greater than zero indicates that an error was made in circularization and that an elliptical orbit has been established. If the orbit period is correct, then the semimajor axis is correct, and we have the situation shown in Fig. 5.6. This error produces a reciprocating drift in longitude with an amplitude of $2e$.²² Correcting this error requires a general coplanar maneuver at one of the intersections shown in Fig. 5.6.

Inclination error. If the orbit plane is not in the equatorial plane, a north-south figure eight motion will be produced. Correcting this error requires a simple plane change maneuver described by

$$\Delta V = 2V \sin i/2 \quad (5.2)$$

where

V = orbital velocity, 3.0747 km/s

i = inclination angle, deg

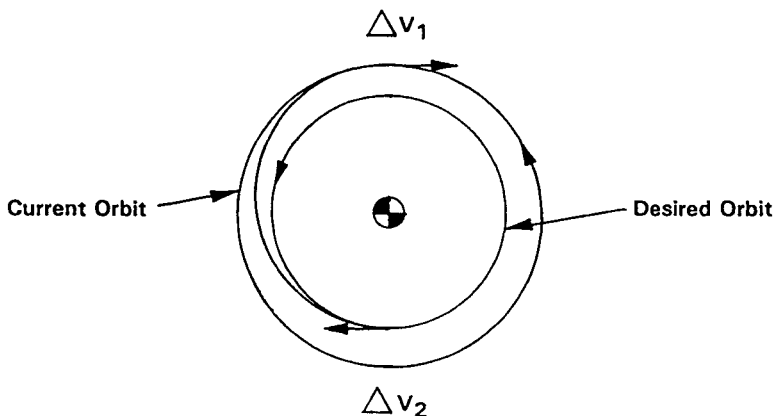


Fig. 5.5 Correcting radius error.

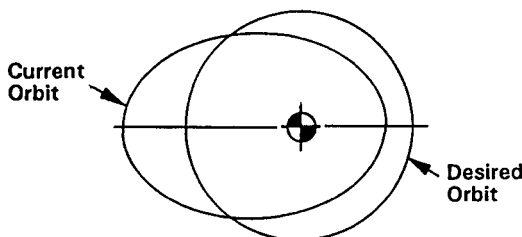


Fig. 5.6 Eccentricity error.

Perturbations. In addition to launch errors, orbital errors are introduced continuously by the Earth's bulge, the attraction of the sun, the attraction of the moon, and solar pressure. The spacecraft propulsion system must also make periodic corrections for these perturbations. These correction maneuvers are called station keeping; they are performed as previously described. The tighter the position tolerance, the more station-keeping maneuvers.

Repositioning

It may also be necessary to change the position of the satellite. This is done by increasing or decreasing the velocity of the spacecraft to produce an elliptical orbit. If velocity is increased, the position of the impulse will become the perigee; if the velocity is decreased, the position of the decrease will become the apogee.

Consider a velocity increase of 1 m/s. The point of impulse will become the perigee, and the new, higher velocity will be $V_p = 3.0757$ km/s. The semimajor axis will be 42,191.64 km, an increase of 27.47 km. The period will increase by 84.22 s. The drift will be 84.22×3.0747 km/s = 258.95 km westward each day. The longitudinal drift rate is

$$\frac{258.95(360)}{2\pi(42,164.2)} = \frac{0.3518^\circ\text{s}}{\text{m-day}}$$

When the spacecraft has drifted to the proper position, a 1-m/s velocity decrease will be necessary. The impulse must occur at the perigee, exactly where the increase in velocity took place. Note that if eastward repositioning is desired, the preceding process is reversed. An excellent description of orbit errors, repositioning, and station keeping is given by Agrawal.²²

5.2 Sun-Synchronous Orbit

The sun-synchronous orbit is an Earth orbit with the curious property of providing a constant sun angle for the observation of Earth. A constant sun angle is very desirable for cameras and other instruments that observe reflected light.

A sun-synchronous orbit is designed by matching the regression of nodes to the rotation of the Earth around the sun. For example, assume that a polar spacecraft is launched with the orbit plane on an Earth–sun line, as shown in Fig. 5.7. As the Earth travels around the sun, the orbit plane would depart from the sun line by 360 deg during the 365 days required to make a complete orbit. The orbit plane would depart from the sun line at a clockwise rate of about 1 deg per day. In 90

SPACECRAFT MISSION DESIGN

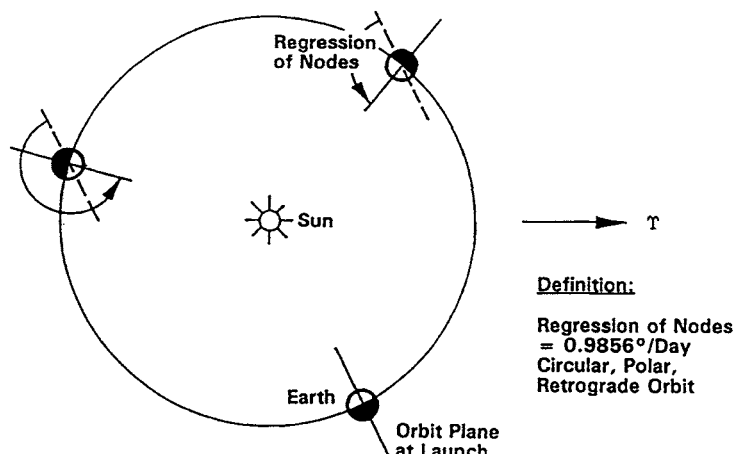


Fig. 5.7 Sun-synchronous orbit.

days the orbit plane would be perpendicular to the sun line. However, suppose we design the orbit such that its regression of nodes is equal and opposite the mean daily motion of

$$360 \text{ deg}/365.242 \text{ days} = 0.9856 \text{ deg/day}$$

In such a case the orbit plane would always be on a sun line. So how do we get a regression of nodes of -0.9856 deg/day ? From Eq. (4.3) it can be seen that there is a range of orbital inclinations and altitudes that will produce the proper regression of nodes. This range is shown in Fig. 5.8. Note that a sun-synchronous orbit must be retrograde.

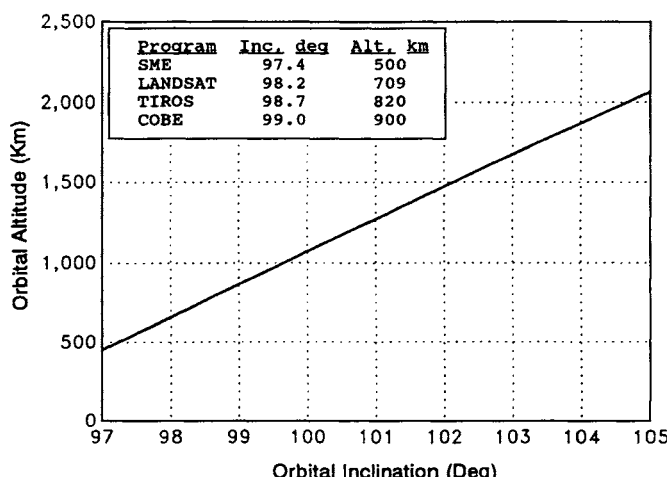


Fig. 5.8 Orbital inclinations and altitudes for sun-synchronous orbits.

SPECIAL EARTH ORBITS

89

LANDSAT is probably the best-known sun-synchronous spacecraft. LANDSAT D was placed in a 709-km-altitude orbit with a 98.2-deg inclination.¹⁷ Circling the globe every 103 min, its sensors view a 185-km strip of the surface running nearly north and south. It covers the entire surface of the Earth every 20 days. The spacecraft crosses the equator at 9:30 a.m. local time every orbit. The spacing of the swath is 138 km at the equator. This orbit produces a consistent and constant lighting of the Earth, the best condition for an imaging system.

5.3 Molniya Orbit

The Molniya orbit, shown in Fig. 5.9, was devised by the USSR to provide features of a geosynchronous orbit with better coverage of the northern latitudes and without the large plane change that would be required from their far northern launch sites. The approximate orbital elements are as follows:

$$P = 43,082 \text{ s (one half of a sidereal day)}$$

$$a = 26562 \text{ km}$$

$$i = 63.4 \text{ deg}$$

Viewed in Earth-fixed coordinates, the orbit rises alternately above the North American continent and the Eurasian continent. As shown in Fig. 5.10, a Molniya spacecraft alternates 12-h periods above each continent.

The time ticks in Fig. 5.10 show that the spacecraft spends most of its time in the high-altitude portion of the orbit. There is an 8-h period over the North American continent each day when Eurasia is also in view. During that period, a single spacecraft can serve as the communication link between continents. A constellation of three spacecraft would provide a continuous direct link. The Molniya ground track is shown in Fig. 5.11. The orbit retraces this ground track each day. Although

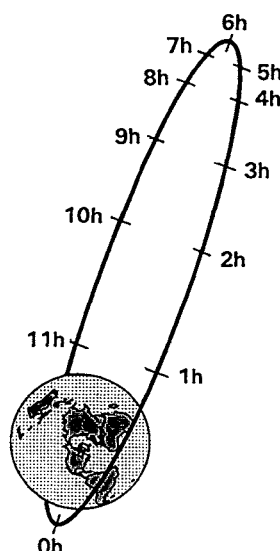


Fig. 5.9 Molniya orbit.

SPACECRAFT MISSION DESIGN

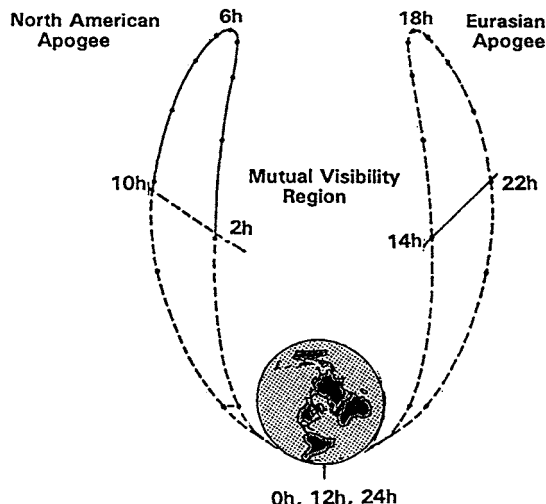


Fig. 5.10 Molniya orbit in Earth-fixed coordinates.

it does not hover in a fixed position as a geosynchronous spacecraft would, it holds a regional position for eight hours a day in two important regions.

A Molniya orbit requires only two impulses to become established:

- 1) Launch to parking orbit
- 2) Velocity increase at perigee to establish the ellipse

Launch to Parking Orbit

A launch due east from Plesetsk, the busiest launch site on Earth, would produce a parking orbit with an inclination of 62.8 deg. A small adjustment in azimuth will produce an inclination of 63.4 deg and thereby eliminate rotation of apsides. The

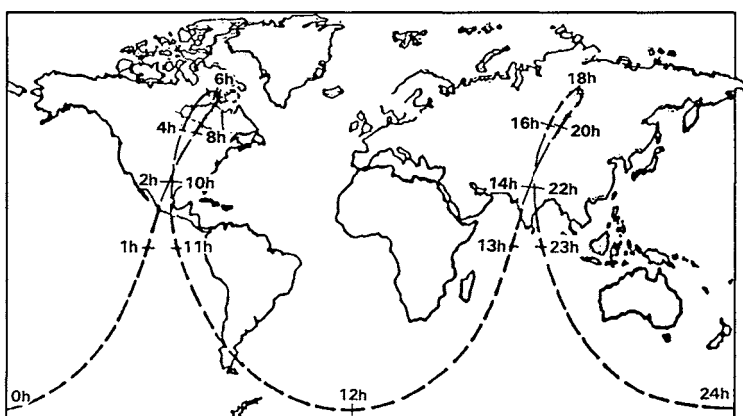


Fig. 5.11 Molniya ground track.

Earth's rotational assist at Plesetsk is 200 m/s compared to 408 m/s for a launch from ETR.

The parking orbit altitude is important because, unlike the geosynchronous orbit, the parking orbit radius becomes the perigee radius of the final orbit. The parking orbit must be high enough to minimize drag; 300 km is an adequate altitude. Several different perigee altitudes have been used; consider the 504-km altitude used by Molniya 1-73.²³ The velocity change for a 504-km parking orbit would be 7.610 km/s.

Parking Orbit to Final Orbit

The orbit period must be half of a sidereal day, or 43,082 s. The semimajor axis, computed directly from the period, must be 26,562 km. Any combination of apogee and perigee radii with a semimajor axis of 26,562 km will have the correct period. The simplest design is one with a perigee radius the same as, and tangent to, the parking orbit radius, which we have assumed to be 6882 km. Therefore, the apogee radius must be 46,241 km. The perigee velocity is 10.04 km/s for this orbit. The velocity increase to place a spacecraft on this orbit is 2.43 km/s from a 504-km parking orbit.

There is no plane change or circularization required. The Molniya orbit requires a ΔV of 2.43 km/s, above the parking orbit velocity, compared to 5.175 km/s for a geosynchronous orbit from Plesetsk. This energy difference translates into twice as much spacecraft mass in a Molniya orbit than in a geosynchronous orbit (for a given launch vehicle—the normal situation).

Table 5.2 compares the example design with two actual Molniya orbits.

5.4 Low Earth Orbit

Low Earth orbits are simple to design but nonetheless important because of their extensive use. Figure 5.12 shows the spacecraft crowd in low Earth orbit.²⁴ Of the 2390 spacecrafts in orbit at the end of 1996, more than 90% were in low Earth orbit.²³ It is clear from Fig. 5.12 why there is growing concern about debris in low Earth orbit.

The low-Earth-orbit family is bounded on the low end by drag considerations. Atmospheric drag places the lower limit at about 200 km. Drag at perigee lowers apogee, which increases drag and ultimately leads to re-entry. The early re-entry of Skylab is one such example. Spacecraft drag is impossible to predict accurately because of uncertainties in the time variance of upper atmospheric density.

Table 5.2 Some Molniya orbits

Spacecraft	i , deg	h_p , km	h_a , km	P , s
Molniya 1-74	62.8	623	39,721	43,044
Molniya 1-73	63.1	504	39,834	43,068
Example	63.4	504	39,863	43,082

Source: Ref. 23, pp. 59 and 62.

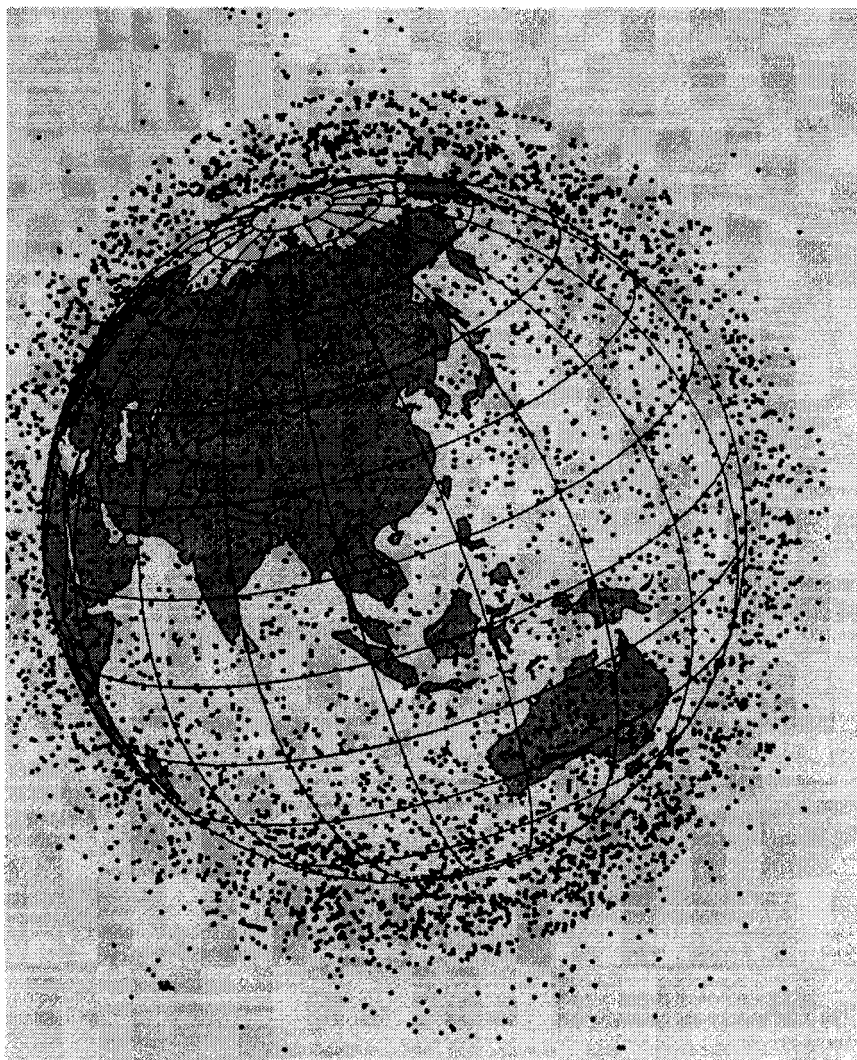


Fig. 5.12 Crowd in low Earth orbit.

These orbits are used because of the low energy required for the launch vehicle and because low Earth orbit can be reached without a restart capability in the upper stage. (It is impractical to reach an orbit over about 1000 km without using a parking orbit and a Hohmann transfer.)

The Space Shuttle and most other manned spacecraft inhabit low Earth orbit in the relatively radiation-free corridor above 200 km and below 600 km. The orbit is also used for atmospheric research, surveillance, Earth resources research, astronomy, and other similar pursuits.

Problems

- 5.1** Design a mission to place a spacecraft in a geosynchronous equatorial orbit from the Russian launch site at Plesetsk. How much velocity change is required? Compare the result with an ETR launch.
- 5.2** Design a geosynchronous orbit for Mars. Give radius, inclination, eccentricity, period, and horizon angle.
- 5.3** An Earth communications satellite has attained an equatorial orbit. However, the apogee altitude is 41,756 km, and the eccentricity is 0.0661. What is the minimum velocity change required to place the satellite in geosynchronous orbit if the altitude requirement is $35,786 \pm 1$ km?
- 5.4** The mean daily motion of Mars is 0.5240 deg/day. Design a sun-synchronous orbit for Mars. Give altitude, inclination, and regression of nodes. The requirement is to match the mean daily motion within 0.01 deg.
- 5.5** What is the maximum radius for a circular sun-synchronous Earth orbit? Why?

This page intentionally left blank

6

Interplanetary Trajectories

Humans have been on Earth for at least 500,000 years. For most of that period they have puzzled over the planets; for the last 35 years we have had the ability to explore these worlds with spacecraft. Understanding interplanetary trajectories was one of the most interesting achievements underlying that capability. This chapter discusses how an interplanetary mission is analyzed and designed.

A brief review of the pertinent geometry of the solar system is in order. Figure 6.1 shows an isometric view of the ecliptic plane with the nine planets in their positions as of January 1, 1992, rotating in direct, slightly elliptical, slightly inclined orbits around the sun. The distances involved are so enormous that two different scales are required to accommodate all planets on one page. The semimajor axis of the Earth's orbit is 149.597870×10^6 km,¹² a distance that is called an astronomical unit (AU). The length of an astronomical unit is shown for both scales used in Fig. 6.1.

As shown in Table 6.1, the perihelion distances vary from 46 million km for tiny Mercury to over 4 billion km for Neptune and Pluto. Pluto is the maverick planet; the inclination of its orbit, 17 deg, is two and a half times greater than that of its nearest rival, and its orbit is so eccentric ($e = 0.25$) that at times Neptune is the outer planet.

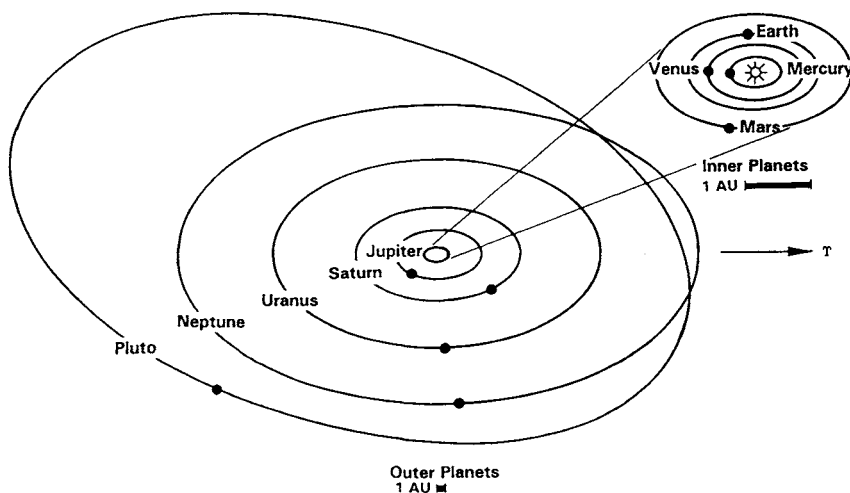


Fig. 6.1 Solar system.

Table 6.1 Mean orbital parameters of the planets

Planet	a , AU	r_p , $\times 10^6$ km	e	i , deg	Velocity, km/s
Mercury	0.387	45.99	0.2056	7.005	47.89
Venus	0.723	107.43	0.0068	3.395	35.05
Earth	1.000	147.10	0.0167	0.001	29.77
Mars	1.524	206.72	0.0933	1.850	24.13
Jupiter	5.203	740.84	0.0482	1.305	13.05
Saturn	9.516	1345.02	0.0552	2.487	9.64
Uranus	19.166	2729.29	0.0481	0.772	6.80
Neptune	30.011	4447.85	0.0093	1.772	5.43
Pluto	39.557	4436.42	0.2503	17.150	4.73

Source: Ref. 12, p. E3; Ref. 25, pp. 14, 15, and Ref. 26, p. 17.

The slight eccentricities of these orbits means that not only are the distances large, but they are time variant. These eccentricities also imply that planetary arrivals and departures must take into account flight path angles.

The planets are not quite in the ecliptic plane. The significance of the inclination of these orbits is that a plane change at high speed must be accounted for in mission design.

The velocities shown in Table 6.1 are the mean velocities of the planets around the sun; since the orbits are elliptical, the velocities are time variant. The velocity of the planets are large compared to the velocities that launch vehicles can provide. It would not be possible to send spacecraft to the planets without taking advantage of the orbital velocity of the Earth; the contribution of the launch vehicle is minor in comparison.

In Table 6.1, semimajor axis, eccentricity, and inclination are given as of January 24, 1991 (JD 244 8280.5) and refer to the mean ecliptic and equinox of J2000.0. The orbital elements of the planets change slowly with time. For precise work *The Astronomical Almanac* should be consulted.¹²

6.1 Patched Conic Approximation

A planetary trajectory is a four-body motion involving the Earth, the target planet, the sun, and the spacecraft. It would be possible and proper to use an N -body simulation to study the trajectory; however, there are numerous disadvantages in this approach. The patched conic technique is a brilliant approximation of this four-body motion; it provides adequate accuracy for almost all purposes.

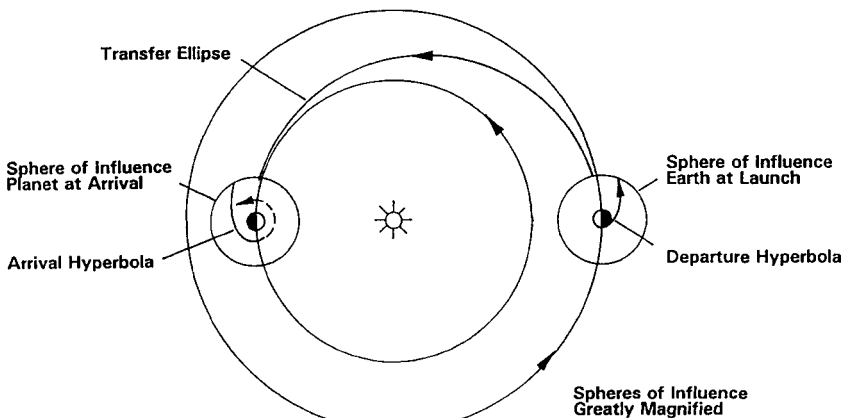
The patched conic approximation subdivides the planetary mission into three parts (see Fig 6.2):

1) *The departure phase*, in which the two relevant bodies are Earth and the spacecraft. The trajectory is a departure hyperbola with Earth at the focus. The influences of the sun and target planet are neglected.

2) *The cruise phase*, in which the two bodies are the sun and the spacecraft. The trajectory is a transfer ellipse with the sun at the focus. The influences of the planets are neglected.

INTERPLANETARY TRAJECTORIES

97

**Fig. 6.2 Patched conic orbit.**

3) *The arrival phase*, in which the two bodies are the target planet and the spacecraft. The trajectory is an arrival hyperbola with the planet at the focus. The influences of the sun and Earth are neglected.

An arbitrary sphere of influence is defined about the Earth and the target planet. The transfer ellipse is “patched” to the hyperbolas at the boundaries of the spheres of influence. The radius of the sphere of influence suggested by Laplace is^{3,15}

$$R_s \approx R \left(\frac{M_{\text{planet}}}{M_{\text{sun}}} \right)^{2/5} \quad (6.1)$$

where

R_s = radius of the sphere of influence of a planet

R = mean orbital radius of the planet

M_{planet} = mass of the planet

M_{sun} = mass of the sun

At radius R_s the gravitational attractions of the planet and the sun are approximately equal. Other definitions of R_s are possible; specifically, an exponent of 1/3 rather than 2/5 is sometimes used in Eq. (6.1). Fortunately, a precise definition of sphere of influence is not critical to planetary trajectory design.

Table 6.2 shows the sphere of influence values found by using the Laplace method. Inside the sphere of influence, spacecraft times and positions are calculated on the departure or arrival hyperbola. Outside the sphere, times and positions are calculated on the transfer ellipse.

Technically, the transfer ellipse should be designed to terminate at the boundary of the sphere of influence. However, the sphere of influence is so small compared to the transfer ellipse that this small correction is negligible. For example, the true anomaly on the transfer ellipse at Earth should be reduced by 0.15 deg to account for Earth’s sphere of influence.

It is important to remember that the actual trajectory converts smoothly from the departure hyperbola to the transfer ellipse and back to the arrival hyperbola.

Table 6.2 Sphere of influence

Planet	$R_s, \times 10^6 \text{ km}$
Mercury	0.111
Venus	0.616
Earth	0.924
Mars	0.577
Jupiter	48.157
Saturn	54.796
Uranus	51.954
Neptune	80.196
Pluto	3.400
Moon	0.0662

Nonetheless, the patched conic technique is a surprisingly accurate approximation—accurate enough for all but the most demanding work (e.g., navigation).

6.2 Highly Simplified Example

To get an overview of a planetary mission, consider the simplest possible case. Take a mission to Venus as an example, and assume the following:

1) The planetary orbits are circular. This assumption will allow the use of mean orbital velocities without the complication of velocity variation and flight path angles.

2) The orbits are coplanar. This assumption will eliminate plane changes. Venus can be arbitrarily placed at arrival such that it is diametrically opposed to the Earth position at departure, thereby eliminating the ephemeris calculations and making the transfer ellipse tangent to the planetary orbits. The resulting trajectory is a simple Hohmann transfer on a grand scale, as shown in Fig. 6.3. The velocities, radii, and positions shown in Fig. 6.3 are given with respect to the sun and are mean values assuming circular orbits.

The periapsis of the transfer ellipse is equal to the radius of the Venus orbit, and the apoapsis radius is equal to the radius of the Earth orbit. The transfer orbit elements can readily be calculated:

$$\begin{aligned} r_a &= 149.59 \times 10^6 \text{ km}, & V_a &= 27.29 \text{ km/s} \\ r_p &= 108.21 \times 10^6 \text{ km}, & V_p &= 37.73 \text{ km/s} \\ a &= 128.90 \times 10^6 \text{ km}, & P &= 292 \text{ days} \\ e &= 0.1605 \end{aligned}$$

The spacecraft velocity at departure must be equal to the apoapsis velocity on the transfer ellipse, or 27.29 km/s. The arrival velocity will be the periapsis velocity, 37.73 km/s. The time of flight will be half the transfer orbit period, or 146 days.

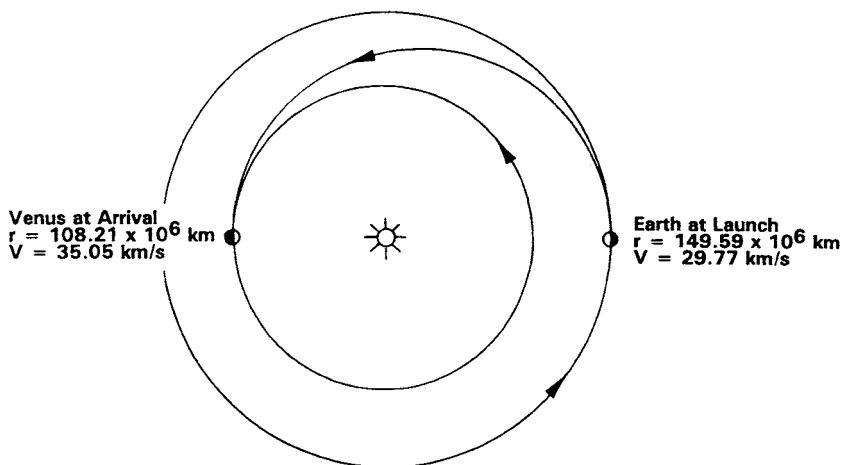


Fig. 6.3 Simplified Venus trajectory.

Hyperbolic Excess Velocity and C3

The vector difference between the velocity of the Earth with respect to the sun and the velocity required on the transfer ellipse is called the hyperbolic excess velocity V_{HE} (see Fig. 6.4). The hyperbolic excess velocity is V_∞ on the departure hyperbola. Recall that the velocity at infinity along a hyperbolic trajectory is the excess amount above the escape velocity (hence the name). In Fig. 6.4,

$V_{s/s}$ = required velocity of the spacecraft with respect to the sun on the transfer ellipse

$V_{e/s}$ = velocity of the Earth with respect to the sun

V_{HE} = hyperbolic excess velocity, which is the required spacecraft velocity with respect to the Earth

α = included angle between $V_{s/s}$ and $V_{e/s}$

In this example it has been assumed that the transfer ellipse and the Earth's orbit are tangent and coplanar; therefore, the included angle α is zero and

$$\begin{aligned} V_{HE} &= V_{s/s} - V_{e/s} \\ V_{HE} &= 27.29 - 29.77 = -2.48 \text{ km/s} \end{aligned} \quad (6.2)$$

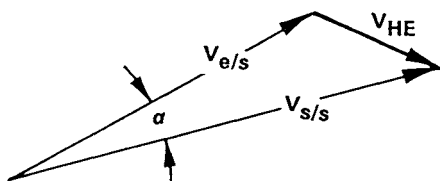


Fig. 6.4 Definition of hyperbolic excess velocity.

Table 6.3 C3 required for various missions

Mission	C3, km ² /s ²
Venus, 1986	11
Mars, 1990	17
Jupiter, 1987	80
Ulysses, 1986	123

V_{HE} is negative for a Venus mission or for any mission to an inner planet, indicating that the Earth's orbital velocity must be reduced to enter the transfer ellipse.

The hyperbolic excess velocity is important because it is a measure of the energy required from the launch vehicle system. It is traditional to use C3, which is V_{HE}^2 , as the major performance parameter agreed on between the launch vehicle system and a planetary spacecraft.

From the point of view of the spacecraft, C3 comes from a mission design calculation as previously shown and represents the minimum energy requirement needed to accomplish the mission. Table 6.3 shows some typical C3 requirements. From the point of view of the launch vehicle, C3 is computed as the maximum energy the launch vehicle can deliver carrying a spacecraft of a given weight. Hopefully the launch vehicle C3 capability at the expected spacecraft weight will be above the C3 required for the mission.

V_{∞} at the Planet

When the spacecraft arrives at the target planet, a velocity condition analogous to departure occurs. The hyperbolic excess velocity on arrival at the planet is called V_{∞} or V_{HP} ; we will use V_{∞} . V_{∞} is the vector difference between the arrival velocity on the transfer ellipse and the orbital velocity of the planet. In this example, the included angle α would be zero at arrival also; therefore,

$$V_{\infty} = V_{s/s} - V_{p/s}$$

$$V_{\infty} = 37.73 - 35.05 = 2.68 \text{ km/s} \quad (6.3)$$

where

$V_{s/s}$ = arrival velocity of the spacecraft on the transfer ellipse with respect to the sun

$V_{p/s}$ = velocity of the target planet with respect to the sun

V_{∞} = velocity at infinity along the arrival hyperbola

V_{∞} at the target planet is positive in this example, indicating that velocity must be reduced for capture.

6.3 Patched Conic Procedure

Consider next a realistic planetary mission with actual planetary positions and elliptical, inclined planetary orbits. This example will use the patched conic procedure, which consists of four steps:

- 1) Pick a launch date and an arrival date during the launch opportunity (the period in which the mission is possible). Accurately determine the position of the Earth and the target planet on the chosen dates.
- 2) Design a transfer ellipse from Earth to the target planet. The transfer ellipse must contain the Earth's position at launch and the planet's position at arrival. The time of flight on the transfer arc must be equal to the time between the launch and arrival dates. This is a trial and error process. Each trial transfer ellipse is defined by an arbitrary selection of the longitude of the line of apsides. Trials are made until the transfer conditions are met.
- 3) Design the departure hyperbola such that it will deliver the spacecraft to the transfer ellipse.
- 4) Design the approach hyperbola and the arrival mission.

Each step will be considered in terms of theory and by example in the subsequent sections of this chapter. The example that will be used is the type I Venus mission in the 1988 launch opportunity.

6.4 Locating the Planets

In the prior simplified design, the planets were placed arbitrarily at locations that were convenient to the calculation. Ephemeris calculations allow the determination of actual locations for the planets at the times needed.

Launch Opportunity

It is desirable for the Earth at launch and target planet at arrival to be directly opposed, as in a Hohmann transfer, to minimize launch energy. The years for which an approximation of this position occurs are said to offer a launch opportunity. To see how this concept works, consider the launch opportunities between the Earth and an imaginary planet with a period exactly twice that of the Earth, as shown in Fig. 6.5. (This situation is similar to that between Earth and Mars.) Assume that Earth and the target planet are perfectly aligned for a Hohmann transfer on January 1 of year 1. In one year the Earth will make one revolution and will be back to its original position. The period of the target planet is two years, so that it will be halfway around the sun on arrival day. Its arrival position will be adjacent to the

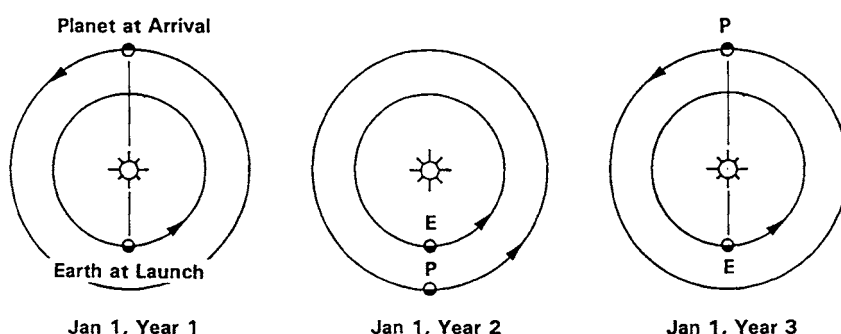


Fig. 6.5 Relative position of Earth and a planet with twice the Earth's period.

Earth departure position. Initiating an interplanetary transfer is impossible in this situation, regardless of launch vehicle capability.

At the end of the second year (January 1, year 3), the Earth has made its second orbit of the sun. The target planet will complete its orbit of the sun on arrival day. The planets are again in ideal positions for a mission.

Synodic Period

For this imaginary planet the synodic period is two years. The synodic period is the time interval between launch opportunities and is a characteristic of each planet. The synodic period of a planet is

$$S = \frac{2\pi}{\omega_e - \omega_p} = \frac{1}{1 - 1/P_p} \quad (6.4)$$

where

S = synodic period, year

ω_e, ω_p = angular velocity of Earth and planet, rad/year

P_p = period of the planet, year

Table 6.4 shows the synodic period of the planets. Note that the derivation of synodic period is based on an assumption of circular orbits. The synodic period of the outer planets is essentially one year because their orbital motion is very slow in comparison to that of the Earth. In one year the Earth is back in a favorable launch position, and the outer planet has not moved much.

Trajectory Type and Class

Planetary trajectories are classified based on the length of the transfer ellipse (see Fig. 6.6). If the spacecraft will travel less than a 180-deg true anomaly, the trajectory is called type I. If the spacecraft will travel more than 180 deg and less than 360 deg, the trajectory is called a type II. Types III and IV exist but are seldom used. Trajectories are also organized into classes. A class I transfer trajectory reaches the target planet before apoapsis (or before periapsis for inbound missions).

Table 6.4 Synodic periods

Planet	S , days
Mercury	116
Venus	584
Mars	780
Jupiter	399
Saturn	378
Uranus	370
Neptune	367
Pluto	367
Moon	30

INTERPLANETARY TRAJECTORIES

103

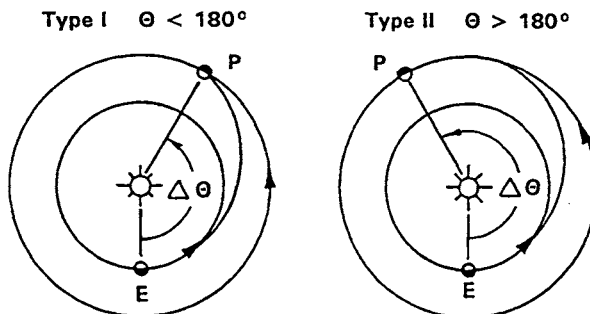


Fig. 6.6 Trajectory types.

Class II trajectories reach the target planet after apoapsis (or after periapsis for inbound missions). The Viking mission to Mars, for example, used a type II, class II trajectory.

A good launch opportunity depends on more than the relative position of the planets. The location of the line of nodes for the target planet's orbit is important in sizing the plane change and therefore is important in setting the energy required of the launch vehicle. Launch opportunities also vary in quality because of the eccentricity of the orbits. Figure 6.7 shows the variation in C_3 for type I and type II trajectories to Venus over five launch opportunities. The variation shown is due to all causes: the relative positions, the plane change, the velocities of the planets, and the eccentricity of the orbits.

Planet Locations

Strangely enough, for a planetary trajectory, the launch and arrival dates may be arbitrarily picked; launch energy is the dependent variable. The Voyager 1 trajectory to Jupiter was designed to launch after Voyager 2 and arrive at Jupiter four months ahead of Voyager 2.

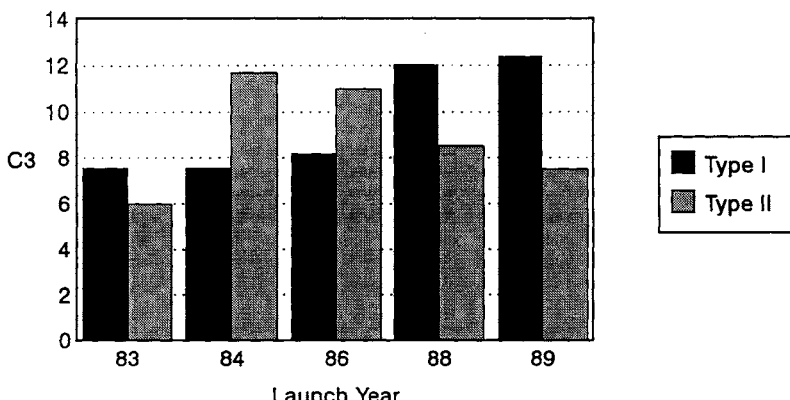


Fig. 6.7 Minimum C_3 for trajectories to Venus (source: Ref. 27).

In 1988 the launch opportunity to Venus ran from March 1 to about April 10. The example trajectory to Venus may be arbitrarily selected as follows:

Launch = April 8, 1988 (JD 244 7259.5)

Arrival = July 26, 1988 (JD 244 7368.5)

Ephemeris Calculations

The sizes, shapes, and locations of the planetary orbits change slowly with time; these changes are caused by perturbations to the orbits. The changes are small but important for ephemeris calculations. To make the situation even more interesting, the ecliptic plane moves slightly with time, as does the location of the vernal equinox vector; thus, the axis system is moving. To accurately locate the two planets we must: 1) arbitrarily fix the reference system, 2) determine the size, shape, and location of planetary orbits in the period of interest, and 3) hold these parameters fixed and determine the latitude and longitude of Earth on launch day and of the target planet on arrival day.

There are two methods currently in use for fixing the axis system. One approach is to pick a date, locate the ecliptic plane and the vernal equinox vector, and assume that the axes are fixed for a period of time (usually 50 years). A calculation of this kind is labeled "of epoch J2000.0" or "of epoch J1950.0." These expressions mean that the measurements are made from the locations of the ecliptic and the vernal equinox vector on January 1, 2000, or January 1, 1950, respectively.

The second method of handling the moving axis system is to measure from the instantaneous position of the ecliptic and the equinox vector. Calculations of this type are labeled "of date."

The standard reference for ephemeris data is *The Astronomical Almanac*,¹² available annually from the U.S. Government Printing Office. Prior to 1981 the publication was referred to as *The American Ephemeris and Nautical Almanac*.

The Astronomical Almanac provides tabulations of the heliocentric latitude, longitude, and radius of the planets. These tabulations were given daily for the inner planets and at longer intervals for the outer planets. Interestingly, the Earth's heliocentric coordinates must be calculated from the geocentric coordinates of the sun by adding (or subtracting) 180° to the longitude and reversing the sign of the latitude. In addition, the almanac gives the instantaneous planetary orbital elements at eleven times spaced equally over a year. The instantaneous two-body elements are known as *osculating orbital elements*.

Another method of obtaining ephemeris information employs the polynomial fit technique, using short numerical series of the form

$$E_{\text{FUTURE}} = E_{\text{REF}} + C_1 T + C_2 T^2 \quad (6.5)$$

where

E_{FUTURE} = an orbital element (parameter) at some future date

E_{REF} = the same orbital element at a reference date in the past

C_1, C_2 = polynomial coefficients

T = Julian centuries from the reference date to the future date

INTERPLANETARY TRAJECTORIES

105

Given the future Julian date JD_{FUTURE} and the reference Julian date JD_{REF} ,

$$T = (JD_{FUTURE} - JD_{REF})/36,525 \quad (6.6)$$

Polynomial coefficients of this form are given in Refs. 28 and 29.

Ephemeris data are also calculated by an alternate relation of the following form:

$$E = a_0 + a_1 p + a_2 p^2 \quad (6.7)$$

The value of p is determined by using the following equation:

$$p = (JD_{FUTURE} - JD_{REF})/2280 \quad (6.8)$$

Polynomial coefficients of this type are given for all planets in *Planetary and Lunar Coordinates for the Years 1984–2000*.³⁰

A convenient way to get the needed ephemeris data is to use the computerized ephemeris calculation method contained in the ORBWIN software included with this book (see Appendix A).

The geometry of the 1988 Venus mission and the corresponding ephemeris data are shown in Fig. 6.8. Figure 6.8 shows a view of the ecliptic plane from the northern celestial sphere. The orbit of Venus is slightly out of plane; Venus is below the ecliptic at arrival. Longitudes are measured in the ecliptic plane counterclockwise

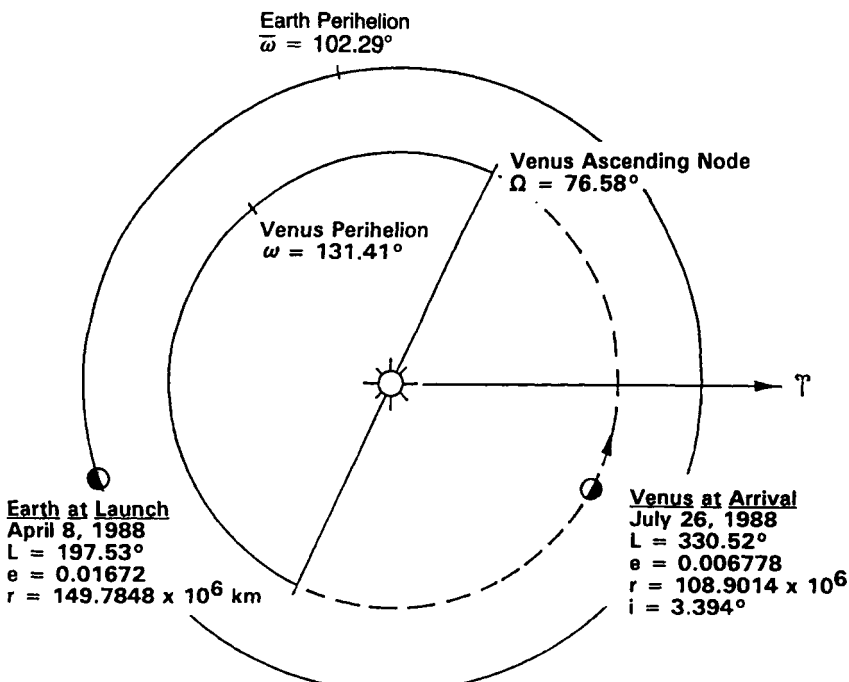


Fig. 6.8 1988 type I mission to Venus.

in the direction of motion, from the vernal equinox vector. The Earth at launch is less than 180 deg from Venus at arrival; therefore, this is a type I trajectory.

From Fig. 6.8, the true anomaly of Earth at launch is

$$\Theta_e = 197.53 - 102.29 = 95.24 \text{ deg}$$

At this position the velocity of the Earth with respect to the sun is, from Eq. (2.14),

$$V_{e/s} = 29.75 \text{ km/s}$$

and the flight path angle is, from Eq. (2.31),

$$\gamma_e = 0.9554 \text{ deg}$$

From Fig. 6.8, for Venus at arrival,

$$\Theta_p = 330.52 - 131.41 = 199.11 \text{ deg}$$

$$V_{p/s} = 34.80 \text{ km/s}$$

$$\gamma_p = -0.1280 \text{ deg}$$

6.5 Design of the Transfer Ellipse

The transfer ellipse of this example is defined by the two following requirements:

- 1) It must pass through the Earth position at launch and through the Venus position at arrival.
 - 2) The time of flight between these positions must be exactly equal to the number of days between April 8, 1988 and July 26, 1988.
- These requirements constitute the rendezvous conditions.

The transfer ellipse can be found by trial and error. The two planet positions define two points on a family of transfer ellipses, each defined by the radial position of the line of apsides. Selecting the position of the line of apsides defines the true anomaly for each planet position and the time of flight between points. The trial and error process then becomes a series of selections of line of apsides positions and subsequent calculations of times of flight on the resulting transfer ellipse.

The required time of flight on the transfer ellipse is the number of days between the Julian dates of launch and arrival:

Arrival:	July 26, 1988	JD 244 7368.5
Launch:	April 8, 1988	JD 244 7259.5
Time of Flight:		109.0 days

For the first attempt, try placing the line of apsides through the Earth position at launch (see Fig. 6.9). The true anomaly of the Earth's position becomes 180 deg. Consulting Fig. 6.8, Venus is 132.99 deg ahead of the Earth position ($330.52 - 197.53$), indicating a true anomaly of $180 + 132.99 = 312.99$ deg. The planet radii and true anomalies define the trial transfer ellipse shown in Fig. 6.9.

The eccentricity of the transfer ellipse, from Eq. (2.28), is

$$e = \frac{(108.9014 \times 10^6) - (149.7848 \times 10^6)}{(149.7848 \times 10^6)(\cos 180) - (108.9014 \times 10^6)(\cos 312.99)}$$

$$e = 0.1825$$

INTERPLANETARY TRAJECTORIES

107

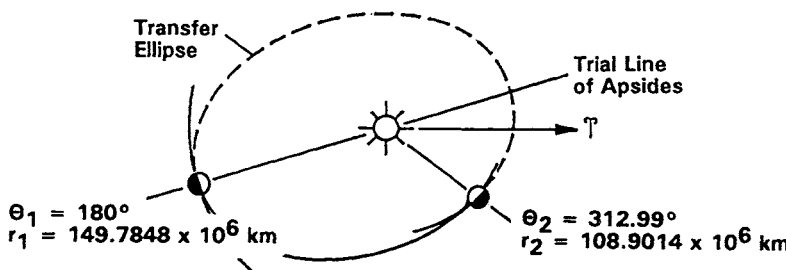


Fig. 6.9 Trial transfer ellipse.

The periapsis radius, from Eq. (2.29), is

$$r_p = \frac{149.7848 \times 10^6 [1 + (0.1825)(-1)]}{(1.1825)} = 103.5550 \times 10^6 \text{ km}$$

The semimajor axis is, from Eq. (2.50),

$$a = \frac{103.555 \times 10^6}{(1 - 0.1825)} = 126.673 \times 10^6 \text{ km}$$

From the Kepler equation comes the time of flight:

	$\theta, \text{ deg}$	$T, \text{ days}$
Periapsis to Earth	180	142.30
Venus to periapsis	312.99	26.15
Transfer time		116.15 (109.0 required)

The first trial transfer ellipse yields a time of flight of 116.15 days vs a requirement of 109.0 days. Subsequent trials must be made holding the following properties on the transfer ellipse constant:

- 1) radius at Earth = $149.7848 \times 10^6 \text{ km}$
 - 2) radius at Venus = $108.9014 \times 10^6 \text{ km}$
 - 3) longitudinal angle from Earth to Venus = 132.99°
- and varying the true anomaly at Earth and Venus. Table 6.5 shows the results of three trials. Trial 3 is the transfer ellipse.

The spacecraft reaches Venus before periapsis; therefore, this is a class I trajectory. The velocities required on the transfer ellipse and the associated flight path

Table 6.5 Trial and error properties of transfer ellipse

	Θ at Earth	Θ at Venus	e	$a \times 10^6$	TOF, days
1	180	312.99	0.1825	126.669	116.15
2	190	322.99	0.1744	127.954	112.16
3	199.53	332.52	0.17194	129.336	109.02

angles can now be calculated:

$$\begin{array}{lll} \text{Near Earth: } & V = 27.312 \text{ km/s}, & \gamma = -3.924 \text{ deg} \\ \text{Near Venus: } & V = 37.566 \text{ km/s}, & \gamma = -3.938 \text{ deg} \end{array}$$

6.6 Design of the Departure Trajectory

On a planetary flight, the launch vehicle sends the spacecraft off on a hyperbolic escape trajectory. As the spacecraft speeds along, the Earth's influence diminishes with distance and the sun's influence increases. The hyperbolic orbit gradually becomes an elliptic orbit about the sun. To send a spacecraft to a planet, send it away on the right hyperbolic orbit (right V_∞) and in the right plane (the transfer plane). We can then sit back and watch physics do the rest. Like a cannon, if we point it correctly, it will hit the target. The key results of the patched conic calculation are the definition of the transfer plane and V_∞ (i.e., how to point the cannon). Calculation of these key results will be discussed in this section.

Plane Change

The plane change is made at departure to take advantage of the energy economy of combining the plane change with injection. In addition, launch vehicle energy is used rather than spacecraft energy. As a result, the transfer ellipse is not in the ecliptic plane; it is in an intersecting plane that contains the center of mass of the sun, the Earth at launch, and Venus at arrival, as shown in Fig. 6.10. In Fig 6.10,

i_t = the inclination of the transfer plane

i_v = the inclination of the Venus orbital plane

$\alpha = 180 - i_v = 180 - 3.394 = 176.61 \text{ deg}$

a, b, c = spherical angles measured on the surface of a sphere of radius r_e centered at the sun

To get the inclination of the transfer plane i_t requires solution of the spherical triangle a, b, c in Fig. 6.10. The side a is in the ecliptic plane and can be obtained directly from longitudes (see Fig. 6.8):

$$\begin{aligned} a &= (\Omega + 180) - L_e \\ a &= 76.58 + 180 - 197.53 = 59.05 \text{ deg} \end{aligned} \quad (6.9)$$

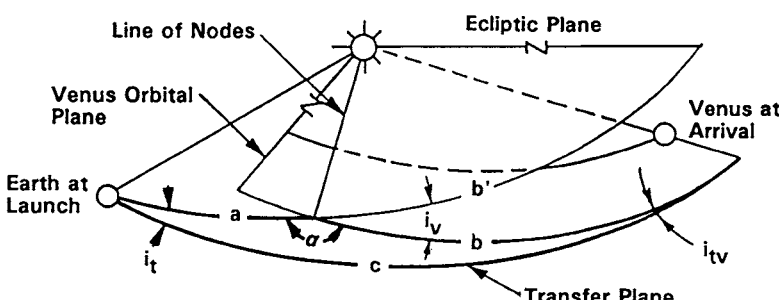


Fig. 6.10 Transfer plane.

The arc b' , measured from the line of nodes to the Venus longitude can be obtained by

$$\begin{aligned} b' &= L_v - (\Omega + 180) \\ b' &= 330.52 - 76.58 - 180 = 73.94 \text{ deg} \end{aligned} \quad (6.10)$$

Since longitudes are measured in the ecliptic plane and the arc b is slightly inclined to the ecliptic, a small adjustment should be made. Solving a right spherical triangle defined by side b' and angle i_v , and hypotenuse b yields $b = 73.967$ deg.

The arc c can be obtained using the law of cosines from spherical trigonometry:

$$\begin{aligned} \cos c &= \cos a \cos b + \sin a \sin b \cos \alpha \\ \cos c &= -0.6807 \\ c &= 132.90 \text{ deg} \end{aligned} \quad (6.11)$$

The inclination of the transfer plane can be obtained by using the law of sines from spherical trigonometry:

$$\begin{aligned} \sin i_t &= \frac{\sin \alpha \sin b}{\sin c} = 0.07768 \\ i_t &= 4.455 \text{ deg} \end{aligned} \quad (6.12)$$

Calculating V_{HE} and $C3$

The V_{HE} vector is designed so that when the spacecraft reaches “infinity” on the departure hyperbola it will have the proper speed and direction to establish the transfer ellipse in the transfer plane. The size of the transfer ellipse is so large compared to the hyperbolic departure orbit that, for preliminary calculations, we do not have to find an X, Y position where the departure (or arrival) hyperbola and the transfer ellipse are patched. As shown in Fig. 6.11, the direction established for V_{HE} accommodates the flight path angle of Earth, the flight path angle of the spacecraft on the transfer ellipse, and the plane change to the transfer plane.

In Fig. 6.11,

$V_{e/s}$ = velocity of Earth with respect to the sun

$V_{s/s}$ = velocity of the spacecraft with respect to the sun on the transfer ellipse

V_{HE} = hyperbolic excess velocity, which is the velocity with respect to Earth at infinity on the departure hyperbola

γ_e = flight path angle of Earth

γ_t = flight path angle of the spacecraft on the transfer ellipse

i_t = inclination of the transfer plane with respect to the ecliptic

The angles in Fig. 6.11 are greatly exaggerated. The vector geometry shown is for the example problem. The geometry will vary widely depending on the sign and magnitude of each angle.

Figure 6.12 shows the geometry as seen when looking down the departure vector. It is necessary to know α because it is the angle between the two vectors of interest

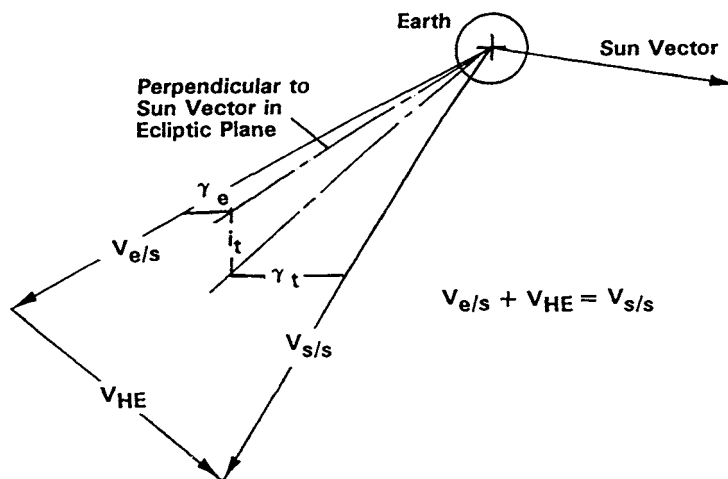


Fig. 6.11 Vector diagram at departure.

and is needed for a cosine law solution. For a right spherical triangle,

$$\begin{aligned}\cos \alpha &= \cos i_t \cos(\gamma_e + \gamma_t) \\ \cos \alpha &= \cos 4.455 \cos(0.9554 + 3.924) = 0.99337 \\ \alpha &= 6.604 \text{ deg}\end{aligned}\quad (6.13)$$

From the law of cosines,

$$C3 = V_{e/s}^2 + V_{s/s}^2 - 2V_{e/s}V_{s/s} \cos \alpha \quad (6.14)$$

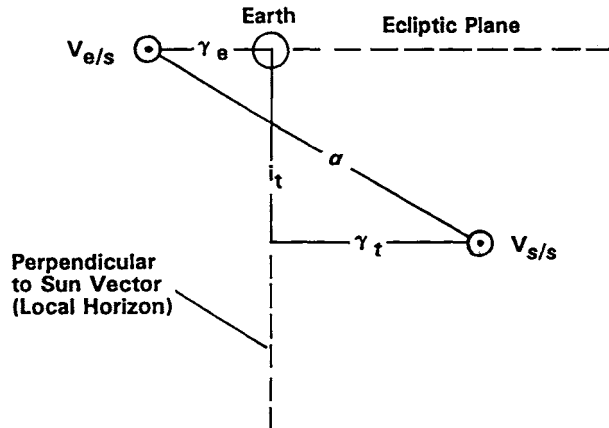


Fig. 6.12 Spherical triangles containing departure vectors.

INTERPLANETARY TRAJECTORIES

111

Since

$$V_{e/s} = 29.75 \text{ km/s}$$

$$V_{s/s} = 27.312 \text{ km/s}$$

C3 for the 1988 type I Venus mission is

$$C3 = 16.73 \text{ km}^2/\text{s}^2$$

$$V_{HE} = 4.090 \text{ km/s}$$

for launch on April 8 and arrival on July 26.

In any year that contains a launch opportunity, there are a number of acceptable launch dates and a number of acceptable arrival dates. Holding the arrival date of July 26 fixed and varying the launch date yields a series of patched conic solutions with various times of flight and various C3 values. The result is that only certain days in a launch opportunity are feasible for any given launch vehicle, as Fig. 6.13 shows.

In a year with a launch opportunity there will be a best day that has relative planetary positions requiring the least launch vehicle energy. There will be a period of a few days on either side of the best day when a mission is possible with a given launch vehicle. For Magellan (Venus, type IV, 1989) the launch opportunity was 28 days long.

Note how rapidly C3 rises at the edges of the opportunity; substantially more launch energy would not greatly extend the window.

It is common practice to calculate a large number of trajectories to obtain contours of C3 for a range of launch dates and arrival dates. Figure 6.14 shows such a plot for the Venus 1988 launch opportunity. Figure 6.14 shows that there are two regions of minimum C3 in the 1988 opportunity. The upper region contains

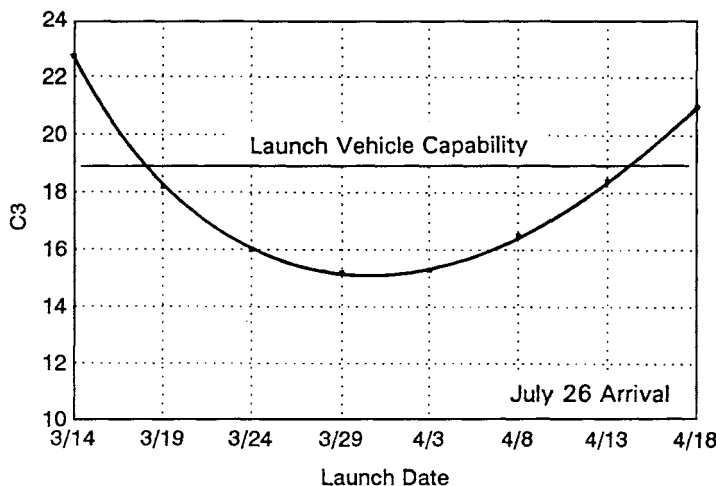


Fig. 6.13 C3 vs launch date for 1988 Venus mission.

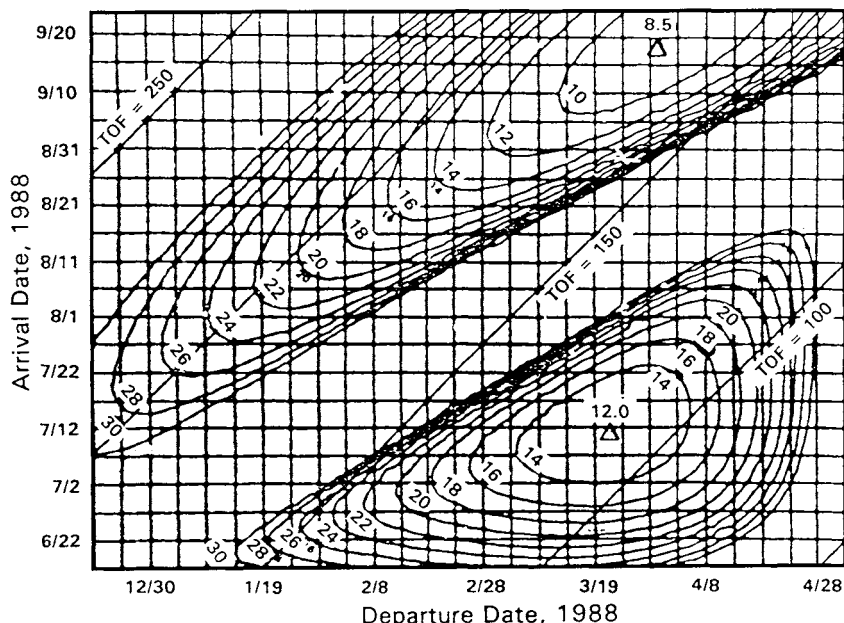


Fig. 6.14 Contours of C3: Earth to Venus 1988 (from Ref. 27, pp. 2–113; provided courtesy of Jet Propulsion Laboratory, California Institute of Technology, Pasadena, California).

the type II missions, and the lower region contains the type I missions. Lower C3 values could be obtained with type II missions in 1988. A C3 of 8.5 is attainable, and time of flight (TOF) is about 200 days. The type I missions have a minimum C3 of 12.0 and a TOF of about 100 days. The type I and II launch periods overlap; it would be possible to launch two spacecraft at close intervals and have widely spaced arrivals (as the Voyager program did at Jupiter). Figure 6.14 also shows how quickly C3 increases on either side of the minimum. In just a matter of days, a mission on any conceivable launch vehicle becomes impossible.

The launch date selected for a project is usually a compromise between C3 and other concerns, usually arrival conditions. Thus a launch seldom takes place at the minimum C3.

Departure Hyperbola

The departure hyperbola, shown in Figure 6.15, has a periapsis radius equal to the radius of the parking orbit and a V_{HE} magnitude and direction that are calculated to place the spacecraft on the proper transfer ellipse as previously discussed. It is convenient to visualize the V_{HE} vector passing through the center of the Earth. The acceptable departure hyperbolas form a body of revolution about the V_{HE} vector, as shown in Fig. 6.16. Departure on any hyperbola in the body of revolution is acceptable. The *point of injection* is the location at which the spacecraft reaches the

INTERPLANETARY TRAJECTORIES

113

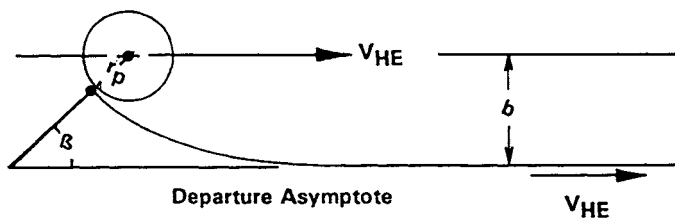


Fig. 6.15 Departure hyperbola.

velocity needed to enter the proper hyperbolic departure trajectory; this point is normally at the periapsis of the hyperbola. The velocity required at the injection point is

$$V = \sqrt{(2\mu/r_p) + V_{HE}^2}$$

where

V = the spacecraft velocity at the point of injection into the departure hyperbola

V_{HE} = hyperbolic excess velocity

r_p = radius at the point of injection (assumed to be at periapsis)

Although the launch vehicle interface is specified in terms of C3, the correct velocity, as defined in Eq. (2.57), is what the launch vehicle must actually achieve.

V_{HE} and r_p define the departure hyperbola; the remaining elements can be obtained using the relations provided in Chapter 2. For the example mission, assuming $h_p = 330$ km, the periapsis velocity is, from Eq. (2.59),

$$V = \sqrt{\frac{(2)398,600}{6708} + 16.73} = 11.64 \text{ km/s}$$

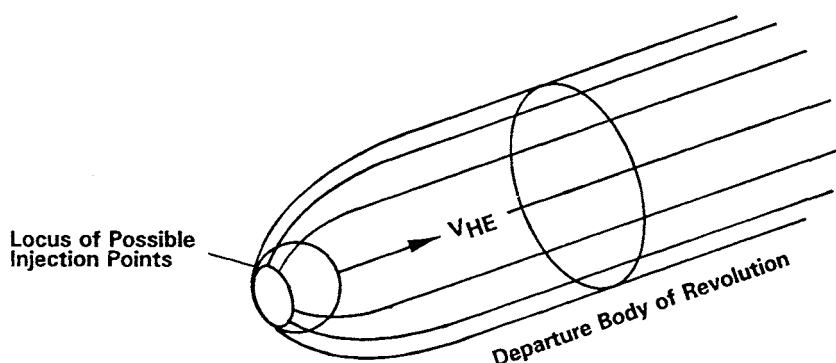


Fig. 6.16 Departure body of revolution.

The semiminor axis of the departure hyperbola, from Eq. (2.82), is

$$b = r_p \sqrt{\frac{2\mu}{r_p V_{\text{HE}}^2} + 1} = 6708 \sqrt{\frac{2(398,600)}{(6708)(16.73)}} + 1 = 19,097 \text{ km}$$

The angle of asymptote, from Eq. (2.66), is

$$\tan \beta = \frac{b V_{\text{HE}}^2}{\mu} = \frac{(19,097)(16.73)}{(398,600)} = 0.8015$$

$$\beta = 38.71 \text{ deg}$$

Launch Window

The acceptable launch azimuth range at the launch site constrains the allowable launch times to a daily launch window. Figure 6.17 shows how this works. The Earth rotates about its axis with the V_{HE} vector passing through its center of mass.

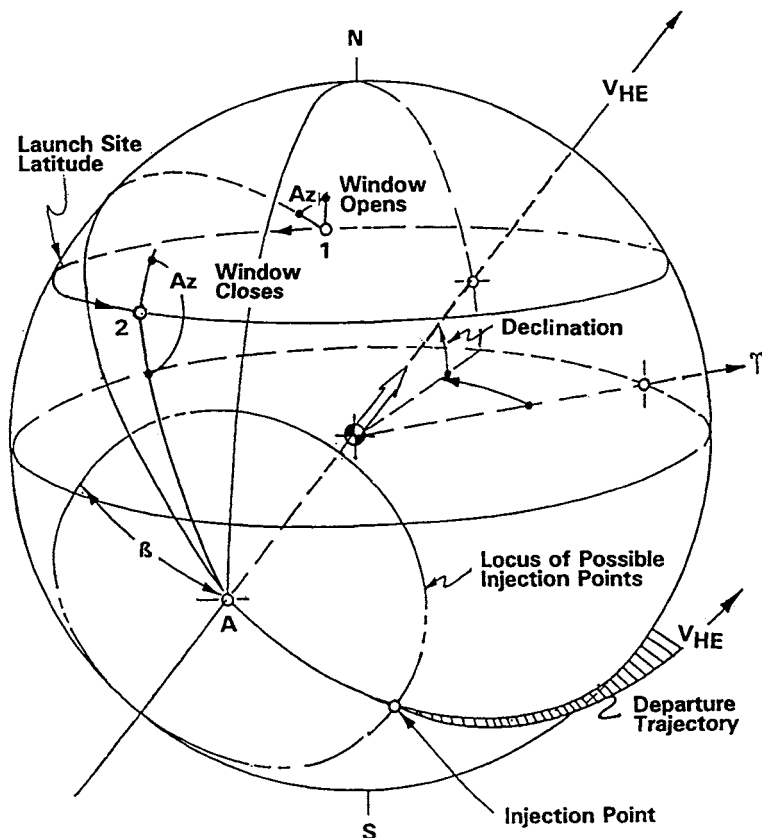


Fig. 6.17 Departure geometry.

The locus of possible injection points is a circle of radius β centered about the V_{HE} vector at point A. To inject the spacecraft onto an acceptable departure hyperbola, the launch trajectory must follow a great circle from the launch site to point A.

Consider all of the features of the figure as fixed in space while the launch site rotates counterclockwise around the Earth's axis on a latitude line. The daily launch window opens at point 1 when the required launch azimuth reaches the minimum acceptable angle for the launch site (about 35 deg for ETR; see Chapter 4).

As time passes the launch site rotates from point 1 to point 2. The required launch azimuth increases with time until the maximum acceptable angle is exceeded at point 2 and the window closes. The departure path shown in Fig. 6.17 assumes that the launch is made at the instant the window opens.

Note from Fig. 6.17 that there are two opportunities to launch on some of the departure trajectories, one early in the window and another late in the window where the great circle crosses the launch site latitude. Also note that many of the acceptable hyperbolas are not achievable.

The position of the V_{HE} vector changes slowly, and as a result the length of the launch window changes with time. The Magellan launch window varied from 28 min on the first day (April 28, 1989) to 126 min on the last, or thirtieth, day.

To recap, a planetary launch can occur only in certain years, only for a few days in those years, and only for a few minutes in those days. If the launch opportunity is missed there will be a significant delay (one synodic period) before another opportunity occurs. These facts are key scheduling and planning factors in any planetary program.

6.7 Design of the Arrival Trajectory

There are three basic arrival mission types:

Mission	Example
Direct impact	Ranger
Gravity-assist	Voyager
Planetary orbiter	Magellan

Arrival design for gravity-assist missions is dominated by targeting considerations; arrival for orbiting missions is dominated by arrival energy considerations.

Arrival Targeting

The objective of arrival targeting is to place the incoming asymptote in the desired location relative to the target planet. Arrival targeting is controlled by small velocity adjustments called midcourse maneuvers or trajectory correction maneuvers. The design of these maneuvers involves using the B plane, which is a plane perpendicular to the asymptote of the approach hyperbola placed at a large distance from the planet (see Fig. 6.18). In Fig. 6.18,

- b = the semiminor axis of the approach hyperbola, the distance between the asymptote of the hyperbola and a line parallel to the asymptote that runs through the center of mass of the target planet
- b_a = atmospheric impact radius in the B plane, the semiminor axis of a hyperbola that is just tangent to the planetary atmosphere

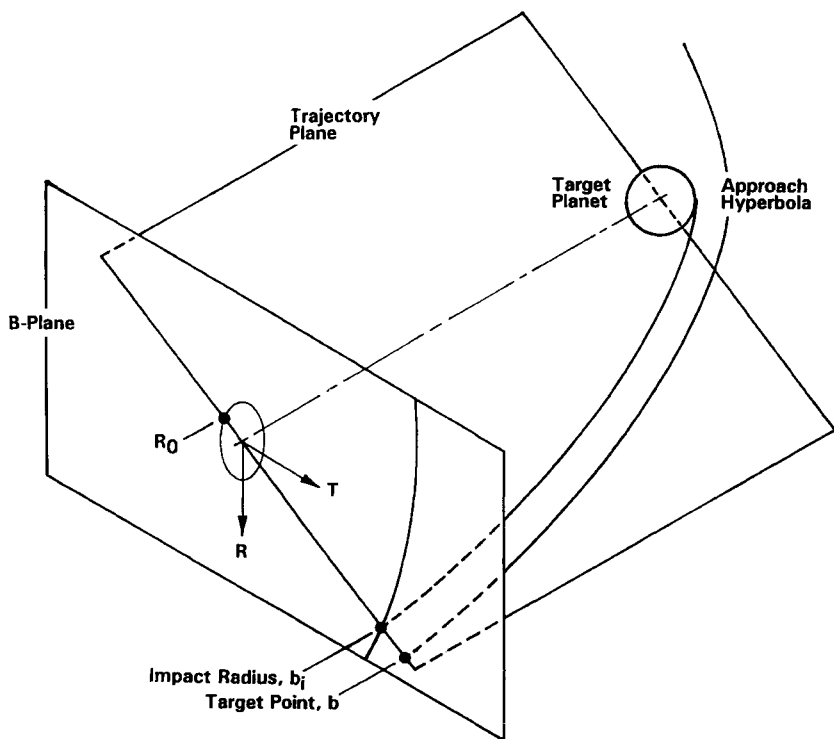


Fig. 6.18 Definition of the B plane.

b_i = surface impact radius in the B plane

R_0 = the mean radius of the surface of the target planet

R = the vertical axis in the B plane that is perpendicular to the ecliptic plane and to the arrival asymptote

T = the horizontal axis in the B plane that is parallel to the ecliptic plane and perpendicular to the approach asymptote

By definition, targeting implies maintaining a proper distance from the projection of the surface and the atmosphere. If a spacecraft pierces the B plane inside the impact circle it will strike the planet. The radius of the impact circle b_i is the semiminor axis of a hyperbola that is just tangent to the surface of the target planet. The impact radius is substantially larger than the radius of the planet R_0 . Using the Venus example and Eq. (2.82) (setting the periapsis radius equal to the mean equatorial radius of Venus), the following value of the impact radius is obtained:

$$b_i = 6052 \sqrt{\frac{(2)(324,858.8)}{(6052)(4.442)^2}} + 1$$

$$b_i = 15,359 \text{ km}$$

(It will be shown later that V_∞ for this approach trajectory is 4.442 km/s.)

The impact radius is 2.5 times the surface radius of the planet. If the V_∞ vector is inside the impact radius, the spacecraft will impact the planet.

The impact radius of the atmosphere can be calculated similarly by selecting a thickness for the atmosphere. For example, $b_a = 15,615$ km for an atmosphere 175 km thick.

Targeting also implies placing the incoming asymptote in the proper position to accomplish the encounter mission. The target point is projected on the B plane surrounded by an ellipse that encompasses the potential position errors. The target radius, or target point b can be readily calculated from the desired periapsis radius using Eq. (2.82):

$$b = r_p \sqrt{\left(2\mu/r_p V_\infty^2\right) + 1}$$

Trajectory correction maneuvers reduce the size of the position error ellipse. Figure 6.19 shows the Magellan B plane. The surface radius of Venus and the semiminor axis b of the approach hyperbola are projected into the plane. The target point is shown surrounded by ellipses that encompass the maximum expected (3σ) position errors after each of the trajectory correction maneuvers.

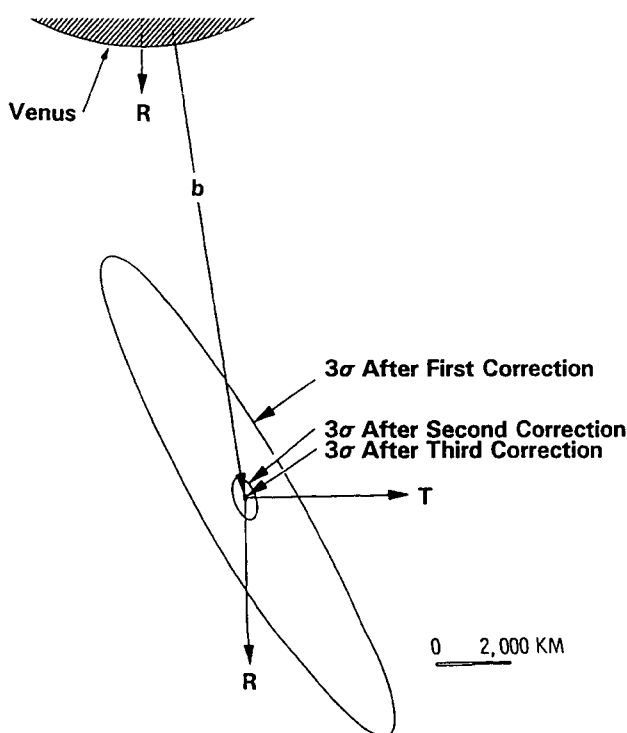


Fig. 6.19 Magellan B plane.

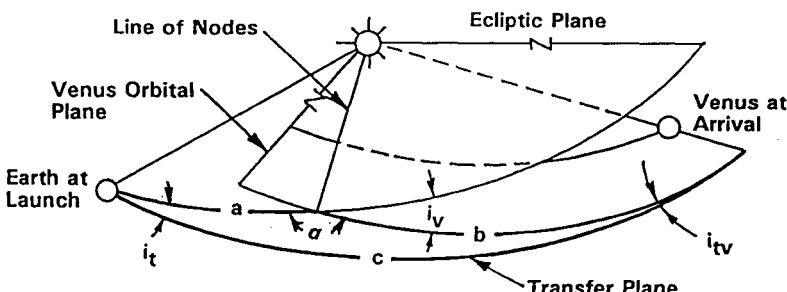


Fig. 6.20 Transfer plane.

Plane Change

The design of the approach hyperbola is similar to the design of the departure hyperbola. The first step is the determination of the inclination of the transfer plane with respect to the orbital plane of the target planet. This calculation requires considering again the spherical triangle formed by the transfer ellipse, the ecliptic plane, and the Venus orbital plane, as shown in Fig. 6.20.

The angle of interest is i_{tp} , the inclination of the transfer plane with respect to the target planet Venus orbital plane. By the sine law of spherical trigonometry, the following equation may be obtained:

$$\sin i_{tp} = \sin \alpha \sin a / \sin c \quad (6.15)$$

$$i_{tp} = 3.975 \text{ deg}$$

Calculating V_∞

V_∞ at the target planet, analogous to V_{HE} at departure, is a dependent variable determined by the departure and transfer trajectories. The arrival vector diagram is conceptually the same as the departure diagram, as shown in Fig. 6.21. In Fig. 6.21,

$V_{p/s}$ = velocity of the target planet with respect to the sun

V_{sa} = velocity of the spacecraft on the transfer ellipse, with respect to the sun, at arrival

V_∞ = spacecraft velocity at infinity on the arrival hyperbola, with respect to the target planet

γ_p = flight path angle of target planet

γ_t = flight path angle of the spacecraft on the transfer ellipse

i_{tp} = inclination of the transfer plane, with respect to the target planet orbital plane

Figure 6.22 shows a spherical triangle, with sides α_a , i_{tp} , and $(\gamma_t - \gamma_p)$, centered on the target planet, looking into the arrival vectors $V_{p/s}$ and $V_{s/a}$. The angle

INTERPLANETARY TRAJECTORIES

119

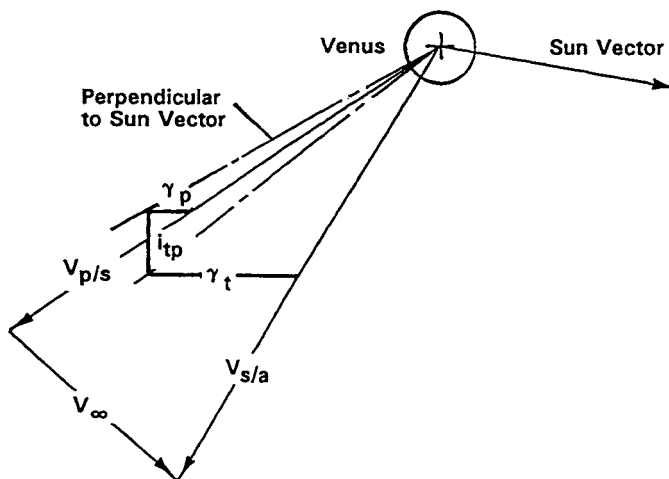


Fig. 6.21 Vector diagram at arrival.

between the two vectors of interest is α_a . For a right spherical triangle,

$$\begin{aligned}\cos \alpha_a &= \cos i_{tp} \cos(\gamma_t - \gamma_p) \\ \cos \alpha_a &= \cos 3.975 \cos(3.938 - 0.1280) \\ \alpha_a &= 5.5039 \text{ deg}\end{aligned}\quad (6.16)$$

Since $V_{p/s} = 34.80 \text{ km/s}$ and $V_{s/a} = 37.57 \text{ km/s}$, using the law of cosines yields the following V_∞ for the 1988 type I Venus mission:

$$V_\infty = 4.442 \text{ km/s}$$

Figure 6.22 is appropriate only for the example problem and is not a general solution. An actual arrival geometry will vary widely depending on the signs and magnitudes of the angles involved.

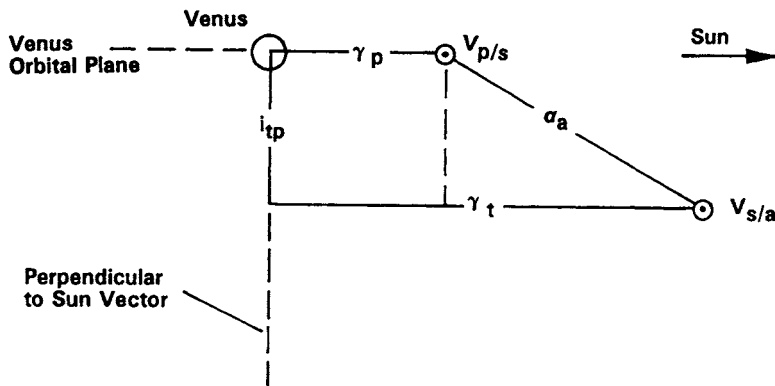


Fig. 6.22 Spherical triangle containing the arrival vectors.

6.8 Gravity-Assist Maneuver

A gravity-assist maneuver is a planetary encounter designed to produce a specific effect on the departure velocity vector of the spacecraft. When a spacecraft passes near a planet, the spacecraft velocity vector is rotated, and the magnitude of the velocity with respect to the sun is changed. This is a very useful maneuver because significant changes can be made to the velocity vector without expending spacecraft resources. After 20 years of analysis, speculation, and debate, the technique was successfully demonstrated by Mariner 10 in 1974.³¹ After the flight of Mariner 10, the maneuver became an indispensable part of planetary mission design; three of the last four planetary missions—Voyager, Galileo, and Ulysses—would not have been possible without it.

Figure 6.23 shows the maneuver, in planet-centered coordinates, designed for an inside pass by the target planet (i.e., between the planet and the sun). In Fig. 6.23,

δ = angle through which the spacecraft velocity vector will be
($180 - 2\beta$) turned

β = the hyperbolic asymptote angle

$V_{\infty a}$ = velocity at infinity on the arrival asymptote

$V_{\infty d}$ = velocity at infinity on the departure asymptote

As shown in Fig. 6.24, the effect of a planetary encounter is to add the vector

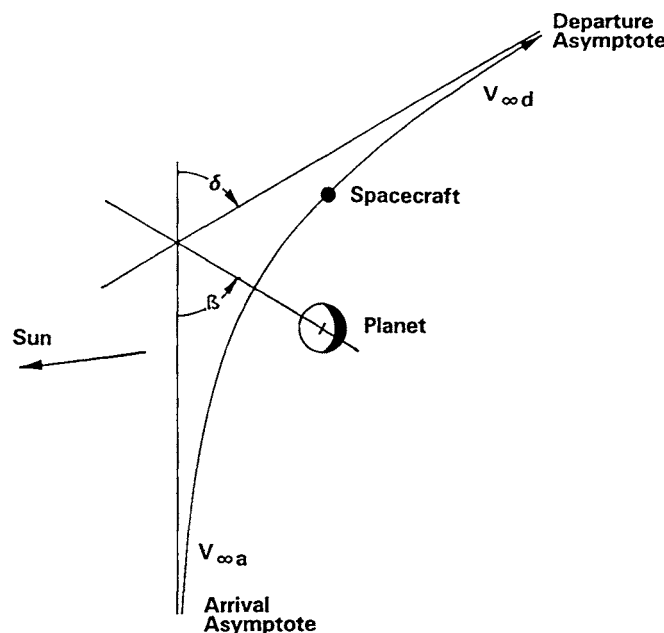
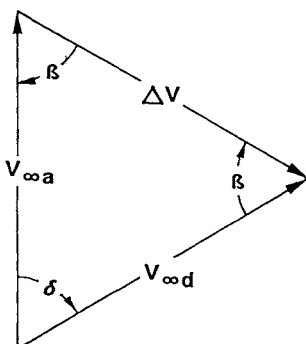


Fig. 6.23 Planetary encounter in geocentric coordinates.

INTERPLANETARY TRAJECTORIES

121



$$|V_{\infty a}| = |V_{\infty d}|$$

Fig. 6.24 Effect of a flyby on V_{∞} .

ΔV to the arrival velocity $V_{\infty a}$. The magnitude of the ΔV vector is

$$\Delta V = 2V_{\infty} \cos \beta \quad (6.17)$$

$$\Delta V = 2V_{\infty}/e \quad (6.18)$$

The spacecraft V_{∞} vector is rotated through the angle δ by the gravitational effect of the planet. The magnitude of the V_{∞} vector is not changed; however, the velocity of the spacecraft with respect to the sun is changed. Recall that V_{∞} is the velocity of the spacecraft with respect to the planet. To obtain the velocity of the spacecraft with respect to the sun, the velocity of the planet with respect to the sun must be added to V_{∞} .

The velocity of the spacecraft with respect to the sun before and after the encounter is shown in Fig. 6.25. In Fig. 6.25,

V_{sa} = spacecraft velocity with respect to the sun on arrival at the sphere of influence of the target planet

V_{sd} = spacecraft velocity with respect to the sun at departure from the sphere of influence of the planet

$V_{p/s}$ = velocity of the target planet with respect to the sun

It can be seen from Fig. 6.25 that the velocity of the spacecraft with respect to the sun has been increased by the encounter. (In Fig. 6.25, the central portions of vectors V_{sa} , V_{sd} , and $V_{p/s}$ have been deleted, so that the area of interest may be seen more clearly.)

The arrival vectors are fixed by the transfer trajectory design; δ , β , ΔV , and V_{sd} can be changed. (The arrival parameters change slightly each day of the launch opportunity but can be considered fixed for any single day.) Selection of any one orbital parameter defines the encounter trajectory. During design, targeting is specified by periapsis radius or altitude; during the mission it is specified by the target point in the B plane.

The angle α_a between the velocity of the planet and the velocity of the spacecraft is determined by the design of the transfer orbit. The angles δ and β are defined by the design of the flyby hyperbola. The angle Γ can be calculated from the law

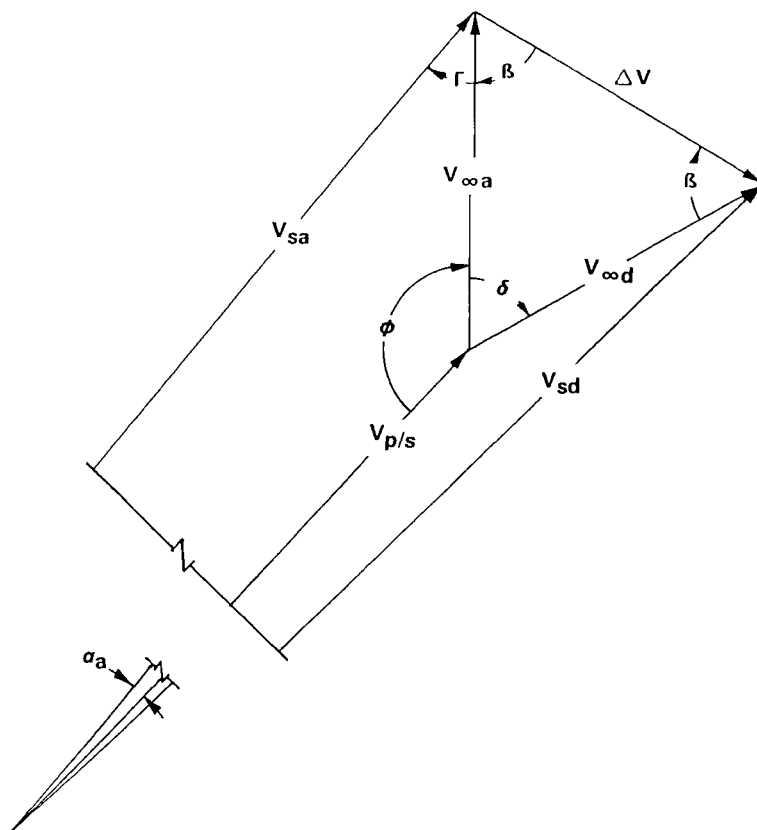


Fig. 6.25 Effect of a flyby on spacecraft velocity.

of sines as follows:

$$\sin \Gamma = \frac{V_{p/s} \sin \alpha_a}{V_{\infty a}} \quad (6.19)$$

and angle $\phi = 180 - \Gamma - \alpha_a$.

The cosine law can now be used to compute V_{sd} :

$$V_{sd}^2 = V_{sa}^2 + \Delta V^2 - V_{sa} \Delta V \cos(\beta \pm \Gamma) \quad (6.20)$$

The sign of gamma may be determined by inspection of the vector diagram.

The departure angle α_d can be obtained from the law of cosines as follows:

$$\cos \alpha_d = \frac{V_{p/s}^2 + V_{sd}^2 - V_{\infty d}^2}{2V_{p/s} V_{sd}} \quad (6.21)$$

For the Venus mission example ($V_{\infty} = 4.442$ km/s), targeting to achieve a periapsis altitude of 5,000 km defines an encounter hyperbola with the following

elements:

Asymptote angle:	$\beta = 53.25 \text{ deg}$
Semiminor axis:	$b = 22,047 \text{ km}$
Semimajor axis:	$a = 16,464 \text{ km}$
Eccentricity:	$e = 1.6713$
Periapsis velocity:	$V_p = 8.861 \text{ km/s}$

To achieve a periapsis altitude of 5000 km requires a target point in the B plane, which is 22,047 km from the center of the planet.

From prior calculations,

$$\begin{aligned} V_{sa} &= 37.57 \text{ km/s} & V_{p/s} &= 34.80 \text{ km/s} \\ \alpha_a &= 5.5039 \text{ deg} & V_\infty &= 4.442 \text{ km/s} \end{aligned}$$

The value of ΔV from Eq. (6.18) is

$$\Delta V = 2(4.442)/1.6713 = 5.316 \text{ km/s}$$

Equation (6.19) yields

$$\begin{aligned} \sin \Gamma &= \frac{34.80}{4.442} \sin 5.5039 = 0.7514 \\ \Gamma &= 48.713 \text{ deg} \\ \delta &= 180 - 48.713 - 5.5039 = 125.783 \text{ deg} \end{aligned}$$

Using the law of cosines to calculate V_{sd} yields

$$\begin{aligned} V_{sd}^2 &= (37.57)^2 + (5.316)^2 - 2(199.72) \cos(48.713 + 53.249) \\ V_{sd} &= 39.02 \text{ km/s} \end{aligned}$$

The spacecraft gained 1.45 km/s in the encounter.

The departure angle, from Eq. (6.21), is

$$\begin{aligned} \cos \alpha_d &= \frac{(34.80)^2 + (39.02)^2 - (4.442)^2}{(2)(34.80)(39.02)} \\ \alpha_d &= 2.156 \text{ deg} \end{aligned}$$

Maximizing Spacecraft Velocity Increase

The departure velocity of the spacecraft with respect to the sun is at a maximum when $V_{p/s}$ and V_{cod} are collinear, as shown in Fig. 6.26. In this case, the velocity of the spacecraft at departure is the arithmetic sum of the velocity of the planet and V_∞ .

The turning angle to maximize V_{sd} can be determined as follows:

$$\delta' = 180 - \phi \quad (6.22)$$

or

$$\beta' = \phi/2 \quad (6.23)$$

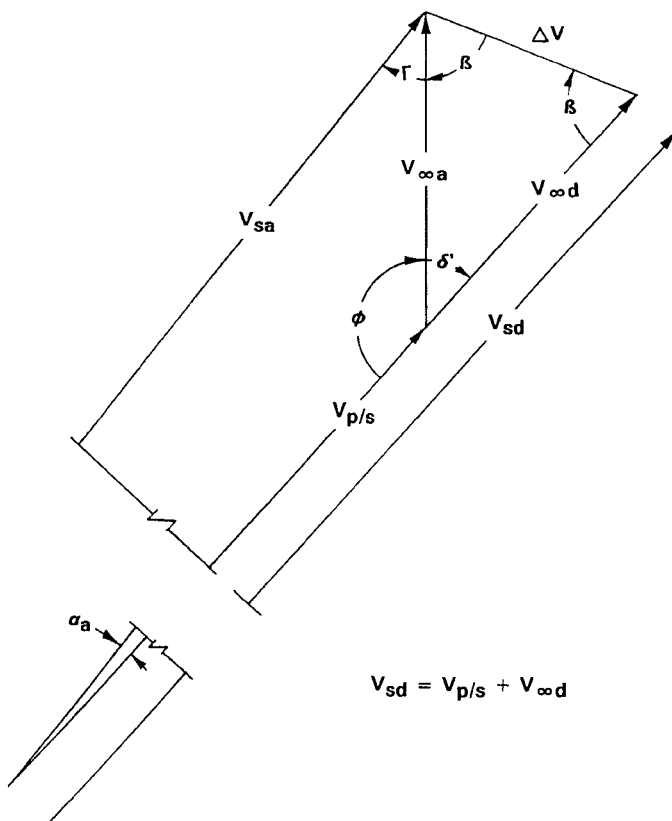


Fig. 6.26 Conditions for maximum departure velocity.

where δ' = the angle of turn that produces maximum spacecraft velocity at departure V_{sd} , and β' = the asymptote angle that produces maximum velocity at departure.

The maximum V_{sd} may not be achievable; the encounter hyperbola for β' may require a periapsis radius lower than the surface of the target planet.

Maximum Angle of Turn

It is sometimes desirable to achieve a given angle of turn rather than a velocity increase; the Ulysses mission offers an example of this situation. The maximum theoretical angle of turn is 180 deg, which occurs when $\beta = 0$ and ΔV is a maximum. From Eq. (6.17),

$$\Delta V_{\max} = 2V_{\infty} \quad (6.24)$$

The theoretical maximum angle of turn represents an elastic collision with the target planet. The largest practical angle of turn occurs with the closest

INTERPLANETARY TRAJECTORIES

125

acceptable approach to the target planet. For the Venus example, selecting a periapsis altitude of 400 km as the closest approach yields the following encounter hyperbola:

Asymptote angle:	$\beta = 44.07 \text{ deg}$
Seminor axis:	$b = 15,940 \text{ km}$
Semimajor axis:	$a = 16,464 \text{ km}$
Eccentricity:	$e = 1.392$
Periapsis velocity:	$V_p = 10.974 \text{ km/s}$

The maximum practical turning angle for the Venus example is

$$\alpha_{\max} = 180 - (2)(44.05) = 91.9 \text{ deg}$$

Spacecraft Velocity Decrease

The examples discussed so far show a velocity increase during the encounter; however, the maneuver can be designed to provide a velocity increase or decrease. As shown in Fig. 6.27, a velocity increase results when the encounter hyperbola passes behind the planet and the spacecraft velocity vector is rotated clockwise. Clockwise rotation tends to align $\vec{V}_{\infty d}$ with the departure velocity, which leads to an increase in departure velocity. Conversely, a velocity decrease results when the encounter hyperbola passes in front of the planet and the velocity vector is rotated counterclockwise.

Velocity Increasing Maneuver

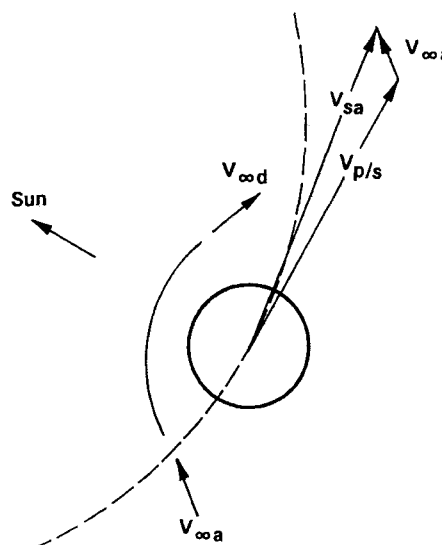


Fig. 6.27a Increasing or decreasing departure velocity.

Velocity Decreasing Maneuver

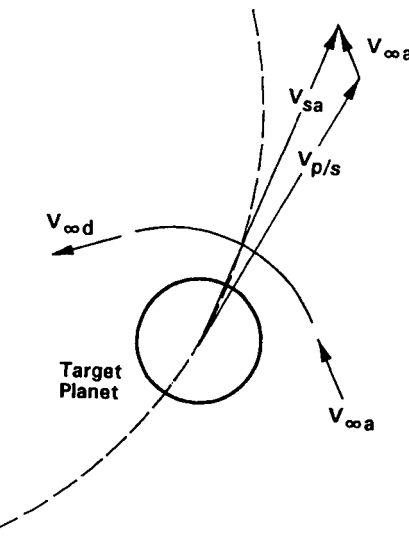


Fig. 6.27b Increasing or decreasing departure velocity.

Suppose the encounter hyperbola in the example problem is relocated such that the spacecraft passes in front of Venus instead of behind it. None of the elements of the hyperbola are changed. The resulting vector diagram is shown in Fig. 6.28.

Comparing Fig. 6.25 and Fig. 6.28, all of the vectors have the same magnitude except V_{sd} , which has been significantly reduced. Solving for V_{sd} as before, except Γ will now subtract from β ,

$$\begin{aligned}V_{sd}^2 &= (37.57)^2 + (5.316)^2 - 2(199.72) \cos(53.249 - 48.713) \\V_{sd} &= 32.27 \text{ km/s}\end{aligned}$$

Moving the target point to the opposite side of the planet changes the spacecraft departure velocity from 39.02 km/s to 32.27 km/s.

6.9 Cycler Orbits

A cycler orbit is one that visits Earth and a target planet at regular intervals. Interest in cycler orbits stems from a desire to make periodic visits to the nearby planets, particularly Mars and Venus. Ideally a cycler orbit would make gravity-assist maneuvers at each encounter that would rotate the line of apsides just enough to send the spacecraft to the new positions of Earth and the target planet on the next orbit. Ideally the dual planet flybys would continue at regular intervals over a long period of time with minimal use of fuel for corrections. Figure 6.29 shows the cycler concept. A spacecraft launched from E1 would encounter Mars at M1. At Mars it would make a gravity-assisted turn to rotate the orbit just enough to

INTERPLANETARY TRAJECTORIES

127

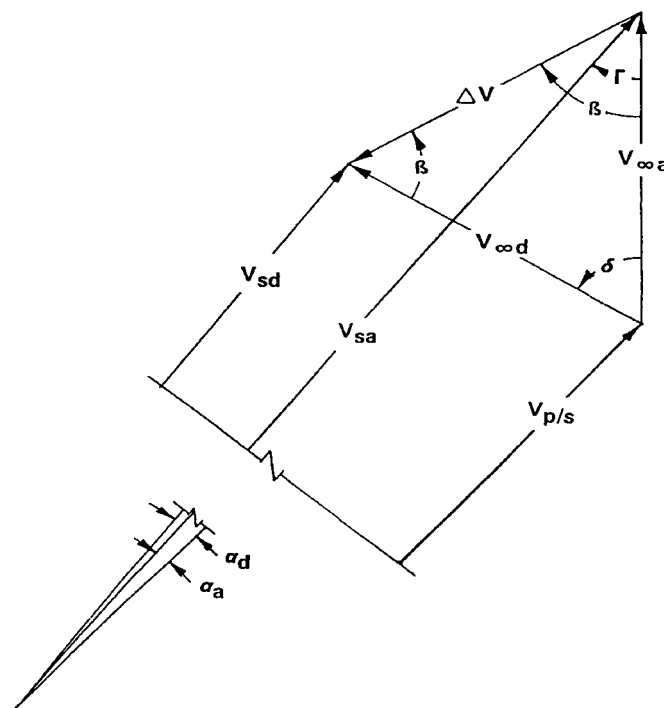


Fig. 6.28 Decreasing spacecraft velocity.

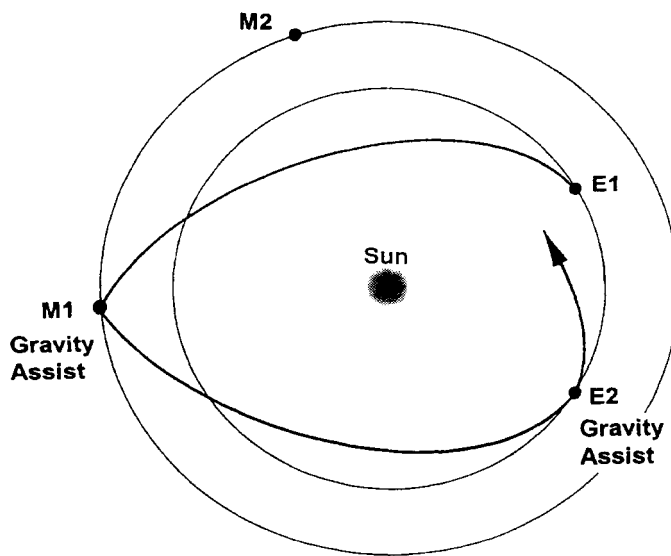


Fig. 6.29 Cycler orbit concept.

encounter Earth at E2 on the next orbit almost a year later. A gravity assist at Earth would rotate the orbit just enough to encounter Mars again at M2 about a year and a half later. Subsequent maneuvers would continue the encounters at regular intervals.

The general approach to the analysis of cycler orbits is to conduct initial investigations using circular coplanar orbits and the patched conic technique previously described; the purpose is to discover potentially useful time periods and planetary geometries. The selected periods can then be analyzed using realistic assumptions. Trajectory opportunities between the planets repeats with the synodic period (see Table 6.4). The synodic period for Venus is 584 days, or 1.60 years. The synodic period of Mars is 780 days, or 2.14 years.

Several cycler orbit designs have been discovered.^{32–34} Full revolution return orbits³⁴ are elliptical sun-centered orbits in the ecliptic plane with a period of exactly one year. Such orbits can be designed to visit a target planet and return to the Earth position exactly one year after launch. There are an infinite number of ellipses that will do this. A half revolution return orbit is an ellipse with both eccentricity and period of the Earth orbit but inclined to the ecliptic. A spacecraft in this orbit encounters Earth twice per year. These orbits are interesting, but are not useful for planet visits; they require high altitude passes for negligible distortion during encounter.

The simplest type of cycler orbit devised so far is the Aldrin cycler named after Astronaut Buzz Aldrin who devised it (see Fig. 6.30). To minimize transit times, two spacecraft are used, one for Earth–Mars transit and one for Mars–Earth transit. When these orbits are designed for position repetition on a 15-year cycle, the angle between the apsides is 51.4 deg as is the rotation of apsides during each orbit.

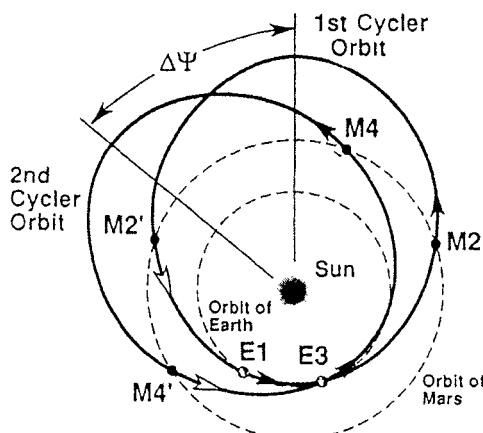


Fig. 6.30 Dual spacecraft Mars cycler orbits. (From Ref. 35, p. 335; reproduced courtesy of AIAA.)

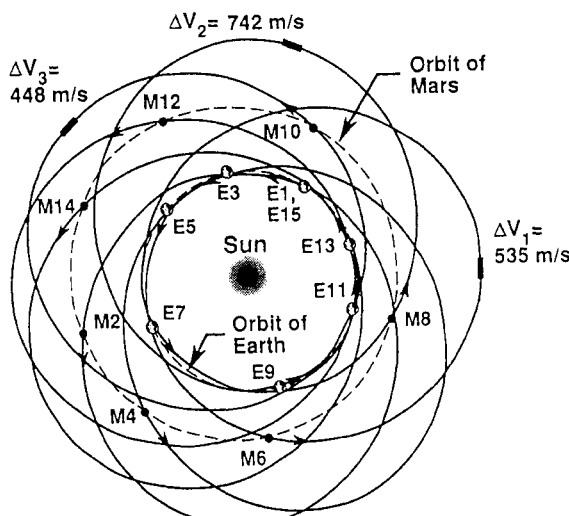


Fig. 6.31 Fifteen-year propagation of outbound cycler orbit. (From Ref. 35, p. 335; reproduced courtesy of AIAA.)

This arrangement has been studied extensively by Byrnes et al.³⁵ The 15-year propagation of one of the Earth–Mars spacecraft, for the period 1995 to 2010, is shown in Fig. 6.31. Periodic adjustments in the orbit are required because Earth–Mars geometry does not repeat exactly; these ΔV requirements are shown in Fig. 6.31. The elements of these orbits are $a = 1.60$ AU and $e = 0.393$. The transit times are between 147 and 170 days for both Earth–Mars and Mars–Earth transits.

6.10 Establishing Planetary Orbit

Frequently it is desired to place a spacecraft in orbit rather than using the encounter for velocity changes. Mariner 9 in 1971 was the first spacecraft to orbit another planet, followed by Viking, Pioneer 10, and Magellan. Establishing a planetary orbit requires a simple orbit change maneuver as shown in Fig. 6.32.

The velocity at periapsis of the approach hyperbola is

$$V_p = \sqrt{V_\infty^2 + 2\mu/r_p} \quad (6.25)$$

The velocity at periapsis of the desired orbit is

$$V'_p = \sqrt{2\mu/r_p - \mu/a} \quad (6.26)$$

To put a spacecraft into a planetary orbit, the velocity at periapsis must be reduced from V_p to V'_p . Substantial spacecraft energy and weight are usually required. For example, 60% of the Magellan cruise weight was dedicated to putting the spacecraft into Venus orbit. The velocity required to establish an orbit is proportional to

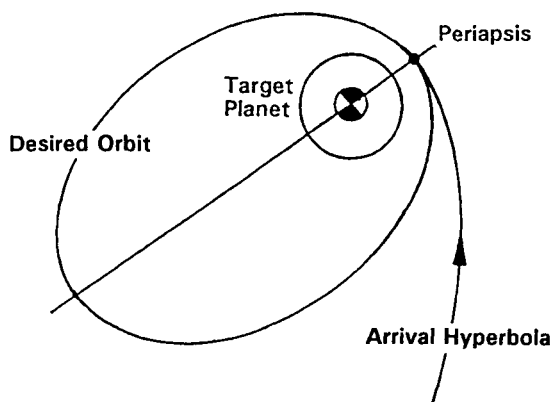


Fig. 6.32 Establishing a planetary orbit.

V_∞ . Therefore, for an orbital mission, the optimum launch date is a compromise between the minimum C3 and the minimum V_∞ .

Note that for capture the velocity of the spacecraft must be reduced to a value below $\sqrt{2\mu/r}$.

Problems

6.1 The Voyager 2 grand tour of the outer planets started with launch on August 20, 1977, from ETR and ended with the encounter of Neptune on August 24, 1989. In transit there were gravity-assist maneuvers at Jupiter, Saturn, and Uranus. (The planetary alignment that allowed this mission occurs once every 176 years.) The mission time from Earth to Neptune was 12 years. How long would the mission have taken by way of a simple Hohmann transfer without the gravity-assist maneuvers?

6.2 The Voyager 2 encounter hyperbola at Neptune had the following elements:

$$\text{Eccentricity} = 2.4586$$

$$\text{Semimajor axis} = 20,649 \text{ km}$$

The periapsis was placed near the north pole.

What was the maximum relative velocity that the camera system had to deal with while the strikingly clear surface pictures were being taken?

6.3 The ephemeris data for Earth on the day of the Magellan launch (May 4, 1989, JD 244 7650.5) were as follows:

$$\text{Semimajor axis} = 1.49598011 \times 10^8 \text{ km}$$

$$\text{Eccentricity} = 0.016703$$

$$\text{Longitude} = 222.0^\circ$$

$$\text{Longitude of perihelion} = 103.0^\circ$$

INTERPLANETARY TRAJECTORIES

131

The Venus transfer ellipse had the following properties:

$$\text{Semimajor axis} = 1.2829322 \times 10^8 \text{ km}$$

$$\text{Eccentricity} = 0.179361$$

$$\text{Inclination} = 0.724 \text{ deg}$$

$$\text{Longitude of ascending node} = 43.347^\circ$$

$$\text{Longitude of perihelion} = 9.231^\circ$$

What C3 was delivered by the Shuttle/Inertial Upper Stage?

6.4 Magellan approached Venus with a velocity at infinity of 4.357 km/s and a semiminor axis b of 16,061.4 km. What was the periapsis radius at Venus? What was the minimum velocity change required for capture by Venus? What is the impact radius of Venus in the B plane?

6.5 The Voyager I's closest approach to Saturn was at a periapsis radius of 124,000 km; the hyperbolic excess velocity was 7.51 km/s. What was the angle through which the spacecraft velocity vector was turned by Saturn?

6.6 Design a mission to Mars for launch in the 1990 type I opportunity given the following information:

Earth at launch: August 16, 1990 (JD = 244 8120)

$$\text{Longitude} = 323.368^\circ$$

$$e = 0.016672$$

$$\text{Longitude of perihelion} = 103.015^\circ$$

Mars at arrival: March 14, 1991 (JD = 244 8330)

$$\text{Longitude} = 117.3988^\circ$$

$$\text{Latitude} = 1.7075^\circ$$

$$a = 227,937,700 \text{ km}$$

$$e = 0.093437$$

$$\Omega = 49.5831 \text{ deg}$$

$$\text{Longitude of perihelion} = 336.0034^\circ$$

$$i = 1.8503 \text{ deg}$$

- (a) Design the transfer ellipse; determine the longitude of the line of apsides, the eccentricity, and the periapsis radius.
- (b) Calculate the inclination of the transfer ellipse with respect to the ecliptic plane.
- (c) Calculate C3.
- (d) Calculate the inclination of the transfer ellipse with respect to the Mars orbit plane.
- (e) Calculate velocity at infinity on the arrival hyperbola.

This page intentionally left blank

7

Lunar Trajectories

Lunar trajectories were the premier problem in mission design in the 1960s. In this chapter the characteristics of this trajectory and the techniques used will be summarized. A patched conic method will be discussed; however, the method is not as accurate for lunar trajectories as planetary ones because of the influence of both the Earth and sun. Accurate solutions must be accomplished by numerical analysis.

7.1 Motion of the Earth–Moon System

The Earth–moon system is unique; the two bodies are so close to the same mass that, had the moon been slightly larger, they would be the only known binary planet system. It is a common misconception that the moon revolves around the Earth. In fact, the Earth and moon revolve around a common center of mass that is 4671 km from the center of the Earth and 379,729 km from the center of the moon; see Fig. 7.1. One sidereal rotation about the common center takes 27.32 days.

Solar perturbations change the rotation period by as much as 7 h. The orbit is slightly elliptical with an eccentricity of 0.0549 and semimajor axis of 384,400 km.

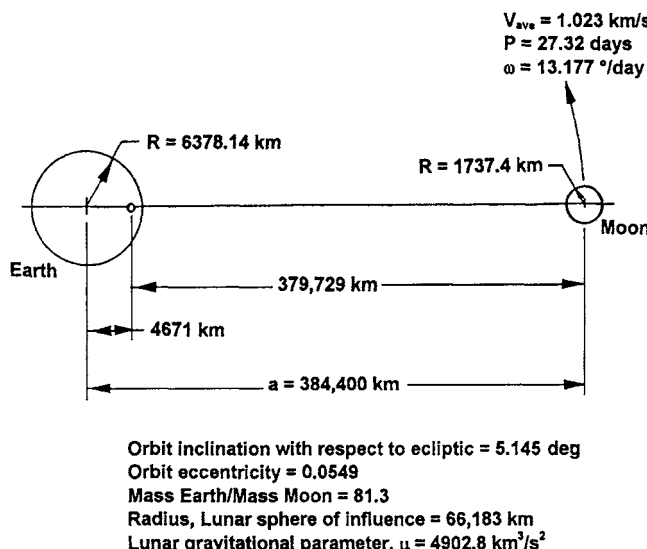


Fig. 7.1 Characteristics of the Earth–moon orbit.

As a result the Earth–moon distance changes slightly with true anomaly. In addition the semimajor axis is increasing with time as the tides about Earth take energy from the moon orbit and slow its orbital velocity. Small changes in eccentricity occur with a period of 31.8 days; this effect is called *evection* and was observed by the Greeks 2000 years ago.³

The average orbit inclination, with respect to the ecliptic, is 5.145 ± 0.15 deg varying with a period of 173 days.³⁶ The inclination of the equatorial plane with the ecliptic is 23.45 deg and the equatorial plane is relatively stable with a period of 26,000 years. When the ascending node of the Earth–moon orbit is aligned with the vernal equinox, the inclination of the moon orbit with the equator is at a maximum of $23.45 + 5.145$ or 28.6 deg. Conversely, when the descending node is at the equinox, the inclination of the moon orbit with the equator is 18.3 deg. The period of this variation is 18.6 years. Recall that the minimum inclination that can be achieved from ETR without a plane change is 28.5 deg; therefore, good launch years are on 18.6 year centers. It is not a coincidence that the moon launches in 1969 were during a good year.

7.2 Time of Flight and Injection Velocity

Time of flight was a very serious consideration in the Apollo manned missions because of the mass of provisions required to sustain life. Injection velocity is a serious consideration in any mission because the chosen launch vehicle imposes an absolute limit. Lunar time of flight and injection velocity can be bounded using a simplified case with the following assumptions:

- 1) The lunar orbit has a circular radius of 384,400 km.
- 2) The transfer ellipse is in the lunar orbit plane.
- 3) The gravitational effect of the moon is negligible.
- 4) The injection point is at the perigee of the transfer ellipse.

Unlike planetary launches, a lunar departure orbit is elliptical rather than hyperbolic. The minimum energy trajectory is an ellipse just tangent to the lunar orbit, orbit 1 in Fig. 7.2. Any less energetic orbit would not reach the lunar radius. The minimum energy trajectory has the longest possible transfer time and the lowest injection velocity. Assuming a transfer ellipse with perigee of 275 km, the nominal

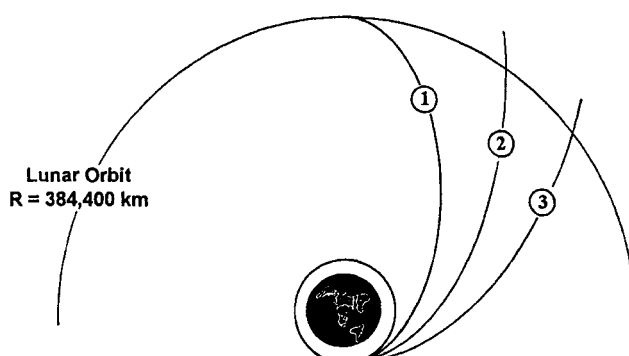


Fig. 7.2 Lunar trajectories.

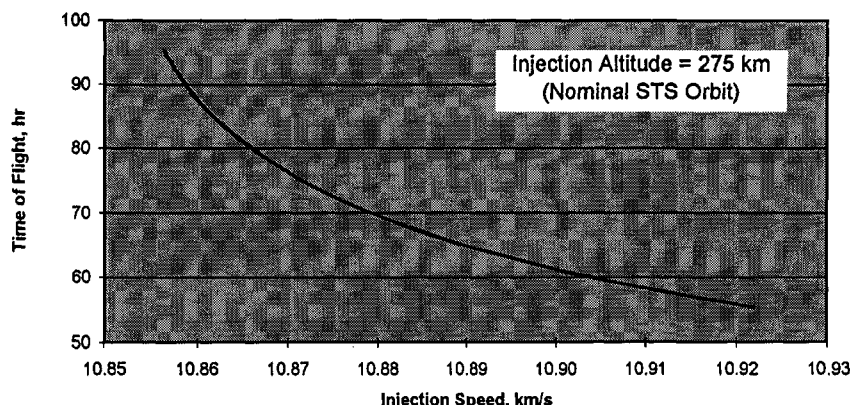


Fig. 7.3 Time of flight vs injection speed.

Shuttle orbit, produces a minimum energy transfer ellipse with a time of flight of 119.5 h and an injection speed of 10.853 km/s.

Shorter flight times can be obtained by increasing the injection speed, orbits 2 and 3 in Fig. 7.2. Figure 7.3 shows the relation between time of flight and injection speed for injection altitudes of 275 km. You can see that the 72-h time of flight used in the Apollo program is a reasonable compromise between time and launch vehicle energy. A curve similar to Fig. 7.4 can be constructed for any chosen injection altitude.

7.3 Sphere of Influence

In the patched conic analysis of a planetary mission, it was possible and accurate to assume that the sphere of influence was negligibly small compared to the transfer ellipse and essentially ignore it. That assumption is not accurate for a lunar trajectory; it is necessary to acknowledge the sphere of influence and make a trajectory patch at its boundary.

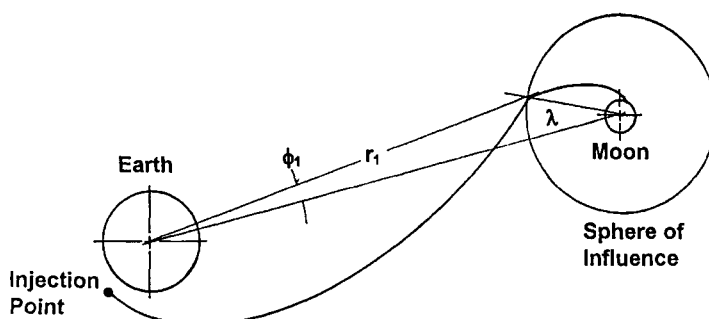


Fig. 7.4 Lunar patched conic.

The radius of the sphere of influence may be calculated by the Laplace method. From Eq. (6.1),

$$r_s = r_1 \left(\frac{M_{\text{moon}}}{M_{\text{Earth}}} \right)^{2/5} \quad (7.1)$$

where

r_s	= radius of the lunar sphere of influence
r_1	= distance between centers of mass for Earth and moon, 384,400 km
$M_{\text{moon}}/M_{\text{Earth}}$	= ratio of mass for moon and Earth, 1/81.3

$$r_s = (384,400)(1/81.3)^{2/5} \quad (7.2)$$

$$r_s = 66,183 \text{ km} \quad (7.3)$$

7.4 Lunar Patched Conic

Using the patched conic method for a moon mission is not as accurate as it is for a planetary mission, primarily because of the influence of the sun on both bodies and the short distance between the two, compared with the sphere of influence. In the following analysis, we will assume that the lunar transfer orbit is coplanar with the lunar orbit. The mission is shown schematically in Fig. 7.4.

Designing a Lunar Mission

The procedure for designing a lunar mission is as follows:

- 1) Set initial conditions. To define the transfer ellipse, it is necessary to pick injection altitude (or radius), velocity, and flight path angle. (If injection is made at perigee the flight path angle is zero.) In addition, it is necessary to define the location of the arrival point at the sphere of influence; the most convenient method is to set the angle λ , as shown in Fig. 7.4.
- 2) Define the transfer ellipse given r , V , and γ at the point of injection using the energy/momenta technique described in Sec. 2.2 and Example 2.2. If the initial velocity is not high enough, the departure ellipse will not intersect the moon sphere of influence and a second set of initial conditions must be chosen. Note that the departure trajectory is an ellipse rather than a hyperbola as it was in a planetary mission. A lunar mission can be done without reaching the escape velocity.
- 3) Find the radius to the sphere of influence, r_1 in Fig. 7.4, from trigonometry.
- 4) Given r_1 , find time of flight to the sphere of influence boundary.
- 5) Define V_2 , and γ_2 inside the sphere of influence at the arrival point. The radius is the radius of the sphere of influence, 66,183 km.
- 6) Given r_2 , V_2 , and γ_2 inside the sphere of influence, define the arrival orbit. (It is not reasonable to assume that the sphere of influence will be pierced at V_∞ on the arrival hyperbola as it is with a planetary mission.)
- 7) If the arrival orbit is satisfactory, find the launch day using the time of flight calculated in step 3 and average orbital velocity.

8) If the arrival orbit is not satisfactory (e.g., if the arrival hyperbola impacts the surface when a lunar orbit was desired), adjust initial conditions and start over at step 1.

Note that all of these steps can be done with the ORBWIN software.

Example 7.1 Lunar Patched Conic

Assume the lunar orbit is circular with radius 384,400 km and is coplanar with the transfer ellipse. Define a lunar trajectory with the following initial conditions:

$$\text{Injection at perigee } \gamma_0 = 0$$

$$\text{Injection radius } r_0 = 6700 \text{ km}$$

$$\text{Injection velocity } V_0 = 10.88 \text{ km/s}$$

$$\text{Arrival angle } \lambda = 60 \text{ deg}$$

Using Eq. (2.8) for the stated initial conditions, the specific energy on the transfer ellipse is

$$\begin{aligned} \varepsilon &= \frac{V_0^2}{2} - \frac{\mu}{r_0} \\ \varepsilon &= \frac{(10.88)^2}{2} - \frac{398600.4}{6700} \\ \varepsilon &= -0.305397 \text{ km}^2/\text{s}^2 \end{aligned} \quad (2.8)$$

The specific momentum is

$$\begin{aligned} H &= r_0 V_0 \cos \gamma_0 \\ H &= (6700)(10.88) \cos(0) \\ H &= 72,896 \text{ km}^3/\text{s} \end{aligned} \quad (2.12)$$

and from Eq. (2.10)

$$\begin{aligned} a &= -\frac{\mu}{2\varepsilon} \\ a &= -\frac{398600.4}{(2)(-0.305397)} = 652,594 \text{ km} \end{aligned} \quad (2.10)$$

From Eq. (7.5),

$$\begin{aligned} e &= \sqrt{1 - \frac{H^2}{\mu a}} \\ e &= \sqrt{1 - \frac{(72896)^2}{(398600)(652594)}} = 0.98973 \end{aligned} \quad (2.13)$$

You can use Eq. (2.14) to assure yourself that the calculated semimajor axis and a periapsis velocity of 10.88 km/s are consistent.

Arrival conditions. Defining arrival as the point on the transfer ellipse at the intersection with the sphere of influence, the radius of the arrival point is r_1 in Fig. 7.4. The radius r_1 can be obtained from trigonometry, specifically the cosine law. The full solution of the triangle containing r_1 is shown in Fig. 7.5. The phase angle ϕ_1 is 9.2662 deg and r_1 is 355,953 km. Given r_1 , the arrival velocity V_1 , the flight path angle γ_1 , the true anomaly θ_1 , and the time of flight can be determined by evaluating parameters at a point. The technique is described in Sec. 2.3 and Example 2.5, or it can be done with the ORBWIN software.

The parameters at a point evaluation yields $V_1 = 1.276$ km/s, $\gamma_1 = 80.766$ deg, $\theta_1 = 166.54$ deg, and time of flight = 49.752 h.

Defining the lunar orbit. The lunar orbit, inside the sphere of influence, is defined by the radius, velocity, and flight path angle. The average velocity of the moon about the Earth–moon center of mass is $V_m = 1.023$ km/s in a counterclockwise direction perpendicular to the Earth–moon radius. The arrival geometry is shown in Fig. 7.6; note that the angle between the known velocity vectors V_m and V_1 is $\gamma_1 - \phi_1$.

The spacecraft velocity with respect to the moon V_2 , can be obtained from the cosine law; the full solution of the vector diagram is shown in Fig. 7.7. You can see from Fig. 7.6, the arrival geometry, that the flight path angle associated with V_2 is

$$\gamma_2 = 180 - \lambda - \beta$$

$$\gamma_2 = 57.05 \text{ deg}$$

The orbital elements inside the sphere of influence are determined:

$$r_2 = 66,183 \text{ km}$$

$$V_2 = 1.359 \text{ km/s}$$

$$\gamma_2 = 57.05 \text{ deg}$$

The lunar orbit can now be defined using the energy/momentum technique. (It is not adequate to assume that the spacecraft arrives at V_∞ on a hyperbolic orbit, as is done in planetary trajectories, because the sphere of influence is relatively

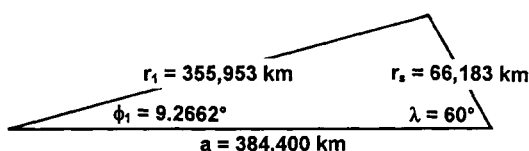


Fig. 7.5 Triangle solution for r_1 .

LUNAR TRAJECTORIES

139

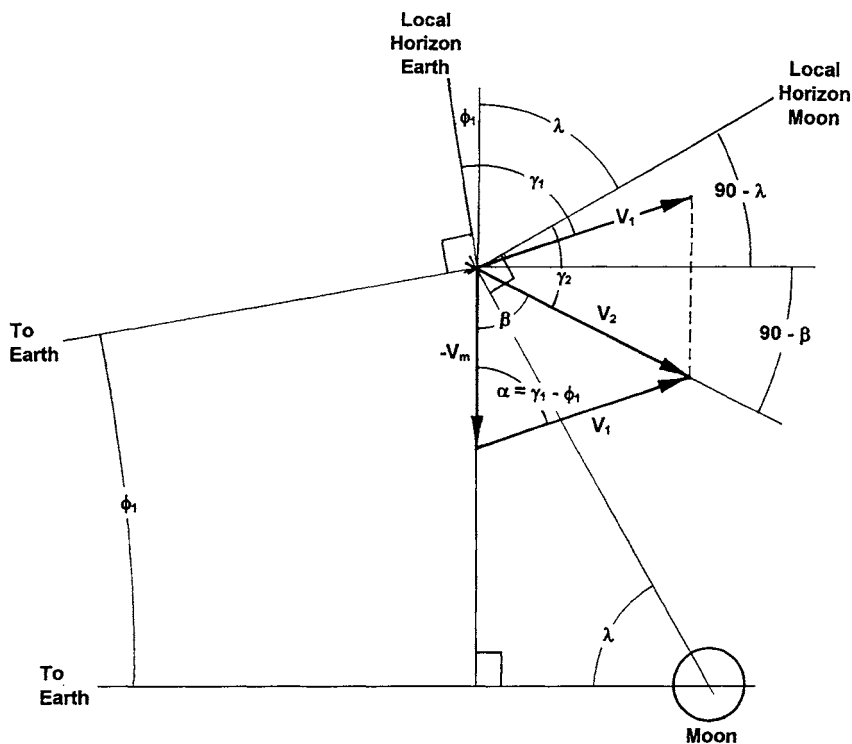


Fig. 7.6 Lunar arrival geometry.

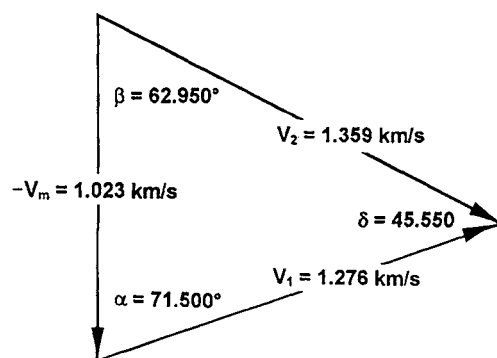


Fig. 7.7 Arrival vector diagram.

small.) From Eq. (2.8), the specific energy of lunar orbit is

$$\varepsilon = \frac{(1.359)^2}{2} - \frac{4902.8}{66183}$$

$$\varepsilon = 0.84936 \text{ km}^2/\text{s}^2$$

(You will recognize that μ for the moon is 4902.8.) A positive specific energy signals a hyperbolic orbit. Calculating specific momentum,

$$H = (66183)(1.359) \cos(57.05)$$

$$H = 48,920.5 \text{ km}^3/\text{s}$$

and from Eq. (2.10)

$$a = -\mu/2\varepsilon$$

$$a = -\frac{4902.8}{(2)(0.84936)} = -2886.2 \text{ km} \quad (2.10)$$

From Eq. (7.5),

$$e = \sqrt{1 - \frac{H^2}{\mu a}} \quad (2.13)$$

$$e = \sqrt{1 - \frac{(48920.5)^2}{(4902.8)(-2886.2)}} = 13.0432$$

A negative semimajor axis and an eccentricity larger than one both confirm the orbit as hyperbolic.

The resulting lunar orbit is the relatively flat hyperbola shown to scale in Fig. 7.8. The periapsis radius is 34,759 km and the time of flight from sphere of influence

Orbital Elements

$a = -2886.2 \text{ km}$
 $e = 13.0432$
 $r_p = 34,759 \text{ km}$
 $V_\infty = 1.3033 \text{ km/s}$

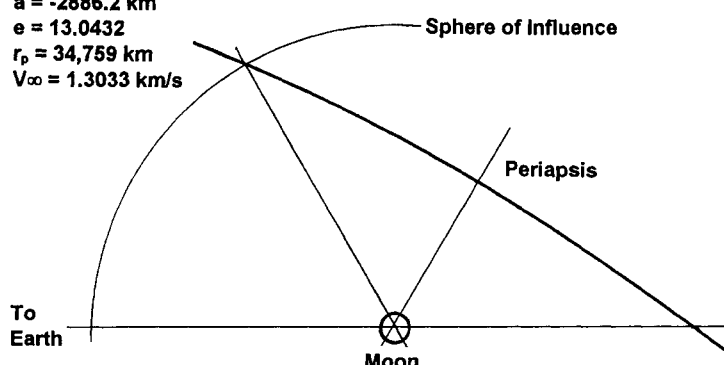


Fig. 7.8 Lunar orbit.

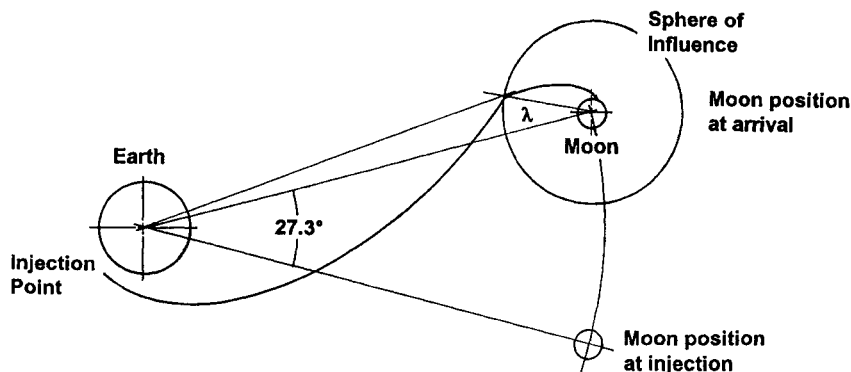


Fig. 7.9 Moon position at injection.

to periapsis is 11.59 h, making the total time of flight from injection to periapsis 61.34 h. Note that V_∞ is 1.3033 km/s, while velocity at the patch point is 1.39 km/s. The common planetary trajectory assumption that velocity at the patch point is V_∞ would have led to a serious error.

Recall the initial assumption that the trajectory was in the lunar orbit plane. If a noncoplanar trajectory is desired, the inclination of the transfer plane can be incorporated into the calculations using the methods described in Chapter 6.

Evaluation of the Orbit

With the lunar trajectory elements in hand, evaluate the orbit against what is needed for the mission. For example, if a lunar landing were desired, this is clearly the wrong orbit. If the orbit is not satisfactory, change the initial conditions, particularly λ , and recalculate.

Phasing

After a satisfactory lunar orbit is found, the phasing of the lunar position at injection can be determined. The time of flight from injection to the sphere of influence is 49.752 h. The average lunar angular speed is 13.177 deg per day; therefore, the moon, at the time of injection, must be 27.3 deg before its position at spacecraft arrival (see Fig. 7.9).

It is worth repeating that a patched conic analysis of a lunar trajectory is for preliminary design only. For accurate work, a numerical analysis is required.

Problems

- 7.1 Assuming a circular lunar orbit of radius 384,400 km, coplanar with the transfer ellipse, injection point at the perigee, and negligible lunar mass, what are the elements a and e of the minimum energy transfer ellipse if the injection altitude is 1000 km?

7.2 Assuming a circular lunar orbit of radius 384,400 km, coplanar with the transfer ellipse, injection point at the perigee, and negligible lunar mass, what is the time of flight to the moon if the injection altitude is 850 km and the injection velocity is 10.425 km/s?

7.3 What is the specific energy and specific momentum of an Earth orbit with the following properties at a point?

$$\text{Radius} = 11,000 \text{ km}$$

$$\text{Velocity} = 10.280 \text{ km/s}$$

$$\text{Flight path angle} = -40.1944 \text{ deg}$$

What type of orbit is it?

7.4 What are the elements a and e of a lunar arrival orbit if the arrival point (at the sphere of influence) has the following properties:

$$\text{Velocity} = 1.3133 \text{ km/s}$$

$$\text{Flight path angle} = -86.1445 \text{ deg}$$

Is this a lunar landing orbit?

7.5 Define a lunar trajectory using the patched conic technique assuming circular coplanar transfer. Calculate the elements of the transfer ellipse and the arrival hyperbola given the following:

$$\text{Injection velocity at perigee of transfer ellipse} = 10.738 \text{ km/s}$$

$$\text{Injection altitude} = 500 \text{ km}$$

$$\text{Arrival angle } \lambda = 30 \text{ deg}$$

What is the time of flight from injection to the arrival at the sphere of influence?
Is this a lunar landing trajectory?

Appendix A

ORBWIN: AIAA Mission Design Software

A.1 Introduction to ORBWIN

Mission design computations can be divided into a few fundamental tools that are versatile enough to accommodate a very wide range of situations and powerful enough to save a lot of work. ORBWIN: AIAA Mission Design Software for Windows™ is a collection of these tools. They are analogous to the lathe, drill press, and power saw of mission design. They can handle a project as ambitious as you can conceive. ORBWIN does the arithmetic, keeps the decimal in the right place, and always remembers that regression of nodes is added to apparent westward progression for direct orbits. However, it does not take the engineering imagination out of your design.

System requirements for the software are Microsoft Windows version 3.1 or later, 1.4 MB of RAM, and one disk drive. Access to a printer is desirable.

A.2 Quick Tour of ORBWIN

This section offers a quick tour through the features and the arrangement and conventions used in ORBWIN. More detail can be obtained in subsequent sections.

Installation

The standard Windows approach is used to install the software.

- 1) Put ORBWIN disk in drive A (or drive B).
- 2) For Windows 3.1, from the **File** menu in the Program Manager, select Run. For Windows 95, from the **Start** menu, select Run.
- 3) Type: *A:Setup* (or *B:Setup*).
- 4) Follow the on-screen directions.

Using ORBWIN

To start, click on the ORBWIN icon. The opening screen will appear, as shown in Fig. A.1. The three frames in the opening window provide for **Orbit Definition**, **Utilities**, and **Central Body**. The **Central Body** frame allows selection of the central body by clicking on the option buttons and review of the planetary data used by ORBWIN by clicking on the **Review** button. The **Utilities** frame provides for **Ephemeris**, **Plane Changes**, **Julian Date**, and **Propellant Mass** calculations. These calculations are described in detail in subsequent sections.

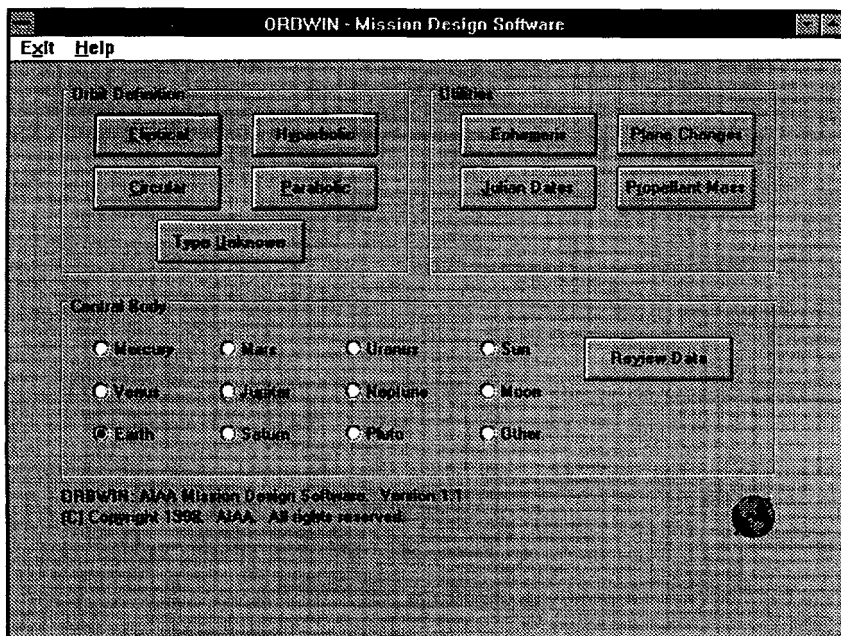


Fig. A.1 ORBWIN opening window.

Defining an Orbit

If the orbit type is known, only three steps are required to define any orbit:

- 1) Select the central body, Earth is the default, from the **Central Body** frame of the opening window.
- 2) Select the type of orbit desired from the **Orbit Definition** frame.
- 3) Enter the known quantities in the **Definition** window; Fig. A.2 shows a typical **Definition** window, this one for circular orbits.

In any **Definition** window, your first action must be to enter the known elements of the desired orbit. For a circular orbit only one element is required. The known element can be either altitude, radius, period, or orbital velocity as shown in Fig. A.2. Taking the Space Shuttle *Atlantis* launch, STS-30, as an example, the orbit period was 5400 s. (Note that the elements must be entered in the units noted in Fig. A.2; altitude in kilometers, radius in kilometers, period in seconds, or velocity in kilometers per seconds.) To move around the input boxes use the Tab key or select the desired box. Enter a period of 5400 s. Use the Backspace key to edit; make your entry in scientific notation (5.4E3) if desired. When you are satisfied with your input, press Enter or select the **Calculate** button. The elements of the defined orbit will be displayed in the **Definition** window as shown in Fig. A.3.

In Fig. A.3 the orbital radius, altitude, and velocity have been computed and displayed. A circular orbit altitude of 274.42 km produces an orbit period of

ORBWIN: AIAA MISSION DESIGN SOFTWARE

145

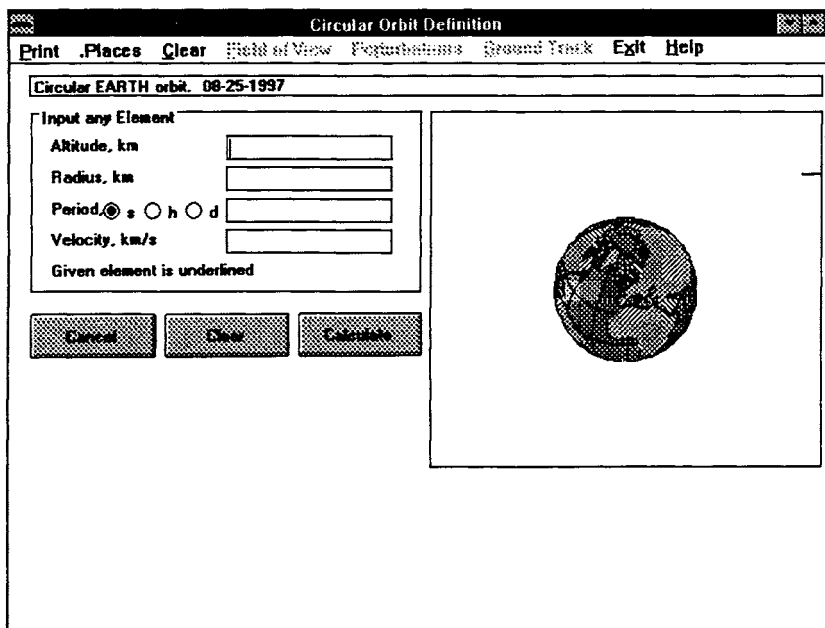


Fig. A.2 Circular orbit definition window.

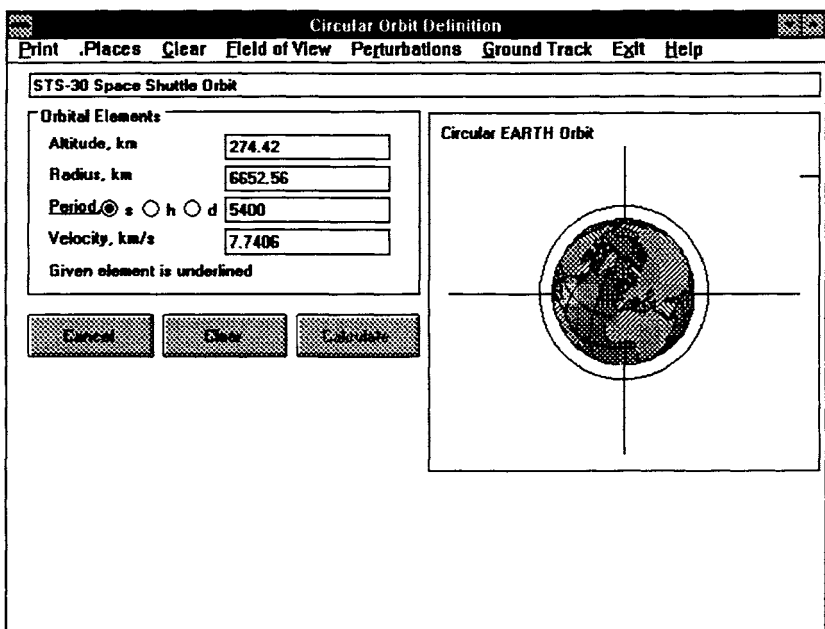


Fig. A.3 STS-30 Space Shuttle orbit.

5400 s. The given element, orbital period, is denoted by an underline. To the right of Fig. A.3 is a scale drawing of the Earth and the orbit. Above the drawing a default title is shown. You can change the title to whatever you like by clicking the title box and overwriting the new title (e.g., "STS-30 Shuttle Orbit").

Once an orbit is defined you can perform eight functions, as shown by the menu bar at the top of the window, by selecting the desired function:

- Print: Produces a copy of the screen via printer. (Control P will also initiate printing.)
- Places: Controls the number of decimal places to which the calculations are taken. The revised number of places takes effect on the next calculation.
- Clear: Empties all of the text boxes in preparation for another calculation. It is important to clear before each calculation; ORBWIN will not overwrite existing results.
- Perturbations: Calculates and displays regression of nodes and rotation of apsidies caused by the equatorial bulge of any planet for which a zonal coefficient has been measured.
- Field of View: Calculates the swath width, measured on the central body surface, the angle to the horizon, and the distance to the horizon for a spacecraft at this altitude.
- Ground Track: Shows a Mercator projection of the spacecraft ground track (locus of nadir points) as a function of time for one orbit.
- Parameters at a Point: (Elliptical and hyperbolic orbits only.) Allows selection of a point of interest by inputting radius, altitude, or true anomaly; ORBWIN fully characterizes conditions at that point. This function is not needed for circular orbits since all points on the orbit have identical properties.
- Exit: Backs up one window from any location in ORBWIN. From the opening screen, Exit returns to Windows. Pressing Esc will also initiate Exit.
- Help: Provides context-sensitive text from any window in ORBWIN. The F1 key also will initiate Help.

As an example, select **Ground Track**; the input window will appear. Input an inclination of 28.5 deg, a longitude of ascending node of -90° , and press Enter. The resulting ground track of a single orbit is shown in Fig. A.4.

Definition of Orbits of Unknown Type

Occasions arise when a point on an orbit is known by radius, speed, and flight path angle, but the orbit type is not known. A spacecraft departing from a planetary flyby is one such a case. Definition of an orbit with these known parameters requires a specific energy/specific momentum solution as described in Chapter 2. To define an orbit of unknown type using ORBWIN, select the **Type Unknown** button in the **Orbit Definition** frame. The input window shown in Fig. A.5 will appear. Enter the known conditions and select **Calculate**. The orbital type will be identified and the orbital elements calculated. These results will be displayed in the proper **Orbit Definition** window; see Fig. A.2 for example.

ORBWIN: AIAA MISSION DESIGN SOFTWARE

147

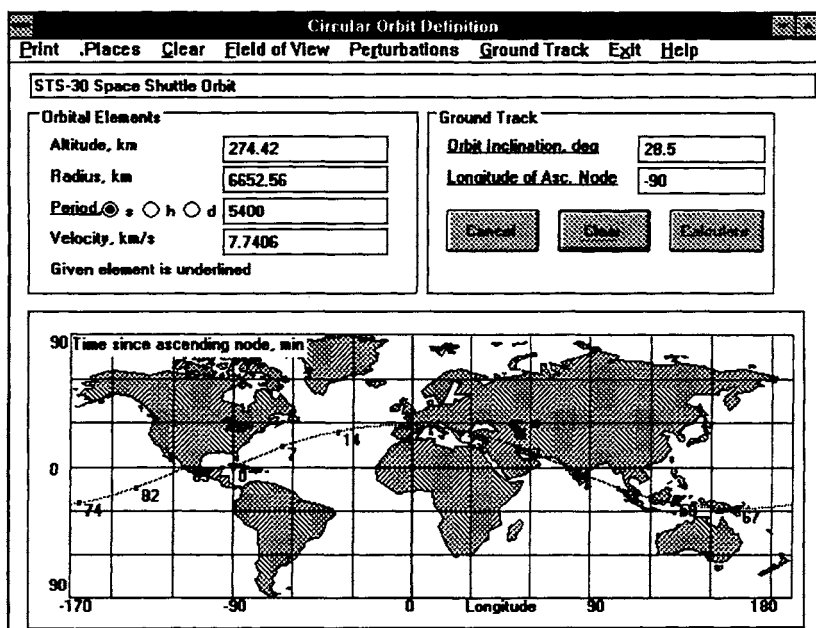


Fig. A.4 STS-30 ground track.

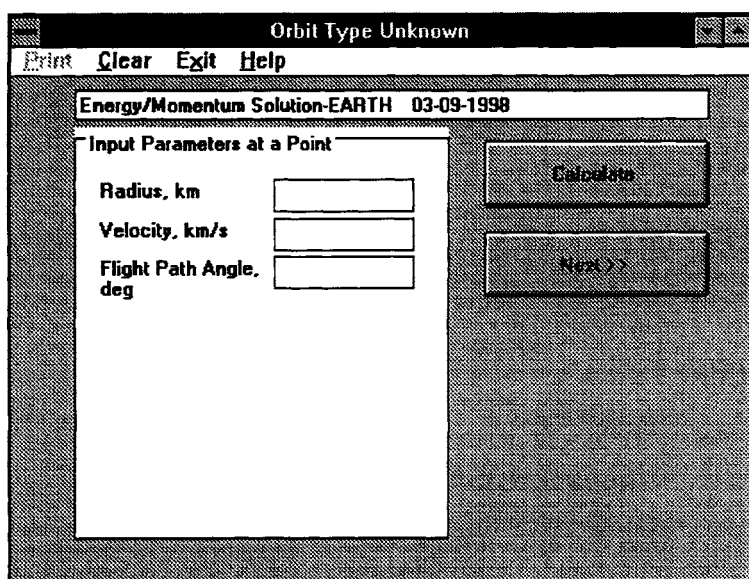


Fig. A.5 Orbit definition—type unknown.

Keyboard Shortcuts

ORBWIN provides the following keyboard shortcut commands.

Keyboard shortcuts	Press
AT A POINT = Determine parameters	Alt-A
CALCULATE	Enter
CLEAR = Clear calculations	Alt-C
EXIT = Back up one window	Alt-X or Esc
FIELD OF VIEW Determination	Alt-F
GROUND TRACK Determination	Alt-G
HELP = Get help	F1 or Alt-H
PERTURBATIONS Determination	Alt-R
PRINT = Print current screen	Alt-P or Ctrl-P

Units

ORBWIN expects inputs in the international unit system (SI), specifically:

Velocity:	kilometers/second
Distance:	kilometers
Time:	mean solar seconds
Angles:	degrees

Nomenclature

This text and the ORBWIN software use the traditional nomenclature of astrodynamics. This nomenclature has its roots in the sixteenth century and is unusually obtuse. Because we cannot change the tradition, a glossary has been included in Appendix B, to help you deal with it.

Central Body Constants

The central body constants used by ORBWIN are the gravitational constant, the radius, the rotation rate, and J2. The constants used are the most accurate currently available; however, the last decade has seen rapid revision to these “constants.” For work requiring high accuracy, it is recommended that a literature search be conducted in this area. If you wish to review or change any of these constants, use the **Review** button in the **Central Body** frame of the initial window; see Fig. A.1. Note that you can use the **Other Body** function to study minor planets or asteroids.

Utilities

ORBWIN is equipped with a set of utilities that are useful in orbital mechanics calculations. These are ephemeris, Julian dates, plane changes, and propellant mass.

Help

Online help can be obtained from any screen by pressing the F1 key, by pressing Alt-H, or by selecting **Help** on the menu bar at the top of the screen. These

ORBWIN: AIAA MISSION DESIGN SOFTWARE

149

instructions are written for Version 1.1 of the software. The manual for new versions will be entirely in the online Help files.

Equations Used

The equations used in ORBWIN are all developed and discussed in the first six chapters and summarized in Appendix C.

A.3 Orbit Definition Example

Elliptical orbits are, by far, the most common orbits. All planets and most spacecraft move in elliptical orbits. The highly elliptical orbit of the Molniya spacecraft is one of the most interesting. The orbit was devised by Russia (at that time the USSR) to provide the features of a geosynchronous orbit with better coverage of the northern latitudes and with less launch vehicle energy required. To study the Molniya orbit, select **Elliptical** from the opening window of ORBWIN; note that the central body Earth is chosen by default. Any two orbital elements define an elliptical orbit. Molniya 3-47, launched August 9, 1995, from Plesetsk has the following orbital elements:

Periapsis altitude (or perigee altitude since it is an Earth orbiter) = 593 km
Apoapsis altitude (or apogee altitude for the same reason) = 39770 km

The **Definition of an Ellipse** window, with these two elements entered, is shown in Fig. A.6.

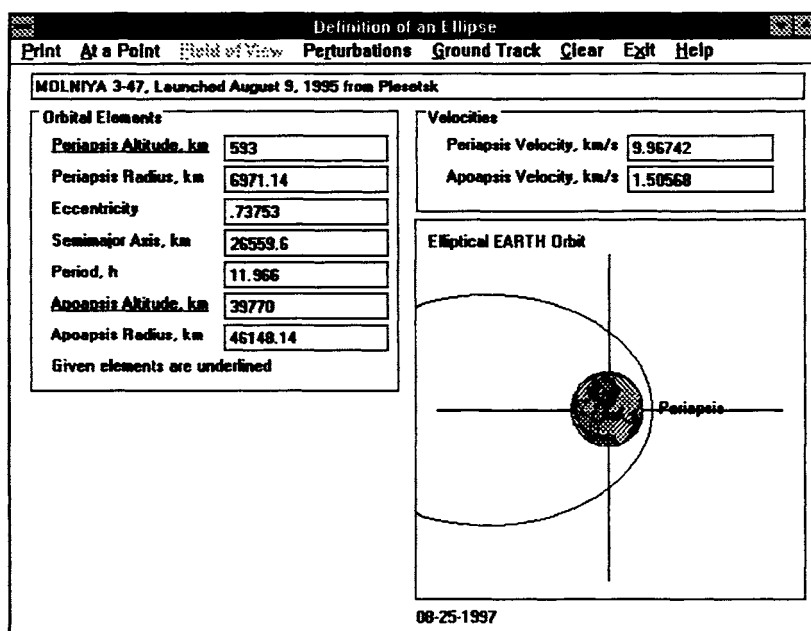


Fig. A.6 Molniya orbit.

The two input elements are underlined and a scale drawing of the highly elliptical orbit is shown in the figure, with periapsis, apoapsis velocities, and remaining calculated elements.

The ellipse input box shows two dependent element pairs; these are altitude and radius, and period and semimajor axis. Each member of a dependent pair carries the same information. Radius and altitude differ by a constant; period and semimajor axis are similarly related. A dependent pair does not define a unique orbit. If two dependent elements had been entered, ORBWIN would show an error message and tell you what to do.

Ground Track

One of the most interesting things about the Molniya orbit is its ground track. The orbit is designed to spend alternate half days over North America and Russia. The North American orbit ground track is shown in Fig. A.7. Note the inclination, longitude of ascending node, and argument of periapsis, which were input to define the North American orbit.

Orbit Perturbations

ORBWIN calculates the perturbations resulting from the equatorial bulge of any of the planets for which J2 has been measured. First you must define the orbit you are interested in and then enter the orbit inclination; ORBWIN will calculate regression of nodes and rotation of apsides for the orbit. If you choose Mercury or

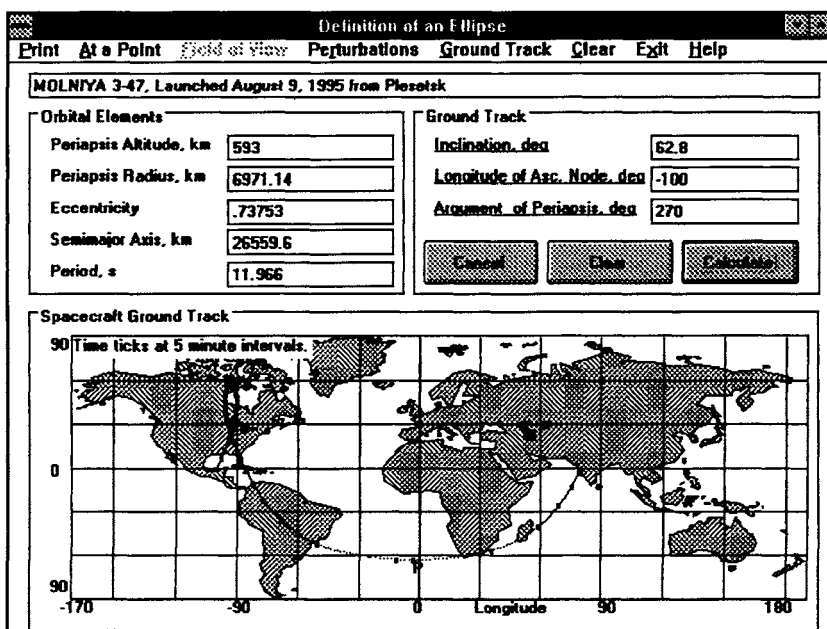


Fig. A.7 Molniya ground track.

ORBWIN: AIAA MISSION DESIGN SOFTWARE

151

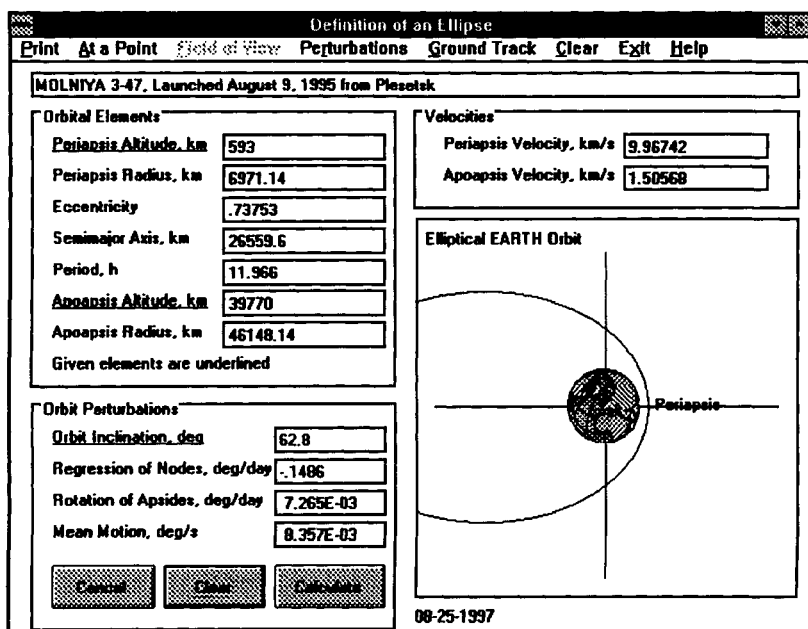


Fig. A.8 Molniya orbit perturbations.

Pluto as the central body, the perturbation will be zero because J2 is not available for these planets.

A due east launch from Plesetsk, at latitude 62.8° , will produce the greatest energy boost from Earth rotation and an orbital inclination of 62.8° . A small adjustment is sometimes made to Molniya orbits to an inclination of 63.4° at which the rotation of apsides (orbit perturbation due to Earth oblateness) would be zero. For Molniya 3-47 this adjustment was not made. To see the resulting rotation of apsides select **Perturbation** on the main menu bar and enter the orbit inclination; the result is shown in Fig. A.8. Without the orbit adjustment the rotation of apsides is not zero, but it is very small, 7 deg every 1000 days.

Field of View

The Molniya field of view in its hover period near apogee is similar to that of a geosynchronous spacecraft. The field of view parameters may be seen by selecting a point; select **At A Point** in the bar menu and enter a true anomaly of 180 deg, apogee. Then select **Field of View** from the bar menu. Notice that **Field of View** is inaccessible and disabled until a point on the orbit is chosen. The field of view results are shown in Fig. A.9. Central angle, distance to horizon, and swath width are calculated based on the assumption that the central body is a sphere of radius equal to the mean equatorial radius without surface irregularities. This assumption leads to an error generally less than 0.1%.

The Molniya apogee altitude is about 4000 km higher than a geosynchronous orbit, and the field of view parameters are similar. The central angle

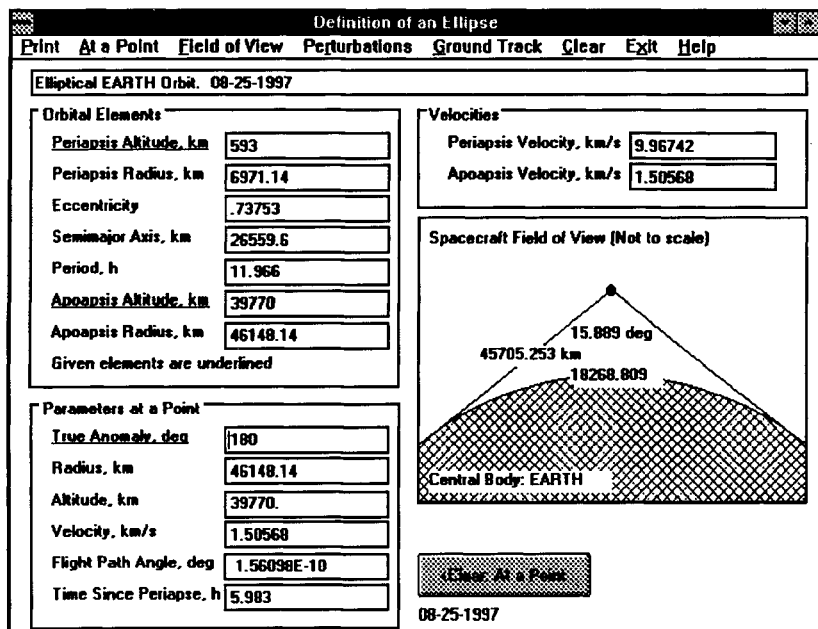


Fig. A.9 Field of view from Molniya orbit apogee.

is 17,402 deg, the distance to the horizon is 41,675 km, and the swath width is 18,100 km.

A.4 Utilities

ORBWIN provides four utility functions that are useful in orbital mechanics calculations. These are

- Ephemeris
- Julian Dates
- Plane Changes
- Propellant Mass

To select one of the utilities click on the appropriate command button from the main window; see Fig. A.1. Each of these functions is discussed in the following sections.

Ephemeris

The ephemeris function calculates the location and orbital elements of any of the major planets for any given date. The calculations are done by a polynomial approximation using coefficients from Meeus,⁴³ for all of the planets but Pluto. The Pluto ephemeris is based on polynomials from Ref. 23. The data are with respect to the ecliptic and equinox of date. The Pluto ephemeris is accurate for dates between October 1, 1989, and January 6, 2002. (Julian days between 244 7800.5 and 245

ORBWIN: AIAA MISSION DESIGN SOFTWARE

153

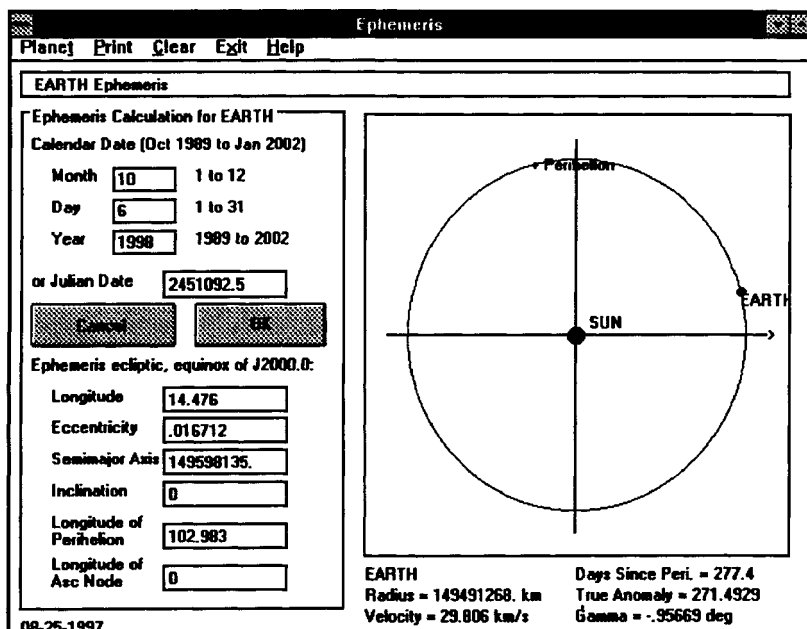


Fig. A.10 Earth ephemeris for 10-16-1998.

2280.5) The ORBWIN software will calculate Pluto orbital elements beyond the stated range; however, the accuracy is questionable.

To use the ephemeris, select **Ephemeris** from the opening window. Then select the planet of interest from the **Ephemeris** window, shown in Fig. A.10. Next enter the date by month, day, and year or by Julian date. Note that the year must be entered fully, 1998 not 98, because the span of possible dates goes into the 2000s. Press Enter or click on OK when you are satisfied with the date.

As shown in Fig. A.10, the ephemeris function calculates the following:

- Planet longitude
- Eccentricity
- Semimajor axis
- Inclination of planetary orbit
- Longitude of perihelion
- Longitude of ascending node
- Radius from sun
- Planet velocity with respect to sun
- Days since periapsis
- True anomaly
- Flight path angle
- And Julian or Gregorian date, whichever was not entered

The planet's position with respect to the vernal equinox vector is shown to scale on the right of the elements, Fig. A.10. The elements are computed with respect to equinox and ecliptic of date. The elements shown are for Earth but the calculation can be done for any planet.

Julian Dates

As described in Sec. 2.6, Julian dates were devised in the sixteenth century to provide astronomers with a standard method for numbering days. Four centuries later it is still the only universally recognized system. Without ORBWIN, calculating a Julian date is messy indeed, and converting Julian dates to calendar dates is even worse. Making this conversion with ORBWIN you first select Julian dates from the Utilities box of the main window. The input window is shown in Fig. A.11.

Figure A.11 shows the conversion of calendar date 9-21-2002 to Julian Day 2452538.5. The conversion can be made in both directions, Gregorian dates (normal calendar) to Julian dates and vice versa. Days between dates may also be calculated. Calendar dates are reported in the standard format: mm-dd-yyyy.

The Julian date fraction, "0.5", results from the 12-h offset between calendar days and Julian days. Unfortunately, this offset means that two Julian days are

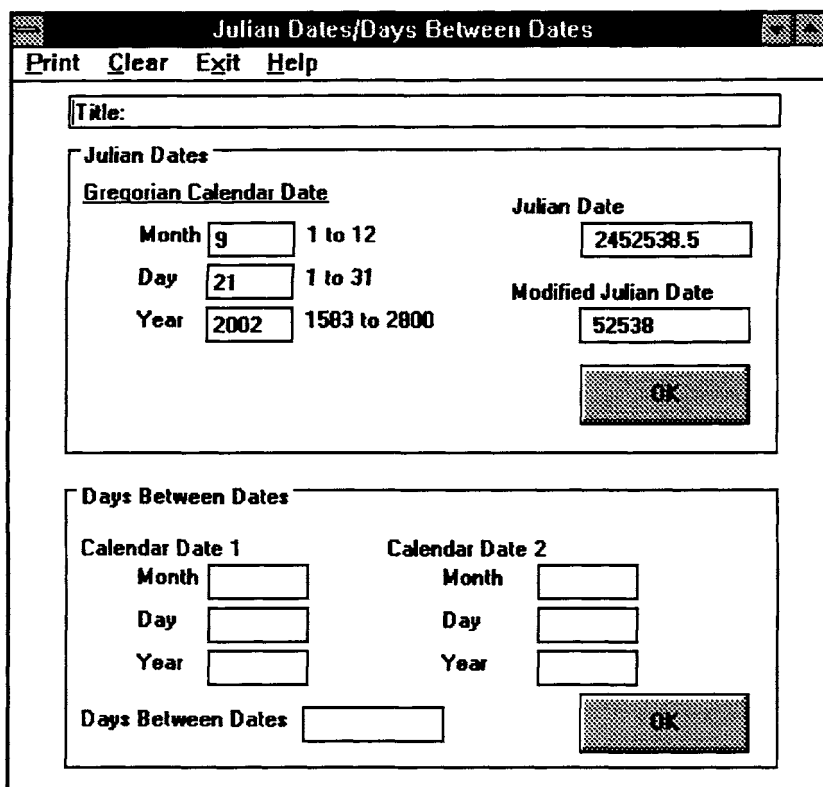


Fig. A.11 Julian day calculation window.

ORBWIN: AIAA MISSION DESIGN SOFTWARE

155

associated with each calendar day and vice versa. The Julian date returned by ORBWIN is Julian date in progress when the calendar day starts at 00:00 Universal Time. At this time the Julian day is half over so ORBWIN will report the Julian date fraction. Similarly, ORBWIN returns the calendar day in progress at the start of the Julian date that is entered.

Modified Julian day numbers are obtained by subtracting 2,4000,000.5 from a Julian day. Modified Julian day numbers are more convenient and less well accepted than Julian days.

Plane Changes

Plane change maneuvers are a frequent calculation required in mission design. ORBWIN provides a rapid calculation utility to obtain the velocity change necessary to make a given plane change. The plane change utility is obtained by selecting the **Plane Change** command button in the main window. Fig. A.12 shows the plane change window. The example shown is a 20 deg change in the direction of a 1.5 km/s velocity vector. The ΔV required calculated by ORBWIN is 0.52094.

Propellant Weight Calculation

The key result of a maneuver calculation is how much propellant weight is required to make the maneuver. The propellant weight computer function of ORBWIN provides this information given the velocity change required, the specific impulse of the propulsion system, and either the initial weight (including the consumed propellant) or final weight (after the propellant is burned). The initial and final weights can be entered in any weight units (pounds, kilograms, or other) the calculated weight will be in the same units. Specific impulse must be input

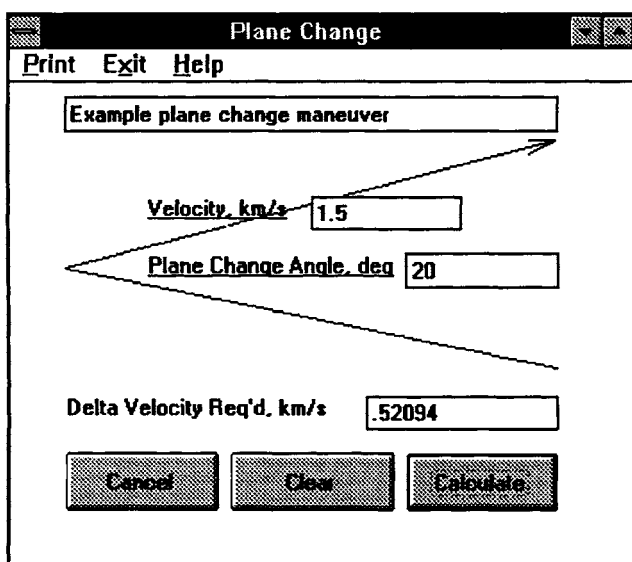


Fig. A.12 Plane change delta velocity.

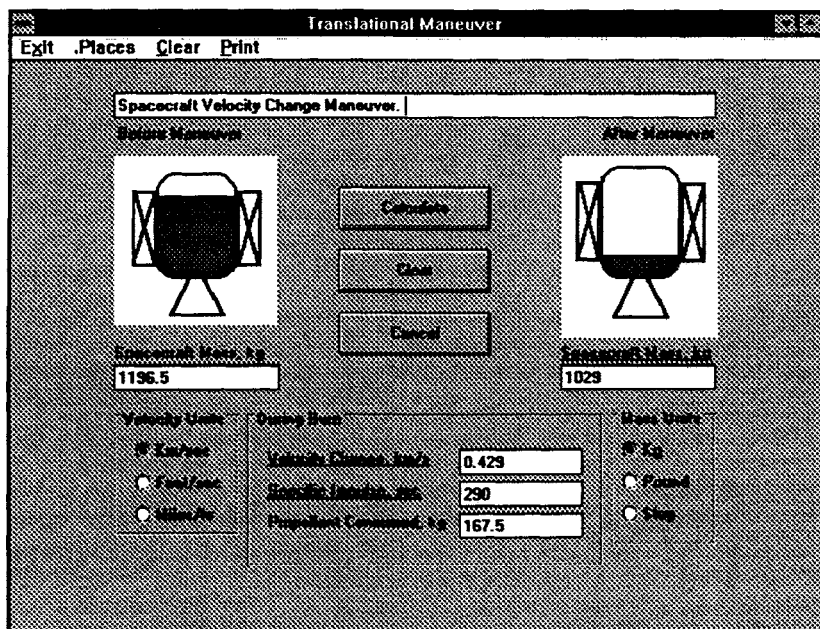


Fig. A.13 Maneuver propellant calculation window.

in seconds; Table 3.2 has some representative values. Velocity change must be in kilometers per second.

Figure A.13 shows the input screen for an example where the velocity change is 429 m/s, the specific impulse is 290 s (typical solid motor), and the weight of the spacecraft at burnout is 1025 kg.

A.5 Interesting Orbits—Examples

In this section the orbits of several interesting and historically significant spacecraft will be analyzed as examples of how ORBWIN works.

The spacecraft selected are

- N-STAR 1—Geosynchronous Orbit
- LANDSAT 7—Sun-synchronous Orbit
- MAGELLAN—Venus Mapping Orbit
- GALILEO—Jupiter Exploration Orbit
- VOYAGER 2—Neptune Encounter
- CLEMENTINE—Lunar Mapping

In each case a brief explanation of the spacecraft and orbit are given along with a figure from ORBWIN showing the orbit. You can use ORBWIN to duplicate any of the orbits in this appendix by entering the orbital elements shown in each figure. The orbital elements that were entered, as opposed to calculated, are underlined.

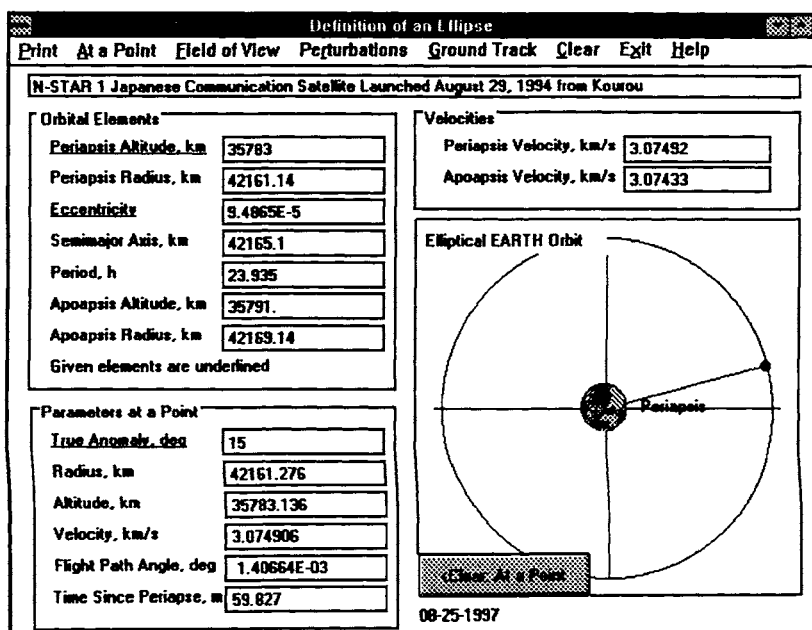


Fig. A.14 N-STAR 1 parameters at a point.

N-STAR 1—Geosynchronous Orbit

N-STAR 1 is a Japanese communications satellite that will deliver telephone service to the remote islands. It was launched on August 29, 1994, by Ariane 44P from Kourou. The ideal geosynchronous orbit is perfectly circular with a radius of 42,164.2 km and an inclination of zero. The orbit shown in Fig. A.14 is the real initial orbit attained by N-STAR 1 and is slightly elliptical, as all real orbits are.

LANDSAT 7—Sun-synchronous Orbit

LANDSAT 7 is the first spacecraft of the third generation of LANDSAT vehicles. It will be launched in 1998 featuring enhanced thermal mapping from a sun-synchronous orbit. The orbit shown in Fig. A.15 is the design orbit. The sun-synchronous orbit has the curious property of providing a constant sun angle at all times. The orbit is very desirable for instruments that observe reflected light. It is a circular retrograde orbit with an inclination designed to match the regression of nodes to the rotation of the Earth.

Magellan—Venus Mapping Orbit

The Magellan spacecraft, launched on Space Shuttle *Atlantis*, in May 1989, produced the first full global map of Venus topography. The map was taken through the dense Venus clouds by synthetic aperture radar techniques. The elliptical mapping orbit, shown in Fig. A.16, had a 3.15-h period; mapping data were taken for

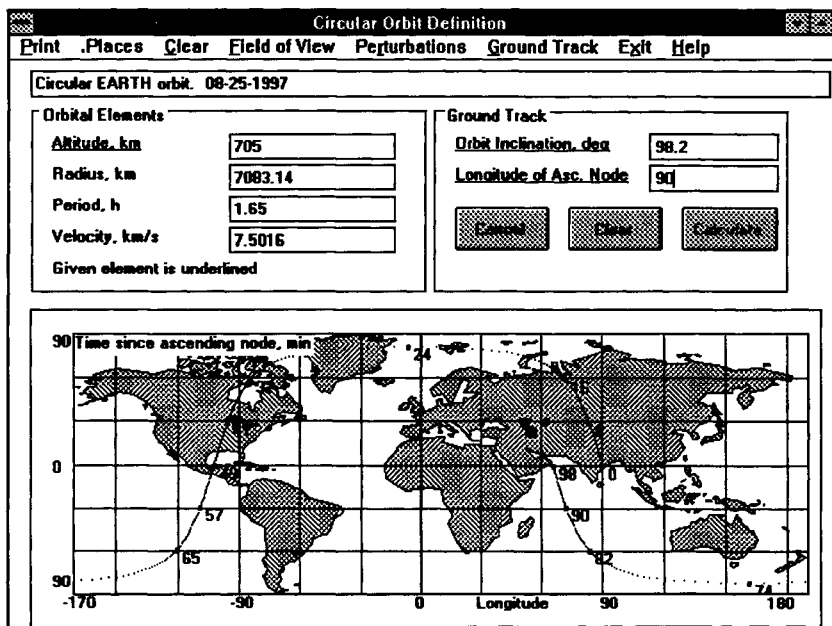


Fig. A.15 LANDSAT 7 sun-synchronous orbit.

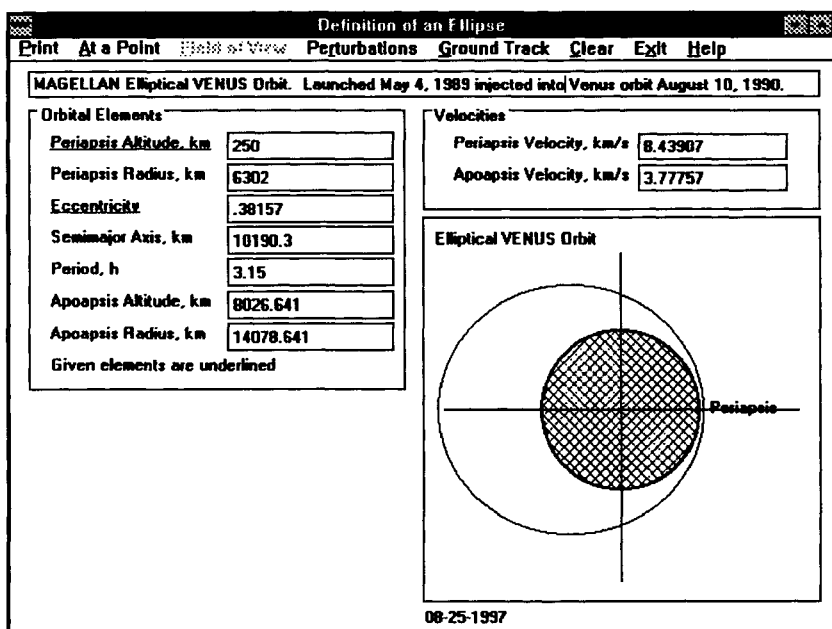


Fig. A.16 Magellan Venus mapping orbit.

ORBWIN: AIAA MISSION DESIGN SOFTWARE

159

37 min near periapsis each orbit. The orbit was designed such that Venus rotated one swath width under the spacecraft each orbit.

Galileo—Jupiter Exploration Orbit

Galileo was launched October 14, 1989, by the Space Shuttle *Atlantis* on a Venus–Earth–Earth gravity-assist trajectory to Jupiter. It was injected into Jupiter orbit on December 7, 1995, after launching a probe into the gaseous planet. The orbit shown in Fig. A.17 is the initial Jupiter orbit. The highly elliptical 230-day orbit was designed to provide observational flybys of Jupiter's moons.

Voyager 2—Neptune Encounter

The Voyager 2 did a remarkable grand tour of the outer planets starting at launch from a Titan III-E in September 1977. After flybys of Jupiter, Saturn, and Uranus, it finally arrived at Neptune for a flyby in August 1989. Its hyperbolic Neptune encounter orbit is shown in Fig. A.18.

Clementine—Lunar Mapping Orbit

The 480-lb Clementine spacecraft, launched in January of 1994, was the first U.S. moon mission in more than two decades, since Apollo 17. It mapped the surface of the Moon from the 5-h polar orbit, shown in Fig. A.19, for two months. It was from this orbit that photographs were taken showing ice on the moon—the first indication of lunar water.

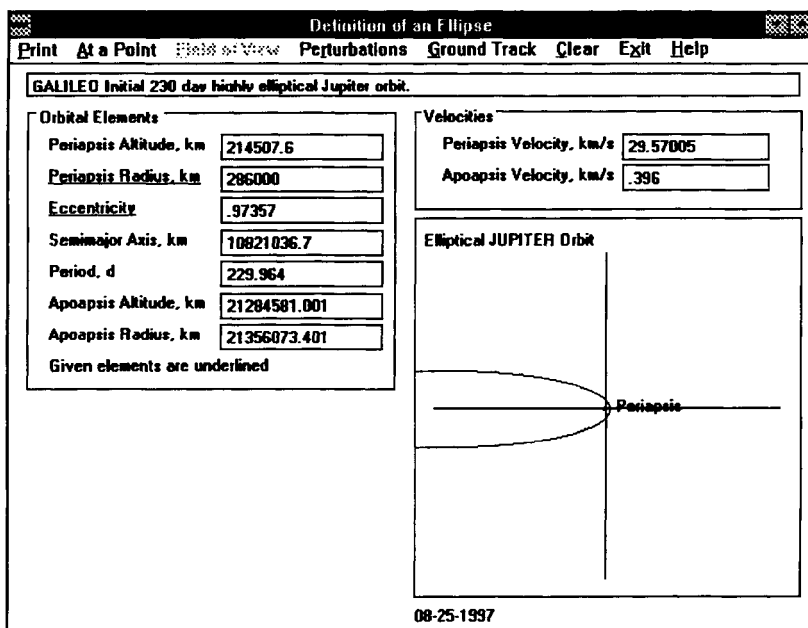


Fig. A.17 Galileo initial Jupiter orbit.

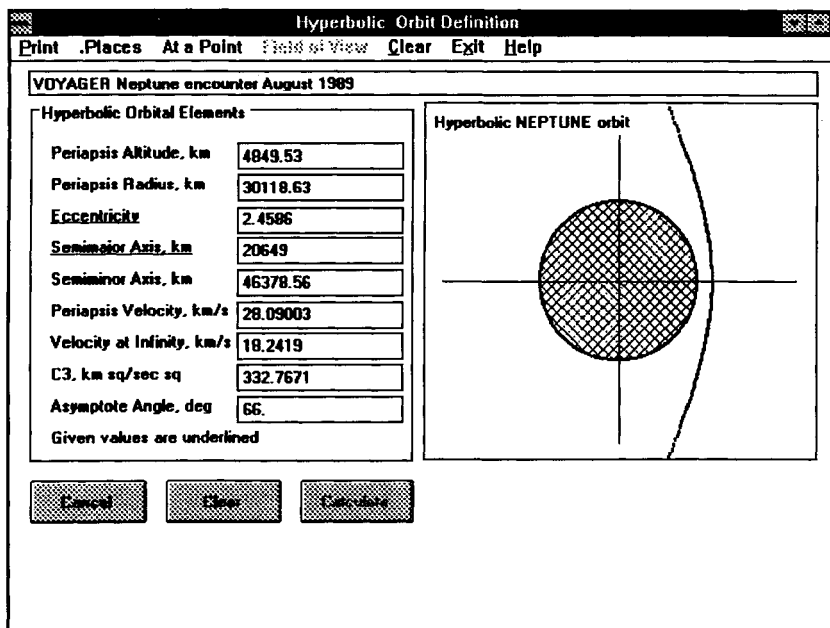


Fig. A.18 VOYAGER 2—Neptune encounter.

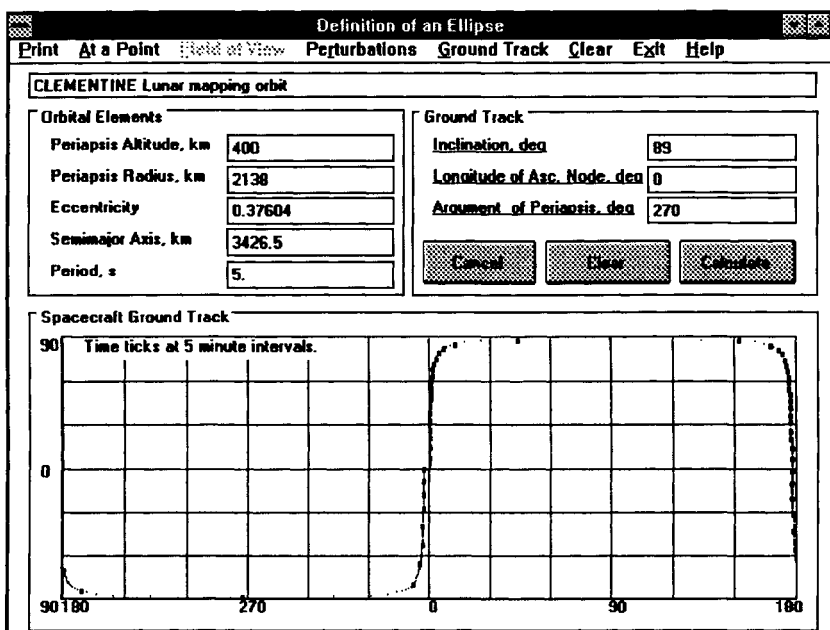


Fig. A.19 Clementine lunar mapping orbit.

Appendix B

Mission Design Glossary

aphelion	The point on an orbit about the sun that is farthest from the sun. See <i>apoapsis</i> .
apoapsis	The point on an orbit farthest from the central body; the point of maximum orbital radius. Apoapsis is a general term for any central body. Apogee is used if the central body is the Earth, aphelion for the sun, apolune for the moon. See <i>periapsis</i> .
apogee	The point on an orbit about the Earth that is farthest from the Earth. See <i>apoapsis</i> .
apolune	The point on an orbit about the Earth's moon that is farthest from the moon. See <i>apoapsis</i> .
argument of latitude, A_{La}	The angle measured in the orbit plane in the direction of motion from the ascending node to the spacecraft. It is numerically equal to the sum of the argument of the periapsis and the true anomaly.
argument of periapsis, ω	The angle from the ascending node of an orbit to the periapsis, measured in the orbital plane in the direction of spacecraft motion.
ascending node	The point where the spacecraft crosses the reference plane headed from south to north.
astronomical unit, AU	A unit of distance equal to the semimajor axis of Earth's orbit around the sun.
autumnal equinox azimuth, Az	See <i>equinox</i> .
B-plane	The angle measured clockwise along the horizon from the north vector to the indicated direction or object.
barycenter	A plane perpendicular to the asymptote of an arrival hyperbola placed at a large distance from the target planet (see Fig. 6.18). The B-plane is used in targeting a planetary arrival.
bielliptic transfer	The center of mass of a pair of bodies; for example, the Earth and the moon.
celestial longitude, Lo	A three-impulse transfer between two nonintersecting orbits that uses two transfer ellipses (see Fig. 3.5).
celestial meridian	An angle measured on the ecliptic eastward from the vernal equinox vector to a plane perpendicular to the ecliptic passing through the object.
	A great circle passing through the zenith and the north celestial pole of the celestial sphere.

celestial sphere	An imaginary sphere on which celestial bodies can be considered to be located; the sphere of the nighttime sky as seen by an observer. The sphere is considered centered at the origin of the coordinate system in use.
central angle, α	The angle, centered at the center of mass of the central body, from the nadir vector to the assigned point on the surface (see Figs. 4.13 and 4.15). See <i>orbital elements</i> and Fig. 2.18.
classical orbital elements	
conjunction	The situation where (or time at which) two celestial bodies have either the same celestial longitude or longitudes 180° apart. A planet is at superior conjunction if the sun is between it and the Earth and at inferior conjunction if it is between the sun and the Earth.
critical inclination	The orbital inclination at which apsidal rotation is zero regardless of orbital eccentricity. The critical inclination is 63.435 deg or 116.565 deg for any celestial body (see Fig. 4.8).
declination	A celestial object's angular distance from the celestial equator, measured north or south along the hour circle through the object.
direct motion	Real or apparent eastward motion; the opposite of retrograde motion; counterclockwise motion when viewed from the north pole.
eccentricity, e	A parameter that defines the shape of a conic section. The eccentricity of a circle is zero, of an ellipse is less than one but greater than zero, of a parabola is exactly one, and of a hyperbola is greater than one.
ecliptic	The plane of the Earth's orbit around the sun, inclined to the Earth's equator by about 23.439 deg.
ephemeris	A tabular statement of the positions of celestial bodies at specified intervals of time. A standard yearly reference called <i>The Astronomical Almanac</i> is published jointly by the United States and Great Britain (prior to 1981 it was called <i>The American Ephemeris and Nautical Almanac</i>).
epoch	An instant of time or a date selected as the time to fix the reference axes (usually the vernal equinox vector and the ecliptic plane) for preparation of ephemeris data.
equatorial bulge	The oblateness of a solar body caused by the axial rotation of the body. The bodies of the solar system are oblate spheroids rather than spheres.
equinox	A day during which the sun is in the intersection of the equatorial plane and the ecliptic plane. The axis of rotation of the Earth is in the horizontal plane with respect to the sun; as a result the length of the day and night is the same everywhere on Earth. There are two equinoxes in a year, one in March called the vernal equinox and one in September called the autumnal equinox.

MISSION DESIGN GLOSSARY

163

escape velocity	The velocity required to escape from the gravitational attraction of a central body.
field of view, FOV	The spherical angle, centered at an observing instrument, that defines the usable region of coverage (see Fig. 4.5). Velocity losses resulting from the fact that real propulsion systems supply impulse over periods of time instead of instantaneously.
finite burn loss	
flight path angle, γ	The angle between local horizontal and the velocity vector.
geocentric	Centered at the center of mass of the Earth.
geosynchronous orbit	A circular, equatorial Earth orbit with a period equal to one sidereal day; an orbit on which a spacecraft has a rotational rate exactly equal to the rotation rate of the Earth's surface below (such a spacecraft appears to be stationary when viewed from the Earth's surface).
gravity-assist maneuver	A maneuver in which a spacecraft encounter with a planet is used to change direction and magnitude of the spacecraft velocity vector (with respect to the sun). These very energetic maneuvers are accomplished at the expense of the energy of the planet rather than spacecraft resources.
heliocentric	Centered at the center of mass of the sun.
Hohmann transfer	A maneuver between two nonintersecting orbits that uses an elliptical transfer orbit that is tangent to both the initial and final orbits (see Fig. 3.4).
hyperbolic excess velocity, V_{HE}	The velocity at infinity on a hyperbolic departure from Earth.
inclination, i	The angle between the orbit plane and the reference plane (equatorial or ecliptic), or the angle between the normals to the two planes; one of the classical orbital elements.
injection point	The point at which a spacecraft velocity is adequate to accomplish a planetary mission.
J2	See <i>zonal coefficient</i> .
latitude, La	The body-centered angle, measured north or south from the reference plane (either the equatorial or the ecliptic), to the position of interest.
launch opportunity	The period of days during which a given planetary launch can be made with available launch vehicles.
launch window	A daily interval of time during which a spacecraft can be launched to accomplish a particular purpose.
line of apsides	The line through periapsis and apoapsis.
line of nodes	The line formed by the intersection of an orbit plane and the reference plane.
longitude, Lo	The body-centered angle, measured east or west of the reference meridian or the vernal equinox vector to a north-south plane containing the position of interest.

longitude of the ascending node, Ω	The angle between the vernal equinox vector and the ascending node, measured in the reference plane in a counterclockwise direction as viewed from the northern hemisphere.
longitude of the perihelion, ϖ	The longitudinal angle, measured in the ecliptic plane, from vernal equinox to the position of the perihelion of the orbit of a planet.
mean anomaly	The product of the mean motion and the time since periaxis passage.
mean distance	The semimajor axis of an elliptical orbit (not the time-average radius).
mean equatorial radius, R_0	The average radius of a celestial body measured at the equator.
mean motion, n	The average angular velocity required to complete one revolution on an orbit in the period of the orbit. For circular orbits it is the angular velocity on the orbit. For elliptical orbits it is the angular velocity on a circular orbit of radius equal to the semimajor axis.
mean solar time	The common time standard, based on a circular orbit with a period exactly equal to that of the Earth and the assumption that the Earth's axis is perpendicular to the ecliptic. A mean solar day is exactly 24 mean solar hours long and exactly 86,400 mean solar seconds long.
nadir	The point on the celestial sphere directly opposite the zenith, i.e., the point directly below the spacecraft.
nadir angle, β_i	The angle, centered at the spacecraft center of mass, measured from the nadir vector to a given position on the surface of the central body. The horizon angle is a specific nadir angle measured to the horizon (see Fig. 4.15).
orbital elements	Quantities that together completely describe the orbit of a spacecraft about a central body. The six classical orbital parameters are as follows (see Fig. 2.18):
a	Semimajor axis (defines the size of an orbit)
e	Eccentricity (defines the shape of an orbit)
i	Inclination of the orbit
Ω	Longitude of the ascending node
ω	Argument of periaxis
t	Time since periaxis passage
osculating elements	The orbital elements giving an instantaneous description of an equivalent, unperturbed orbit.
periapsis	The point on an orbit closest to the central body; the point of minimum orbital radius. Periapsis is a general term for any central body. Perigee is used if the central body is the Earth, perihelion for the sun, perilune for the moon. See <i>apoapsis</i> .

MISSION DESIGN GLOSSARY

165

perigee	The point on an orbit about the Earth that is closest to the Earth. See <i>periapsis</i> .
perihelion	The point on an orbit about the sun that is closest to the sun. See <i>periapsis</i> .
perilune	The point on an orbit about the earth's moon that is closest to the moon. See <i>periapsis</i> .
period, P	The time required to make one revolution around an orbit.
precession	The reactive motion of a gyroscopic object in a direction normal to that of the disturbing torque and to the angular momentum vector.
reference plane	The ecliptic plane or the equatorial plane.
regression of nodes	A phenomenon in which Earth oblateness causes a regression of the line of nodes, decreasing with increasing orbital inclination until the nodes are stationary for polar orbits.
retrograde motion	Real or apparent westward motion; clockwise motion when viewed from the north celestial sphere; the opposite of direct motion.
right ascension	The angular position measured eastward along the celestial equator from the vernal equinox vector to the hour circle of the object.
rotation of apsides	A phenomenon in which Earth oblateness causes the line of apsides to precess forward for orbital inclinations less than $i = 63.4$ deg, for higher inclinations the motion is retrograde.
semimajor axis, a	Either half of the line containing the apoapsis, periapsis, and foci of an elliptical orbit. The semimajor axis of a circle is equal to the radius, is infinite for a parabola, and is negative for a hyperbola.
semiminor axis, b	Half of the width of an ellipse measured at the center and perpendicular to the line of apsides (see Fig. 2.3). For a hyperbola it is the distance from the asymptote to a line parallel to the asymptote that contains the focus (see Fig. 2.10).
sidereal time	A time system based on the motion of Earth with respect to the stars or inertial space (see Fig. 2.13).
solstice	The point and time when the sun is at its northernmost (summer solstice, June 22) or southernmost (winter solstice, December 22) point on the ecliptic.
spacecraft horizon	A circle on the surface of the central body that circumscribes the area that can be seen from the spacecraft.
specific impulse, I_{sp}	The thrust per unit propellant flow rate obtained from a given engine with a given propellant combination; a figure of merit for rocket engines and propellant combinations.

sphere of influence	An imaginary sphere, centered on the central body, inside of which the planet is the only gravitational influence on a spacecraft. Outside that sphere the sun is the only gravitational influence.
sun-synchronous orbit	A retrograde orbit that exactly matches the orbital regression of nodes and the motion of the planet about the sun. The plane of the resulting orbit maintains a fixed angle with respect to the sun vector as the planet moves around the sun.
swath width, S_w	A measurement on the spherical surface of a central body from horizon to horizon (see Fig. 4.14).
synodic period	The time period between which two planets will have the same relative positions with respect to the sun, usually the time between conjunctions.
time since periaxis, t	the elapsed time since a spacecraft passed the point of closest approach to the central body.
true anomaly, θ	The angle in the orbit plane from the periaxis to the spacecraft position, measured in the direction of motion.
Universal time, UT	The mean solar time at the meridian of Greenwich, England.
vernal equinox vector	The vector from the center of mass of Earth to the center of mass of the sun on the spring (northern hemisphere) equinox (which occurs about March 21).
zenith	That point on the celestial sphere toward which the local vertical is directed, i.e., the point directly overhead.
zonal coefficient, J	One of the polynomial coefficients used to describe the gravitational force of an oblate central body. The dominant term is J_2 . See Table C.1 for zonal coefficients of the planets.

Appendix C Mission Design Data

Appendix C is the professional reference appendix. Once you understand how to make mission design calculations, this is the place to look up all of those numbers you are going to need. The parameters in Table C.1 are the most frequently used planetary constants. These are the default values used by the ORBWIN software. They may be updated in ORBWIN by using the Review Data function as described in Appendix A. The gravitational parameters are from Lyons and Dallas.³⁷ The mean equatorial radii and zonal coefficients are from *The Astronomical Almanac*.³⁸ The axial rotation rates A_r are calculated from sidereal rotation periods given in *The Astronomical Almanac* using the relation:

$$A_r = \frac{0.0041667}{\text{rotational period}} = \text{deg/mean solar s} \quad (\text{C.1})$$

Rotation rate is with respect to an inertial frame. Negative rates indicate retrograde motion.

Table C.2 lists the physical characteristics of the planets, sun, and moon extracted from Lang,³⁶ Boyce,³⁹ and *The Astronomical Almanac*.³⁸

Table C.3 lists the orbital elements of the planets for December 13, 1998 (JD 2451160.5) referred to the mean ecliptic of date. Semimajor axis, eccentricity, and longitude are from *The Astronomical Almanac*,³⁸ the remaining elements are

Table C.1 Default parameters used by ORBWIN

Body	μ , km^3/s^2	R_0 , km	A_r , deg/s	J_2
Mercury	22,032.1	2439.7	0.0000711	
Venus	324,858.8	6051.8	-0.0000171	0.000027
Earth	398,600.4	6378.14	0.0041781	0.00108263
Mars	42,828.3	3397	0.0040613	0.001964
Jupiter	126,711,995.4	71,492	0.0100756	0.01475
Saturn	37,939,519.7	60,268	0.0093843	0.01645
Uranus	5,780,158.5	25,559	-0.0058005	0.012
Neptune	6,871,307.8	24,764	0.0062073	0.004
Pluto	1020.9	1195	-0.0006524	
Moon	4902.8	1737.4	0.0001525	0.0002027
Sun	132,712,439,935.5	696,000	0.0001642	

Table C.2 Physical characteristics of the planets, sun, and moon

Symbol												
Planet	Mercury	Venus	Earth	Mars	Jupiter	Saturn	Uranus	Neptune	Pluto	Sun	Moon	
Natural satellites	0	0	1	2	16	18	15	8	1	9	0	
Equatorial radius, R_0	$\oplus = 1$ km miles	0.383 2439.7 1516.0	0.949 6051.8 3760.4	1.00 6378.14 3963.19	0.533 3397.0 2110.9	11.20 71492 44423.1	9.45 60268 37449.0	4.01 25559 15881.9	3.88 24764 15387.6	0.19 1195 742	109.12 696000 432474	0.272 1737.4 1080
Oblateness	J2	—	2.7E-5	0.00108	0.00196	0.01475	0.01645	0.012	0.004	—	—	202.7E-6
Mean density	$\odot = 1$ $\oplus = 1$ gm/cc lb/ft ³	3.85 0.985 5.43 339	3.72 0.950 5.24 327	3.91 1.00 5.515 344.29	2.80 0.71 3.94 246	0.94 0.241 1.33 83	0.50 0.127 0.70 43.7	0.92 0.236 1.30 81.2	1.25 0.319 1.76 109.9	0.78 0.2 1.1 69	1.0 0.255 1.409 87.96	2.37 0.606 3.34 208.8
Mass ^a	$\odot = 1$ $\oplus = 1$ kg $\times 10^{24}$	1.66E-7 0.0552 0.33022	2.45E-6 0.815 4.869	3.00E-6 1.00 5.9742	3.23E-7 0.1074 0.64191	9.55E-4 317.83 1898.8	2.858E-4 95.16 568.5	4.36E-5 14.50 86.625	5.17E-5 17.20 102.78	8E-9 0.0025 0.015	1.00 3.329E-5 1.9891E-6	3.7E-8 0.0123 0.073483
Surface gravity (Equatorial)	$\oplus = 1$ cm/s ² ft/s ²	0.377 370 12.130	0.904 887 29.085	1.00 980.665 32.1740	0.378 371 12.162	2.351 2312 75.641	0.914 896 29.407	0.792 777 25.482	1.12 1100 36.035	0.72 720 23.165	27.94 27398 898.942	0.165 162 5.309
Inclination of equator ^b	deg	0.01	177.36	23.45	25.19	3.13	26.73	97.77	28.32	122.53	—	6.68
Period of rotation ^c	days	58.6462	-243.019	0.99727	1.02596	0.41354	0.44401	-0.71833	0.67125	-6.3872	25.38	27.32166
Rotation rate, A_r	deg/s $\times 10^{-4}$	0.7111	-0.171	41.781	40.613	100.756	93.843	-58.005	62.073	-6.524	1.6417	1.525
Albedo ^d		0.106	0.65	0.367	0.150	0.52	0.47	0.51	0.41	0.30	—	0.12
Surface Temperature	°F °K	322 440	854 730	59 288	-67 218	-140 129	-290 97	-360 58	-362 56	-370 50	9944 5780	-72 215°
Pressure	bar	2E-15	90	1	0.007	—	—	—	—	1.2E-5	—	—

^a Excludes satellites; includes atmosphere.^b Inclination of the equator to the orbital plane of the planet.^c Period of rotation is the rotation of the equator with respect to a fixed reference frame in sidereal days. A negative sign indicates a retrograde rotation with respect to the pole in the northern hemisphere. The period is measured in days of 86,400 sidereal seconds.^d Albedo listed is the ratio of illumination of the planet at zero phase angle to the illumination produced by a plane, absolutely white Lambert surface at the same radius and position as the planet.^e Lunar surface temperature is for the sunny side; dark side = 123°K.

Table C.3 Orbital elements of the planets^{a,b}

Symbol Planet		α Mercury	β Venus	\oplus Earth	σ Mars	ϖ Jupiter	γ Saturn	δ Uranus	ψ Neptune	ρ Pluto
Semimajor axis, a	AU	0.387098	0.723327	0.99998	1.52372	5.2033	9.58078	19.2709	30.1927	39.3782
	Mil km	57.90904	108.2082	149.5979	227.9423	778.4026	1433.2643	2882.8856	4516.7636	5890.8948
Perihelion radius	Mil km	46.0015	107.474	147.204	206.673	740.580	1355.061	2758.835	4467.034	4438.990
Aphelion radius	Mil km	69.817	108.942	152.092	249.212	816.225	1511.467	3006.936	4566.493	7342.800
Sphere of influence	Mil km	0.111	0.616	0.924	0.577	48.157	54.796	51.954	80.196	3.400
Eccentricity, e		0.205625	0.006785	0.01667	0.09331	0.04859	0.054563	0.043030	0.01101	0.246466
Inclination, i	deg	7.0050	3.3946	0.0	1.8498	1.3047	2.4853	0.7730	1.7677	17.1365
Period	days	87.969	244.699	365.26	686.986	4335.28	10831.77	30899.498	60597.03	90257.27
	$\oplus = 1$	0.240	0.6699	1.0	1.881	11.869	29.654	84.59	165.897	247.097
Synodic period	days	115.88	583.92	—	779.94	398.88	378.09	369.66	367.49	366.73
Perihelion velocity	km/s	58.976	35.259	30.285	26.496	13.708	10.163	7.083	5.481	6.105
Aphelion velocity	km/s	38.859	34.784	29.292	21.974	12.4376	9.111	6.499	5.361	3.690
Mean motion	deg/day	4.0923	1.6021	0.9856	0.5240	0.8308	0.0536	0.04303	0.01101	0.2464
Longitude:										
Ascending node, Ω	°	48.318	76.671	—	49.550	100.468	113.632	74.048	131.785	110.321
Perihelion, ϖ	°	77.438	131.25	103.059	336.011	15.627	88.626	172.887	22.04	224.462

^a Elements for December 13, 1998, referred to the mean ecliptic of date. Elements change slowly with time.^b Data for Earth are actually for the moon-Earth barycenter.

Table C.4 Worldwide launch sites

Launch Site	Country	Latitude			Longitude	
ETR	United States	28°	30'	N	80°	33' W
WTR	United States	34°	36'	N	120°	36' W
Wallop Island	United States	37°	51'	N	75°	28' W
Kourou	Europe, ESA	5°	32'	N	52°	46' W
San Marco	Italy	2°	56'	S	40°	12' E
Plesetsk	Soviet Union	62°	48'	N	40°	24' E
Kapustin Yar	Soviet Union	48°	24'	N	45°	48' E
Tyuratam (Baikonur)	Soviet Union	45°	54'	N	63°	18' E
Thumba	UN/India	8°	35'	N	76°	52' E
Sriharikota	India	13°	47'	N	80°	15' E
Shuang-Ch'Eng-Tzu	China	40°	25'	N	99°	50' E
Xichang	China	28°	06'	N	102°	18' E
Tai-yuan	China	37°	46'	N	112°	30' E
Wuzhai	China	38°	35'	N	111°	27' E
Kagoshima	Japan	31°	14'	N	131°	05' E
Osaki	Japan	30°	24'	N	130°	59' E
Takesaki	Japan	30°	23'	N	130°	58' E
Woomera	Australia/U.S.	31°	07'	S	136°	32' E
Yavne	Israel	31°	31'	N	34°	27' E

Source: Ref. 11, p. 617; reproduced courtesy of Wertz and Larson.

Table C.5 Conversions

Multiply	By	To Get
ft/s	0.3048 (exact)	m/s
kg	2.204623	lb
km/s	3280.84	ft/s
km	0.6214	miles
km	0.5396	n mile
n mile	6080.2	ft
n mile	1.852 (exact)	km
miles	5280 (exact)	ft
miles	0.8684	n mile
miles	1.609344 (exact)	km
rad	57.2957795131	deg
rad/s	4.950355×10^6	deg/day

Conversion to Julian days¹⁰:

$$J = 367Y - 7 \left[\frac{(Y + (M + 9)/12)}{4} \right] + \frac{275M}{9} + D + 1,721,013.5 \quad (2.83)$$

MISSION DESIGN DATA

171

Table C.6 Mission design constants

Astronomical unit (AU)	149,597,870 km
Gravitational constant	32.1740 lb _m -ft/lb _f -s ²
	9.80665 m/s ²
Julian century	36,525 days
Mean sidereal day	86,164.091 mean solar s
Mean solar day	86,400 mean solar s
	86,636.55536 sidereal s
Pi	3.1415926535

Sources: Refs. 3, 8, and 12.

Table C.7 General equations defining any conic orbit

$$\varepsilon = (V^2/2) - (\mu/r) \quad (2.8)$$

$$\varepsilon = -\frac{\mu}{2a} \quad (2.9)$$

$$a = -\frac{\mu}{2\varepsilon} \quad (2.10)$$

$$\mathbf{H} = \mathbf{r} \times \mathbf{V} \quad (2.11)$$

$$H = rV \cos \gamma \quad (2.12)$$

$$e = \sqrt{1 - (H^2/\mu a)} \quad (2.13)$$

$$V = \sqrt{(2\mu/r) - (\mu/a)} \quad (2.14)$$

Table C.8 Equations for circular and parabolic orbits

Circular orbits

$$V = \sqrt{\mu/r} \quad (2.6)$$

$$P = 2\pi\sqrt{r^3/\mu} \quad (2.7)$$

$$r = (P^2\mu/4\pi^2)^{1/3} \quad (5.1)$$

Escape velocity

$$V = \sqrt{2\mu/r} \quad (2.15)$$

calculated assuming two-body motion. Orbital elements change with time; for precise work, see *The Astronomical Almanac*.

Tables C.4, C.5, and C.6 contain the most frequently used constants and conversions.

Tables C.7–C.12 list the most important equations from the text.

The equations in Table C.10 have been arranged to accept semimajor axis as a positive number. V_{HE} denotes an Earth-centered hyperbola; V_∞ is the general case. V_∞ and V_{HE} are used interchangeably in Table C.10

Table C.9 Relations defining an elliptical orbit

 Eccentricity e

$$e = \frac{c}{a} \quad (2.19) \quad e = \frac{r_a}{a} - 1 \quad (2.39)$$

$$e = \frac{(r_a - r_p)}{(r_a + r_p)} \quad (2.20) \quad e = 1 - \frac{r_p}{a} \quad (2.40)$$

$$e = \frac{r_2 - r_1}{r_1 \cos \theta_1 - r_2 \cos \theta_2} \quad (2.28)$$

 Flight path angle γ

$$\tan \gamma = \frac{e \sin \theta}{1 + e \cos \theta} \quad (2.31)$$

 Mean motion n

$$n = \sqrt{\mu/a^3} \quad (2.36)$$

 Period P

$$P = 2\pi/n \quad (2.37)$$

$$P = 2\pi \sqrt{a^3/\mu} \quad (2.38)$$

 Radius (general) r

$$r = \frac{a(1 - e^2)}{1 + e \cos \theta} \quad (2.22)$$

$$r = \frac{r_p(1 + e)}{1 + e \cos \theta} \quad (2.23)$$

 Radius of apoapsis r_a

$$r_a = a(1 + e) \quad (2.41)$$

$$r_a = 2a - r_p \quad (2.42)$$

$$r_a = r_p \frac{(1 + e)}{(1 - e)} \quad (2.43)$$

(continued)

MISSION DESIGN DATA

173

Table C.9 Relations defining an elliptical orbit (continued)Radius of periapsis r_p

$$r_p = a(1 - e) \quad (2.44)$$

$$r_p = r_a \frac{(1 - e)}{(1 + e)} \quad (2.45)$$

$$r_p = 2a - r_a \quad (2.46)$$

$$r_p = \frac{r_i(1 + e \cos \theta_i)}{1 + e} \quad (2.29)$$

Semimajor axis a

$$a = \frac{(r_a + r_p)}{2} \quad (2.17)$$

$$a = \frac{\mu r}{2\mu - V^2 r} \quad (2.47)$$

$$a = \frac{r_p}{(1 - e)} \quad (2.48)$$

$$a = \frac{r_a}{(1 + e)} \quad (2.49)$$

Time since periapsis t

$$t = \frac{(E - e \sin E)}{n} \quad (2.34)$$

$$\cos E = \frac{e + \cos \theta}{1 + e \cos \theta} \quad (2.35)$$

True anomaly θ

$$\cos \theta = \frac{r_p(1 + e)}{re} - \frac{1}{e} \quad (2.24)$$

$$\cos \theta = \frac{a(1 - e^2)}{re} - \frac{1}{e} \quad (2.25)$$

Velocity V

$$V = \sqrt{\frac{2\mu}{r} - \frac{\mu}{a}} \quad (2.14)$$

$$r_p V_p = r_a V_a \quad (2.33)$$

Table C.10 Relations defining a hyperbolic orbit

 Angle of asymptote β

$$\tan \beta = b/a \quad (2.63) \qquad \tan \beta = b V_{\text{HE}}^2 / \mu \quad (2.64)$$

$$\tan \beta = \frac{2br_p}{b^2 - r_p^2} \quad (2.65) \qquad \cos \beta = 1/e \quad (2.50)$$

 Eccentricity e

$$e = \frac{1}{\cos \beta} \quad (2.66) \qquad e = (1 + r_p/a) \quad (2.67)$$

$$e = \sqrt{1 + (b^2/a^2)} \quad (2.68)$$

 Flight path angle γ

$$\tan \gamma = \frac{e \sin \theta}{1 + e \cos \theta} \quad (2.31)$$

 Mean motion n

$$n = \sqrt{\mu/a^3} \quad (2.36)$$

 Radius (general) r

$$r = a(e^2 - 1)/(1 + e \cos \theta) \quad (2.51)$$

 Radius of periapsis r_p

$$r_p = b\sqrt{(e-1)/(e+1)} \quad (2.69) \qquad r_p = a(e-1) \quad (2.70)$$

$$r_p = c - a \quad (2.71) \qquad r_p = b \tan(\beta/2) \quad (2.72)$$

$$r_p = \frac{\partial \mu + \mu(e-1)}{V_p^2} \quad (2.73) \quad r_p = -\frac{\mu}{V_{\text{HE}}^2} + \sqrt{\left(\frac{\mu}{V_{\text{HE}}^2}\right)^2 + b^2} \quad (2.44)$$

$$r_p = -a + \sqrt{a^2 + b^2} \quad (2.75)$$

 Semimajor axis a

$$a = b/\sqrt{e^2 - 1} \quad (2.76) \qquad a = r_p/(e-1) \quad (2.77)$$

$$a = \mu/V_{\text{HE}}^2 \quad (2.78) \qquad a = (b^2 - r_p^2)/2r_p \quad (2.79)$$

$$a = \frac{\mu r_p}{r_p V_p^2 - \partial \mu} \quad (2.80)$$

(continued)

MISSION DESIGN DATA

175

Table C.10 Relations defining a hyperbolic orbit (continued)Semiminor axis b

$$b = r_p \sqrt{(e+1)/(e-1)} \quad (2.81)$$

$$b = a\sqrt{e^2 - 1} \quad (2.82)$$

$$b = r_p \sqrt{2\mu/r_p V_{\text{HE}}^2 + 1} \quad (2.83)$$

Time since periaxis t

$$t = (e \sinh F - F)/n \quad (2.59)$$

$$\cosh F = \frac{(e + \cos \theta)}{(1 + e \cos \theta)} \quad (2.60)$$

$$F = \ln(\cosh F + \sqrt{\cosh^2 F - 1}) \quad (2.61)$$

$$\sinh F = \frac{1}{2}[\exp(F) - \exp(-F)] \quad (2.62)$$

True anomaly θ

$$\cos \theta = \frac{a(e^2 - 1)}{re} - \frac{1}{e} \quad (2.52)$$

True anomaly of asymptote θ_a

$$\theta_a = 180 \text{ deg} \pm \beta \quad (2.53)$$

$$\cos \theta_a = -\frac{1}{e} \quad (2.54)$$

Velocity V

$$V_\infty = V_{\text{HE}} = \sqrt{\mu/a} \quad (2.56)$$

$$V = \sqrt{(2\mu/r) + V_{\text{HE}}^2} \quad (2.57)$$

$$V = \sqrt{(2\mu/r) + (\mu/a)} \quad (2.16)$$

$$C3 = V_{\text{HE}}^2 \quad (2.58)$$

Table C.11 Summary of equations governing maneuvers

Cosine law

$$\Delta V^2 = V_i^2 + V_f^2 - 2V_i V_f \cos \alpha \quad (3.2)$$

General plane change

$$\Delta V = 2V_i \sin(\alpha/2) \quad (3.7)$$

$$\cos \alpha = \cos i_i \cos i_f + \sin i_i \sin i_f \cos(\Delta\Omega) \quad (3.9)$$

$$\sin(A_{La})_i = \frac{\sin i_f \sin(\Delta\Omega)}{\sin \alpha} \quad (3.10)$$

Propulsion for maneuvers

$$\Delta V = g_c I_{sp} \ell_n(M_i/M_f) \quad (3.18)$$

$$M_i/M_f = \exp(\Delta V/g_c I_{sp}) \quad (3.19)$$

$$M_p = M_i[1 - \exp(-\Delta V/g_c I_{sp})] \quad (3.20)$$

$$M_p = M_f[\exp(\Delta V/g_c I_{sp}) - 1] \quad (3.21)$$

Table C.12 Equations for observing the central body

Launch site

$$\cos i = \cos La \sin Az \quad (4.1)$$

Regression of nodes

$$\frac{d\Omega}{dt} = \frac{-3n J_2 R_0^2 \cos i}{2a^2(1-e^2)^2} \quad (4.2)$$

For Earth

$$\frac{d\Omega}{dt} = -2.06474 \times 10^{14} \frac{\cos i}{a^{3.5}(1-e^2)^2} \quad (4.3)$$

Rotation of apsides

$$\frac{d\omega}{dt} = \frac{3n J_2 R_0^2 (4 - 5 \sin^2 i)}{4a^2(1-e^2)^2} \quad (4.4)$$

For Earth

$$\frac{d\omega}{dt} = 1.0324 \times 10^{14} \frac{4 - 5 \sin^2 i}{a^{3.5}(1-e^2)^2} \quad (4.5)$$

(continued)

MISSION DESIGN DATA

177

Table C.12 Equations for observing the central body (continued)

Ground track

$$\sin La = \sin i \sin A_{La} \quad (4.6)$$

$$\sin lo = \tan La / \tan i \quad (4.7)$$

Sign of adjustments

Direct orbit
Retrograde orbit

Eastern Hemisphere:

$$Lo = \Omega + lo - \Delta\Omega - Re \quad (4.10) \quad Lo = \Omega - lo + \Delta\Omega - Re \quad (4.11)$$

Western Hemisphere:

$$Lo = \Omega - lo + \Delta\Omega + Re \quad (4.12) \quad Lo = \Omega + lo - \Delta\Omega + Re \quad (4.13)$$

Spacecraft horizon

$$\cos \alpha_h = R_s / (R_s + h_s) = R_s / r \quad (4.15)$$

$$\sin \beta_h = R_s / r \quad (4.16)$$

$$D_h = r \cos \beta_h \quad (4.17)$$

$$S_w = 2\alpha_h R_s \quad (4.18)$$

Field of view

$$\beta_i = Fov/2 \quad (4.19)$$

$$\sin \Gamma' = r \sin \beta_i / R_s \quad (4.20)$$

$$\Gamma = 180 - \Gamma' \quad (4.21)$$

$$\alpha_i = 180 - (\beta_i + \Gamma) = \Gamma' - \beta_i \quad (4.22)$$

$$D_i = R_s \sin \alpha_i / \sin \beta_i \quad (4.23)$$

$$S_i = 2\alpha_i R_s \quad (4.24)$$

This page intentionally left blank

References

- ¹Pasachoff, J. M., *Contemporary Astronomy*, Saunders, Philadelphia, PA, 1977.
- ²Newton, I., *Sir Isaac Newton's Mathematical Principles of Natural Philosophy and His System of the World*, translated by Andrew Motte, 1729. Revised translation by F. Cajori, Univ. of California Press, Berkeley, CA, 1934.
- ³Bate, R. R., Mueller, D. D., and White, J. E., *Fundamentals of Astrodynamics*, Dover Publications, Inc., New York, 1971.
- ⁴Koelle, H. H. (ed.), *Handbook of Astronautical Engineering*, McGraw-Hill, New York, 1961.
- ⁵Wood, K. D., *Aerospace Vehicle Design*, Vol. II, Johnson, Boulder, CO, 1964.
- ⁶O'Neil, W. J., Rudd, R. P., Farless, D. L., Hildebrand, C. E., Mitchell, R. T., Rourke, K. H., and Euler, E. A., *Viking Navigation*, Jet Propulsion Lab., Pub. 78-38, Pasadena, CA, 1979.
- ⁷*Voyager at Neptune: 1989*, Jet Propulsion Lab., JPL 400-353, Pasadena, CA, 1989.
- ⁸Taff, L. G., *Computational Spherical Astronomy*, Wiley, New York, 1981.
- ⁹Wertz, J. R. (ed.), *Spacecraft Attitude Determination and Control*, D. Reidel, The Netherlands, 1978.
- ¹⁰Van Flandern, T. C., "Bits and Bytes," *Sky and Telescope*, Sky Publishing, Cambridge, MA, Aug. 1991, pp. 1-183.
- ¹¹Wertz, J. R., and Larson, W. J. (eds.), *Space Mission Analysis and Design*, Kluwer Academic Press, Dordrecht, The Netherlands, 1991.
- ¹²*The Astronomical Almanac For The Year 1991*, U.S. Naval Observatory and The Royal Greenwich Observatory, U.S. Government Printing Office, Washington, DC, 1991.
- ¹³Hohmann, Walter, *Erreichbarkeit der Himmelskörper*, Munich, Germany, 1925.
- ¹⁴Chobotov, V. A. (ed.), *Orbital Mechanics*, AIAA Education Series, AIAA, Washington, DC, 1991, pp. 1-365.
- ¹⁵Griffin, M. D., and French, J. R., *Space Vehicle Design*, AIAA Education Series, AIAA, Washington, DC, 1991.
- ¹⁶Fortescue, P., and Stark, J., *Spacecraft Systems Engineering*, 2nd ed., Wiley, New York, 1995.
- ¹⁷Bachofer, B. T., *Landsat D Case Study in Spacecraft Design*, AIAA, Washington, DC, 1979.
- ¹⁸Easton, R. L., and Brescia, Continuously Visible Satellite Constellations, Naval Research Laboratory Rept. 6896, 1969.
- ¹⁹Walker, J. G., "Some Circular Orbit Patterns Providing Continuous Whole Earth Coverage," *Journal of the British Interplanetary Society*, Vol. 24, 1971, pp. 369-384.
- ²⁰Draim, J., "Three- and Four-Satellite Continuous-Coverage Constellations," *Journal of Guidance, Control, and Dynamics*, Vol. 8, No. 6, 1985, pp. 725-730.
- ²¹Clarke, A. C., "Extra-Terrestrial Relays," *Wireless World*, Vol. 51, No. 10, 1945, pp. 305-308.

- ²²Agrawal, B. N., *Design of Geosynchronous Spacecraft*, Prentice-Hall, Englewood Cliffs, NJ, 1986.
- ²³Thompson, T. D. (ed.), *1988 TRW Space Log*, TRW Space and Technology Group, Redondo Beach, CA, 1989.
- ²⁴*Air & Space*, National Air and Space Museum, Washington, DC, April/May 1987, pp. 1-49.
- ²⁵Kendrick, J. B. (ed.), *TRW Space Data*, TRW Systems Group, Redondo Beach, CA, 1967.
- ²⁶Hunten, D. M., Colin, L., Donahue, T. M., and Moroz, V. I. (eds.), *Venus*, Uni. of Arizona Press, Tucson, AZ, 1983.
- ²⁷Sergeyevsky, A. B., *Mission Design Data for Venus, Mars and Jupiter Through 1990*, Jet Propulsion Lab., TM 33-736, Pasadena, CA, 1975.
- ²⁸*American Ephemeris and Nautical Almanac*, U.S. Government Printing Office, Washington, DC, published annually prior to 1981.
- ²⁹Michaux, C. M., *Handbook of the Physical Properties of Mars*, NASA SP-3030, U.S. Government Printing Office, Washington, DC, 1967.
- ³⁰*Planetary and Lunar Coordinates for the Years 1984-2000*, U.S. Naval Observatory and The Royal Greenwich Observatory, U.S. Government Printing Office, Washington, DC, 1983.
- ³¹Dunne, J. A., and Burgess, E., *The Voyage of Mariner 10*, NASA SP-424, U.S. Government Printing Office, Washington, DC, 1978.
- ³²Neihoff, J., "Pathways to Mars: New Trajectory Opportunities," AAS Paper 86-1782, July 1986.
- ³³Aldrin, E. E., "Cyclic Trajectory Concepts," Science Applications International Corp., Aerospace Systems Group, Hermosa Beach, CA, Oct. 1985.
- ³⁴Hollister, W. M., "Periodic Orbits for Interplanetary Flight," *Journal of Spacecraft and Rockets*, Vol. 6, No. 4, 1969, pp. 366-369.
- ³⁵Byrnes, D. V., Longuski, J. M., and Aldrin, E. E., "Cycler Orbit Between Earth and Mars," *Journal of Spacecraft and Rockets*, Vol. 30, No. 3, 1993, pp. 334-336.
- ³⁶Lang, K. R., *Astrophysical Data: Planets and Stars*, Springer-Verlag, New York, 1992.
- ³⁷Lyons, D. T., and Dallas, S. S., *Magellan Planetary Constants and Models Document*, Jet Propulsion Lab., PD 630-79, Rev. C, Pasadena, CA, 1988.
- ³⁸*The Astronomical Almanac For The Year 1998*, U.S. Naval Observatory and The Royal Greenwich Observatory, U.S. Government Printing Office, Washington, DC, 1998.
- ³⁹Boyce, J. M., and Maxwell, T., *Our Solar System—A Geological Snapshot*, NASA, Washington, DC, 1992.
- ⁴⁰Fordyce, J., Kwok, J. H., Cutting, E., and Dallas, S. S., *Magellan Trajectory Characteristics Document*, Jet Propulsion Lab., PD 630-76, Pasadena, CA, 1988.
- ⁴¹"STS 30 Mission Chart," Defense Mapping Agency, St. Louis, MO, 1988.
- ⁴²*The Magellan Final Mission Design*, Jet Propulsion Lab., JPL-D-2331, Pasadena, CA, 1986.
- ⁴³Meeus, J., *Astronomical Algorithms*, Willmann-Bell, Richmond, VA, 1991.

Index

- Aldrin cycler, 128
Angle of turn, 123–125
Apoapsis radius, 11–12
Apollo, 134
Apparent solar time, 26
Apsidal rotation, 60–63
Argument of periapsis, 35–36
Arrival targeting, 115–117
Arrival trajectory design, 115–119
Atmospheric drag, 91

Bielliptical transfer, 45, 49

C3, 99–100, 103, 109–113, 130–131
Central body observation
 constellations, 74–78
 ground track, 63–68
 launch site effect, 53–57
 orbit perturbations, 57–63
 spacecraft horizon, 68–74
Circular orbit, 5–8, 39–40, 42–43, 47, 52, 59, 75, 78, 141–142
Circularization, 83–84
Classical orbital elements, 35–36
Combined maneuvers, 48–49, 51
Communication time, 73–74, 79
Communications satellites, 93
Conic sections, 5, 7
Constellation design, 77–78
Coordinate systems, 32–35
 geocentric-inertial, 33
 geographic-body-fixed, 34
 heliocentric-inertial, 33–34
 IAU cartographic, 34–35
 vernal equinox, 32–33
Cycler orbit, 126–129

Delta launch vehicle, 56
Departure hyperbola, 112–114
Departure trajectory design, 108–115
Direct orbit, 56

Earth-moon system, 133–134
Earth
 oblateness, 57–58
rotation, 54
satellite, 36
Eccentric anomaly, 16, 18
Eccentricity, 10–12, 36, 86
Elliptical orbit, 7–8, 11–20, 39, 42, 60, 62, 73, 75, 100
 definition, 11–13
Ephemeris, 26, 31, 101, 130
 calculations, 104–106
Equatorial orbit, 93
Escape velocity, 21
ETR, 55–57, 63, 82, 130

Field of view, 71–72, 78
Finite burn loss, 40–41
Flight path angle, 14–15, 17
Flyby, 22, 122

Galileo, 24, 120
General coplanar maneuver, 41–42
GEOS-A, 52
Geosynchronous orbit, 37, 48, 51, 60, 81–87, 93
 launch to low Earth orbit, 82–83
 mission design, 82
 orbital errors, 85–87
 parking orbit to transfer ellipse, 83
 plane change and circularization, 83–84
 repositioning, 87
 view from orbit, 84–85
GOES-B, 78
GPS, 74, 78
Gravity-assist maneuvers, 22, 24–25, 120–127
Gregorian-to-Julian conversion, 31–32
Ground track, 63–68

Hohmann transfer, 43–45, 49, 52, 83, 86, 92, 98, 101, 130
Hyperbolic Earth departure, 24, 37, 108–109
Hyperbolic excess velocity, 99–100, 109–110, 112–115
Hyperbolic orbit, 8, 22–28, 108
 orbital parameters, 22–23

Inclination, 35, 59–60, 87
Injection velocity, 134–135

- In-plane orbit changes, 40–42
Interplanetary mission design, 33, 95–96
Interplanetary trajectories, 95–96

Julian day, 30–32, 105–106

Kepler equation, 16–17
Kepler's laws, 2, 7, 17
Kick stage, 84

LANDSAT, 36, 70, 72, 74, 89
Laplace method, 97
Launch azimuth, 53–57
Launch latitude, 55
Launch opportunity, 101–104
Launch site effect, 53–57
Launch sites, 55–57
Launch to low Earth orbit, 82–83
Launch to parking orbit, 90–91
Launch window, 114–115
Longitude of the ascending node, 36
Low Earth orbit, 40, 82–83, 91–92
Lunar injection velocity, 134–135
Lunar mission design, 136–137
Lunar orbit, 136–142
Lunar patched conic, 136–142
Lunar time of flight, 134–135, 142
Lunar trajectories, 133–141

Magellan, 17–18, 37, 51–52, 111, 115, 117, 129–131
Mariner, 120, 129
Mars
mission, 126, 128–129, 131
orbit, 44, 52, 93
Mean solar time, 29–30
Mercury orbiter, 5
Molniya orbit, 63, 78, 89–91
Multispectral scanner, 72

Neptune, 25, 79, 130
Neptune mission, 130

Orbit
circular, 5–8, 39–40, 42–43, 47, 52, 59, 75, 78, 141–142
conic, 10
coplanar, 40, 42
cycler, 126–129
definition, 10
direct, 56
elements, 11–13, 35–36
elliptical, 7–8, 11–20, 39, 42, 60, 62, 73, 75, 100
energy, 8, 10
equatorial, 93
errors, 85–87
geosynchronous, 37, 48, 51, 60, 81–87, 93
hyperbolic, 8, 22–28, 108
low Earth, 40, 82–83, 91–92
lunar, 136–142
Mars, 44, 52, 93
Molniya, 63, 78, 89–91
parabolic, 8, 18, 21–22
parking, 83–84, 90–91
period, 17
perturbations, 57–63, 87
planetary, 129–130
polar, 78
retrograde, 56
sun-synchronous, 57, 60, 87–89, 93
Venus mapping, 17–18, 51–52
ORBWIN software, 143
central body selection, 150
ephemeris calculation, 152–154
field of view calculation, 146, 151–152
ground track calculation, 146, 150
installation, 143
Julian date conversion, 152, 154–155
keyboard shortcuts, 148
menus, 143
nomenclature, 148
opening screen, 143
orbit definition, 144
 circular, 144, 157
 elliptical, 149, 157
 examples, 144, 156–159
parameters at a point, 146
perturbations, 146, 150–151
plane change, 152, 155
propellant weight, 152, 155–156
start, 143
system requirements, 143
utilities, 148, 152–156
Osculating orbital elements, 104

Parabolic orbit, 8, 18, 21–22
Parking orbit, 83–84, 90–91
Patched conic, 96–98, 100–101, 136–142
Periapsis, 11–12, 16–18, 25–26
Perturbations, 57–63, 87
Pioneer 10, 129

INDEX

183

- Plane change, 45–49, 83–84, 108–109, 118
Planet location, 101–106
ephemeris calculations, 104–106
launch opportunity, 101–102
synodic period, 102
trajectory type and class, 102–103
Planetary flights, 22
Planetary orbit, 129–130
Planetary orbital parameters, 96
Pluto, 14
Polar orbits, 78
Propellant
maneuvers, 49–51
mass, 49–50
specific impulse, 50–51
thrust force, 49–50
weight savings, 51

Radar altimeter, 69
Radius errors, 86
Regression of nodes, 58–60, 65, 67
Repositioning, 87
Retrograde orbit, 56

Saturn
approach, 37
mission, 131
Semimajor axis, 10–12, 35, 96
Sidereal time, 29–30
Sign of adjustments, 65–66
Skylab, 91
Slant angle, 72
Solar Mesosphere Explorer, 56
Solar system, 95–96
Specific momentum, 10–11
Space Shuttle, 7, 52, 60, 66–68, 92, 135
Spacing, 76–77
Spacecraft communication, 72–74
Spacecraft constellations, 74–78
Spacecraft horizon, 68–74

Spacecraft velocity, 123–126
Specific impulse, 50–51
Sphere of influence, 135–136
Station-keeping, 87
Sun-synchronous orbit, 57, 60, 87–89, 93
Swath width, 70–72, 79
Synodic period, 102, 128

TDRSS, 74
Thor-Delta launch vehicle, 52
Thrust force, 49–50
Thrust-to-weight ratio, 41
Time of flight, 25, 134–135
Time systems, 26, 29–32
Titan IIIE launch vehicle, 24
Transfer ellipse, 14, 106–108, 131
Triton, 25
True anomaly, 12–14, 16, 18, 36
Two-body motion, 1–3, 5

Ulysses mission, 24–25, 120, 124
Universal time, 30

Van Allen belt, 13
Velocity, 15–16, 18, 125–126
Venus
approach, 37, 51, 131
mapping orbit, 17–18, 51–52
mission, 98–100, 104–108, 111–112, 116,
122–123, 125–126
orbit insertion burn, 40
Vernal equinox, 32
Viking, 24, 79, 103, 129
Voyager, 25, 37, 79, 103, 112,
120, 130–131

Walker constellations, 76
WTR, 55–57

Zonal coefficients, 59